Treatment of Textile Wastewater Using Soil as a Low-Cost Adsorbent

This thesis is submitted as a partial fulfilment of the PhD programme in Engineering

by

PRIYA

ID: 2013RCE9062

DEPARTMENT OF CIVIL ENGINEERING
MALAVIYA NATIONAL INSTITUTE OF TECHNOLOGY
JAIPUR
DECEMBER-2016

© Malaviya National Institute of Technology Jaipur, 2016. All rights reserved.

DECLARATION

I hereby certify that the work which is presented in the thesis entitled **"Treatment of Textile Wastewater Using Soil as a Low-cost Adsorbent"** in partial fulfilment of the requirements for the award of Doctor of Philosophy, in the Department of Civil Engineering, Malaviya National Institute of Technology, Jaipur, is an authentic record of my own work unless otherwise referenced or acknowledged. The thesis was completed under the supervision of Dr. Urmila Brighu, Associate Professor, Department of Civil Engineering, Malaviya National Institute of Technology, Jaipur. The results presented in this thesis have not been submitted in part or full, to any other University or Institute for the award of any degree. The content of the thesis has been checked using online software "Turnitin".

Priya
2013RCE9062
Department of Civil Engineering,
MNIT, Jaipur.

DEPARTMENT OF CIVIL ENGINEERING
MALAVIYA NATIONAL INSTITUTE OF TECHNOLOGY
JAIPUR (RAJASTHAN)-302017

CERTIFICATE

This is to certify that the work reported in this thesis entitled **"Treatment of Textile Wastewater Using Soil as a Low-Cost Adsorbent"** has been carried out by Ms. **Priya** and submitted to Malaviya National Institute of Technology, Jaipur for the award of **Doctor of Philosophy**. It is a bonafide record of research work carried out by her under my supervision. The thesis work has reached the requisite standard, fulfilling the requirements for the degree of Doctor of Philosophy. The thesis embodies the original work done by her and has not been carried out earlier to the best of my knowledge and belief.

Dr. Urmila Brighu
Associate Professor
Department of Civil Engineering,
MNIT, Jaipur.

Acknowledgements

No work in this world is a solo effort. Neither is this thesis. I take this opportunity to express my gratitude to the people who have been supportive in the successful completion of this work.

I wish to express my sincere gratitude to my supervisor Dr. Urmila Brighu for her guidance, support and encouragement. Under her guidance, I successfully overcame many difficulties and learned a lot. The joy and enthusiasm she had for this research was motivational for me, even during tough times in Ph.D. pursuit. During the most difficult time of writing this thesis, she gave me the moral support and freedom I needed to move on. She always knew where to look for the answers to obstacles while leading me to the right source, theory and perspective. Her patience, flexibility, genuine concern and faith in me during the dissertation process are highly appreciated.

I am also deeply thankful to Dr. A.B. Gupta for his helpful suggestions and assistance throughout this research. I thank Dr. Sanjay Mathur and Dr. Nivedita Kaul for sharing their expertise.

I gratefully acknowledge the financial assistance provided by Rajasthan State Pollution Control Board, Jaipur to carry out this research. I am also thankful to the team of MRC at MNIT Jaipur, SAIF at IIT Bombay and ACMS at IIT Kanpur for their help and support for performing various tests needed for research.

I would also like to express my gratitude to Rajesh Saxena and S. Ansari for being a support in timely completion of necessary academic paperwork.

I highly appreciate the moral support from all my friends at MNIT especially Kavita and Richa, who always stood by me and helped me surviving the stress.

Lastly, I would like to thank my family for their love and encouragement. For my parents who supported me in all my pursuits. For my brother, Raghvendra, whose sense of humor gave me much needed reprieve from the work. And most of all for my loving, supportive, encouraging and patient husband, Soumitra, whose faithful support during the final stages of this Ph.D is so appreciated. I love you all dearly and dedicate this thesis to you.

Abstract

Water is the basic necessity of life and is available in limited quantity. The rapid industrialization is polluting this limited resource. Textile industry comes under one of such polluting entities, taking into consideration the volume of discharge and effluent composition. This demands for the treatment technologies for water reclamation and reuse. However, for low income countries, effluent treatment is a matter of concern as it incurs cost. Therefore, stress is being made on treatment technologies which would cost less but provide good treatment. Adsorption using low-cost adsorbents can fulfill this requirement.

The present study was proposed to find a low-cost adsorption solution using an adsorbent which is easily and abundantly available for treatment of textile wastewater. Therefore, locally available soil was used as an adsorbent. The purpose of the study was to assess the feasibility and potential of locally available soil for colour removal. Two different classes of dyes; Direct Red 81 and Methylene Blue, were used for their removal from aqueous solution using soil. The adsorption efficiency of soil examined at various parameters like pH, contact time, adsorbent dose, dye concentration and particle size. Out of these parameters, pH was found to have a significant effect on adsorption of these dyes. Hence, soil was modified in accordance to optimum pH obtained for the removal of these dyes to enhance its adsorption capacity. For DR81 removal, soil was modified using 1N H_2SO_4 as maximum removal for this dye was observed at pH 3. Maximum removal for MB was observed at pH 11, therefore soil was modified with 1N NaOH for its removal. Further parametric study was also conducted on modified soils. Inferences made from batch study revealed that alkali modified soil had best adsorption capacity among all the three soils. It showed adsorption capacity of 6.4mgg^{-1} for MB whereas acid modified soil showed adsorption capacity of 2.4 mgg^{-1} for DR81 at contact time of 10 minutes. However, non-modified soil had adsorption capacity of 3.04mgg^{-1} for MB and 0.96mgg^{-1} for DR81 at contact time of 10 minutes.

Kinetic modeling and equilibrium study was also performed on the experimental data obtained from all the three soils. Kinetic modeling showed that Lagergren's pseudo second order model describes the reaction mechanism. From intraparticle diffusion model, it was found that intraparticle diffusion was not only rate-limiting step but boundary layer diffusion also controlled the adsorption of dyes. Equilibrium study revealed that Freundlich isotherm fit best for non-modified soil, Redlich-Peterson isotherm for acid-modified soil and Sips isotherm for alkali-modified soil, suggesting multilayer adsorption of dye molecule on the adsorbent.

To evaluate the actual field application viability of soil, fixed bed study was conducted using simulated and actual textile wastewater. Alkali modified soil was used as an adsorbent in the column. For actual textile wastewater, adsorption was preceded by an additional step of coagulation in the treatment process to reduce the suspended impurities. Alum was used as coagulant. The removal of colour and COD from both the textile wastewaters was studied. It was found that an increase in bed height and a decrease in flow rate improved the colour removal and COD reduction. The combination of bed height of 4.5 cm and flow rate of 0.5 L/hr was found to give best results. Three models, namely; BDST, Thomas and Yoon and Nelson were used to evaluate design parameters. The study concluded that colour and COD in effluent

were meeting the standard limits of disposal and the choking of the bed was also not observed which is a common problem reported for other clays. Therefore, the locally available soil, with modification could be used as a viable low-cost adsorbent for textile wastewater treatment.

Keywords: Dyes, Textile wastewater, Adsorption, Low-cost adsorbent

Contents

Acknowledgements ..... **iii**

Abstract ..... **iv**

List of Tables ..... **xii**

List of Figures ..... **xv**

Nomenclature ..... **xix**

Chapter 1 ..... **1**

Introduction 1

1.1 Context and Background 1

1.2 Environmental Impact of Dyes 3

1.3 Various Techniques for Textile Wastewater Treatment 4

1.3.1 Low-Cost Adsorbents as an Alternative to Treat Textile Wastewater 5

1.4 Need for the Present Study 6

1.5 Aim & Objectives of the Study 7

1.6 Scope of the Study 7

1.7 Novelty of the Study 8

1.8 Outline of the Work 8

1.9 Structure of the Thesis 10

1.10 Summary 11

Chapter 2 ..... **12**

Adsorption of Dyes and Low-Cost Adsorbents: A Literature Review 12

2.1 Introduction 12

2.2 Dyes: Structure and Classification 12

2.2.1 Cationic dyes 13

2.2.2 Anionic Dyes 14

2.3 Dye Removal Techniques 14

2.4 Adsorption of Dyes 19

2.4.1 Factors affecting adsorption of dye 19
2.5 Adsorbent Materials 20
2.5.1 Activated Carbon 20
2.5.2 Low-cost Adsorbents 22
2.5.2.1 Agro-Based Adsorbents 23
2.5.2.2 Industrial Wastes 28
2.5.2.3 Zeolite and Other Siliceous Materials 29
2.5.2.4 Clay 32
2.6 Fixed Bed Study 37
2.7 Summary 37
Chapter 3 39
Research Methodology 39
3.1 Research Stages 39
3.2 Formulation of Research Methods 39
3.3 Batch Study 41
3.3.1 Materials 41
3.3.1.1 Adsorbent 41
3.3.1.2 Adsorbate 41
3.3.1.3 Stock solution 42
3.3.2 Experimental Analysis 42
3.3.2.1 Effect of pH 43
3.3.2.2 Effect of Contact Time 43
3.3.2.3 Effect of Adsorbent Dose 43
3.3.2.4 Effect of Initial dye concentration 43
3.3.2.5 Effect of Particle Size 44
3.3.3 Data Analysis 44
3.3.3.1 Kinetic Modelling 44

3.3.3.2 Equilibrium Studies 47
3.4 Fixed Bed Study 52
3.4.1 Materials 52
3.4.1.1 Simulated Textile Wastewater 52
3.3.4.2 Actual Textile Wastewater 53
3.4.2 Experimental Analysis 53
3.4.2.1 Effect of flow rate and bed height on Breakthrough of Fixed Bed 55
3.4.3 Data Analysis 57
3.5 Analytical Procedure 61
3.6 Summary 62
Chapter 4 63
Removal of Direct Red 81 and Methylene Blue onto Non-Modified Soil 63
4.1 Introduction 63
4.2 Materials & Methods 64
4.2.1 Adsorbent 64
4.2.2 Adsorbate 64
4.2.3 Adsorption Study 64
4.3 Result & Discussion 64
4.3.1 Effect of Operating Parameters on Dye Removal 64
4.3.1.1 Effect of pH 64
4.3.1.2 Effect of Contact Time 68
4.3.1.3 Effect of Adsorbent Dose 71
4.3.1.4 Effect of Initial Dye Concentration 72
4.3.1.5 Effect of Particle Size 74
4.3.2 Kinetic Modelling 76
4.3.2.1 Lagergren's Pseudo First Order Kinetic Model 76
4.3.2.2 Lagergren's Pseudo Second Order Kinetic Model 77

4.3.2.3 Intraparticle Diffusion Model 82
4.3.3 Equilibrium Study 87
4.3.4 Characterisation of the Non-modified Soil 91
4.3.4.1 X-Ray Diffraction Analysis 91
4.3.4.2 X-Ray Fluorescence Analysis 92
4.3.4.3 Surface Area 92
4.3.4.4 Scanning Electron Microscopy (SEM) – Energy Dispersive X-Ray (EDX) Analysis 93
4.3.4.5 Fourier Transform Infrared Spectroscopy Analysis and Zeta Potential of the soil surface 95
4.4 Summary 98
Chapter 5 100
Removal of Direct Red 81 onto Acid-Modified Soil 100
5.1 Introduction 100
5.2 Materials & Methods 100
5.2.1 Adsorbent 100
5.2.2 Adsorbate 101
5.2.3 Adsorption Studies 101
5.3 Results & Discussion 101
5.3.1 Parametric analysis 101
5.3.2 Kinetic modelling 104
5.3.3 Equilibrium Studies 110
5.3.4 Characterisation of the Acid Modified Soil 116
5.4 Summary 123
Chapter 6 124
Removal of Methylene Blue onto Alkali-Modified Soil 124
6.1 Introduction 124
6.2 Materials & Methods 124

6.2.1 Adsorbent 124
6.2.2 Adsorbate 125
6.2.3 Adsorption Studies 125
6.3Results & Discussion 125
6.3.1 Parametric analysis 125
6.3.2 Kinetic modelling 128
6.3.3 Equilibrium Studies 134
6.3.4 Characterisation of the Alkali Modified Soil 140
6.4 Summary 146
Chapter 7 148
Fixed Bed Study for the Treatment of Simulated and Actual Textile Wastewater.... 148
7.1 Introduction 148
7.2 Materials & Methods 149
7.2.1 Adsorbent 149
7.2.2 Adsorbate 149
7.2.3 Fixed Bed Studies 149
7.3 Results & Discussion 149
7.3.1 Treatment of Simulated Wastewater 149
7.3.1.1 Effect of Flow Rate and Bed Height on Breakthrough of Fixed Bed..... 149
7.3.1.2 Analysis and modelling of Fixed Bed Parameters in Columns 153
7.1.3 COD Removal from Simulated Textile Wastewater 160
7.3.2 Treatment of Actual Textile Wastewater 162
7.3.2.1 Coagulation-Flocculation 163
7.3.2.2 Adsorption on Fixed Bed Column 164
7.4 Summary 165
Chapter 8 167
Conclusion 167

Limitations of the Study 173

Overall Conclusion to the Research Problem 174

Scope for Future Research 175

References 176

Appendix A 191

Appendix B 196

Appendix C 202

Appendix D 206

Biographical Profile of Researcher 210

List of Publications 211

List of Tables

Table 1.1: Effluent discharge limits for textile wastewater (*The Environment (Protection) Rules, 1986)* 2
Table 2.1: Classification of dyes (Verma et al. 2012)(Gupta & Suhas 2009)(O'Neill et al. 1999) 15
Table 2.2: Some dye removal techniques (Anjaneyulu et al. 2005)(Verma et al. 2012)(Robinson et al. 2001)(Vandevivere et al. 1998) 17
Table 2.3: Adsorption capacities and other parameters for removal of dyes using agro-based adsorbents. 26
Table 2.4: Adsorption Capacity and other Parameters for Dye Removal by Siliceous Materials 31
Table 2.5: Adsorption capacity and particle size of various clays (Mundada et al. 2016) 34
Table 3.1: Research objectives and data information 40
Table 3.2: List of adsorption isotherm models (Foo & Hameed 2010) 51
Table 3.3: Physicochemical properties of simulated textile wastewater 53
Table 3.4: Physicochemical properties of actual textile wastewater 53
Table 3.5: Parameters for Column design 54
Table 3.6: Instruments used in the study 61
Table 4.1: Effect of adsorbent dose on DR81 and MB removal (Condition: dye concentration: 1000 mg/L; pH: 3 for DR81 & 11 for MB, contact time: 10 minutes) 72
Table 4.2: Effect of initial dye concentration on DR81 and MB removal (Condition: adsorbent dose: 25g/100mL, pH: 3 for DR81 & 11 for MB, contact time: 10 minutes) 74
Table 4.3: Particle Size Distribution of soil 76
Table 4.4: Isotherm parameters obtained using linear method for DR81 and MB removal on non-modified soil 90
Table 4.5: XRF of Non-modified soil 92
Table 4.6: BET surface area analysis of non-modified soil 92
Table 4.7: Elemental Composition of Non-modified Soil 94
Table 5.1: Effect of initial dye concentration on DR81 removal (Condition: adsorbent dose: 12.5g/100ml, contact time: 10 minutes) 103

Table 5.2: Effect of adsorbent dose on DR81 removal (Condition:dye concentration: 1000 mg/L, contact time: 10 minutes) 104
Table 5.3: Isotherm parameters obtained using non-linear regression method for DR 81 removal onto acid modified soil 114
Table 5.4: XRF of Acid-modified soil 117
Table 5.5: BET surface area analysis of acid-modified soil 117
Table 5.6: Elemental Composition of Acid-modified Soil 118
Table 6.1: Effect of initial dye concentration on MB removal (Condition: adsorbent dose: 12.5g/100mL, contact time: 10 minutes) 127
Table 6.2: Effect of adsorbent dose on MB removal (Condition: dye concentration: 1000 mg/L; contact time: 10 minutes) 128
Table 6.3: Isotherm parameters obtained using non-linear regression method for MB removal onto alkali modified soil 138
Table 6.4: XRF of Alkali-modified soil 140
Table 6.5: BET surface area analysis of alkali-modified soil 141
Table 6.6: Elemental Composition of Alkali-modified Soil 142
Table 7.1: Breakthrough and exhaustion times for adsorption of simulated wastewater on alkali-modified soil for different flow rates and bed heights. 151
Table 7.2: Column Parameters for adsorption of simulated wastewater on alkali modified soil for different flow rates and bed heights 152
Table 7.3: Adsorption capacities of different fixed bed columns for adsorption of simulated wastewater onto alkali modified soil for different flow rates and bed heights. 152
Table 7.4: Parameters obtained by BDST Model at different flow rates 155
Table 7.5: Critical Bed Depth and Bed efficiency at different flow rates 155
Table 7.6: Data obtained using BDST equation for different flow rates for adsorption of simulated wastewater onto alkali modified soil 155
Table 7.7: Parameters predicted from Thomas model at various flow rates and bed heights 156
Table 7.8: Parameters predicted from the Yoon and Nelson model at various flow rates and bed heights 158
Table 7.9: Breakthrough times and volume treated of simulate wastewater on alkali modified soil for different flow rates and bed heights for COD removal 162

Table B.1: Lagergren's Pseudo First Order Kinetic Parameters for Adsorption of DR81 and MB on non-modified soil 196
Table B.2: Lagergren's Pseudo Second Order Kinetic Parameters for Adsorption of DR81 and MB on non-modified soil 197
Table B.3: Intraparticle Diffusion Parameters for Adsorption of DR81 and MB 198
Table B.4: FTIR spectra for non-modified soil..... 199
Table B.5: FTIR spectra for DR81 adsorbed non-modified soil 200
Table B.6: FTIR spectra for MB adsorbed non-modified soil..... 201
Table C.1: Lagergren's Pseudo first order and Pseudo second order model for DR81 removal on acid modified soil..... 202
Table C.2: Intraparticle diffusion model for DR 81 removal on acid modified soil.. 203
Table C.3: Isotherm parameters obtained using linear regression method for DR81 removal onto acid modified soil 204
Table C.4: FTIR of acid modified and DR 81 adsorbed acid modified soil 205
Table D.1: Lagergren's Pseudo first order and Pseudo second order model for MB removal on alkali modified soil 206
Table D.2: Intraparticle diffusion model for MB removal on alkali modified soil ... 207
Table D.3: Isotherm parameters obtained using linear regression method for MB removal onto alkali modified soil 208
Table D.4: FTIR of alkali modified and MB adsorbed alkali modified soil..... 209

List of Figures

Figure 1.1: Conceptual framework – Approach towards the research problem 3
Figure 1.2: Outline of the work..... 9
Figure 2.1: Structure of dyes (Verma et al. 2012) 13
Figure 3.1: Research stages of the present study 39
Figure 3.2: Structure of DR81 41
Figure 3.3: Structure of Methylene Blue 42
Figure 3.4: Set- up for Fixed Bed Study 54
Figure 4.1: Effect of pH on dye removal (a) & (b) DR81; (c) MB (Condition: dye concentration: 1000 mg/L; contact time: 10 minutes, adsorbent dose: 100g/100mL) 66
Figure 4.2: Point zero charge of soil 67
Figure 4.3: Effect of contact time on dye removal (a) DR81 and (b) MB (Condition: initial dye concentration: 1000 mg/L; pH: 3 for (a) & 11 for (b), adsorbent dose (per 100mL): 12.5g, 25g, 50g, 75g, 100g) 69
Figure 4.4 : Effect of adsorbent dose on percent dye removal (a) DR81 and (b) MB (Condition: dye concentration: 1000 mg/L; pH: 3 for DR81 & 11 for MB , contact time: 10 minutes, adsorbent dose(per 100mL): 12.5g, 25g, 50g, 75g, 100g; Particle size:300-150µm) 71
Figure 4.5: Effect of initial dye concentration on dye removal (a) DR81 and (b) MB (Condition: adsorbent dose: 25g/100mL, pH: 3 for DR81 & 11 for MB, contact time: 10 minutes, initial dye concentration: 125mg/L, 250mg/L, 500mg/L, 1000mg/L) 73
Figure 4.6: Effect of particle size of non-modified soil on dye removal (a) DR81 and (b) MB (Condition: initial dye concentration: 1g/L; pH: 3 for (a) & 11 for (b), adsorbent dose: 12.5g/100mL)..... 75
Figure 4.7: Particle Size Distribution curve of soil..... 76
Figure 4.8: Lagergren's Pseudo Second Order Kinetic Plot for Adsorption of DR81 79
(a) 100g/100mL (b) 75g/100mL (c) 50g/100mL (d) 25g/100mL (e) 12.5g/100mL.... 79
Figure 4.9: Lagergren's Pseudo Second Order Kinetic Plot for Adsorption of MB.... 81
(a) 100g/100mL (b) 75g/100mL (c) 50g/100mL (d) 25g/100mL (e) 12.5g/100mL.... 81
Figure 4.10: Intraparticle Diffusion Parameters for Adsorption of DR81 (a)100g/100mL (b) 75g /100mL (c) 50g/100mL (d) 25g/100mL (e) 12.5g/100mL.... 84
Figure 4.11: Intraparticle Diffusion Parameters for Adsorption of MB 86
(a)100g/100mL (b) 75g /100mL (c) 50g/100mL (d) 25g/100mL (e) 12.5g/100mL.... 86

Figure 4.12: Freundlich isotherm plots For DR81 (a) 100g/100mL (b) 75g/100mL (c) 50g/100mL (d) 25g/100mL (e) 12.5g/100mL 88
Figure 4.13: Freundlich isotherm plots for MB (a) 100g/100mL (b) 75g/100mL (c) 50g/100mL (d) 25g/100mL (e) 12.5g/100mL 89
Figure 4.14: XRD pattern for Non-modified soil 91
Figure 4.15: Energy Dispersive X-Ray Analysis of Non-modified soil 93
Figure 4.16: SEM images for (a) Non-modified Soil (b) DR81 adsorbed Non-modified Soil and (c) MB adsorbed Non-modified Soil 94
Figure 4.17: FTIR spectra for (a) non-modified soil, (b) DR81 adsorbed non-modified soil, (c) MB adsorbed non-modified soil, (d) zeta potential for non-modified soil 96
Figure 5.1: Effect of initial dye concentration and contact time on DR81 removal. (Condition: dose: 12.5g/100ml) 102
Figure 5.2: Effect of acid modified soil dose on DR81 removal. (Condition: time: 10 min) 103
Figure 5.3: Lagergren's Pseudo Second Order Kinetic Plot for Adsorption of DR81 on Acid Modified Soil (a) 100g/100ml (b) 75g/100ml (c) 50g/100ml (d) 25g/100ml (e) 12.5g/100ml 107
Figure 5.4: Intraparticle Diffusion Parameters for Adsorption of DR81 on Acid Modified Soil (a) 100g/100ml (b) 75g/100ml (c) 50g/100ml (d) 25g/100ml (e) 12.5g/100ml 110
Figure 5.5: Non-Linear Regression Analysis for Isotherms (a) Langmuir 113
(b) Fruendlich (c) Redlich-Peterson (d) Sips (e) Toth 113
Figure 5.6: XRD pattern for Acid modified soil 116
Figure 5.7: Energy Dispersive X-Ray Analysis of (a) Acid-modified soil and (b) DR81 adsorbed Acid-modified Soil 119
Figure 5.8: SEM images for (a) & (b) Acid-modified Soil (c) DR81 adsorbed Acid-modified Soil 120
Figure 5.9: Zeta Potential for Acid modified soil 121
Figure 5.10: FTIR spectra for (a) Acid-modified soil (b) DR81 adsorbed Acid-modified soil 122
Figure 6.1: Effect of initial dye concentration and contact time on MB removal onto alkali modified soil (Condition: dose: 12.5g/100mL) 126
Figure 6.2: Effect of alkali modified soil dose on MB removal. (Condition: time: 10 min) 127

Figure 6.3: Lagergren's Pseudo Second Order Kinetic Plot for Adsorption of MB on Alkali Modified Soil (per 100mL) (a) 100g (b) 75g (c) 50g (d) 25g (e) 12.5g 131
Figure 6.4: Intraparticle Diffusion Parameters for Adsorption of MB on Alkali Modified Soil (per 100mL) (a) 100g (b) 75g (c) 50g (d) 25g (e) 12.5g 133
Figure 6.5: Non-Linear Regression Analysis for Isotherms (a) Langmuir (b) Freundlich (c) Redlich-Peterson (d) Sips (e) Toth 137
Figure 6.6: XRD pattern for Alkali modified soil 140
Figure 6.7: Energy Dispersive X-Ray Analysis of (a) Alkali-modified soil and (b) MB adsorbedAlkali-modified Soil 143
Figure 6.8: SEM images for (a) & (b) Alkali-modified Soil (c) MB adsorbed Alkali-modified Soil 144
Figure 6.9: Zeta Potential for Alkali modified soil 144
Figure 6.10: FTIR spectra for (a) Alkali-modified soil (b) MB adsorbed Alkali-modified soil 145
Figure 7.1: Breakthrough curves for adsorption of simulated wastewater onto alkali modified soil at varying bed depths for flow rates of (a) 0.5 L/hr, (b) 0.7 L/hr and (c)1.0 L/hr. 150
Figure 7.2: BDST model for adsorption of simulated wastewater onto alkali modified soil at varying bed depths for flow rates of (a) 0.5 L/hr, (b) 0.7 L/hr and (c) 1.0 L/hr 154
Figure 7.3: Comparison of experimental breakthrough curves with those predicted by Thomas model for adsorption of simulated wastewater at varying bed heights for flow rate (a) 0.5 L/hr, (b) 0.7 L/hr, (c) 1.0 L/hr 157
Figure 7.4: Comparison of experimental breakthrough curves with those predicted by Yoon and Nelson model for adsorption of simulated wastewater at varying bed heights for flow rate (a) 0.5 L/hr, (b) 0.7 L/hr, (c) 1.0 L/hr 160
Figure 7.5: COD removal from simulated wastewater onto alkali modified soil at varying bed depths for flow rates of (a) 0.5 L/hr, (b) 0.7 L/hr and (c) 1.0 L/hr. 161
Figure 7.6: The curve of absorbance in the visible spectrum for the treated wastewater by alum. 163
Figure 7.7: COD reduction at various alum doses 164
Figure 7.8: COD removal for actual wastewater at 0.5 L/hr flow rate and 4.5cm bed height 164

Figure 7.9: The curve of absorbance in the visible spectrum for the treated wastewater at 0.5 L/hr flow rate and 4.5cm bed height 165

Nomenclature

List of Symbols

m^2/g	Meter square per gram
mg/L	Milligram per litre
mol/g	Moles per gram
$mmolg^{-1}$	Millimoles per gram
µm	micrometer
nm	nanometer
NaOH	Sodium Hydroxide
HCl	Hydrochloride Acid
H_2SO_4	Sulphuric Acid
SiO_2	Silica
Al_2O_3	Alumina
Fe_2O_3	Iron oxide
OH^-	Hydroxyl ion
H^+	Hydrogen ion
L/hr	Litre per hour
%	Percent
N	Normal
M	Molar
K_l	Langmuir constant
K_f	Freundlich constant
K_r	Redlich-Peterson constant
K_s	Sips constant
K_T	Toth constant

List of abbreviations

MB	Methylene Blue
DR81	Direct Red 81
COD	Chemical Oxygen Demand
CPCB	Central Pollution Control Board
LCA	Low-cost adsorbent
AC	Activated Carbon
ASTM	American Society of Testing and Materials
BET	Brunauer-Emmett-Teller
rpm	Rotations per minute
FTIR	Fourier Transmission Infrared Spectrometer
FE-SEM	Field Emission- Scanning Electron Microscope
EDX	Energy Dispersive X-ray Spectrometry
XRD	X-ray Diffraction
XRF	X-ray Fluorescence
GAC	Granular Activated Carbon
PAC	Powdered Activated Carbon
BDST	Bed Depth Service Time

CHAPTER

1

Chapter 1

Introduction

This chapter presents the background of the study and formulation of objectives based on the need of the study. The scope of the work is followed by the novel elements of the research. The last section describes the outline of the research and structure of this thesis.

1.1 Context and Background

Water is the prime necessity of life and extremely essential for the survival of living organisms. It is noteworthy that only 0.02% of the total available water on the earth is immediately available for use in the form of rivers, lakes and streams (Bhatnagar & Minocha 2006). However, due to rapid industrialization, water pollution has become a serious environmental concern around the world. Though, the textile industry is one of the fastest growing industries and contributes significantly to the economy of various Asian and other countries (Mondal 2008), it is also rated amongst high water polluters (El Qada et al. 2008). The large volume of effluent from this industry mainly contains dyes. The discharge of dyes during textile fibre dyeing and finishing processes cause surface and groundwater pollution. Though, the exact quantity of production of dyestuffs in the world is still not known, but, it is estimated that more than 1,00,000 types of commercially available dyes exist, and an annual amount of 7,00,000-10,00,000 tons is produced worldwide. India itself contributes to 6.6% of the total world output which accounts for around 60,000 tons of dyes. It is also estimated that 2,80,000 tons of textile dyes are discharged as industrial effluent every year across the world (Pang & Abdullah 2013) (Singh & Arora 2011). And, this makes the untreated textile wastewater high in chemical oxygen demand (COD), biological oxygen demand, total organic carbon, suspended solids, pH, temperature and toxicity (Ergas et al. 2006).

Textile operations are extremely water intensive. The high water consumption of this industry accounts for 3% of the annual water withdrawals from natural resources in India. And, wastewater generated in this sector has been estimated as 55×10^6 m^3 per

day, of which 68.5×10^3 m^3 are dumped directly into local rivers and streams without prior treatment (Verma et al. 2012). Direct disposal of effluent into water resources is not only harmful to human and animal life, but also eradicates the limited water available. This has prompted the government of many developing countries for the implementation of stringent directives. These directives help in the reduction of the water pollution by forcing textile industries to use new and less polluting technologies, treating the effluent to specified discharge requirements and recycling the waste several times before discharging it. In India, the main legislations that are relevant to water pollution are the Water (Prevention and Control of Pollution) Act, 1974, the Water (Prevention and Control of Pollution) Cess Act, 1977 and the Environment (Protection) Act, 1986. The Central Pollution Control Board (CPCB) sets uniform discharge standards as minimum acceptable standards for industrial and municipal discharges to be enforced by state pollution control boards (Singh & Arora 2011). Table 1.1 shows the effluent discharge limits for textile wastewater.

Table 1.1: Effluent discharge limits for textile wastewater (*The Environment (Protection) Rules, 1986)*

Parameter	**Concentration not to exceed, milligram per litre (mg/L), except pH**
pH	5.5 – 9.0
Total suspended solids	100
Bio-chemical oxygen demand	30
Chemical oxygen demand	250
Total residual chlorine	1
Oil and grease	10
Total chromium as Cr	2
Sulphide as S	2
Phenolic compounds as C_6H_5OH	1

Section 1.1 helps in formulating research approach of the present study. Figure 1.1 shows the conceptual framework for research problem. The highlighted area in this figure defines the direct approach while rest suggests the alternatives for the corresponding issues. The figure clearly indicates that the research problem of the proposed study originated due to the scarcity of fresh water availability and the stringent laws enforced by the government. Therefore, three ways have been suggested to overcome this problem: demand reduction, water reclamation and innovation in technology. This research is focused on developing a low-cost solution for wastewater treatment so that it can be discharged safely or reused. Treated

wastewater can be reused for agricultural irrigation, landscape irrigation, industrial recycling and reuse, groundwater recharge and non-potable urban uses. Thus, we can clearly see the approach (highlighted area in Figure 1.1) of the present research study through viewing the conceptual framework.

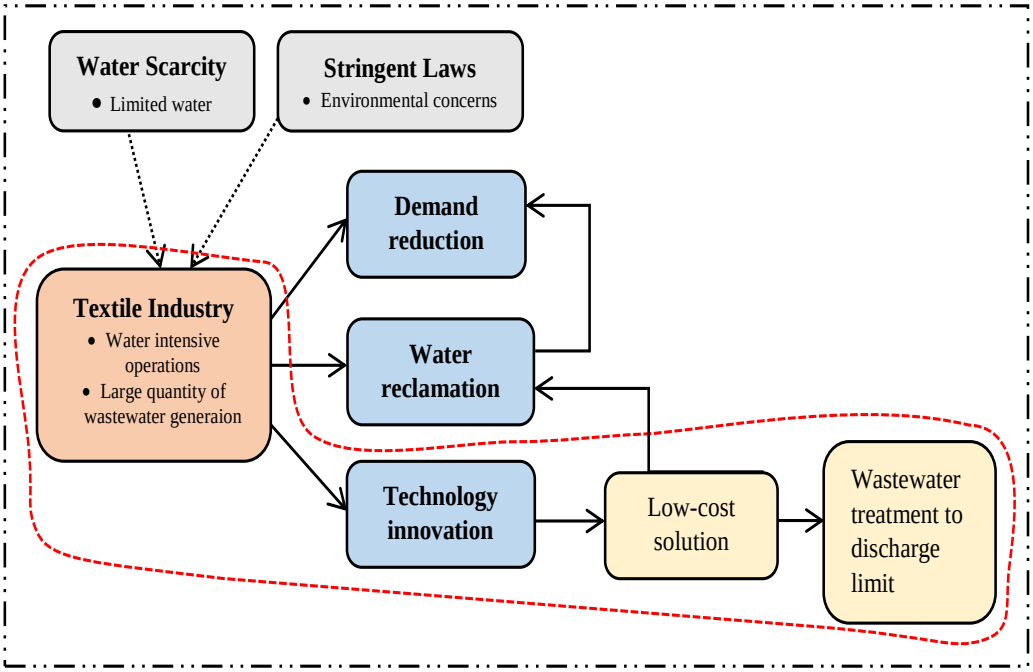

Figure 1.1: Conceptual framework – Approach towards the research problem

1.2 Environmental Impact of Dyes

Dyestuffs have a considerable negative environmental impact. It is not only the coloured effluents which are offensive to the eyes but also the toxicity of the colouring agents in the effluent creates environmental hazards (Mondal 2008). Many dyes are made from known carcinogens, such as benzidine, naphthalene and other aromatic compounds, all of which might be transformed as a result of microbial metabolism. It has been shown that azo and nitro compounds are reduced in sediments and in the intestinal environment which results in the regeneration of the parent toxic amines (Anjaneyulu et al. 2005). Aromatic amines are reported to have the potential of inducing cancer and tumors in humans. Some of them are competent enough to cause irritations to the skin, eyes, allergic dermatitis, and respiratory tract if swallowed. For example, triphenylmethane dyes (Malachite Green, Acid Violet 19, and Crystal Violet) are phytotoxic in agricultural plants, cytotoxic in mammalian cells, and also

promoting tumor growth in some species of fish. These dyes will cause irritation to the gastrointestinal tract upon ingestion and lead to permanent injury upon contact with the eyes (Pang & Abdullah 2013). Metal-based complex dyes, such as chromium-based dyes can result in the release of chromium ion which is carcinogenic in nature. Some disperse dyes have also shown a tendency to bioaccumulate. Anthraquinone-based dyes are the most resistant to degradation due to their fused aromatic structure and thus remain coloured for a longer period. Due to the non-biodegradability of organic dyes and their high color intensity, these dyes can reduce aquatic diversity by blocking the passage of sunlight through the water (Khraisheh et al. 2005). Basic dyes have high brilliance and color intensity even in a very low concentration (Anjaneyulu et al. 2005).

1.3 Various Techniques for Textile Wastewater Treatment

There are several methods available for the treatment of the textile wastewater which is divided into three broad categories: physical, chemical and biological. Conventional biological processes are the most economical for the treatment of textile effluents but are unable to treat dye wastewater effectively because most commercial dyes are toxic to the organisms present in the process and result in problems of sludge bulking, rising sludge and pin point floc formation (Ahn et al. 1999). Furthermore, anaerobic processes are also not effective for textile wastewater. The presence of azo dyes in textile wastewater makes anaerobic biological processes unsuitable for the treatment because degradation of azo dyes under anaerobic conditions results in the breakdown of azo bonds which leads to the formation of toxic aromatic amines (Meriç et al. 2004). To decrease the toxicity of the dyestuff, wastewater pretreatment by physical and chemical processes like chemical coagulation/flocculation (Tan et al. 2000), ozonation (Mezzanotte et al. 2013), Fenton’s oxidation (Meriç et al. 2004), electrocoagulation (Do & Chen 1994), membrane filtration process (Van der Bruggen et al. 2005), adsorption (Goswami & Purkait 2011) has been reported. However, these processes also have some drawbacks.

In coagulation process, a significant amount of sludge is produced, which may become a pollutant itself and thus, increases the treatment cost. Also, oxidation process, such as ozonation effectively decolorizes almost all dyes except disperse dyes, but does not remove COD effectively. Ozone attacks the double bonds of the

dye that impart colour which decolourises the water but does not necessarily lead to a reduction in COD. The effectiveness of decolorization by the oxidation process will also be reduced by the amount of ozone used and hence the treatment cost (Ahn et al. 1999)(Babu et al. 2007). The major disadvantage of the Fenton's process is that this mechanism involves flocculation; impurities are transferred from the wastewater to the sludge, which is still ecologically questionable. The performance is dependent on the final floc formation and it's settling quality (Anjaneyulu et al. 2005). The main drawbacks of the electrocoagulation process are high electricity cost and sludge production and also pollution from chlorinated organics, heavy metals produced due to indirect oxidation (Gupta & Suhas 2009). In membrane processes, the high cost of the membrane and other membrane equipment is a major constraint. There is a decrease in productivity with time due to the deposition of precipitated dyestuff, i.e. fouling. Another problem faced is the disposal of concentrates from the membrane processes (Joshi et al. 2004). Thus, it could be well noticed that all the above mentioned physical and chemical treatment methods face the problem of disposal of sludge and concentrates after the treatment of wastewater.

1.3.1 Low-Cost Adsorbents as an Alternative to Treat Textile Wastewater

Among all the treatment techniques discussed above, adsorption is the most popular since it is a very simple technique due to its convenience, ease of operation, and versatility. This process can minimize or remove different types of pollutants and is thus having a broad range of applications in wastewater treatment (Robinson et al. 2001).

Most commercial systems currently use activated carbon as an adsorbent to remove dyes in wastewater because of its excellent adsorption capacity. Though it is a preferred adsorbent; its widespread use is restricted due to high cost. To decrease the cost of treatment, attempts have been made to find inexpensive alternative adsorbents (Crini & Ndongo Peindy 2006).

Since cost is an important parameter in most developing countries, efforts have been made to explore the possibility of using various low-cost adsorbents. A low-cost adsorbent (LCA) can be defined as any natural material or the waste/by-product of industries or synthetically prepared material, which is cost effective and can be used as such or after some minor treatment and also can be disposed off easily (Gupta & Suhas 2009) (Sanghi & Bhattacharya 2002).

A number of low-cost adsorbents have been reported like fly ash (Al-Degs et al. 2000), bagasse fly ash (Mall et al. 2006), clay (Gürses et al. 2006), montmorillonite (Almeida et al. 2009), kaolinite (Ghosh & Bhattacharyya 2002), bentonite (Bulut et al. 2008), fuller's earth (Atun et al. 2003), diatomite (Khraisheh et al. 2005), siliceous materials like zeolite (Wang & Zhu 2006), perlite (Vijayakumar et al. 2009) , sepiolite (Doğan et al. 2007), alunite (Özacar & Şengil 2003), agricultural wastes like rice husk (Shih & Husk 2012) , saw dust (Garg et al. 2003), etc.

1.4 Need for the Present Study

The reason which made the research on low-cost adsorbents popular is their cost. However, when it comes to using them at commercial scale, low-cost adsorbent should be easily, locally and abundantly available.

Most of the available literature is on batch scale studies for the treatment of single dyes. Also, these studies have focused mainly on colour removal. However, in the real world textile sector, the final effluent is always a mixture of different dyes. COD in the effluent is also a parameter of concern in addition to colour. Thus, the efficiency of low-cost adsorbents for the treatment of these parameters should be analysed. For adsorbents to be used at commercial scale, fixed bed studies should be conducted on the basis of the results obtained from the batch studies. But, the low particle size of reported adsorbents like clay causes choking of bed, though they may provide good treatment at batch scale.

Adsorptive capacity of an adsorbent depends on its surface morphology, the role of functional groups and chemical composition. Many studies have reported these factors, but detailed critical investigation and adsorption process analysis is still lacking.

Colour removal is influenced by the dye-adsorbent interactions. Specificity of the adsorbent for a particular class of dye limits its use for commercial purpose. Although modification of adsorbents has been studied to address this constraint in the treatment of textile wastewater containing a mixture of different dyes but the understanding of the topic still requires detailed investigation and research.

Many low-costs and some modified adsorbents have been studied previously, but almost all the studies are lab scale, with single dye treatment and focuses mainly on colour removal. There exists a need to enlarge the scope of research to fixed bed

studies to include simulated/actual textile wastewater. Therefore, there is a requirement of low-cost adsorbent which addresses the above issues.

1.5 Aim & Objectives of the Study

The overall aim of the present research was to find out a low-cost solution for textile wastewater treatment. Thus, for the accomplishment of this aim, efforts were made to use the locally available soil from Rajasthan as a low-cost adsorbent, which would help in the treatment of wastewater generated from the textile industries in Rajasthan. However, initially the basic goal was to assess the feasibility and potential of locally available soil for colour removal. Following this goal, four objectives were identified for the present study.

1. To study the effect of various operating parameters to identify the set of optimum parameters for colour removal on the soil.
2. To modify soil by acid/alkali, based on optimum parameters as identified from objective 1 and analyse surface characteristics of soil after modification.
3. To assess the potential of modified soil by acid/alkali vis-a-vis colour removal.
4. To conduct fixed bed study to evaluate design parameters of using modified soil by acid/alkali, as an adsorbent.

1.6 Scope of the Study

The scope of the study was limited to laboratory scale development of adsorption process for the treatment of textile industry wastewater. Management and disposal of saturated adsorbent are beyond the scope of the present research.

Within the scope of the study, following points were covered to fulfil the purpose of research:

- Feasibility study of non-modified soil for adsorption of two different classes of dyes based on various operational parameters.
- Kinetic modelling and equilibrium study to understand the mechanism of adsorption on the non-modified soil.
- Modification of the non-modified soil based on the optimum parameters for both the dyes.

- Parametric study on modified soil to compare its adsorption capacity with non-modified soils.
- Kinetic modelling and equilibrium study to understand the mechanism of adsorption on the modified soils.
- Characterization of the surface properties of the non-modified and modified soils.
- Fixed bed study for simulated and actual textile wastewater for color and COD removal.
- Evaluation of the design parameters obtained from the fixed bed study for various bed heights and flow rates.

1.7 Novelty of the Study

In the present study, the adsorption capacity of the locally available soil from Rajasthan has been tested for the removal of two different classes of dyes – anionic and cationic. Since, Rajasthan is a desert area (Roy et al. 1978), therefore the availability of soil is enormous and easy. This is the main advantage of using locally available adsorbent, and also this makes it low-cost adsorbent. The soil has been modified to improve its efficiency for dye removal. Modification of the soil was done by two methods: acid modification and alkali modification. Serious efforts have been made to explore the adsorption property of soil used in this research work for colour and chemical oxygen demand removal in the fixed bed study.

1.8 Outline of the Work

The present work can be broadly classified into two parts: batch study and fixed bed study. Figure 1.3 gives the outline of the work.

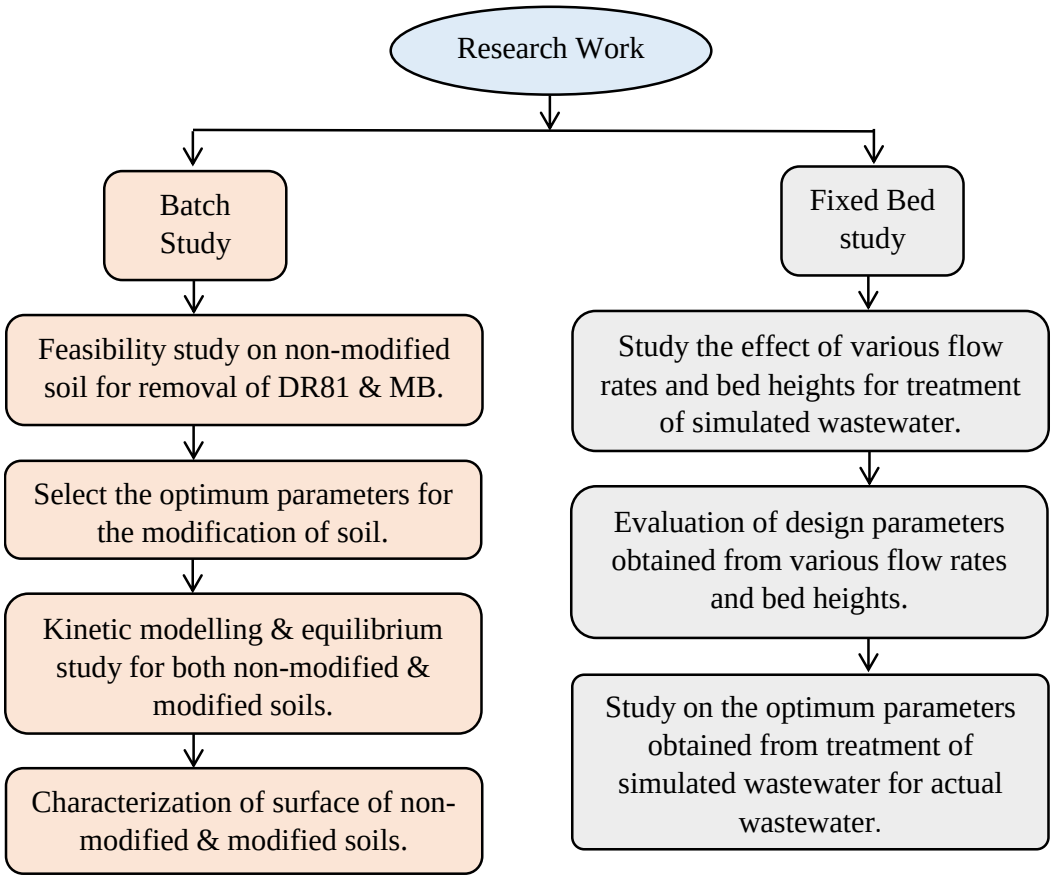

Figure 1.2: Outline of the work

Batch study: To begin with the research, the feasibility of the non-modified soil to remove dye from aqueous solution was tested for two dyes i.e. anionic Direct Red 81 and cationic Methylene Blue. The effect of operational parameters like pH, contact time, adsorbent dose, initial dye concentration and particle size were investigated for dye adsorption. These findings helped in modifying the adsorbent characteristics according to optimized operational parameters. Kinetic modelling and equilibrium studies were conducted on the data obtained from the parametric study for non-modified and modified soils. This helps to understand the mechanism of adsorption of dyes. Surface characterization of non-modified and modified soils was conducted.

Fixed bed study: To check the competence of the adsorbent, fixed bed study was conducted for simulated and actual textile wastewater. Three different bed heights and flow rates were used to understand the breakthrough curve. Three models were used to evaluate the design parameters obtained from fixed bed study was done.

1.9 Structure of the Thesis

Chapter 1: Introduces the present research. It presents a general introduction, the environmental impacts due to dyes and the need for research. It finally outlines the tasks performed in the present research.

Chapter 2: Includes a literature review designed to provide a summary of the base knowledge already available involving the issues.

Chapter 3: Describes the materials and methods used in the present study along with the different theoretical considerations and experimental protocols employed to meet the objectives. Various instrumental techniques employed have also been discussed.

Chapter 4: Marks the beginning of results & discussion of the present study. It discusses various parametric study for the adsorption of dyes onto non-modified, which forms baseline data for further research.

Chapter 5: Presents detailed study on the adsorption of Direct Red 81 dye onto the acid-modified soil.

Chapter 6: Presents detailed study on the adsorption of Methylene Blue dye onto the alkali-modified soil.

Chapter 7: Includes detailed theoretical and mathematical analysis of data and discussion on fixed bed studies.

Chapter 8: Discusses conclusions drawn from investigations done in above chapters. Scope for future work has also been discussed in the end.

Lastly, a list of references is given towards the end of the report.

1.10 Summary

Untreated effluent discharges from textile industries pose several environmental concerns. Various treatment technologies are available, however for present study low-cost treatment for textile wastewater was chosen. A number of low-cost adsorbents have been reported. But, the present study focuses on finding a low-cost adsorbent which addresses research gaps present in the literature available on low-cost adsorbents.

This Chapter enlists research objectives and delineates the research work carried out in this thesis. The next Chapter discusses the available literature on low-cost adsorbents in detail.

CHAPTER 2

Chapter 2

Adsorption of Dyes and Low-Cost Adsorbents: A Literature Review

The chapter begins with the classification of various types of dyes used in the textile industry. An overview of various treatment techniques available for the removal of dyes in the textile wastewater is also covered. Several investigations that have been carried out in the recent past for adsorption of dyes onto various low-cost adsorbents have been reported.

2.1 Introduction

To address the research problem, this literature review provides detailed information and discussion about dyes, current treatment technologies and low-cost adsorbents. It also provides insight into various parameters affecting adsorption of dyes. Adsorption capacity and other parameters for dye removal have also been summarised.

2.2 Dyes: Structure and Classification

A dye is a molecule which imparts colour to the material by becoming an integral part of it (Verma et al. 2012). The colour imparting molecule of dye is chromophore. It is an aromatic structure which absorbs visible light and anchors the dye into or within the fibers. There are about 12 classes of chromophoric groups (Vandevivere et al. 1998), some of which are: -C=C- (ethenyl), -C=O (carbonyl), -C=N-(imino), -CH=S (thiocarbonyl), -N=N- (azo), -N=O (nitroso), $-NO_2$ (nitro) (Verma et al. 2012). The azo chromophore makes up to 60-70% of all textile dyes produced (Vandevivere et al. 1998). To be a dye, a compound must contain not only a chromophore, but also the additional group(s) called auxochrome(s). These groups are the electron withdrawing or donating substitutes which have the potential to intensify the colour of chromagen. Some of the auxochromes are $-NH_2$ (amino), -COOH (carboxylic), $-SO_3H$ (sulphonyl) and -OH (hydroxyl) (Verma et al. 2012). Figure 2.1 illustrates the structure of various dyes.

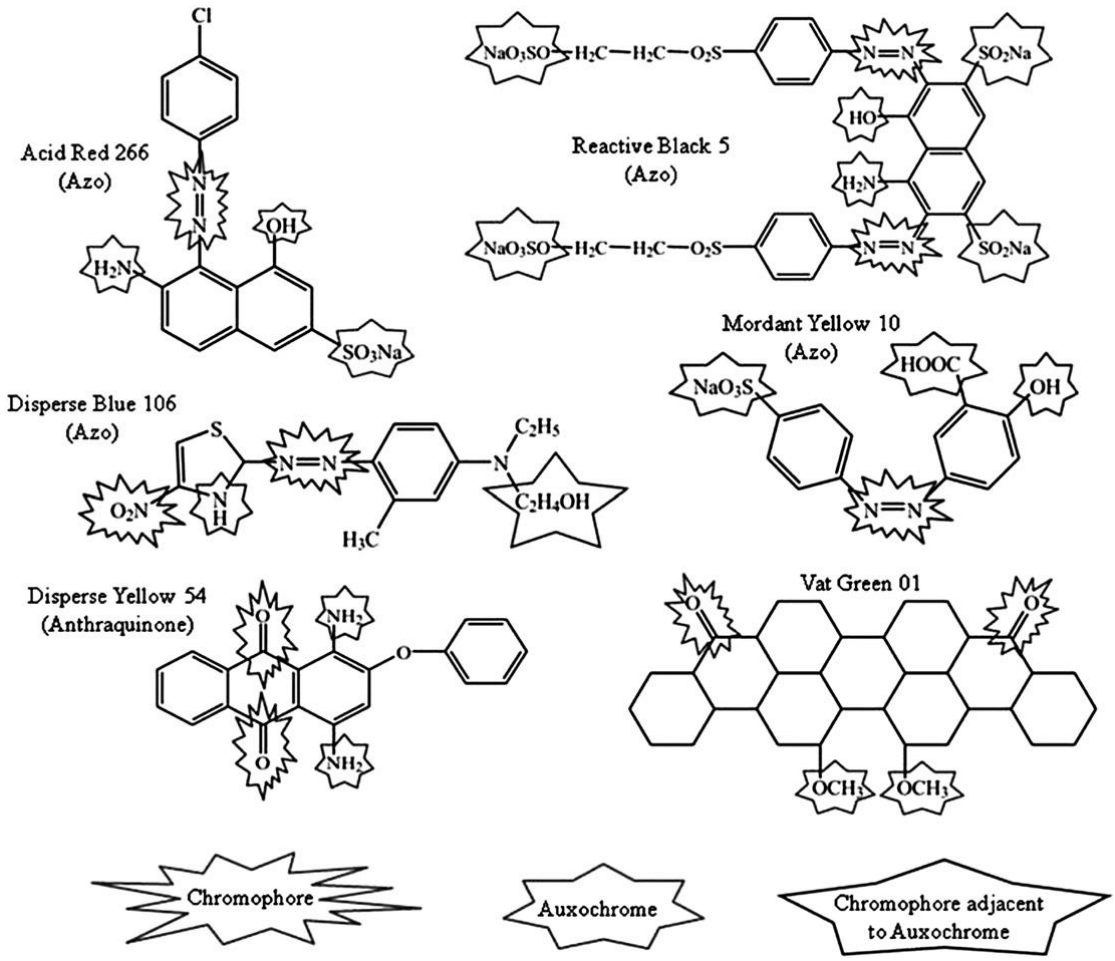

Figure 2.1: Structure of dyes (Verma et al. 2012)

Under broad classification, textile dyes can be categorised as anionic, cationic and non-ionic dyes. Of which, direct, acid and reactive dyes are of anionic type of dyes while all basic dyes and disperse dyes belongs to cationic and non-ionic dyes category (Joshi et al. 2004). Table 2.1 illustrates the classification of dyes.

2.2.1 Cationic dyes: This group of dyes is considered as toxic colorants and can cause harmful effects such as allergic dermatitis, skin irritation, mutations and cancer. These dyes are also called basic dyes and depend on a positive ion, which are generally hydrochloride or zinc chloride complexes. Cationic dyes carry a positive charge in their molecule. Furthermore it is water soluble and yield colored cations in solution. Cationic functionality is found in various types of dyes, mainly in cationic azo dyes and methane dyes, also in anthraquinone, di- and tri-arylcarbenium, phthalocyanine dyes, various polycarbocyclic and solvent dyes. The anthraquinone dyes are expensive and weak while the azo dyes have good properties, strong thus reducing cost. Basic dyes are highly visible and have high brilliance and intensity of colors. Cationic dyes

were used intensely as a model in dye adsorption studies such as Crystal Violet, Methylene Blue, Basic Blue 41 and Basic Red 46 (Salleh et al. 2011) (El Qada et al. 2008).

2.2.2 Anionic Dyes: Anionic dyes depend on a negative ion. Anionic dyes include many compounds from the most varied classes of dyes, which exhibit characteristic differences in structure (e.g., azoic, anthraquinone, triphenylmethan and nitro dyes) but possess as a common feature, water-solubilizing, ionic substituents. The anionic dyes also include direct dyes, and from the chemical standpoint, the group of anionic azo dyes includes a large proportion of the reactive dyes (Salleh et al. 2011).

2.3 Dye Removal Techniques

Various dye removal techniques with their benefits and limitations are given in Table 2.2. Despite the development of various technologies for dye waste water treatment, economic effectiveness and rapid water treatment at a commercial level is still a challenging problem. However, previous research efforts have revealed that adsorption technology for the dye remediation from wastewater can handle fairly large flow rates, producing a high quality effluent that does not result in the formation of harmful substances. Moreover, it can remove or minimize different types of organic pollutants and thus has a wider applicability in pollution control (Mohammed et al. 2014). Thus, adsorption is recognized as the most versatile process used in lesser developing countries. In the next sections, adsorption technique and low-cost adsorbents for dye removal are discussed in detail.

Table 2.1: Classification of dyes (Verma et al. 2012)(Gupta & Suhas 2009)(O'Neill et al. 1999)

Dye	Characteristics	Substrate	Chemical class	Loss to effluent	Method of Application
Acid	Water soluble, anionic	Nylon, wool, silk, acrylics	Azo, anthraquinone, triphenylmethane, azine, xanthene, nitro and nitorso	5-20%	Usually from neutral to acidic dyebaths
Basic	Water soluble, cationic	Silk, wool, cotton, nylon, polyester	Diazahemicyanine, triarylmethane, cyanine, hemicyanine, thiazine, oxazine and acridine	0-5%	Applied from acidic dyebaths
Disperse	Water-insoluble, non-ionic	Polyester, nylon, cellulose acetate, acrylic fibres	Azo, anthraquinone, styryl, nitro and benzodifuranone	0-10%	Fine aqueous dispersions often applied by high temperature pressure or lower temperature carrier methods
Direct	Water soluble, anionic	Cotton, rayon, nylon	Polyazo, stilbenes, phthalocyanines and oxazines	5-30%	Applied from neutral or slightly alkaline baths containing additional electrolytes
Reactive	Water soluble, anionic	Cotton, cellulosics, wool, nylon	Azo, anthraquinone, triarylmethane, phthalocyanine, formazin, oxazine	10-50%	Reactive site on dye reacts with functional group on fibre to bind dye covalently under the influence of heat and pH(alkaline)

Sulphur	Water insoluble, Colloidal	Cotton, rayon, silk, polyamide	Intermediate structures	10-40%	Aromatic substrate vatted with sodium sulfide and re-oxidised to insoluble sulfur-containing products on fibre
Vat	Water insoluble, Colloidal	Cotton, rayon, wool	Anthraquinone, indigoids	5-20%	Water insoluble dyes solubilised by reducing with sodium hydrosulfite, then exhausted on fibre and re-oxidised

Table 2.2: Some dye removal techniques (Anjaneyulu et al. 2005)(Verma et al. 2012)(Robinson et al. 2001)(Vandevivere et al. 1998)

Treatment Methodology	**Method Description**	**Stage of treatment**	**Benefits**	**Limitations**
Ozonation	Oxidation using ozone gas	Post/ main treatment	Useful in water soluble dye removal, applied in gaseous state, therefore, no alteration in volume	Short half-life (20 min), high cost, little contribution to COD removal
Fenton's Reagent	Oxidation using H_2O_2-Fe(II)	Pre treatment	Useful in both water soluble and insoluble dye removal	Sludge generation, requires acidic pH
Photochemical oxidation	Oxidation using mainly H_2O_2-UV	Pre/ post treatment	No sludge production, efficiently decolorizes all types of dyes, significantly removes TOC	Formation of byproducts, high cost of UV irradiation
Sonolysis	Destruction of chemical bond by producing free radical using ultrasound	Pre treatment	No sludge production, simple to use, effective in integrated systems	Requires a lot of dissolved oxygen, high cost, awaiting full-scale application
Adsorption	Dye removal based on a solid support	Pre / post treatment	Excellent removal of wide variety of dyes	Regeneration difficulties, costly disposal of adsorbent
Membrane filtration	Physical separation	Post / main treatment	Removes all types of dyes, recovery and reuse of chemical and water	Production of sludge, high cost

Ion-exchange	Ion exchange resin	Main treatment	Easy regeneration with negligible loss of adsorbents	Not effective for all dyes
Electro-coagulation	Treatment based on anode and cathode	Main treatment	Efficiently removes reactive, disperse and acid dyes, no additional chemicals are required, cheaper than chemical coagulation	High cost, low electrode reliability, lower COD removal performance than chemical coagulation
Irradiation	Treatment based on ionizing radiation	Post treatment	Effective removal for a wide range of dyes at low volumes	High dissolved oxygen requirement, ineffective for light resistant dyes
Biological process	Treatment based on microbiological degradation	Main treatment	Colour removal is facilitated along with COD removal, biogas produced during anaerobic treatment is used for steam generation	High maintenance cost, large area requirement, slow process, narrow operating temperature range, microbes less resistant to recalcitrant
Chemical coagulation/flocculation	Addition of coagulants and flocculants	Pre/ post/ main treatment	Short detention time and low capital costs, good removal efficiencies	High cost of chemicals for pH adjustment, dewatering and sludge handling problems.

2.4 Adsorption of Dyes

"Adsorption of dyes can be described as a rapid phenomenon of passive sequestration separation of dyes from an aqueous phase onto a solid phase." This process occurs between two phases in transporting dye from one phase to another. The transfer of dye onto adsorbent is considered to be a complex phenomenon and depends mostly on the surface chemistry or nature of the adsorbent, nature of dye and the system conditions in between the two phases (Sanghi & Bhattacharya 2002). To be specific, adsorption processes usually occur in interfacial layers which are regarded as two regions: the surface layer of the adsorbent and the adsorption space, in which the enrichment of the adsorptive can occur (El Qada et al. 2008).

Depending on the type of forces involved, adsorption processes can be classified as physical or chemical. Physical adsorption occurs when weak interparticle bonds exist between dye and adsorbent. Examples of such bonds are van der Waals, hydrogen and dipole-dipole. In the majority of cases, physical adsorption is easily reversible. Chemical adsorption occurs when strong interparticle bonds are present between dye and adsorbent due to an exchange of electrons. Examples of such bonds are covalent and ionic bonds. Chemisorption is regarded as irreversible in the majority cases (Koumanova & Allen 2005).

2.4.1 Factors affecting adsorption of dye

Adsorption phenomena are dependent on experimental conditions like pH, adsorbent dose, initial dye concentration, nature of the adsorbent and type and structure of the dye.

- *pH*: The pH value of the dye solution plays a significant role in the whole adsorption process and particularly on the adsorption capacity. Any functional group present on the adsorbent surface creates a charge (positive or negative) on its surface. This charge is proportional to the pH of the solution which surrounds the functional group on the adsorbent. A convenient index of the susceptibility of a surface to become either positively or negatively charged as a function of pH is the value of the pH required to give zero net surface charge. This value is called point of zero charge (pH_{ZPC}) or isoelectric point (pH_{IEP}). pH_{ZPC} or pH_{IEP} is a critical value for determining quantitatively the net charge carried on the

adsorbent surface during adsorption of dyes (Koumanova & Allen 2005). Due to the presence of functional group such as OH^- group, cationic dye adsorption is favoured at pH > pHpzc, whereas, anionic dye adsorption is favoured at pH > pHpzc where the surface becomes positively charged (Yagub et al. 2014).

- *Adsorbent dose*: Adsorbent dosage is an important parameter to determine the adsorption capacity of an adsorbent for a given amount of the adsorbent at the operating conditions. Generally, the percentage of dye removal increases with increasing adsorbent dosage, where the quantity of adsorption sites on the surface of adsorbent will increase by increasing the amount of the adsorbent. The effect of adsorbent dosage gives an idea for the ability of a dye adsorption to be adsorbed with the smallest amount of adsorbent, so as to recognise the capability of dye from an economical point of view (Salleh et al. 2011).
- *Initial dye concentration*: The amount of adsorption for dye removal is highly dependent on the initial dye concentration. The effect of initial dye concentration depends on the immediate relation between the concentration of the dye and the available sites on an adsorbent surface. In general, the percentage of dye removal decreases with an increase in the initial dye concentration, which may be due to the saturation of adsorption sites on the adsorbent surface. On the other hand, the increase in initial dye concentration will cause an increase in the capacity of the adsorbent, and this may be due to the high driving force for mass transfer at a high initial dye concentration (Yagub et al. 2014).
- *Nature of the adsorbent*: The extent of the adsorption depends on the textural properties of the adsorbent especially porosity and surface area. The pore size distribution determines the fraction of the adsorbent structure that can be accessed by the dye molecule of given size and shape. Therefore, a good adsorbent has high porosity ad larger surface area with more specific adsorption sites. High porosity not only increases the surface area but also the kinetics of the adsorption (Bello, Bello, et al. 2013; Bhatnagar & Minocha 2006).

2.5 Adsorbent Materials

2.5.1 Activated Carbon

Adsorption on activated carbon is a widely used technique for several pilot plant and commercial-scale systems (Joshi et al. 2004). Carbonaceous material – coal is used

for the production of activated carbon for its easy availability and cheapness. Coal based adsorbents have been efficiently used for dye removal. However, coal is not a pure material, so it has a variety of surface properties which results in different adsorption properties (Gürses et al. 2004). In particular, the adsorption capacity of carbons depends upon the sources of raw material used, the history of its preparation and treatment conditions such as pyrolysis temperature and activation time (Crini 2006) (Rafatullah et al. 2010). The high surface area and the micro porous structure also enhance the adsorption capacity of activated carbon (Iqbal & Ashiq 2007). Besides this, surface chemistry (heteroatom content) and surface charge also strongly influence the adsorption potential of carbon (Crini 2006)(Rafatullah et al. 2010).

It is well known that activated carbon is most effective with volatile organic compounds (VOC) which can be readily and effectively adsorbed and desorbed from the activated carbon (Cooper 1995). However, the adsorption of dyes onto the carbon is significantly affected by the solubility and polarity of the dye molecule. According to (Joshi et al. 2004), adsorption of insoluble dyes like disperse dyes, vat dyes, and pigments onto the carbon is exorbitantly slow at room temperature. Even, the water soluble dyes like acid, basic, direct, mordant and reactive dyes are also not readily adsorbed on carbon. The possible reason for the poor adsorption is the polar nature of these dyes versus the non-polar nature of the carbon. Also, factors such as choice of activated carbon, temperature, pH, contact time and dosage may greatly enhance the removal of dyes from wastewater.

Commercially, activated carbon is available in two forms: Powdered activated carbon (PAC) and Granular activated carbon (GAC). Both the ACs has a huge network of pores, and the internal surface area might range from 500 to 1500 m^2/g (Sanghi & Bhattacharya 2002). Out of these two forms of activated carbon, GAC has been widely researched, because it is more adaptable to continuous contacting, and there is no need to separate the carbon from the bulk fluid. The problem with PAC is that it has to be separated from the fluid after use. In spite of these challenges PAC is also used for wastewater treatment due to low capital cost and lesser contact time requirement as compared to GAC (Gupta & Suhas 2009).

Several studies have been conducted for the adsorption capacities of the activated carbon vis-à-vis colour removal. Granular Activated Carbon (GAC) Filtrasorb 400 has

been extensively studied. (Walker & Weatherley 2000) and (Walker & Weatherley 2001) used it for treating a ternary solution of acid, simulated and real effluent from nylon printing plant in a fixed bed column. (Al-Degs et al. 2000) studied the adsorption of three reactive dyes namely; Remazol Reactive Yellow, Remazol Reactive Black and Remazol Reactive Red and reported that Filtrasorb 400 provides the high adsorption of these dyes. (Maurya et al. 2008) reported the adsorption potential of an another commercial activated carbon FS300 for the uptake of cationic dyes, namely, Methylene Blue and Rhodamine B. (Iqbal & Ashiq 2007) examined the adsorption capacities of several dyes, namely, Bromophenol Blue, Alizarine Red-S, methyl blue, Methylene Blue, Eriochrome Black-T, Malachite Green, phenol and Methyl Violet from aqueous media on activated charcoal. Their observation indicated that adsorption of dyes was favoured at low temperature and that the dyes are chemisorbed on activated charcoal. In an another study by (Sauer et al.), the adsorption capacity of an adsorbent carbon with high iron oxide concentration was compared with that of a commercial activated carbon in the removal of dye used in tannery from an aqueous solution. Activated carbon showed a better adsorption capacity than the adsorbent carbon due to its higher surface area.

Although activated carbon has been proved as an excellent adsorbent, but the major consideration is its high price. Nonetheless, this is not the only restriction for its massive employment. Regeneration by desorption is also a difficult task which results in the loss of carbon and it further adds to the cost. Furthermore, the regenerated product may have a lower adsorption capacity in comparison with the virgin activated carbon. Thus, when this technique is used for full-scale plants, the pay-back becomes poor (Cooper 1995) (Gupta & Suhas 2009).

2.5.2 Low-cost Adsorbents

According to (Bailey et al. 1999), any by-product or waste material present in an abundant quantity from another industry and which requires additional disposal cost can be considered as a low-cost adsorbent (LCA) after little processing (Crini 2006) (Rafatullah et al. 2010). LCAs can be classified on the basis of their availability (i.e. source) and nature (i.e. organic or inorganic) (Gupta & Suhas 2009).

The reason that activated carbon has always been the first choice as an adsorbent for dye removal from wastewater is that of its high surface area and porous texture.

However, (Gou et al. 2003) showed that the adsorption does not always increase with surface area. Besides the physical structure, the adsorption capacity of a given carbon is strongly influenced by the chemical nature of the surface. The acid and base character of a carbon influences the nature of the dye isotherms. The adsorption is a complicated process depending on several interactions such as electrostatic and non-electrostatic interactions. Thus, attention has now been shifted from commercially available activated carbon towards adsorbents that can remove pollutants from contaminated water and are cost effective too.

2.5.2.1 Agro-Based Adsorbents

Several types of agro-based adsorbents have been utilized to remove dyes from wastewater. A large amount of work has been reported on bagasse pith. Bagasse pith is the term used for the by-product/waste obtained when sucrose content from the sugarcane has been removed. The major composition of bagasse pith is α-cellulose (53.7%), pentosan (27.9%), lignin (20.9%), alcohol (7.5%) and ash (6.6%) (McKay 1998). Various other agricultural wastes have also been reported like maize cob (El-Geundi 1991), corn cob (Kavitha & Senthamilselvi 2015), banana and orange peels (Annadurai et al. 2002), pomelo (*Citrus grandis*) peel (Hameed et al. 2008b), spent tea leaves (Hameed 2009).

Sawdust is one of the most appealing materials among agricultural waste materials, used for removing pollutants, such as dyes, salts and heavy metals from water and wastewater. It is a by-product of the timber industry. The material consists of lignin, cellulose and hemicellulose, with polyphenolic groups playing an important role for binding dyes through different mechanisms. Adsorption takes place by complexation, ion exchange and hydrogen bonding (Gupta & Suhas 2009), (Garg et al. 2003). (Journal & Engineering 2013) examined removal of Methylene Blue using sawdust. A quality work has been done by (Khattri & Singh 2009) using Neem sawdust (*Azadirachta indica*) for the removal of Methylene Blue from aqueous solutions. The authors found that removal capacity of neem sawdust is appreciably high for basic dyes. And, because it is abundantly available and inexpensive too, it can be easily used for basic dye treatment. (Laasri et al. 2007) used fir and beech sawdust for the removal of Basic Red 46 and Basic Yellow 28.

Agro-residues like wheat bran, rice husk and barley husk have also been used as the source of adsorbent for the dyes. Rice husk is a by-product of the rice milling industry and accounts for about 20% of rice as a whole. The characteristics of rice husk such as granular structure, insolubility in water, chemical stability, high mechanical strength and local availability at almost no cost make it ideal adsorbent for dyes. Modified and unmodified rice husk was used for the adsorption of Methylene Blue and it was found that unmodified rice husk gave 98% of dye removal whereas it was 67% for nitric acid treated rice husk, 59% for hydrochloric acid treated rice husk and 55% for sulfuric acid treated rice husk (Shih & Husk 2012). When rice husk is burnt in the boilers of various industries to produce steam, a waste by-product called rice husk ash is produced. The authors used this ash to remove Brilliant Green from aqueous solution (Mane et al. 2007). (Sulak & Yatmaz 2012) used wheat bran for the removal of Remazol Red F3B (Reactive Red 180) from aqueous solution. The adsorption behaviour of Methylene Blue was studied on unmodified wheat straw and modified wheat straw(carboxylated) in fixed bed column, and it was found that Methylene Blue uptake for unmodified straw was only 23.1mgg^{-1} which was merely 10% of that of modified straw (Zhang et al. 2011). Barley is widely distributed in a large geographic region-ranging west from Turkey, Syria, and Egypt, eastward to Pakistan, India, and into western China. (Haq et al. 2011) utilized barley husk to remove Solar Red BA.

Other non-conventional adsorbents used are palm ash (Ahmad et al. 2007), eucalyptus bark (Morais et al. 1999), sea shell powder (Chowdhury & Saha 2010), hazelnut shells (Fathi et al. 2011), roots of water hyacinth (Soni et al. 2012), etc.

Various researchers prepared activated carbon from agro-based materials. They also compared the adsorption capacity and cost effectiveness of these low-cost activated carbons with the commercially available activated carbon. In many of the cases, the prepared low-cost activated carbon gave promising results. Activated carbons from agro-based materials could be prepared by either physical (thermal) activation or chemical activation. Thermal activation involves carbonisation or calcination of the raw materials at elevated temperatures (500-900°C) in an inert atmosphere followed by mild oxidation (gasification) of the substance with steam, air and/or carbon dioxide at high temperatures (800-1000°C). Simultaneous carbonisation and activation can also be obtained chemically by impregnation with dehydrating agents such as phosphoric acid and zinc chloride (Banat et al. 2003).

The coconut shells are waste material and can be obtained at negligible cost. The activated carbon obtained from coconut shells is strong, dense and even resistant to mechanical abrasion (Sanghi & Bhattacharya 2002). Methylene Blue and Methyl Orange removal from wastewater were successfully achieved with the coconut shell activated carbon with the adsorption capacity of 5.24 x 10^{-5} mol/g and 2.88 x 10^{-5} mol/g respectively for the two dyes (Singh et al. 2003). In another study, (Ahmad & Hameed 2009) treated real textile wastewater from a cotton industry using activated carbon from bamboo. Under the conditions of pH = 3, adsorbent dose= 0.30 g/100mL solution and time = 10 hr, the prepared activated carbon reduced color and COD to 91.84% and 75.21%, respectively. Saw dust is also used to prepare activated carbon amongst other materials. (Garg et al. 2003) compared adsorption capacity of saw dust of *Dalbergia sissoo* (Indian Rosewood) tree with commercially available activated carbon. The authors prepared two types of activated carbon by treating the sawdust with sulphuric acid and formaldehyde. The adsorption efficiency of sulphuric acid treated saw dust was higher than formaldehyde treated saw dust for the treatment of Malachite Green. Although, both of them had lower adsorption efficiency than commercially available activated carbon at higher dye concentration. (Gupta et al. 2007) demonstrated the removal of Vertigo Blue 49 and Orange DNA13 from synthetic textile wastewater onto activated carbon slurry. This waste material is obtained as a result of partial in-combustion of fuel with a high cost for disposal from fuel oil-based generators. Dye adsorption capacities of activated carbon slurry for the two dyes were 11.57 & 4.57 mgg^{-1} of adsorbent respectively at pH 7. (Attia et al. 2008) prepared activated carbons derived from peach stone shells for the removal of Methylene Blue from aqueous solutions. Table 2.3 shows adsorption capacities and another parameter for removal of dyes using agro-based adsorbents.

From the author's viewpoint, the limitation of using agro-based adsorbents like orange peel (Khaled et al. 2009), coconut waste (Hameed et al. 2008a), wheat bran (Sulak & Yatmaz 2012) and many others also, is that their use for commercial scale would be restricted because of limited availability.

Table 2.3: Adsorption capacities and other parameters for removal of dyes using agro-based adsorbents.

Adsorbent	Dye	Modification	pH	Isotherm	Removal	Reference
Date pits	Methylene Blue	Carbonisation & activation by CO_2 flush followed by washing 0.1M H_2SO_4	8	Langmuir	12.94 mgg^{-1} (activation at 500°C) 17.9494 mgg^{-1} (activation at 700°C)	(Banat et al. 2003)
Orange peel	Direct Yellow 12	Activation with 98% H_2SO_4	1.5	Dubinin-Radushkevich	75.76 mgg^{-1}	(Khaled et al. 2009)
Date pits	MB	-	8	Langmuir	80.29 mgg^{-1}	(Banat et al. 2003)
Palm ash	Direct blue 71	-	-	Freundlich	400.01 mgg^{-1}	(Ahmad et al. 2007)
Almond shell	Direct Red 80	-	6	Internal: BET External: Freundlich Mixture: Langmuir	16.4 mgg^{-1} 16.96 mgg^{-1} 20.5 mgg^{-1}	(Doulati Ardejani et al. 2008)
Eucalyptus Bark	Remazol BB	-	2.5	-	90 mgg^{-1}	(Morais et al. 1999)

Orange peel	Direct Red 23 Direct Red 80	-	2	Langmuir	10.72 mgg^{-1} 21.05 mgg^{-1}	(Arami et al. 2005)
Spent Tea Leaves	Methylene Blue	-		Langmuir	300.052 mgg^{-1}	(Hameed 2009)
Hazelnut Shells	Direct Red 12B	-	2.5	Langmuir & Tempkin	99.8%	(Fathi et al. 2011)
Bamboo	Methylene Blue	Activation with KOH and CO_2 at 850°C for 2 hrs	-	Langmuir	454.2 mgg^{-1}	(Hameed et al. 2007)
Yellow passion fruit peel	Methylene Blue	-	9	-	0.0068 $mmolg^{-1}$	(Pavan et al. 2008)
Jute Fibre	Methylene Blue	Carbonized with 15% phosphoric acid for 12hrs	5-10	Langmuir	225.64mgg^{1}	(Senthilkumaar et al. 2005)

2.5.2.2 Industrial Wastes

The industrial waste materials are available almost free of cost and cause major disposal problem. If they could be used as adsorbents, it would not only reduce the volume of waste material but also help in wastewater treatment at a reasonable cost. Some of the industrial wastes are discussed in this section. Red mud is an unwanted by-product produced during the production of alumina from bauxite. The authors activated this red mud with hydrochloric acid for the removal of Congo red from aqueous solution (Tor & Cengeloglu 2006).

Another industrial waste is fly ash. Fly ash is a waste material generated from the combustion of coal at the power plants. It is mostly used in the cement industry because of its cementation property or otherwise, for the disposal at landfills. According to ASTM standards, fly ash can be classified as Type F when the sum of SiO_2, Al_2O_3 and Fe_2O_3 is 70% but if the sum is upto 50% then it is classified as Type C. The good adsorption property of fly ash helps in removal of organics and dye colour from the textile waste water. Due to its availability at negligible or no cost as compared to activated carbon by (Bello et al. 2013), it can be effectively used for dye removal from wastewater and industrial effluents. The presence of species like SiO_2, lime and metal oxide in fly ash gives anionic charge to it. On reaction with water, pH of fly ash reaches somewhere between 10-12 and it shows great affinity for the cationic charge (Pansuk 2011). This negative charge helps in the removal of basic dyes like Methylene Blue, Malachite Green and Rhodamine B as shown by (Khan et al. 2009). (Pansuk 2011) prepared unmodified fly ash and cationic surfactant modified granule (Mo-G) for the removal of two anionic dyes; Acid Brown 75 and Direct Yellow 162 from aqueous solution. The surfactant used was Hexadecyltrimetylammonium Bromide (HDTMA-Br) and it increased the dye adsorption ability of fly ash. However, according to (Hsu 2008) raw coal fly ash (CFA) had superior adsorbing ability for the anionic dye Acid Red 1 than did two modified coal fly ashes (CFA-600 and CFA-NaOH). The adsorption capacities were directly proportional to temperature and followed the order CFA > CFA-600 > CFA-NaOH as 92.59–103.09, 32.79–52.63, and 12.66–25.12 mgg^{-1}, respectively. In this study authors found that changing the nature of the raw coal fly ash through heating or modification with NaOH solution did not improve its ability to adsorb Acid Red 1. To increase the adsorption efficiency, mixtures of fly ash with other low-cost absorbents

were also studied. (Albanis et al. 2000) studied adsorption and removal of various commercial dyes namely, Acid Orange 7, Acid Yellow 23, Disperse Blue 79, Basic Yellow 28 and Direct Yellow 28 in aqueous suspensions of fly ash mixtures with a sandy clay loam soil of low organic matter content. While, (Moghaddam et al. 2010) compared three types of adsorbent; fly ash, clay and pretreated walnut shells for the removal Methylene Blue. The maximum adsorption capacity of clay, fly ash and walnut shell was found to be 7.14, 7.87 and 5.78mgg^{-1}, respectively.

The major issue in using fly ash for treatment purpose is that it has a fine particle size which causes inconvenience during filtration and settling (Pansuk 2011). To overcome this problem, (Nidheesh et al. 2012) and (Gandhimathi et al. 2012) used bottom ash for the removal of basic dyes namely; Methylene Blue, Malachite Green and crystal violet. Bottom ash is also a by-product of power plants like fly ash, but it is coarse, granular and incombustible.

2.5.2.3 Zeolite and Other Siliceous Materials

Zeolite is hydrated aluminosilicate mineral with a micro porous structure (Halimoon & Yin 2010). It has a three-dimensional crystal structure in which the unit cell lattice bears the formula either $Na_6[(AlO_2)_6(SiO_2)_{30}].24H_2O$ or $(Na_2, K_2, Ca, Mg)_3[(AlO_2)_6(SiO_2)_{30}].24H_2O$. Due to the presence of ion exchangeable cations such as Na, K, Ca and Mg in its structure, zeolite possesses a high cation exchange capability. The ion exchange capacity of zeolites varies in the range of 1.9 and 2.2 meq/g (Armagan et al. 2004). The adsorption of anionic reactive dyes using natural zeolite is very limited due to the surface of the zeolite and the dye molecules having negative charges (Alver & Metin 2012). Many investigations on the adsorption of dyes onto natural and modified zeolites have been reported.

Several siliceous materials have been studied for their adsorption properties and efficacy. Alunite ore, $Al_2(SO_4)_3{\cdot}K_2SO_4{\cdot}4Al(OH)_3$, is one of the minerals of the jarosite group, and it is insoluble in water. It forms when volcanic rocks are changed hydrothermally, and it occurs with SiO_2 minerals and contains about 10- 50% SiO_2. Alunite gives thermal decomposition reaction products such as Al_2O_3, $Al_2(SO_4)_3$ and K_2SO_4 when it is calcined at 973–1023K (Tunali et al. 2006), (Ozacar 2002).

Perlite is another naturally occurring glassy siliceous rock with a distinct, concentric onion-like structure due to fractures, caused by contractions during cooling. Perlite expands to about 20 times its original volume when heated at a temperature range between 760 to 1100°C to form a lightweight, glasslike material with a cellular structure. The main components of perlite are silica, aluminium, potassium and sodium. The silicon atom in perlite is surrounded by molecular water and hydroxyl groups. Perlite has been extensively used for the adsorption of heavy metals and dyes (Vijayakumar et al. 2009),(Ateş et al. 2014),(Doğan & Alkan 2003). Adsorption of several dyes like Congo red (Vijayakumar et al. 2009), Methyl Violet (Doğan & Alkan 2003), Methylene Blue (Doğan et al. 2004) has been studied.

Diatomite is a siliceous mineral derived from fossilized diatom skeleton. It is not pure hydrous silica but also contains other associated elements. But, the silanol group is an active one which tends to react with many polar organic compounds and various functional groups. The OH groups and oxygen bridges on the diatomite surface act as the adsorption sites. Adsorption of Methylene Blue, Cibacron Reactive Black and Reactive Yellow dyes has been studied on diatomite. And, the affinity of these dyes to diatomite was as follows: Methylene Blue > hydrolysed Reactive Black > hydrolysed Reactive Yellow (Al-Ghouti et al. 2003), (Khraisheh et al. 2005).

Another type of siliceous material reported for its adsorption potential is sand. Sand has been used for the adsorption of Methylene Blue (Bukallah et al. 2006), Neutral Red (Rauf et al. 2007), and Coomassie Blue, Malachite Green and Safranin Orange (Rauf et al. 2007). These authors also tried to find out the effect of various ions like thiosulphate, potassium, nickel, zinc, chloride, sodium and copper ions on adsorption of the above mentioned dyes. (Saha et al. 2010) used clayey soil of Indian origin to remove Malachite Green. The authors observed that the maximum adsorption capacity at 303K was 78.57 mgg^{-1} at pH 6. Other siliceous materials used are modified and original pumice (Canci & Kilic 2013), beach sand and beach sand coated with polyaniline (Ansari et al. 2013), etc.

Table 2.4: Adsorption Capacity and other Parameters for Dye Removal by Siliceous Materials

Adsorbent	Dye	Modification	pH	Isotherm	Removal	Reference
Zeolite	Rhodamine B Methylene Blue	-	-	Langmuir & Fruendlich	2.8×10^{-5} molg^{-1} 7.9×10^{-5} molg^{-1}	(Wang & Zhu 2006)
MCM-22	Methylene Blue Crystal Violet Rhodamine B	-	-	Langmuir Freundlich	1.8×10^{-4} molg^{-1} 1.2×10^{-4} molg^{-1} 1.1×10^{-4} molg^{-1}	(Wang et al. 2006)
Diatomite	SB EBR IY	-	-	Freundlich	10.11mgg^{-1} 5.92 mgg^{-1} 117.75 mgg^{-1}	(Erdem et al. 2005)
Zeolite	Reactive Red-239 Reactive Blue-250	Stirred with HMDA solution for 5hrs, then washed and dried	7	Freundlich & Redlich-Peterson	28.57 mgg^{-1} 17.63 mgg^{-1}	(Alver & Metin 2012)
Alunite	Acid Blue 40 Acid Yellow 17	Calcined from 373K-1073K for 15-120 min	2	Langmuir	212.8 mgg^{-1} 151.5 mgg^{-1}	(Ozacar 2002)
Alunite	Reactive Blue 114 Reactive Yellow 64 Reactive Red 124	Calcined from 373K-1073K for 15-120 min	-	Langmuir	170.7 mgg^{-1} 236 mgg^{-1} 153 mgg^{-1}	(Özacar & Şengil 2003)

2.5.2.4 Clay

Natural clay minerals are strong candidates as adsorbents because of their low-cost, high adsorption properties and potential for ion exchange. Clay is chiefly comprised of silica, alumina and water, frequently with appreciable quantities of iron, alkalies and alkali earths. With these elements present in a layered fashion, clay act as the negatively charged host material to adsorb positively charged species. Two structural units are involved in the atomic lattices of most clay minerals. One unit consists of closely packed oxygens and hydroxyls in which aluminium, iron and magnesium atoms are embedded in an octahedral combination so that they are equidistant from six oxygens or hydroxyls. The second unit is built of silica tetrahedrons. The silica tetrahedrons are arranged to form a hexagonal network that is repeated indefinitely to form a sheet of composition, $Si_4O_6(OH)_4$ (Al-Degs et al. 2000).

According to the differences in their layered structures, several classes of clays has been classified, such as smectites (montmorillonite, saponite), mica (illite), kaolinite, serpentine, pylophyllite (talc), vermiculite and sepiolite (Crini 2006).

Bentonite is an absorbent aluminium phyllosilicate, which is essentially impure clay consisting mostly of montmorillonite. There are different types of bentonite, each named after the respective dominant element, such as potassium (K), sodium (Na), calcium (Ca) and aluminium (Al) (Ajibola et al. 2015). The clay has adsorbent properties and an alkaline pH due to the presence of potassium, sodium and calcium ions (Koumanova & Allen 2005).

Kaolin is a soft, white plastic clay consisting mainly of the mineral kaolinite which is a hydrated aluminium silicate $Al_2Si_2O_5(OH)_4$. The general structure of the kaolinite group is composed of silicate sheets (Si_2O_5) bonded to aluminium oxide/hydroxide layers ($Al_2(OH)_4$) called gibbsite layers, which is a layered silicate mineral with one tetrahedral sheet linked through oxygen atoms to one octahedral sheet of alumina octahedral. Kaolinite is a non-swelling clay (Ajibola et al. 2015).

Montmorillonite is a very soft phyllosilicate mineral and is a member of smectite family. It has 2:1 expanding crystal lattice. The smectite group refers to a family of non-metallic clays primarily composed of hydrated sodium calcium aluminium silicate, a group of monoclinic clay-like minerals with general formula (Ca, Na,

H)(Al, Mg, Fe, Zn)$_2$(Si, Al)$_4$O$_{10}$(OH)$_2$.nH$_2$O. Chemically, it is hydrated sodium calcium aluminium magnesium silicate hydroxide Na,Ca)x(Al,Mg)$_2$(Si$_4$O$_{10}$)(OH)$_2$.nH2O (Ajibola et al. 2015).

Sepiolite is a fibrous hydrated magnesium silicate with a unit cell formula (Si$_{12}$)(Mg$_8$)(O$_{30}$)(OH)$_4$(OH)$_2$·8H$_2$O and a general structure formed by an alternation of blocks and tunnels that grow up in the fibre direction. Each block consists of two tetrahedral silica sheets enclosing a central magnesia sheet but the silica sheets are discontinued and inversion of the silica sheets that give rise to structural tunnels. These characteristics of sepiolite make it a powerful adsorbent for organic dye molecules. In addition, some isomorphic substitutions in the tetrahedral sheets of the lattice of sepiolite, such as Al^{3+} instead of Si^{4+} form negatively adsorption sites. Such sites are occupied by exchangeable cations that compensate for the electrical charge (Özcan et al. 2006).

To improve the removal efficiency and adsorption capacity of above mentioned clayey minerals, modification of surfaces has also been reported. There are two types of surface modification: physical and chemical.

Physical process: It is an impregnation or organic modification process which is accomplished through the replacement of inorganic exchangeable cations, like Na^+, K^+ and Ca^{2+}, within the clay crystalline structure with organic cations, typically with quaternary ammonium cations of the form $[(CH_3)_3NR]^+$ or $[(CH_3)_2NR_2]^+$ such as hexadecyltrimethyl ammonium bromide, bromize hexadecyl pyridine, 2-mercaptobenzimidazole rendering the surface of clays from hydrophilic and organophobic to hydrophobic and organophilic character. After this replacement, organic molecules are adsorbed within the crystalline structure of the clay that then swells in the presence of organic contaminants. These organic ions attached to the clay readily adsorb other organic species, mainly the phenols.

Chemical Process: This process is of organo functionalization or grafting of organic molecules on clay surfaces. The surface of clays can be changed from hydrophilic to hydrophobic or organophilic by organo-functional molecules, with surface hydroxyl groups, Lewis and Brönsted acidic sites, etc., by grafting organic groups on the clay surface. Grafting coupling agents are generally silanes like $(RO)_3SiRVX$ where X is CH = CH_2, Cl, NH_2 or SH and RV is $(CH_2)_3$. Hydrolysis of the alkoxy groups yields silanol groups that react with surface groups of the clay. The usual organic derivatives

of clays are generally obtained by using coupling agents, mainly various types of silanes, amino-, mercapto-, methacryloxy-, ureidosilanes. After the modification, the surface properties of clays are changed to interact with metal ions and/or organic molecules (Erdemoğlu et al. 2004).

Table 2.4 shows adsorption capacity and other parameters for dye removal using clayey minerals. Despite having chemical and mechanical stability, high surface area and structural properties, low particle size of clay creates separation/filtration problems after adsorption (Gupta et al. 2015). Table 2.5 shows adsorption capacity and particle size of various clays.

Table 2.5: Adsorption capacity and particle size of various clays (Mundada et al. 2016)

Adsorbent	Particle size	Adsorption Capacity	Dye
Montmorillonite clay	53-105 µm	86.32-348.89 mgg^{-1}	Methylene Blue
Organo-attapulgite	<200 µm	189.39 mgg^{-1}	Congo red
Calcined pure kaolin	<230 µm	8.88 mgg^{-1}	Methylene Blue
Calcined raw kaolin	<230 µm	7.59 mgg^{-1}	Methylene Blue
Bentonite	80-125 µm	500 mgg^{-1}	Methylene Blue
Acid-Activated Bentonite	<63 µm	416.3 mgg^{-1} 119.1 mgg^{-1}	Acid Red 57 Acid Blue 294
Activated Clay	<38 µm	208-54.3 mgg^{-1}	Basic Red81
Activated Clay	<38µm	7.29-58.2 mgg^{-1}	Acid Blue 9
Clay	<= 53 µm	6.93 mgg^{-1}	Methylene Blue

Table 2.6: Adsorption Capacity and other Parameters for Dye Removal by Clayey Minerals

Adsorbent	Dye	Modification	pH	Isotherm	Removal	Reference
Activated clay	Methylene Blue	Thermal treatment at 300°C and boiling with 0.5dm^3 HNO_3 for 2 hrs	-	Toth	500 mgg^{-1}	(El Mouzdahir et al. 2010)
Vermiculite	Methylene Blue	-	7	Langmuir	11.77 mgg^{-1}	(Zhao et al. 2008)
Pryophyllite	Methylene Blue Procion Crimson H-EXL	-	2-12	Langmuir	70.42 mgg^{-1} 71.43 mgg^{-1}	(Gücek et al. 2005)
Clay	Methylene Blue	-	5.6	Langmuir	58.2 mgg^{-1}	(Gürses et al. 2006)
Calcined pure kaolin	Methylene Blue	-	>4	Langmuir & Freundlich	8.88 mgg^{-1}	(Ghosh & Bhattacharyya 2002)
Calcined pure kaolin	Methylene Blue	-	>4	Langmuir & Freundlich	7.59 mgg^{-1}	(Ghosh & Bhattacharyya 2002)
Sepiolite	Acid Blue193	-	1.5	Freundlich	1.19×10^{-4} molg^{-1}	(Özcan et al. 2006)

DEDMA-Sepiolite	Acid Blue193	Sepiolite stireed with DEDMA bromide salt for 24 hrs , then washed and dried	1.5	Freundlich	2.57×10^{-4} $molg^{-1}$	(Özcan et al. 2006)
DEDMA-Sepiolite	Acid Red 57	Sepiolite stireed with DEDMA bromide salt for 24 hrs , then washed and dried	2	Freundlich	425.0 mgg^{-1}	(Özcan & Özcan 2005)
BTMA-Bentonite	Acid Blue193	Bentonite stireed with BTMA chloride salt for 24 hrs , then washed and dried	1.5	Langmuir, Fruendlich & Dubinin-Radushkevich	505.3 mgg^{-1} (20°C) 480.4 mgg^{-1} (30°C) 472.4 mgg^{-1} (40°C)	(Özcan Safa et al. 2005)
Organo-attapulgite	Congo red	Attapulgite stirred with HTMAB for 24 hrs, then washed and dried	7-9	Langmuir	189.39 mgg^{-1}	(Chen & Zhao 2009)
Bentonite	Congo Red	TA: heating at 100°C AC: activation with 0.5M HCl at 30°C ATA: activation using 0.1M HCl at 30°C then thermal activation followed by calcination at 100°C for 20min.	3-11	Freundlich	TA: 52.6mg/g AC: 61.5mg/g ATA: 74.5mg/g	(Zaghouane-Boudiaf et al. 2014)

2.6 Fixed Bed Study

The above discussed literature on various low-cost absorbents is on batch adsorption studies. The data given on adsorption capacity is for laboratory purposes. However, for practical application of low-cost adsorbent, the data is not suitable. At field scale, large volumes of wastewater are continuously generated. Therefore, a fixed bed column is preferred where fresh adsorbent is always in contact with wastewater, providing the essential concentration gradients between adsorbate and adsorbent for adsorption. This permits far more effective utilization of adsorbent capacity and also results in improved effluent quality. The design and theory of packed column adsorption systems focus on determination of the shape of the breakthrough curve and its kinetics through the bed. The performance of fixed bed is described by the theory of the breakthrough curve (Pathak et al. 2015) (Charumathi & Das 2012) (Srivastava et al. 2008). Very little literature is available on fixed bed studies. Moreover, treatment of synthetic and real textile wastewater is not much discussed. Some of the reported studies are: treatment of Methylene Blue on rice husk column (Han et al. 2007), removal of crystal violet using agro-waste column of *Citrullus lanatus rind and Cyperus rotundus* (Bharathi & Ramesh 2013), oil palm empty fruits bunch activated carbon for rhodamine B removal (Auta 2012), phoenix tree leaf powder for removal of Methylene Blue (Abdulla 2009), surfactant-modified zeolite to remove color from real textile wastewater (Ozdemir et al. 2009).

2.7 Summary

This chapter reviewed the chemical composition of dyes related to textile industry applications and the amount of dye lost in the effluent. A detailed account of all the available technique for dye removal technique is provided. The benefits and limitations of current dye removal technique are summarized. Adsorption is one of the most effective techniques for dye removal. Unfortunately, the use of adsorption for dye removal is restricted due to the high cost of activated carbon, which is a widely used adsorbent for industrial adsorption processes. This limitation highlights the need for low-cost adsorbents.

Some low-cost adsorbents with effective adsorption capacity have been reported. But their use at commercial scale is restricted due to limited availability. With most of the

available literature on batch studies, the feasibility of the adsorbent at industrial scale could not be judged. Clays showed good colour removal capacity, sometimes better than activated carbon. However, not many fixed bed studies on clay have been reported which can help in assessing its performance on handling large volumes of effluent. Also, the low particle size of clays may create hydrodynamic problems. Treatment of synthetic and real textile wastewater is also an area of study which needs focus. Surface modification of many adsorbents has shown an increase in adsorption capacity. However, critical investigation on surface characteristics after modification is still lacking. Thus, this research gap in the available literature led to the formation of four earlier mentioned objectives of the present study.

CHAPTER 3

Chapter 3

Research Methodology

This Chapter illustrates in detail the research methodology used in the present study. It gives an insight into the experimental setup and analysis done in collecting the data. The entire work was carried out in the PHE laboratory of Department of Civil Engineering in Malaviya National Institute of Technology, Jaipur.

3.1 Research Stages

The experimental analysis of the present study has been divided into two parts: batch study and fixed bed study. Figure 3.1 shows the flowchart for research stages.

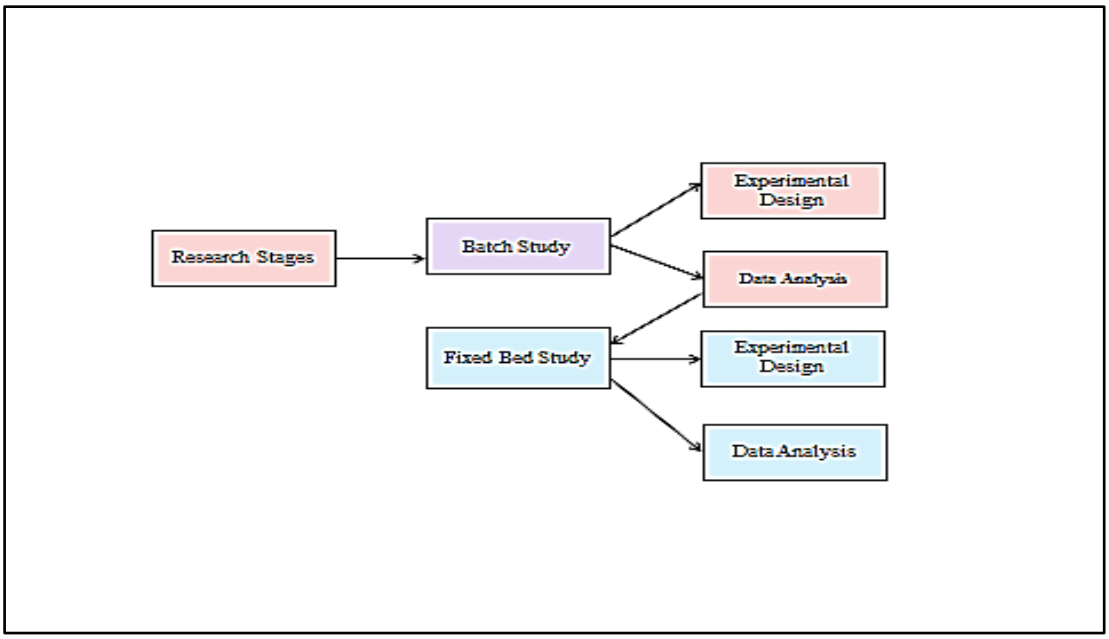

Figure 3.1: Research stages of the present study

3.2 Formulation of Research Methods

The logical stepwise methodologies were adopted during the research study to accomplish the key objectives of the study that were formulated within the aim of the study. The data and information required with respect to each objective were collected to perform various analyses. All such information is collectively well defined in Table 3.1.

Table 3.1: Research objectives and data information

Research Objectives	**Data required**	**Data Sources**	**Data analysis**
To study the effect of various operating parameters to identify the set of optimum parameters for colour removal on the soil.	Detailed information related to the structure of dyes, physical characteristics of the soil, adsorbent-adsorbate reaction mechanism.	Electronic sources and experimental trials.	Experimental Analysis, Kinetic Modelling, Equilibrium study
To modify soil based on optimum parameters as identified from objective 1 and analyze surface characteristics of soil after modification.	Detailed knowledge of modification process. Descriptive information on surface characterisation procedures.	Electronic sources	Data comparison of objective 1 & 3. Literature review and data comparison
To assess the potential of modified soil vis-a-vis colour removal.	Comparative data for the concerned parameters from objective 1.	Electronic sources and also data from objective 1.	Experimental Analysis, Kinetic Modelling, Equilibrium study
To conduct fixed bed study to evaluate commercial feasibility of soil.	Knowledge of continuous flow parameters, bed design	Electronic sources and optimized parameters from above objectives	Experimental Analysis, Evaluation of design parameters by various models

3.3 Batch Study

The batch study was performed to determine the adsorption rate and equilibrium adsorption capacity of soil. It helped in understanding the reaction mechanism between dye and soil. The subsections enlist the materials required to perform the batch study.

3.3.1 Materials

3.3.1.1 Adsorbent

Three different types of adsorbents were used in the present study. Adsorbent preparation details are given subsequent chapters.

- **Non-modified soil**
- **Acid- modified soil**
- **Alkali modified soil**

3.3.1.2 Adsorbate

Two types of dyes were used as adsorbate to test the adsorption capacity of adsorbent used in the present study.

- **Direct Red 81(DR81)**

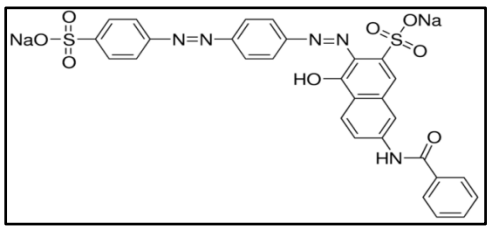

Figure 3.2: Structure of DR81

The dye (Figure 3.2) was obtained from Sigma-Aldrich (dye purity ~ 50%). It has chemical formula $C_{29}H_{19}N_5Na_2O_8S_2$. The IUPAC name of the dye is Disodium 7-benzamido-4-hydroxy-3-[[4-[(4-sulphonatophenyl)azo]phenyl]azo]naphthalene-2-sulphonate. It has a molecular weight of 675.60 $molg^{-1}$. DR81 is characterised by azo bonds (N=N) having $–SO_3$, $-COO^-$ and OH^- groups which make it highly soluble and is not likely to be flocculated (Gupta et al. 2007). When this dye is dissolved in aqueous solutions, the sulfonate groups of the dye ($D\text{-}SO_3Na$) are dissociated and

converted to anionic dye ions (Bulut et al. 2008). It has a maximum visible absorbance (λ_{max}) at a wavelength of 548 nm.

- **Methylene Blue (MB)**

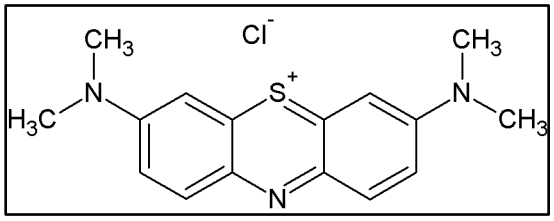

Figure 3.3: Structure of Methylene Blue

The dye (Figure 3.3) was obtained from Merck (CI 52015) (dye purity ≥ 82%). It has chemical formula $C_{16}H_{18}ClNS.xH_2O$ (x=2 or 3). The IUPAC name for the dye is Methylthioninium chloride, 3,7-Bis(dimethylamino)phenothiazinium chloride, Tetramethylthionine chloride. The molecular mass of the dye is 319.86 $molg^{-1}$. MB is a thiazine (cationic) dye. It dissociates in aqueous solution into MB cation and the chloride ion. The cationic property originates from positively charged nitrogen or sulphur centers(Almeida et al. 2009) (Al-wahbi et al. 2011) (Alzaydien 2009). It has a maximum visible absorbance (λ_{max}) at a wavelength of 663 nm.

3.3.1.3 Stock solution

The stock solution for both the dyes was prepared by dissolving an accurately weighed amount of dye in distilled water to achieve a concentration of 5000 mg/L and subsequently diluted to the required concentrations.

3.3.2 Experimental Analysis

The batch study was conducted as a function of the adsorbent dose, initial dye concentration, contact time and pH. The batch tests were carried out in 500 mL capped-Erlenmeyer flasks. A given amount of soil was added with 100 mL of dye solution to the flask. The contents of the flasks were then agitated at a constant speed of 150 rpm for one hour in an incubator shaker (Model MSW-232) at 30°C. At regular intervals, an accurately measured content was taken out and centrifuged in a centrifuge (Model Remi R8C-BL) at 2000 rpm. The supernatant solution was pipetted out and without dilution was monitored instantaneously on a spectrophotometer

(Model UV-1800 Shimadzu UV-Vis Spectrophotometer) for absorption values. After recording the absorption values, the supernant was returned to the flask. The procedure to determine the influence of various parameters is explained in following subsections.

3.3.2.1 Effect of pH

For determination of optimum pH for adsorption of Direct Red 81 and Methylene Blue, the experiments were carried out at different pH values ranging from 1 to 11 for 10 minutes. The dye concentration was kept as 1000 mg/L, agitation speed 150rpm and temperature 30°C. Samples were analysed after 10 minutes for the amount of dye adsorbed.

3.3.2.2 Effect of Contact Time

The flasks were agitated at 150rpm at 30°C at various adsorbent doses and dye concentrations for a contact time of 60 minutes. The contents were pipetted out at an interval of 3, 6, 10, 20, 30, 40, 50 and 60 minutes and analysed for the amount of dye adsorbed.

3.3.2.3 Effect of Adsorbent Dose

To determine the effect of adsorbent dose on adsorption of Direct Red 81 and Methylene Blue, the experiments were carried out at optimum pH and contact time obtained from the tests above. The experiments were performed at adsorbent doses ranging from 12.5 g/100mL to 100 g/100mL and various dye concentrations. The agitation speed and temperature were kept at 150 rpm and 30°C respectively.

3.3.2.4 Effect of Initial dye concentration

Effect of initial dye concentration was studied at an adsorbent dose ranging from 12.5 g/100mL to 100 g/100mL. The study was conducted at optimum pH and contact time obtained from the tests above. The agitation speed was kept at 150 rpm and temperature at 30°C. The dye concentrations tried were 125 mg/L, 250 mg/L, 500 mg/L and 1000 mg/L.

3.3.2.5 Effect of Particle Size

Effect of two particle size range 300-150 µm and 150-75 µm was studied at a constant adsorbent dose and pH for a contact time of 10 minutes. The agitation speed was kept at 150rpm and temperature at 30°C. The dye concentration was kept as 1000 mg/L.

3.3.3 Data Analysis

3.3.3.1 Kinetic Modelling

The prediction of the rate at which adsorption takes place for a given adsorption system is one of the most important factors in adsorption system design, with adsorbate residence time and the reactor dimensions controlled by the system's kinetics (Ho 2006). At equilibrium, a relationship exists between the concentration of the dye molecules in the aqueous phase and the concentration of dyes molecules adsorbed onto the adsorbent (i.e. number of dye molecules adsorbed per unit mass of adsorbent). The amount of dye at equilibrium on the adsorbent was calculated from the Equation 3.1.

$$q_e = (C_0 - C_t)\frac{V}{m} \tag{3.1}$$

Where q_e (mgg^{-1}) is the amount of dye adsorbed per unit weight of adsorbent at equilibrium; C_0 and C_t are, respectively, the initial and liquid-phase concentrations of the dye solution at any time t (mg/L); V is the volume of the dye solution; m is the mass of the adsorbent.

Kinetic models have been developed to investigate the mechanism of adsorption and to elucidate potential rate controlling step based on alternative approaches discussed in the forthcoming sections.

The two main types of adsorption kinetic models, namely reaction-based and diffusion-based models, were adopted to fit the experimental data. Pseudo first-order and pseudo second order were considered as the reaction based models and intraparticle diffusion model as the diffusion based model (Goswami & Purkait 2011).

a. Lagergren's Pseudo First Order Kinetic Model

Lagergren developed the pseudo-first order kinetic model to explain the mechanism of adsorption. This model assumed that the rate of change of solute uptake with time was directly proportional to the difference in saturation concentration and the amount of solid uptake with time (Ho 2004a). The Equation 3.2 in its differential form is given as below:

$$\frac{dq}{dt} = k_1(q_e - q_t) \tag{3.2}$$

Where k_1 is the pseudo first order kinetic constant, q_e is the amount of dye adsorbed on the soil at equilibrium (mgg^{-1}), q_t is the amount of dye adsorbed on the soil at any time t (mgg^{-1}). Integrating Equation 3.2 for the boundary conditions t = 0 to t = t and q_t = q_e and rearranging, we get the linearized form of the Equation 3.3 as follows:

$$\ln(q_e - q_t) = \ln(q_e) - k_1 t \tag{3.3}$$

The linearized plot of $\ln(q_e - q_t)$ versus t gives straight line. The first order rate constant k_1 is calculated from slope and q_e is calculated from intercept of this plot. Values of k_1, predicted uptake of adsorbate (q_e^{pred}) and experimental uptake of adsorbate (q_e^{exp}) along with the coefficient of regression (R^2) for 125 mg/L, 250 mg/L, 500 mg/L, and 1000 mg/L of dye adsorbed onto soil respectively were determined and compared.

b. Lagergren's Pseudo Second Order Kinetic Model

The rate expression for Lagergren's pseudo second order kinetic model is given by Equation 3.4. The model assumes that adsorption capacity is proportional to the number of active sites occupied on the sorbent (Ho & McKay 1999).

$$\frac{dq}{dt} = k_2(q_e - q_t)^2 \tag{3.4}$$

where k_2 is the pseudo second order rate constant (gmg^{-1}hr^{-1}), q_e is the amount of dye adsorbed on the soil at equilibrium (mgg^{-1}) and q_t is the amount of dye adsorbed on the soil at any time t (mgg^{-1}) . Rearranging the variable in Equation 3.4, it gives:

$$\frac{dq}{(q_e - q_t)^2} = k_2 dt \tag{3.5}$$

Integrating the Equation 3.5 for the boundary conditions t = 0 to t = t and q_t = 0 to q_t = q_t gives:

$$\frac{1}{(q_e - q_t)^2} = \frac{1}{q} k_2 t \tag{3.6}$$

Linearised form of Equation 3.6 is given in the Equation 3.7.

$$\frac{t}{q_t} = \frac{1}{h} + \frac{1}{q_e} t \tag{3.7}$$

Where h is the initial adsorption rate ($gmg^{-1}hr^{-1}$) and is given by $h = k_2 {q_e}^2$. A plot between $\frac{t}{q_t}$ and t gives straight line having slope $\frac{1}{q_e}$ and intercept $\frac{1}{h}$.

For pseudo second order kinetics, $\frac{t}{q_t}$ is plotted with respect to t. The straight line is obtained. Slope gives the value of q_e and the intercept gives the value of h, from which k_2 is calculated. The values obtained from experimentally compared with the predicted values. Based on the second-order model, the values of k_2, initial adsorption rate (h), predicted uptake of dye (${q_e}^{pred}$) and experimental uptake of dye (${q_e}^{exp}$) along with the coefficient of regression (R^2) for 125 mg/L, 250 mg/L, 500 mg/L and 1000 mg/L of dye adsorbed onto soil respectively were determined and compared.

c. Intraparticle Diffusion Model

In adsorption studies, it is necessary to determine the rate-limiting step. The general mechanism for dye removal by adsorption on a sorbent material may be assumed to involve the following four steps: (i) migration of dye from bulk of the solution to the surface of the adsorbent (bulk diffusion); (ii) diffusion of dye through the boundary layer to the surface of the adsorbent (film diffusion); (iii) transport of the dye from the surface to the interior pores of the particle (intraparticle diffusion or pore diffusion); (iv) adsorption of dye at an active site on the surface of material (chemical reaction via ion exchange, complexation and/or chelation). The dye adsorption is usually governed by either the liquid phase mass transport rate or the intraparticle mass transport rate. Hence diffusive mass transfer is incorporated into the adsorption process. In diffusion studies, the rate can be expressed in terms of the square root time. The mathematical dependence of q_t versus $t^{0.5}$ is obtained if the process is considered to be influenced by diffusion in the particles and convective diffusion in

the solution. According to the intraparticle diffusion model proposed by Weber and Morris (Weber & Morris 1963), the root time dependence may be expressed by Equation 3.8.

$$q_t = k_i t^{0.5} + C \tag{3.8}$$

where q_t is the amount of solute on the surface of the sorbent at time t (mg/g), k_i the intraparticle diffusion rate constant ($mgg^{-1}min^{-1/2}$), t the time (min), and C is the intercept (mgg^{-1}). For this analysis, q_t was plotted with $t^{0.5}$. The k_i values were determined and analysed from the slopes of q_t versus $t^{0.5}$ plots.

3.3.3.2 Equilibrium Studies

Establishment of the most appropriate adsorption equilibrium correlation is an indispensable part of reliable prediction of adsorption parameters and quantitative comparison of adsorbent behaviour for various experimental conditions (Gimbert et al. 2008). In this perspective, adsorption isotherms describe how dye molecules interact with the adsorbent and therefore, they are critical for optimization of the adsorption mechanism pathways, expression of the surface properties and capacities of adsorbents, and effective design of the adsorption systems (Thompson et al. 2001).

For the present study, the plots were made for five values of adsorbent dose (12.5g, 25g, 50g, 75g, and 100g). The concentration of adsorbate at equilibrium was calculated using varying initial dye concentration (125 mg/L - 1000 mg/L). Five isotherms namely, Langmuir, Freundlich, Redlich-Peterson, Sips and Toth have been considered for the study.

a. Langmuir Isotherm

Langmuir isotherm is based on the assumption of monolayer adsorption i.e. the adsorbed layer is one molecule in thickness. It describes that adsorption can only occur at a finite number of definite localized sites, that are identical and equivalent, with no lateral interaction and steric hindrance between the adsorbed molecules, even on adjacent sites (Vijayaraghavan et al. 2006). The mathematical aspect of the Langmuir isotherm models is illustrated in Table 3.2, where; q_e is equilibrium solid phase concentration (mg/g) and C_e is equilibrium liquid phase concentration (mg/L) in all isotherm models. In all models, q_m parameter is relevant with adsorption capacity.

In Langmuir equation K_l are the Langmuir constants related to the adsorption capacity.

b. Freundlich Isotherm

Freundlich isotherm describes the multilayer adsorption of the adsorbate molecules on the adsorbent surface. The model applies to adsorption onto heterogeneous surfaces with a uniform energy distribution and reversible adsorption. It is not restricted to the monolayer formation. Table 3.2 illustrates the mathematical Freundlich equation. K_f and n are isotherm parameters characterizing adsorption capacity and intensity of adsorption, respectively. The heterogeneity factor $1/n$ indicates the non-linearity between adsorbate and adsorbent. If the value of $1/n$ is equal to unity, the adsorption is linear; if the value is below unity, this implies that the adsorption process is chemical; if the value is above unity, adsorption is a favorable physical process; the more heterogeneous the surface, the closer $1/n$ value is to 0 (Gimbert et al. 2008).

c. Redlich-Peterson Isotherm

Redlich-Peterson isotherm combines elements of both Langmuir and Freundlich isotherms. This model has a linear dependence on concentration in the numerator and an exponential function in the denominator. The mechanism of adsorption is hybrid and does not follow ideal monolayer adsorption (Foo & Hameed 2010). The mathematical expression is given in Table 3.2. K_r (L/g) and a_r (L/mg) are Redlich–Peterson isotherm constants and β is the exponent which lies between 0 and 1. Since, it is a three parameter equation solver add-in function in Microsoft Excel was used to calculate the parameters of the equation. When the exponent β tends zero, the equation approaches Freundlich isotherm. While, when β is closer to one, ideal Langmuir condition is approached (Chan et al. 2012).

d. Sips Isotherm

Sips isotherm is an improvement of the Freundlich and Langmuir equations. At low adsorbate concentrations, it reduces to Freundlich isotherm; while at high concentrations, it predicts a monolayer adsorption capacity characteristic of the Langmuir isotherm (Foo & Hameed 2010). The mathematical expression of the Sips equation is given in Table 3.2. a_s constant is related to energy of adsorption and βs is related to surface characteristics. The smaller is the value of this parameter, the more

heterogeneous is the adsorbent surface. If βs is equal to 1, the Sips equation is reduced to the Langmuir equation and the surface is homogeneous (Srenscek-Nazzal et al. 2015).

e. Toth Isotherm

Toth isotherm is designed to improve Langmuir isotherm fittings. It is applicable to heterogeneous adsorption systems. Its correlation presupposes an asymmetrical quasi-Gaussian energy distribution, with most of its sites has an adsorption energy lower than the peak (maximum) or mean value (Foo & Hameed 2010). The mathematical expression is given in the Table3.2. K_T is the Toth model constant and $\frac{1}{t}$ the Toth model exponent ($0 < \frac{1}{t} \leq 1$).

f. Linear Regression Method

Linear regression method of analysis has been the most commonly used technique to determine the most fitted isotherm. It quantifies the distribution of adsorbates and mathematically analyses the adsorption systems. The linear least-square method to the linearly transformed isotherm equations has been applied to confirm the consistency of the predicted and experimental equilibrium data using the coefficient of determination (Vasanth Kumar & Sivanesan 2007) (Ho 2004b). Langmuir and Freundlich isotherms were plotted for five adsorbent doses 12.5g, 25g, 50g, 75g, and 100g. C_e is the equilibrium dye concentration at contact time of 10 minutes for initial dye concentration (125 mg/L – 1000 mg/L) and q_e is calculated by linear equation given in Table 3.2.

g. Non-Linear Regression Method

Transformations of the non-linear form of isotherms to linear form alter their error structure, violate the error variance and normality assumptions of standard least squares. The error distribution may vary either to better or to worse depending on the way the equation is linearized. This leads to the bias in the adsorption data. However, the non-linear method has an advantage that the error distribution does not get altered, as all the equilibrium parameters are fixed on the same axis. Therefore, a trial and error procedure was used for a non-linear method by using the solver add-in with Microsoft spreadsheet, Microsoft Excel. Five isotherms were analysed, namely; Langmuir, Freundlich, Redlich-Peterson, Sips and Toth. The experimental q_e^{exp} was

calculated by the Equation 3.1 and the predicted q_e^{pred} is obtained from the non-linear expressions of the above mentioned isotherms, given in the Table 3.2

The evaluation of fitness of the model equations with experimental data requires an error function with optimization. The model's fitness for the non-linear method in the present study was determined by the coefficient of determination (R^2), non-linear error functions: the residual root mean square error (RMSE) and the chi-square test (χ^2). The standard equations are as follows:

Coefficient of determination (R^2): It gives the proportion of the variance of one variable that is predictable from the other variable. The coefficient of determination is such that $0 < R^2 < 1$, and denotes the strength of the linear association between experimental data, q_e^{exp} and prediction data, q_e^{pred}. The coefficient of determination represents the percent of the experimental data that is the closest to the line of best fit. R^2 is described by the expression in Equation 3.9 (Foo & Hameed 2010).:

$$R^2 = \frac{\sum_{n=1}^{n}(q_e^{exp} - q_e^{pred})^2}{\sum_{n=1}^{n}(q_e^{exp} - \overline{q_e^{pred}})^2} \tag{3.9}$$

where, q_e^{exp} is the equilibrium adsorption capacity found from the batch experiment, q_e^{pred} is the prediction from the isotherm model for corresponding to C_e and n is the number of observations.

Residual root mean square error (RMSE) and Chi-square test (χ^2): Residual root mean square error (RMSE) and the chi-square test (χ^2): Non-linear error functions such as the residual root mean square error (RMSE) and the chi-square test (χ^2) are used to judge the equilibrium model with the optimal magnitude. Equation 3.10 and 3.11 shows the standard equation of RMSE and χ^2 respectively.

$$RMSE = \sqrt{\frac{1}{n-1}\sum_{n=1}^{n}\frac{(q_e^{exp} - q_e^{pred})^2}{q_e^{exp}}} \tag{3.10}$$

$$\chi^2 = \sum_{n=1}^{n}\frac{(q_e^{exp} - q_e^{pred})^2}{q_e^{exp}} \tag{3.11}$$

The small values of RMSE and χ^2 indicate the better model fitting and the similarity of the model with the experimental data respectively (Hossain et al. 2012).

Table 3.2: List of adsorption isotherm models (Foo & Hameed 2010)

Isotherm	Non-Linear Expression	Linear Expression	Plot
Langmuir-I		$\frac{C_e}{q_e} = \frac{1}{q_m} C_e + \frac{1}{K_l\, q_m}$	$\frac{C_e}{q_e}\ vs.\ C_e$
Langmuir-II	$q_e = \frac{qmK_l\, C_e}{1+K_l\, C_e}$	$\frac{1}{q_e} = (\frac{1}{K_l q_m})\frac{1}{C_e} + \frac{1}{q_m}$	$\frac{1}{q_e}\ vs.\ \frac{1}{Ce}$
Langmuir-III		$q_e = q_m - (\frac{1}{K_l})\frac{q_e}{C_e}$	$q_e\ vs. \frac{q_e}{C_e}$
Langmuir-IV		$\frac{q_e}{C_e} = K_l\, qm - K_l\, q_e$	$\frac{q_e}{C_e}\ vs. q_e$
Freundlich	$q_e = K_f {C_e}^{1/n}$	$\log(q_e) = \log(K_f) + \frac{1}{n}\log(C_e)$	$\log(q_e)\ vs.\ \log(C_e)$
Redlich-Peterson	$q_e = \frac{K_r C_e}{1 + a_r {C_e}^{\beta}}$	$\ln\left(K_r \frac{C_e}{q_e} - 1\right) = \beta \ln(C_e) + \ln(a_r)$	$\ln\left(K_r \frac{C_e}{q_e} - 1\right)\ vs.\ \ln(C_e)$
Tempkin	$q_e = \frac{R_T}{b_T} lnA_T\, C_e$	$q_e = \frac{R_T}{b_T} lnA_T + \left(\frac{R_T}{b_T}\right) lnC_e$	$q_e\ vs. lnC_e$
Sips	$q_e = \frac{K_s\, {C_e}^{\beta s}}{1 + a_s {C_e}^{\beta s}}$	$\beta_s \ln(C_e) = -\ln\left(\frac{K_s}{q_e}\right) + \ln(a_s)$	$\ln\left(\frac{Ks}{q_e}\right)\ vs.\ \ln(C_e)$
Toth	$q_e = \frac{K_T\, C_e}{(a_T + C_e)^{\frac{1}{t}}}$	$\ln\left(\frac{q_e}{K_T}\right) = \ln(C_e) - \frac{1}{t}\ln(a_T + C_e)$	$\ln\left(\frac{q_e}{K_T}\right)\ vs. \ln(C_e)$

3.4 Fixed Bed Study

Practically, the fixed bed adsorption studies are more competent than the batch type adsorption studies. Column operation allows more efficient utilization of the adsorptive capacity of the adsorbent than the batch type. The adsorbent at the inlet end is contacted continuously by the solution at the initial adsorbate concentration. The bed can be assumed to consist of several layers stacked one over other. Each layer remains in contact with a fresh solution of constant adsorbate concentration. During the passage of adsorbate solution, the concentration of adsorbate in solution changes in every sub-layers. The change in concentration is small at each subsequent layer. At constant adsorbate concentration, maximum loading of adsorbent occurs through this mechanism. In column operation, a concentration gradient is more in the beginning, and it continuously declines as one goes above the column. This is the reason for expected adsorption capacity and the removal rate to be different among batch and column environments(Pathak et al. 2015). The column design and details of the fixed bed study are discussed in the next sections.

3.4.1 Materials

3.4.1.1 Simulated Textile Wastewater

To conduct fixed bed study, synthetic textile wastewater was prepared (Manu & Chaudhari 2002). The composition of the synthetic textile wastewater was as follows: sodium chloride; NaCl (0.15g/L), ammonium sulphate; $(NH_4)_2SO_4$ (0.28g/L), ammonium chloride; NH_4Cl (0.23g/L), disodium hydrogen phosphate; Na_2HPO_4 (0.03g/L), acetic acid; CH_3COOH (0.53g/L), hydrolyzed starch (0.005g/L) and methylene blue (0.2g/L). The above mentioned composition was mixed in tap water and heated at a temperature of 80°C for 2 hours to hydrolyze the added chemicals. After 2 hours, the prepared wastewater was allowed to cool down to room temperature and further study was carried out at using this synthetic textile wastewater. The physicochemical properties of simulated textile wastewater are tabulated in Table 3.3.

Table 3.3: Physicochemical properties of simulated textile wastewater

Parameter	Wastewater
pH	8.76
COD(mg/L)	874.90
Temperature	Room temperature (25-27°C)
Color	Dark blue

3.3.4.2 Actual Textile Wastewater

In order to test the efficiency of the adsorbent, real textile wastewater was also treated. Wastewater was collected from the local dyeing mill from Khatri Nagar, Sanganer, Jaipur. The composition of the dyeing water was not disclosed due to legal reasons. The physiochemical properties of actual wastewater are tabulated in Table 3.4.

Table 3.4: Physicochemical properties of actual textile wastewater

Parameter	Wastewater
pH	11.35
COD(mg/L)	1215.14
Temperature	Room temperature (25-27°C)
Color	Turbid dark blue

3.4.2 Experimental Analysis

The fixed bed tests were conducted as a function of the flow rate and bed height. Dynamic experiments were performed to obtain breakthrough curves of dyes through a fixed bed. Fixed bed studies were performed using alkali modified soil and simulated wastewater of required composition in Perspex columns. Parameters for column design are given in Table 3.5. Three Perspex columns of the internal diameter of 6.5cm and a total height of 14.5cm were used for the study. Each column was packed with the adsorbent of size range 150-75 µm. The bed of the adsorbent was sandwiched between the layer of gravels (bottom layer) of 5.5cm, coarse sand (middle layer) of 3cm and then the varying layer of the adsorbent of 2.5cm, 3.5cm and 4.5cm respectively. The size of the gravels used was 8-12mm, and coarse sand was 0.45 to 0.55mm. At the top of the adsorbent layer, a layer of gravels of 1 cm was kept. This arrangement of layers was made to support the bed and to prevent any flow disturbances. Simulated wastewater of required composition was passed in the upflow

direction through the column at required flow rate with the help of the peristaltic pump (Model Enertech ENDP 200). The effluent flow was kept constant and was assured by measurement regularly throughout the experiment. Effluent samples were collected from the outlet provided in the column at an interval of 10 minutes. For getting smooth curves, a number of samples were collected. The color and COD removal were measured in the influent and effluent samples collected. The data was used for plotting the breakthrough curves.

Figure 3.4: Set- up for Fixed Bed Study

Table 3.5: Parameters for Column design

Volume (mL)	Bed depth (cm)	Weight of soil (g)	Flow rate (L/hr)
82.9	2.5	125	0.5 0.7 1.0
116	3.5	175	0.5 0.7 1.0
150	4.5	225	0.5 0.7 1.0

3.4.2.1 Effect of flow rate and bed height on Breakthrough of Fixed Bed

Experimental breakthrough curves were obtained at all three bed heights of 2.5cm, 3.5cm and 4.5cm for three different flow rates 0.5 L/hr, 0.7 L/hr and 1.0 L/hr respectively for simulated wastewater having methylene blue concentration of 200mg/L. Breakthrough time and exhaustion time were calculated from the plots of breakthrough curves when the effluent concentration reached 0.05 times influent concentration and 0.9 times influent concentration, respectively. The breakthrough curves were used for evaluating design parameters for colour removal in fixed bed studies as per the equations mentioned in next subsection. The data collected during experiments formed the basis for analysis and modelling of fixed bed reactors.

- **Evaluation of the adsorption column design parameters**

The time required (t_Z) for the adsorption zone to move the length of its own height up the column once it is established is given by the Equation 3.12.

$$t_Z = \frac{V_s}{Q_w} \tag{3.12}$$

Where V_s is the total volume of water treated between breakthrough and exhaustion point (mL) and $Q_w$is the influent flow rate (mL/min). V_s is given by Equation 3.13.

$$V_s = V_E - V_B \tag{3.13}$$

Where V_B and V_E are the volume of water treated up to breakthrough and exhaustion point, respectively (mL).

The time required (t_E) for the adsorption zone to be established and to move completely out of the bed is given by following Equation 3.14.

$$t_E = \frac{V_E}{Q_w} \tag{3.14}$$

The rate at which the adsorption zone is moving up or down through the bed (U_Z) is given by the Equation 3.15.

$$U_Z = \frac{h_Z}{t_Z} = \frac{h}{t_E - t_f} \tag{3.15}$$

Where h_Z is the height of adsorption zone (cm), h is the total bed height (cm) and t_f is the time required for the adsorption zone to initially form (min). Rearranging Equation 3.15 gives an expression for the height of the adsorption zone as shown in the Equation 3.16.

$$h_Z = \frac{h\, t_Z}{t_E - t_f} \tag{3.16}$$

The value of t_f can be calculated as follows:

$$t_f = (1 - F)\, t_Z \tag{3.17}$$

Where F is that fraction of adsorbent present in the adsorption zone at breakthrough which has ability to remove solute and can be calculated using the Equation 3.18.

$$F = \frac{S_Z}{S_{max}} = \frac{\int_{V_B}^{V_E} (C_0 - C_t)\, dv}{C_0 [V_E - V_B]} \tag{3.18}$$

Where S_Z is the amount of solute that has been removed by the adsorption zone from breakthrough to exhaustion (mg), S_{max} is the amount of solute removed by the adsorption zone if completely exhausted (mg), C_0 and C_t are the initial concentration of simulated wastewater and that at a given instant of time t (mg/L).

The percentage of the total column saturated at breakthrough is given by the Equation 3.19.

$$\%\, Saturation = \frac{h + (F-1) h_Z}{h} \times 100 \tag{3.19}$$

The maximum column capacity (q_{total}) for a given feed concentration and flow rate is equal to the area under the plot of the adsorbed solute C_{ad} i.e. $(C_0 - C_t)$ versus time (min) and is calculated from Equation3.20.

$$q_{total} = \frac{Q\, A}{1000} = \frac{Q}{1000} \int_0^{t_{total}} C_{ad}\, dt \tag{3.20}$$

Where, Q is the volumetric flow rate (mL/min), A is the area under the breakthrough curve and t_{total} is the total flow time (min).

The total amount of simulated wastewater passed through the column can be calculated from Equation 3.21.

$$m_{total} = \frac{C_0 Q t_{total}}{1000} \quad (3.21)$$

Total percentage removal of simulated wastewater (Y) may be calculated using Equation 3.22.

$$Y = [\frac{q_{total}}{m_{total}}] \times 100 \quad (3.22)$$

The equilibrium adsorbate uptake (q_{eq}), which is the maximum capacity of the column, is defined as the total amount of adsorbate adsorbed (q_{total}) per unit dry weight of adsorbent at the end of the total time flow (g) and is calculated by the Equation 3.23.

$$q_{eq} = \frac{q_{total}}{X} \quad (3.23)$$

Where X is the total dry weight of adsorbent in the bed (g) (Ozdemir et al. 2009),(Kundu & Gupta 2005) .

3.4.3 Data Analysis

The adsorption process is very complex and is governed by many variables. Prediction of the concentration-time profile or breakthrough curve and adsorption capacity for the effluent under given specific operating conditions are required for the successful design of a column used for adsorption process. A number of mathematical models have been developed for use in design of fixed bed system. Few of them are Bohart and Adams, Thomas, Klotz, Erskine and Schuliger, Yoon and Nelson, Clark, Wolbraska, etc (Xu et al. 2013). These are more popular and well cited by many authors for the analysis and design of fixed bed columns. In the present study, the basic laboratory data on column runs are used to model the breakthrough behaviour of adsorption column with a high degree of accuracy. Three mathematical models which are simpler, suitable, more accurate and logical with immediate practical benefits are adopted in the present research work.

a. Bed Depth Service Time (BDST) Model

It is the most widely used model. In this model, characteristic parameters, such as the maximum adsorption capacity, the adsorption rate constant and the critical bed depth, etc. required for scale up of column design are estimated (Ko et al. 2000). The model

is derived on the basis of surface reaction rate theory proposed by Bohart and Adams and is given by Equation 3.24.

$$\ln\left(\frac{C_0}{C_B} - 1\right) = \ln\left(e^{KN_o\left(\frac{X}{F}\right)} - 1\right) - KC_0T \tag{3.24}$$

Where C_0 is the influent concentration (mg/L), C_B is the breakthrough concentration (mg/L), K is the adsorption rate constant (cm^3/mg-hr), N_o is the maximum adsorption capacity (mg/g), X is the bed depth (cm), F is the linear flow rate (cm/min) and T is the service time of the bed (hr). The expression $KN_o\left(\frac{X}{v}\right)$ in the Equation 3.24 is usually much greater than unity, hence the equation 3.24 can be further simplified to Equation 3.25.

$$\ln\left(\frac{C_0}{C_B} - 1\right) = KN_o\left(\frac{X}{F}\right) - KC_0T \tag{3.25}$$

Solving the Equation 3.25, the service time is given by Equation 3.26.

$$t = \frac{N_oX}{C_0F} - \frac{1}{C_0K}ln\left(\frac{C_0}{C_B} - 1\right) \tag{3.26}$$

The form of the Bohart-Adams equation, shown in Equation 3.26, can be used to determine the service time (T) of a column of bed depth (X) given the values of N_o, C_0 and K, which must be determined from a set of nine laboratory columns operated over a range of velocity values (F). The critical depth, a theoretical parameter, is defined as the minimum bed depth required to obtain the desired effluent quality at time t_0. Numerically, it is the bed depth (X_o) just sufficient to prevent penetration of concentration in excess of C_B at zero time. Hence, at t = 0,

$$X_o = \frac{F}{N_oK}\,ln\left(\frac{C_0}{C_B} - 1\right) \tag{3.27}$$

Hutchins (1973) modified the Bohart and Adams equation such that only three fixed bed tests are required to collect the necessary data. This is called Bed Depth Service Time (BDST) approach (Ozdemir et al. 2009). Equation 3.28 has the form of a straight line and represented as

$$t = aX + b \tag{3.28}$$

Where slope is given by

$$a = \frac{N_o}{C_0 F} \tag{3.29}$$

The intercept is given by

$$b = \frac{1}{C_0 K} ln\left(\frac{C_0}{C_B} - 1\right) \tag{3.30}$$

The intercept (b) on the abscissa or X-axis of the BDST graph gives the critical bed-depth (X_o). It is a measure of the adsorption rate and is defined as the time required for the adsorption wave front to pass through the critical bed depth. Using the above linearization equation, the value of N_o and K can be calculated.

The slope constant for a different flow rate can be directly calculated by the Equation 3.31.

$$a' = a\frac{F}{F'} = a\frac{v}{v'} \tag{3.31}$$

In Equation 3.31, a and F are the old slope and influent linear velocity, respectively, and $a'$and F' are the new slope and influent linear velocity. As the column used in experiment has the same diameter, the ratio of original (F) and the new influent linear velocity (F') and original flow rate (v) and the new flow rate (v') is equal.

b. Thomas Model

The Thomas model (Thomas 1943) is one of the most general and widely used models for analysing column performance. Thomas model assumes Langmuir kinetics of adsorption-deadsorption with no axial dispersion. It has been derived with the assumption that the rate driving force obeys second order reversible reaction kinetics. The model predicts concentration-time profile or breakthrough curve for the effluent and gives an idea about the adsorption capacity of adsorbent. The Thomas model also assumes a constant separation factor but it is applicable equally to either favourable or unfavourable isotherms (Han et al. 2007). The model has the following form:

$$\frac{C}{C_0} = \frac{1}{1+exp\left[\frac{k_{Th}}{Q}(q_o M - C_0 V_{eff})\right]} \tag{3.32}$$

Where $k_{Th}$is the Thomas rate constant (mL/min.mg), Q is the flow rate (mL/min), q_o is the maximum solid-phase concentration of the solute (mg/g), M is the mass of adsorbent (g) and V_{eff} is the effluent volume (mL).

The linearized form of Thomas model is as follows:

$$ln\left(\frac{C}{C_0}-1\right)=\frac{k_{Th}q_oM}{Q}-\frac{k_{Th}C_0V_{eff}}{Q} \quad (3.33)$$

The kinetic coefficient (k_{Th}) and the adsorption capacity of the bed (q_o) can be determined from a plot of $ln\left(\frac{C}{C_0}-1\right)$against time t at a given flow rate. The value of time t (min) is t = $\frac{V_{eff}}{Q}$.

c. Yoon and Nelson Model

Yoon and Nelson model is based on the assumption that the rate of decrease in the probability of adsorption for each adsorbate molecule is proportional to the probability of adsorbate adsorption and the probability of adsorbate breakthrough on the adsorbent. Compared to other models, the Yoon and Nelson model is less complicated. No detailed data concerning the characteristics of adsorbate, the type of adsorbent and the physical properties of adsorption bed are required for this model (Bharathi & Ramesh 2013). The Yoon and Nelson equation for the single-component system is expressed as Equation 3.34.

$$\frac{C}{C_0}=\frac{1}{1+exp\{k_{YN}(\tau-t)\}} \quad (3.34)$$

Where k_{YN} is the Yoon and Nelson rate constant (min^{-1}), τ is the time required for 50% adsorbate breakthrough (min) and t is the sampling time (min).

The linearized form of Yoon and Nelson model is as follows:

$$ln\left(\frac{C}{C_0-C}\right)=k_{YN}t-\tau k_{YN} \quad (3.35)$$

The calculation of theoretical breakthrough curves for a single-component system requires the determination of the parameters k_{YN} and τ for the adsorbate of interest. These values may be determined from available experimental data. The approach involves a plot of $ln\left(\frac{C}{C_0-C}\right)$ versus sampling time (t).

The derivation of equation 3.35 was based on the definition that 50% breakthrough occurs at $t=\tau$. Thus, the adsorption bed should be completely saturated at $t=2\tau$. Owing to the symmetrical nature of breakthrough curves due to the Yoon-Nelson

model, the amount of atrazine being adsorbed in the fixed bed is half of the total atrazine entering the adsorption bed within 2τ period. Hence, the following equation can be obtained for a given bed:

$$q_{oYN} = \frac{q_{total}}{M} = \frac{(1/2)C_0(Q/1000)(2\tau)}{M} = \frac{C_0 Q\tau}{1000M} \quad (3.36)$$

This equation also permits one to determine the adsorption capacity of the column (q_{oYN}) as function of inlet atrazine concentration (C_0), flow rate (Q), biomass quantity in the column (M) and 50% breakthrough time (τ) by using the Yoon –Nelson model.

3.5 Analytical Procedure

The detail of analytical procedures used in the present study in given in Appendix A. The Table 3.6 shows the instruments used for analytical procedure and their model.

Table 3.6: Instruments used in the study

S.No.	Instruments Used	Model
1.	pH Meter	Hanna HI-98128
2.	Incubator Shaker	MSW-232
3.	Centrifuge	Remi R8C-BL
4.	Spectrophotometer	Shimadzu UV- Vis 1800
5.	Particle size Analyzer	Malvern Mastersizer-2000
6.	Fourier Transform Infrared Spectrophotometer	Perkin Elmer Spectrum 2
7.	Field Emission Scanning Electron Microscope and Energy Dispersive X-ray	Nova Nano FE-SEM 450
8.	X-ray Diffraction	PANanalytical Xpert
9.	Zeta Potential	Malvern Zetasizer Nano ZSP (ZEN5600)
10.	BET Surface Area	Model AutosorbI, Quantachrome
11.	X-ray Fluoresence Spectroscopy	PANanlytical PW 2404

3.6 Summary

This Chapter has provided the description of materials and methodology used for performing the experiments. It has the details of the experimental setup and solutions prepared for the study. The detailed procedure of experiments has been given which explains the technique used for colour removal and COD removal.

The next chapter marks the beginning of results and discussions.

CHAPTER

4

Chapter 4

Removal of Direct Red 81 and Methylene Blue onto Non-Modified Soil

In this chapter, the feasibility of the non-modified soil for the adsorption of the two dye classes: anionic and cationic; has been discussed. The effect of operational parameters like pH, adsorbent dose, initial dye concentration, contact time and particle size of the adsorbent, which governs the adsorption process for dye removal, has been elucidated. The findings discussed in this Chapter form the baseline data for the present study and also explain the motive of using selected range of operational parameters employed in the later part of the study.

4.1 Introduction

This section of the study deals with the removal of dye using non-modified soil as a low-cost adsorbent. The competence of clay and several other siliceous materials like zeolite (Wang et al. 2006), perlite (Vijayakumar et al. 2009), etc. for dye removal have been reported earlier. However, adsorption property of sandy soil of Rajasthan in India for colour removal has not been reported so far. The clayey and other siliceous particles in the non-modified soil can act as the natural scavenger for the dye removal from aqueous solutions. Methylene Blue and Direct Red 81 are chosen as the model adsorbates for the present study because of their high toxicity. MB is highly soluble in water which makes it one of the difficult dyes to be removed by adsorption process (El Qada et al. 2008). DR 81 is lost in the effluent to a significant amount, next to reactive dyes. Also, both these dyes have opposite charges which will help in determining the effectiveness of the non-modified soil in removing different types of dyes.

4.2 Materials & Methods

4.2.1 Adsorbent

The adsorbent used for the present study is locally available sandy soil from Rajasthan. It was collected from the premises of Malaviya National Institute of Technology, Jaipur. The collected soil was then washed with distilled water to remove the suspended impurities and then oven dried at 100°C for 2 hours. The dried soil was crushed and sieved to give particle sizes in the range of 300-150 μm and 150-75 μm using ASTM Standard sieves. Initially, the adsorption study was conducted on the soil of particle size in the range 300-150μm.

4.2.2 Adsorbate

Direct Red 81 and Methylene blue stock solutions were prepared as discussed in section 3.3.1.3.

4.2.3 Adsorption Study

The adsorption measurements were carried out by the batch method given in section 3.3.2.

4.3 Result & Discussion

4.3.1 Effect of Operating Parameters on Dye Removal

It is well known that the efficiency of dye adsorption onto the adsorbent surface depends on the parameters like pH, contact time, adsorbent dose, initial dye concentration and particle size of the adsorbent.

The present parametric study was conducted to determine adsorption capacity of the locally available non-modified soil for DR81 and MB samples prepared in the laboratory. The findings from this study were also used to determine optimum operational parameters for the treatment of aqueous solutions of DR81 and MB.

4.3.1.1 Effect of pH

pH is considered to be the most important parameter in the adsorption process. It affects the dye solution chemistry, functional group activity on the soil surface, and the composition of the dye (Pathak et al. 2015).

In this study, two classes of dyes were examined for their removal onto the soil surface. DR81 is an anionic dye and MB is a cationic dye. The experiments were conducted to find the optimum value of pH, for which maximum efficiency of colour removal can be attained. Therefore, experiments were performed at varying pH in the range of 1-11 while keeping the initial dye concentration, adsorbent dose and contact time constant. The optimum pH for maximum removal of DR81 and MB is reported in Figure 4.1(a) and (c).

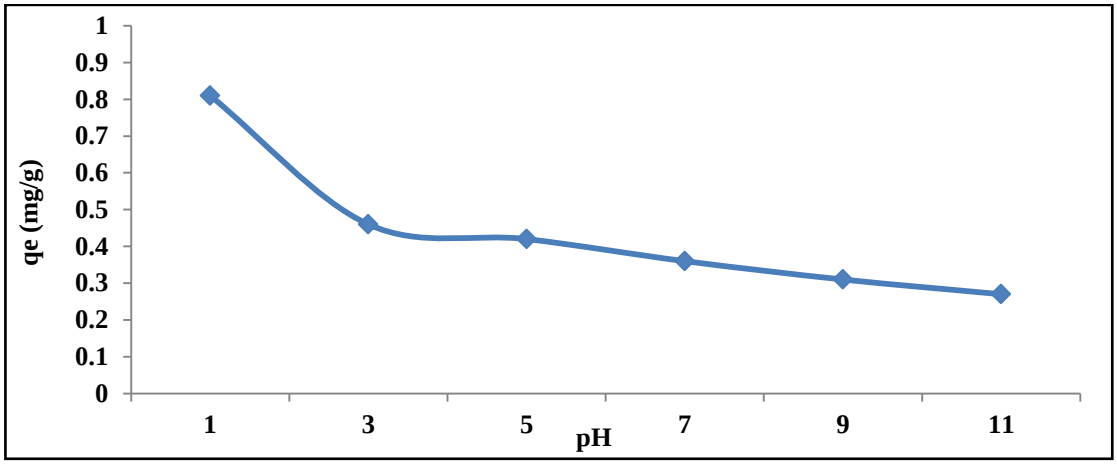

(a)

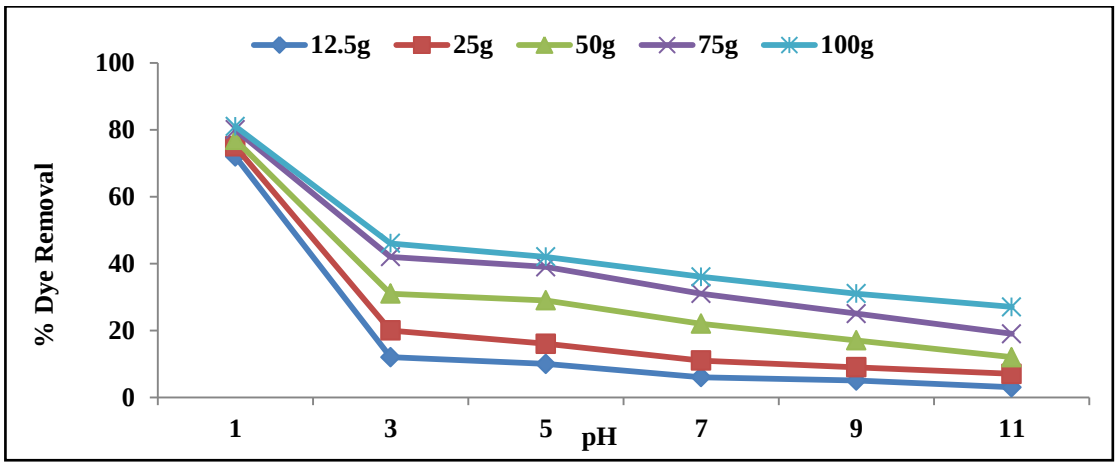

(b)

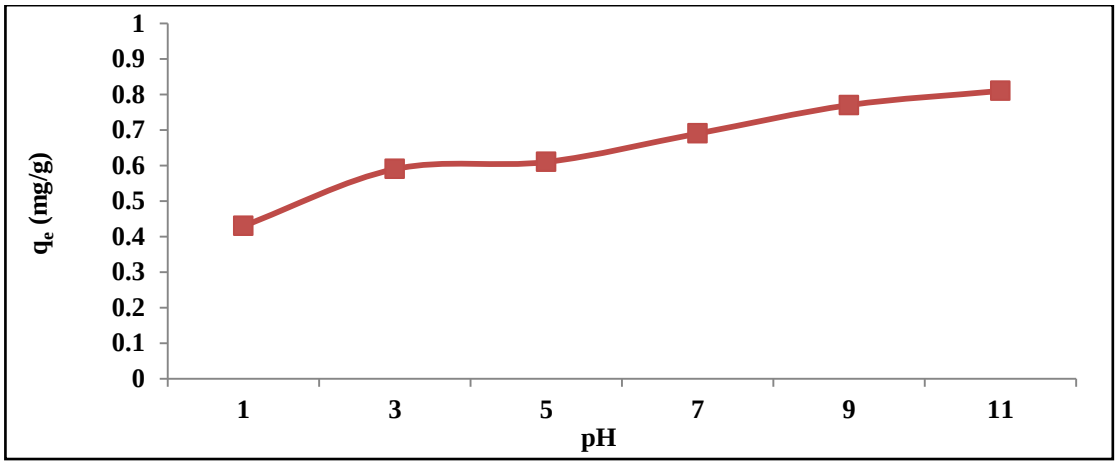

(c)

Figure 4.1: Effect of pH on dye removal (a) & (b) DR81; (c) MB (Condition: dye concentration: 1000 mg/L; contact time: 10 minutes, adsorbent dose: 100g/100mL)

Figure 4.1 (a) and (c) show the effect of pH on DR81 and MB removal from aqueous solution, respectively. It can be seen from the Figure 4.1(b) that at pH 1 almost 80% of the dye is removed, irrespective of the adsorbent concentration. Thus, it can be said that only pH is affecting the colour removal at pH 1. One more noteworthy fact observed at pH 1 was that the red colour of the dye was different from the original red colour, before adsorbent was added to it. The above observation suggests that at pH 1, the dominant mechanism for colour removal is chemical precipitation. However, when pH rises, surface adsorption becomes the primary mechanism for dye removal (Zhu et al. 2007). A similar finding was observed by (Bulut et al. 2008) for Congo Red (DR28) removal onto bentonite, for Congo Red onto Indian Jojoba seeds (Somasekhara Reddy et al. 2012) and for Acid Blue 80 onto alkaline white mud (Zhu et al. 2007). Therefore, it can be said that at certain pH, colour and its intensity change occurs due to the structural changes being affected in the dye molecule (Hao et al. 2000).

However, after that when pH shifts from acidic to basic condition i.e. from pH 3 to pH 11, a slow decrease in DR81 could be seen, varying according to the adsorbent concentration.

Whereas it can be observed, from Figure 4.1(c), that removal of MB increases with the increase in pH from 1 to 11. Dye removal constantly increases when the pH moves towards alkaline range. No colour change was observed for MB at this pH range as it

was observed for DR81. This could be due to high solubility of MB in water (El Qada et al. 2008).

Figure 4.2 shows the influence of the solution pH on the dye uptake can be explained on the basis of the pH zero point charge or isoelectric point of the adsorbent. The pH at which the surface charge of the adsorbent is zero is called the point of zero charge (pH_{zpc}) and is typically used to quantify or define the electrokinetic properties of the adsorbent surface. The value of pH is used to describe point zero charge only for systems in which H^+/OH^- are the potential determining ions. Due to the presence of functional group such as OH^-group, cationic dye adsorption is favoured at $pH>pH_{zpc}$, whereas, anionic dye adsorption is favoured at $pH<pH_{zpc}$ where the surface becomes positively charged (Salleh et al. 2011). The pH point of zero charge (pH_{zpc}) of the adsorbent is determined by powder addition method (Ponnusami et al. 2008). For this method, 10g of non-modified soil was added to 100ml capped conical flask containing 50ml of 0.1M NaCl solution. Several batches were carried out for various initial solution pH. The pH was adjusted using 0.01N H_2SO_4 and 0.01N NaOH solution. The electrolyte solution with non-modified soil was equilibrated for 2 hours. After equilibration, the final pH; pH_f, was recorded. Both positive & negative ΔpH (pH_i-pH_f) values recorded for the non-modified soil are plotted against the initial pH values. The zero point charge on the non-modified soil was found to be at pH 9.0.

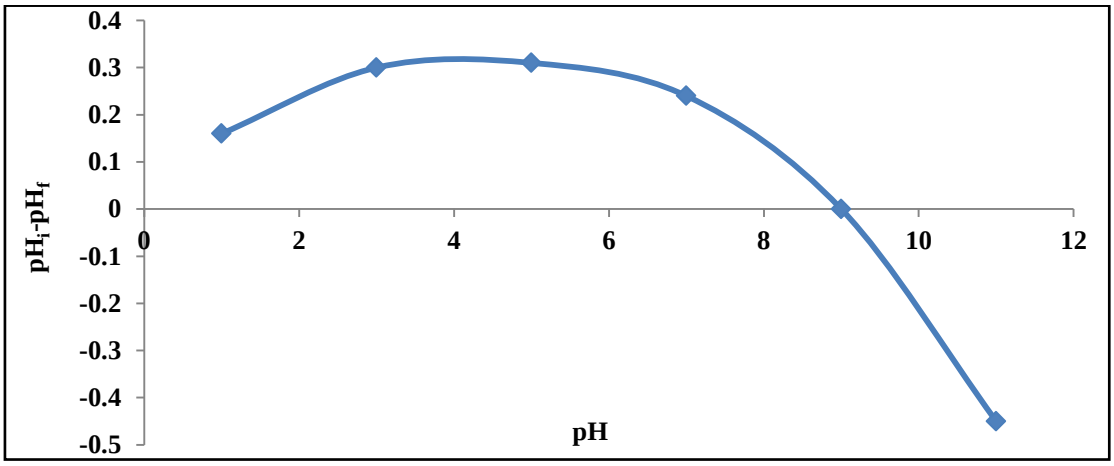

Figure 4.2: Point zero charge of soil

The major oxides present in the soil are Si, Al, Fe and Ca as shown in Table 4.9. The zero point charge of SiO_2, Al_2O_3, Fe_2O_3 and CaO are 2.2, 8.3, 8.5 and 11.0 respectively (Papić et al. 2004) (Mall et al. 2005). Therefore, except SiO_2, all the

mentioned oxides possess positive charge for the studied range of pH. The removal of DR81 may be influenced most by these positively charged oxides. A high electrostatic force exists between the positively charged sites of the non-modified soil and DR81. As seen from the Figure 4.1(a), at high pH dye removal decreased. This is due to the increase in the negatively charged sites, as the pH of the system is increased. The repulsion between the negatively charged sites and the dye anions reduces the rate of DR81 from the system. Also, there exists a competition between the OH^- ions and the dye anions at higher pH (Khaled et al. 2009). Similar results for the adsorption of anionic dye are observed on bagasse fly ash (Mall et al. 2005), almond shells (Doulati Ardejani et al. 2008). The removal of the MB as shown in Figure 4.1 (c) may be mostly influenced by the by the negatively charged silica oxides present on the non-modified soil surface. However, at acidic pH, the presence of an excess of H^+ ions reduces the adsorption of dye cations on active sites (Pavan et al. 2008). Similar results for the adsorption of methylene blue are observed on sepiolite (Doğan et al. 2007), jute fibre carbon (Senthilkumaar et al. 2005), montmorillonite clay (Almeida et al. 2009).

As the maximum removal of DR81 was found to be at pH 3 and for MB at pH 11, further all the tests were performed at these pH values for respective dye removal.

4.3.1.2 Effect of Contact Time

Contact time is the time required for the adsorption system to reach equilibrium. Some of the mass transfer steps in adsorption could be comparatively slow. Therefore, it is necessary to determine the contact time to make sure that the equilibrium is reached (Pathak et al. 2015).

In the present study, the optimum contact time for which maximum efficiency of colour removal can be attained was analysed. Experiments were conducted at varying contact time in the range of 0-60 minutes while keeping the initial dye concentration, adsorbent dose and pH constant. The optimum contact time for maximum removal of both the dyes is shown in Figure 4.3 (a) and (b).

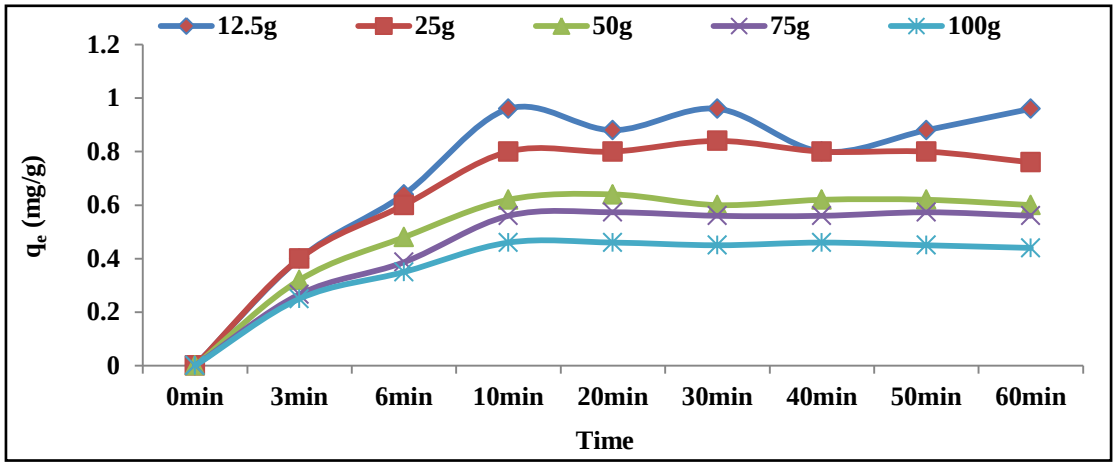

(a)

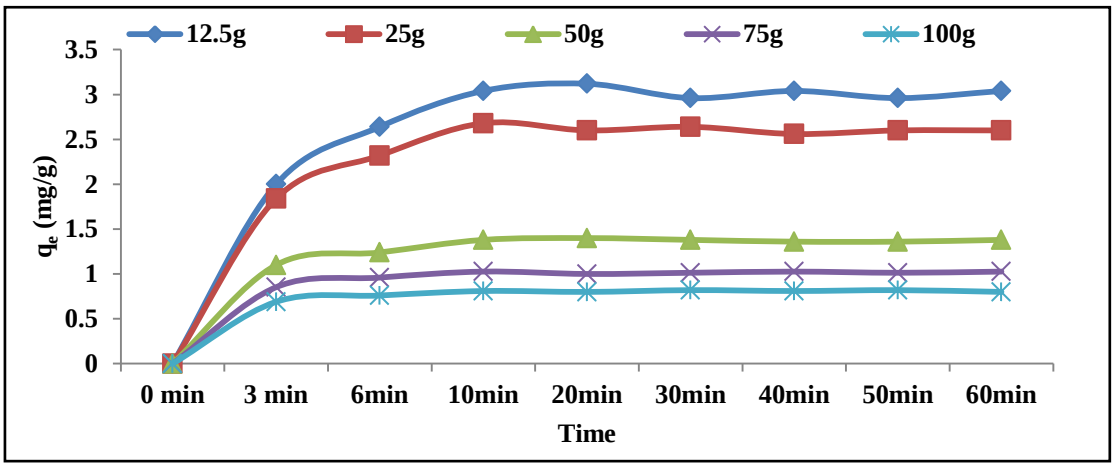

(b)

Figure 4.3: Effect of contact time on dye removal (a) DR81 and (b) MB (Condition: initial dye concentration: 1000 mg/L; pH: 3 for (a) & 11 for (b), adsorbent dose (per 100mL): 12.5g, 25g, 50g, 75g, 100g)

The Figure 4.3 (a) and (b) shows the effect of contact time on removal of DR81 and MB from aqueous solution, respectively. From the Figure 4.3 (a) and (b), it can be analysed that there is a fast uptake of the dye molecules till 10 minutes* of contact time and thereafter, the uptake becomes almost constant. However, the experimental data is measured till 60 minutes to make sure that a complete equilibrium is attained. Therefore, it can be said that the optimum contact time for the establishment of equilibrium is within 10 minutes.

The contact time between the dye molecule and the adsorbent is of significant importance in dye removal by adsorption. Rapid removal of colour and the relatively short period for the establishment of equilibrium signifies the efficacy of that

*These results may have been influenced because of limited data and therefore must be read accordingly.

adsorbent for its use at a commercial level. Generally, in physical adsorption, most of the dye molecules are adsorbed within a short interval of contact time. However, strong chemical binding of the dye molecule with adsorbent requires a longer contact time for the attainment of equilibrium. Available adsorption studies in literature reveal that the uptake of the dye molecule is fast at the initial stages of the contact period, and thereafter, the rate of adsorption is found to be nearly constant. At this point, the amount of the dye being adsorbed onto the adsorbent surface is in a state of dynamic equilibrium with the amount being desorbed from the adsorbent surface. The time required to attain this state of equilibrium is termed as the equilibrium time (t_e in min) and the amount of dye adsorbed at t_e reflected the maximum dye adsorption capacity of the adsorbent under these conditions. The high adsorption rate at the initial stages may be due to the high availability of the vacant sites for adsorption (Mall et al. 2006) (Rodr̀iguez et al. 2009) (Crini & Ndongo Peindy 2006)

For both the dyes, the adsorption was found to be extremely rapid for first 10 minutes and then become constant as the equilibrium was achieved. For the contact time range under which the experiments were conducted, the percent removal of MB was found to be higher than DR81. The percent removal increased from 21% to36% for DR81 and 38% to 81% for MB with an increase in adsorbent dose from 12.5g/100mL to 100g/100mL. However, the adsorption capacity decreased from 1.68 mgg^{-1} to 0.36 mgg^{-1} for DR81 and 3.04mgg^{-1} to 0.81mgg^{-1} for MB with an increase in adsorbent concentration as shown in Figure 4.3 (a) and (b). The reports indicate that a relatively larger contact time is required for the adsorption of MB and direct red dyes with classical adsorbents like sepiolite (Doğan et al. 2007), montmorillonite clay (Almeida et al. 2009), activated carbon (Lorenc-Grabowska & Gryglewicz 2006), orange peel (Doulati Ardejani et al. 2007), Ca-bentonite (Lian et al. 2009), etc. and they are some of the most difficult dyes to remove from aqueous solutions. Thus the high affinity shown by the locally available sandy soil for the adsorption of these dyes can result in an excellent low-cost alternative for treating the wastewater containing these dyes. Since a contact time of 10 minutes can be considered as the optimum time for MB and DR81 adsorption, so further tests in the next sections were performed at this contact time only.

4.3.1.3 Effect of Adsorbent Dose

To know the effect of adsorbent dose on the dye removal, the experiments were conducted at constant pH, initial dye concentration and contact time while varying the adsorbent dose in the range of 12.5g/100mL to 100g/100mL.

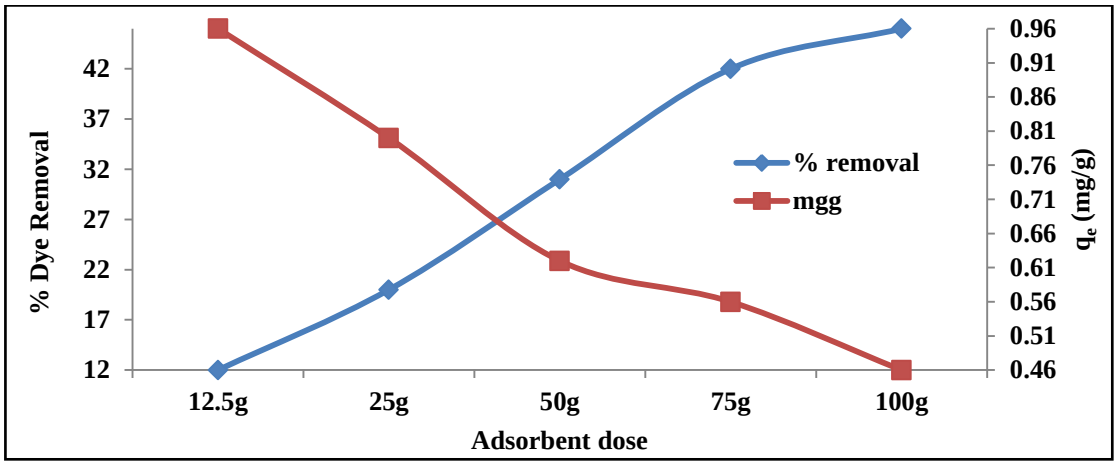

(a)

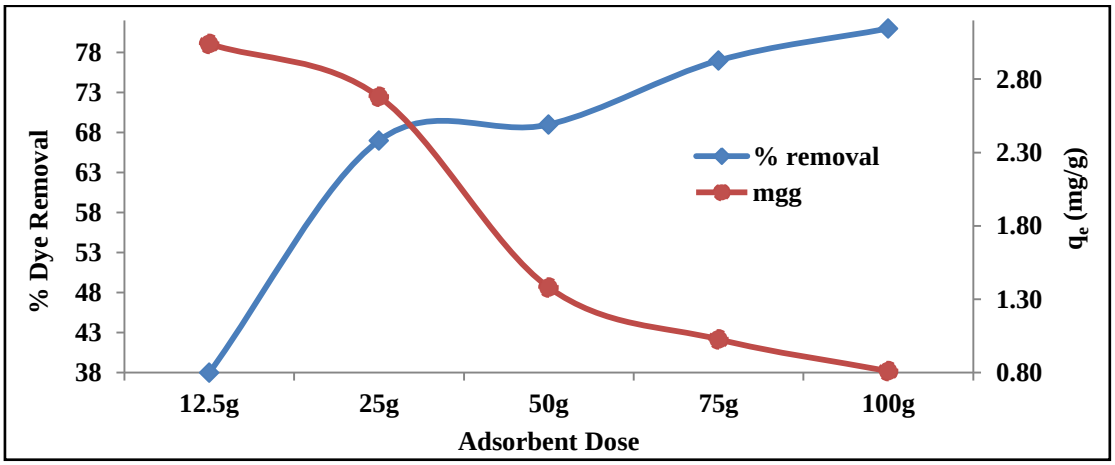

(b)

Figure 4.4 : Effect of adsorbent dose on percent dye removal (a) DR81 and (b) MB (Condition: dye concentration: 1000 mg/L; pH: 3 for DR81 & 11 for MB , contact time: 10 minutes, adsorbent dose(per 100mL): 12.5g, 25g, 50g, 75g, 100g; Particle size:300-150µm)

The effect of adsorbent dose on DR81 and MB removal has been shown in Figure 4.4 (a) and (b). It can be observed from Figure 4.4 (a) and (b) that there is an increase in the percent removal of both the dyes with the increase in the adsorbent dose. The plausible reason for this observation could be a greater number of exchangeable or

adsorption sites are available at a higher concentration of the adsorbent (Erdem et al. 2005), (Pathak et al. 2015). However, there is a decrease in the milligram of dye removal per gram of dye. This can be attributed to overlapping or aggregation of adsorption sites resulting in a decrease in the total adsorbent surface area available to dye and increase in diffusion path length (Crini et al. 2007). Table 4.1 illustrates the data obtained in percent removal and mgg^{-1} for de removal. Similar results have been reported on melon husk (Olajire et al. 2015), montmorillonite clay (Almeida et al. 2009).

Adsorbent dose	**% removal**		**q_e mgg^{-1}**	
	MB	DR81	MB	DR81
12.5g/100mL	38	12	3.04	0.96
25g/100mL	67	20	2.68	0.80
50g/100mL	69	31	1.38	0.62
75g/100mL	77	42	1.03	0.56
100g/100mL	81	46	0.81	0.46

Table 4.1: Effect of adsorbent dose on DR81 and MB removal (Condition: dye concentration: 1000 mg/L; pH: 3 for DR81 & 11 for MB, contact time: 10 minutes)

The amount of DR81 dye removal per unit mass of non-modified soil at equilibrium is very less in the chosen adsorbent dose range. Therefore, the lower range of adsorbent dose was not tried. It was also observed that MB showed better adsorption at equilibrium onto soil surface as compared to DR81. Thus, this adsorbent range was considered for further experiments.

4.3.1.4 Effect of Initial Dye Concentration

Effect of initial dye concentration was analysed at a constant adsorbent dose, pH and contact time while varying the dye concentration in the range of 125 mg/L to 1000 mg/L. The initial dye concentration provides a necessary driving force to overcome the mass transfer resistance between the dye in the bulk phase and non-modified soil. Higher initial concentrations give higher loading capacity (Pathak et al. 2015) (Almeida et al. 2009).

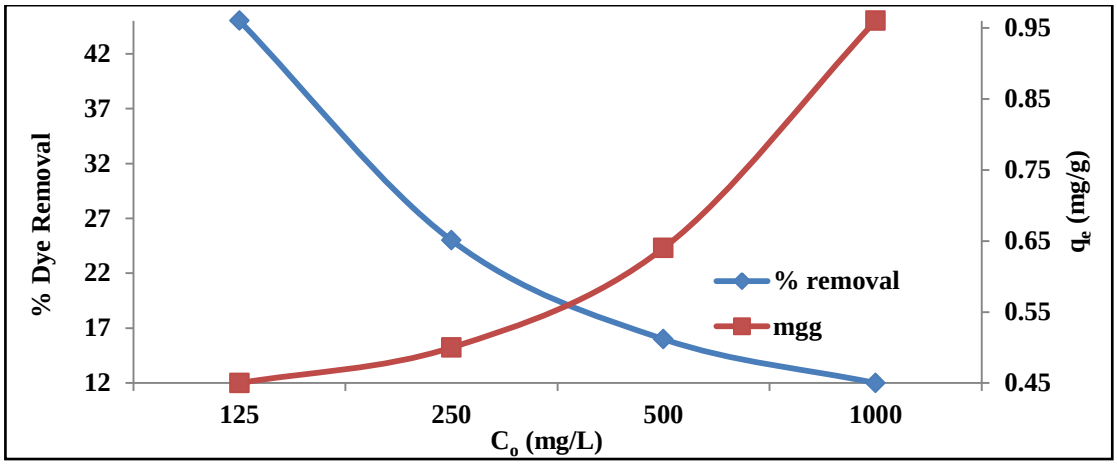

(a)

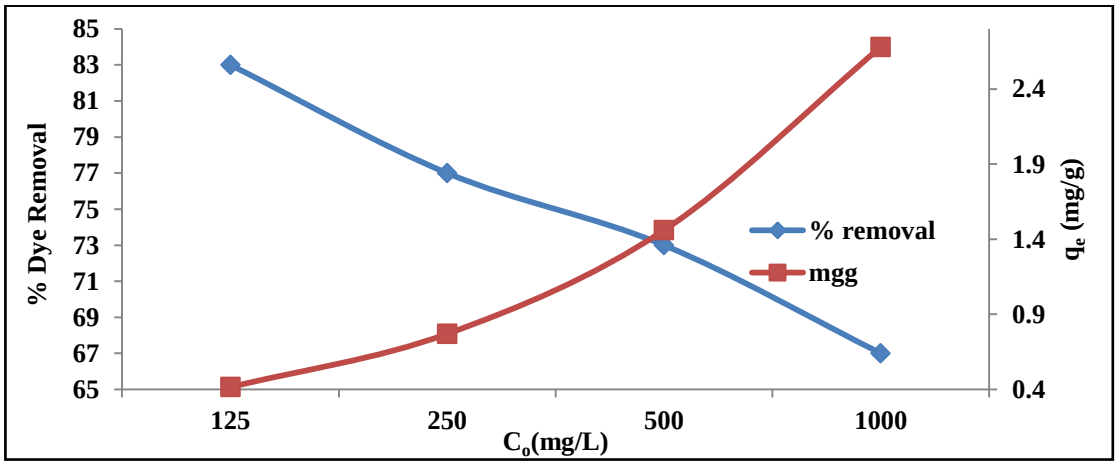

(b)

Figure 4.5: Effect of initial dye concentration on dye removal (a) DR81 and (b) MB (Condition: adsorbent dose: 25g/100mL, pH: 3 for DR81 & 11 for MB, contact time: 10 minutes, initial dye concentration: 125mg/L, 250mg/L, 500mg/L, 1000mg/L)

Effect of initial DR81 and MB concentration has been shown in Figure 4.5 (a) and (b). It can be observed from the Figure 4.5 (a) and (b) that there is a decrease in the percent dye removal with the increase in dye concentration. But the actual amount of MB and DR81 adsorbed per unit mass of non-modified soil was increased with increase in dye concentration. Table 4.2 illustrates the data obtained in percent removal and mgg^{-1} for dye removal. Similar research has been reported on the removal of MB on jute fibre carbon (Senthilkumaar et al. 2005), Congo Red on activated carbon and activated sawdust (Jain & Sikarwar 2008), Direct Red80 on almond shells (Doulati Ardejani et al. 2008).

Dye Concentration	% removal		q_e mgg^{-1}	
	MB	DR81	MB	DR81
125mg/L	83	55	0.42	0.28
250mg/L	77	42	0.77	0.42
500mg/L	73	28	1.46	0.56
1000mg/L	67	20	2.68	0.80

Table 4.2: Effect of initial dye concentration on DR81 and MB removal (Condition: adsorbent dose: 25g/100mL, pH: 3 for DR81 & 11 for MB, contact time: 10 minutes)

It was also observed that MB removal was better than DR81 in the considered dye concentration range. Therefore, this concentration range was further used in the later part of the research.

4.3.1.5 Effect of Particle Size

Surface area increases with a decrease in particle size. A higher surface area gives more number of binding sites for adsorption. Small particle size lowers the mass transfer driving force per unit area of adsorbent particles, which increases the uptake/saturation capacity per unit mass of soil (Pathak et al. 2015).

The effect of particle size on the percent dye removal was analysed on two different particle sizes of soil i.e. 300-150 µm and 150-75 µm respectively.

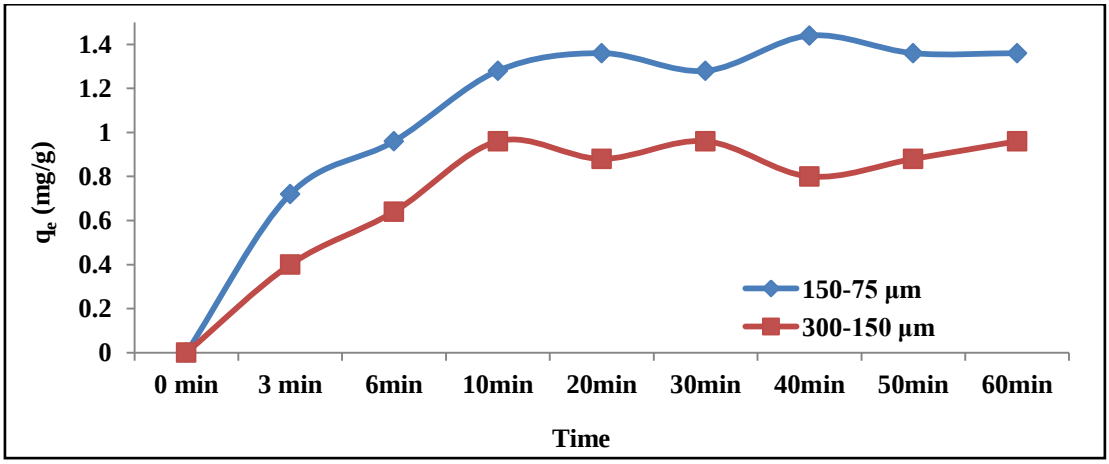

(a)

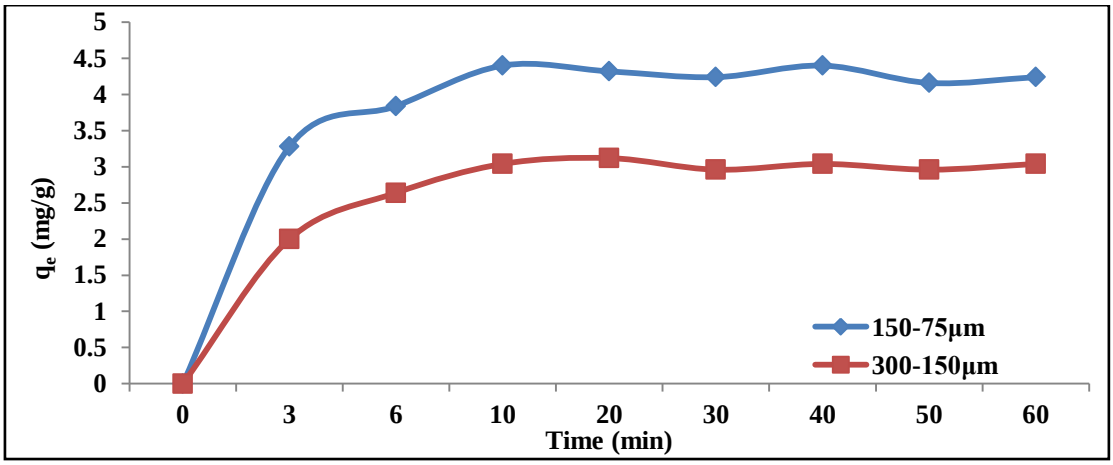

(b)

Figure 4.6: Effect of particle size of non-modified soil on dye removal (a) DR81 and (b) MB (Condition: initial dye concentration: 1g/L; pH: 3 for (a) & 11 for (b), adsorbent dose: 12.5g/100mL)

Fig 4.6 (a) and (b) shows the effect of the particle size of soil on DR81 and MB adsorption, respectively. Two different particle size ranges (300-150µm & 150-75µm) were analysed for this purpose. When the particle size was decreased from 300-150µm to 150-75µm, the adsorption capacity of soil was increased from 0.96mgg^{-1} to 1.28 mgg^{-1} for DR81 and 3.04mgg^{-1} to 4.4 mgg^{-1} for MB. Adsorption is a surface phenomenon; therefore, specific surface area (m^2/g) of the adsorbent particle plays an important role in dye removal. The value of specific surface area increased from 0.0441 m^2/g to 0.0783 m^2/g as the particle size decreased from 300-150µm to 150-75µm (Table 4.3). And, as a consequence, adsorption capacity per unit mass of non-modified soil increased. Increase in the external surface area of smaller particles removes more dye in the initial stages of the adsorption process than large particles (Erdem et al. 2005)(Crini et al. 2007). (McKay 1982) and (Robinson et al. 2002) reported the similar kind of observations. Also, non-modified soil provides good colour removal at reasonably larger size than other low-cost adsorbents like clay minerals. Therefore, it reduces the hydraulics problem (Mundada et al. 2017). All the further experiments were conducted on the soil of particle size 150-75µm as it showed better adsorption. Figure 4.7 & Table 4.3 represents the particle size distribution curve.

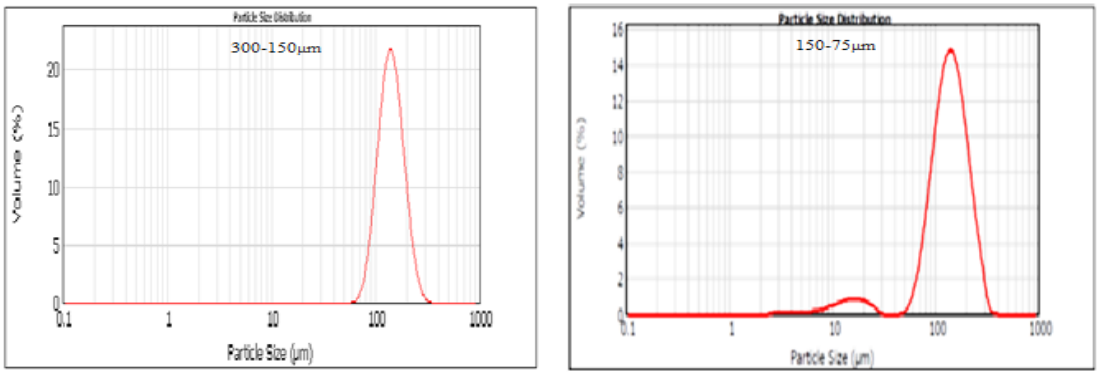

Figure 4.7: Particle Size Distribution curve of soil

Table 4.3: Particle Size Distribution of soil

Parameter	300-150 µm	150-75 µm
Uniformity	0.2	0.35
Specific surface area	0.0441m^2/g	0.0783 m^2/g
Surface weighted mean	135.948 µm	76.655 µm
Volume weighted mean	146.194 µm	140.556 µm
D(0.1)	99.690 µm	74.173 µm
D(0.5)	140.532 µm	135.622 µm
D(0.9)	200.237 µm	122.907 µm

4.3.2 Kinetic Modelling

Kinetic models are used to test experimental data, predict the mechanism of adsorption and find out the potential rate controlling steps such as mass transport and chemical reaction processes in adsorption (Kumar 2006). To investigate the adsorption kinetics of MB and DR81 on non-modified soil, three equations have been tested in the following sections; namely, Lagergren's pseudo first order model, Lagergren's pseudo second order model and intraparticle diffusion model.

4.3.2.1 Lagergren's Pseudo First Order Kinetic Model

The linearised plot of $\ln(q_e - q_t)$ versus t gives straight line. The first order rate constant k_1 is calculated from slope and q_e is calculated from intercept of this plot. The Table B.1 from Appendix B illustrates Lagergren's pseudo first order kinetic

parameters at various adsorbent doses for the adsorption of 125 mg/L, 250 mg/L, 500 mg/L, and 1000 mg/L of MB and DR81 concentration. This model assumes adsorption rate to be proportional to the first power of concentration, where the adsorption is characterized by diffusion through a boundary (Salleh et al. 2011).

From the Table B.1, it can be observed for both the dyes that the correlation coefficient (R^2) values do not fit well with the experimental data. The experimental data deviates greatly from linearity. Also, the predicted equilibrium adsorption capacities do not agree with experimental values. Thus, it could be said that adsorption on non-modified soil does not follow Lagergren's pseudo first order model.

4.3.2.2 Lagergren's Pseudo Second Order Kinetic Model

Kinetic data were further analysed with the pseudo-second-order kinetic model. This model assumes that chemisorption may be the rate-controlling step in the adsorption processes (Salleh et al. 2011). If the pseudo-second-order kinetics is applicable, the plot of $\frac{t}{q_t}$ and t should show a linear relationship as shown in Figure 4.8. The correlation coefficients (R^2), the second-order rate constants (k_2) and predicted (q_e^{pred}) and experimental (q_e^{exp}) equilibrium adsorption capacities are shown in Table B.2 in Appendix B for both dyes; DR81 and MB. The experimental data q_e^{exp} agreed well with predicted data q_e^{pred} under all work conditions for two dyes. The correlation coefficients for the second-order kinetic model are higher than 0.99 in all cases. The values of q_e^{exp} increased with increasing concentration of both dyes presumably due to the enhanced mass transfer of dye molecules to the surface of non-modified soil. This observation suggested that the boundary layer resistance was not the rate-limiting step (Doğan et al. 2009). However, values of k_2 declines gradually with an increase in the initial dye concentration for both the dyes, which suggests that there exists a competition between dye molecules at higher concentration for the adsorbent active sites (Albadarin et al. 2012). These results, which confirmed that the adsorption of dyes by non-modified soil is best described by the pseudo-second-order model are in agreement with many work in literature (Lian et al. 2009), (Khaled et al. 2009), (Doulati Ardejani et al. 2007).

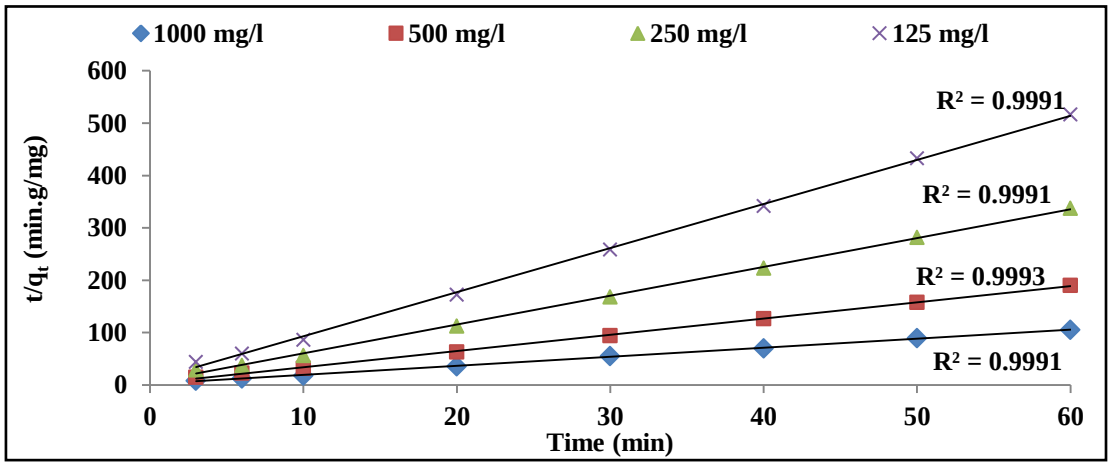
1000 mg/l
500 mg/l
250 mg/l
125 mg/l
t/qt (min.g/mg)
Time (min)
R² = 0.9991
R² = 0.9991
R² = 0.9993
R² = 0.9991

(a)

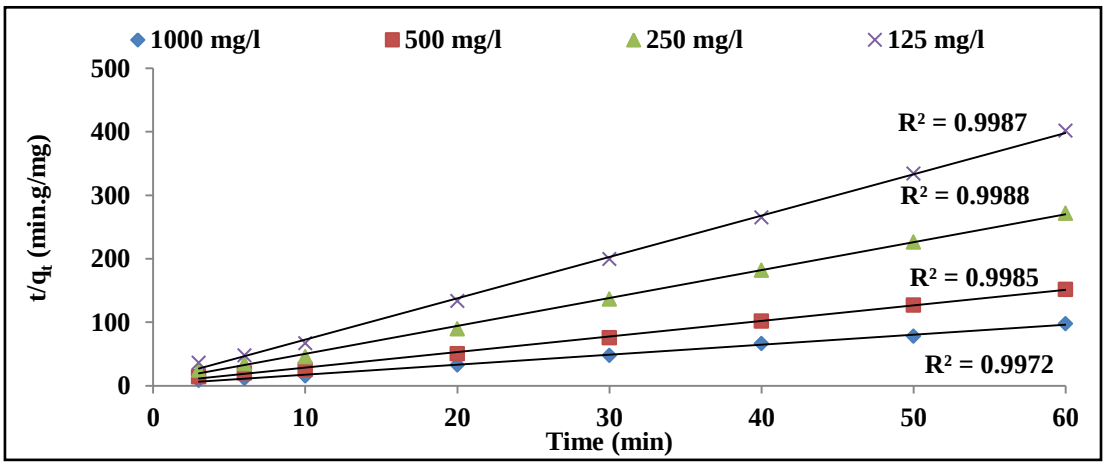
1000 mg/l
500 mg/l
250 mg/l
125 mg/l
t/qt (min.g/mg)
Time (min)
R² = 0.9987
R² = 0.9988
R² = 0.9985
R² = 0.9972

(b)

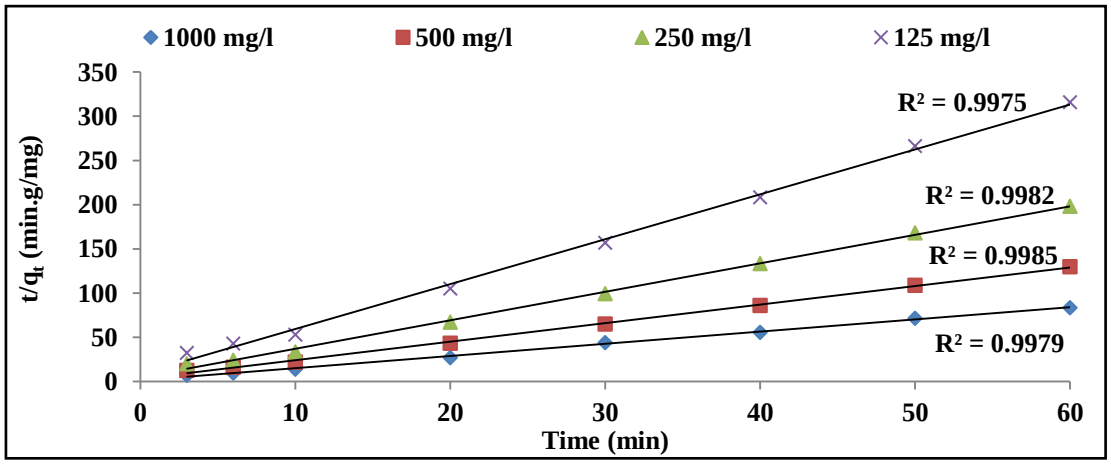
1000 mg/l
500 mg/l
250 mg/l
125 mg/l
t/qt (min.g/mg)
Time (min)
R² = 0.9975
R² = 0.9982
R² = 0.9985
R² = 0.9979

(c)

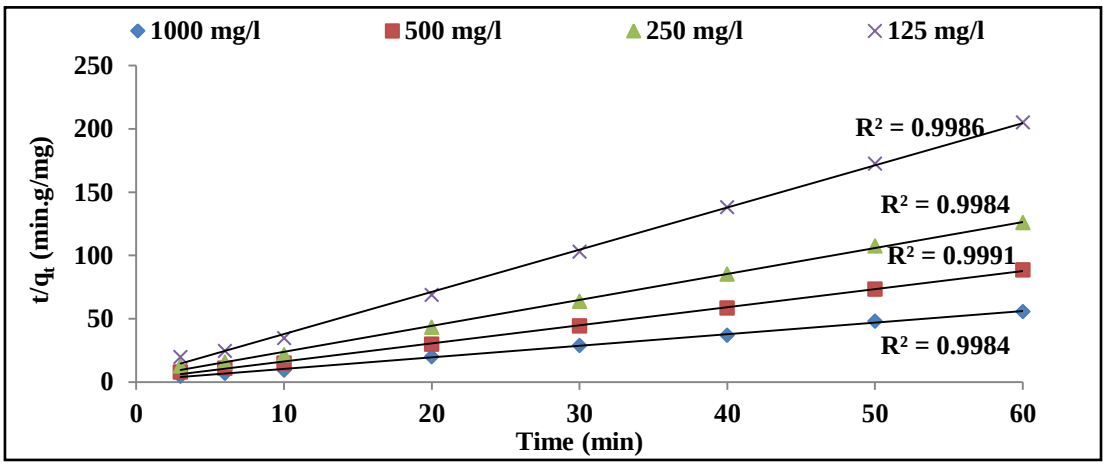

(d)

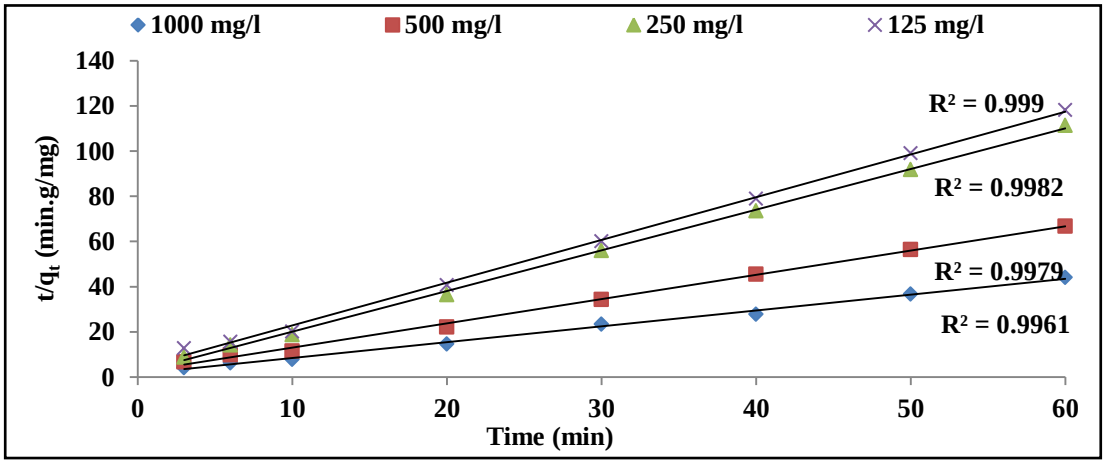

(e)

Figure 4.8: Lagergren's Pseudo Second Order Kinetic Plot for Adsorption of DR81 (a) 100g/100mL (b) 75g/100mL (c) 50g/100mL (d) 25g/100mL (e) 12.5g/100mL

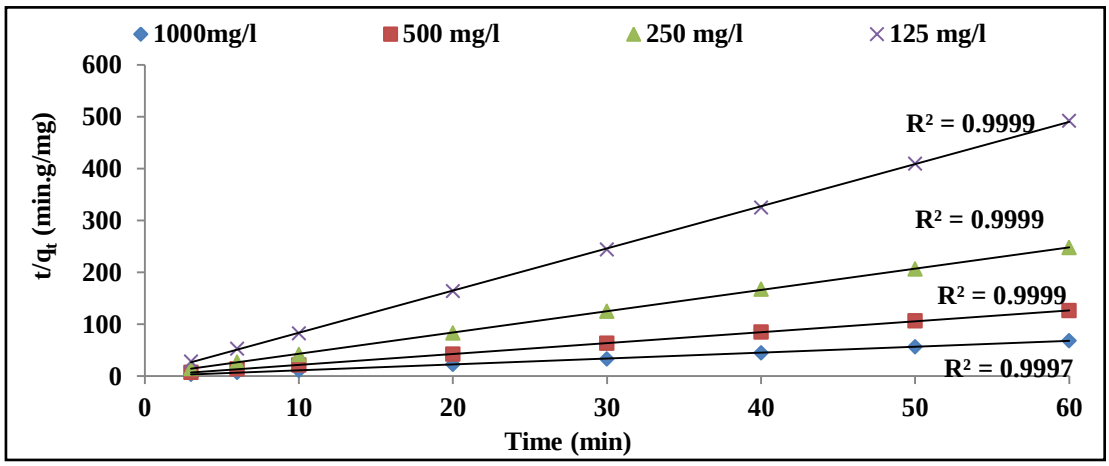
1000mg/l
500 mg/l
250 mg/l
125 mg/l
t/qt (min.g/mg)
600
500
400
300
200
100
0
0
10
20
30
40
50
60
Time (min)
R² = 0.9999
R² = 0.9999
R² = 0.9999
R² = 0.9997

(a)

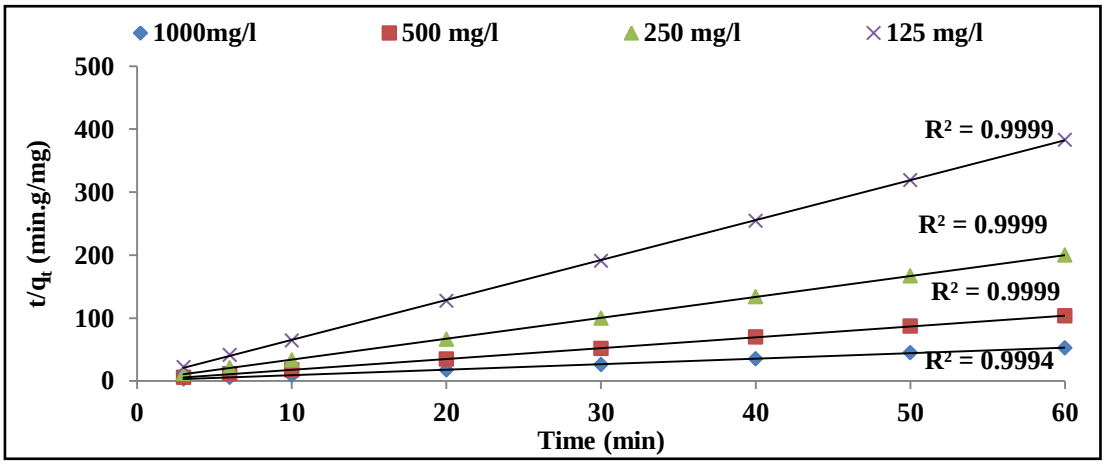
1000mg/l
500 mg/l
250 mg/l
125 mg/l
t/qt (min.g/mg)
500
400
300
200
100
0
0
10
20
30
40
50
60
Time (min)
R² = 0.9999
R² = 0.9999
R² = 0.9999
R² = 0.9994

(b)

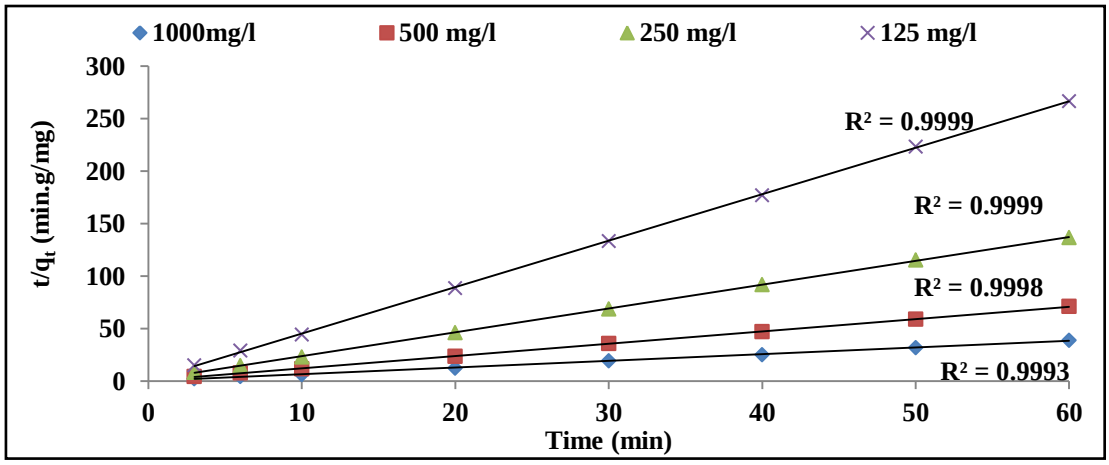
1000mg/l
500 mg/l
250 mg/l
125 mg/l
t/qt (min.g/mg)
300
250
200
150
100
50
0
0
10
20
30
40
50
60
Time (min)
R² = 0.9999
R² = 0.9999
R² = 0.9998
R² = 0.9993

(c)

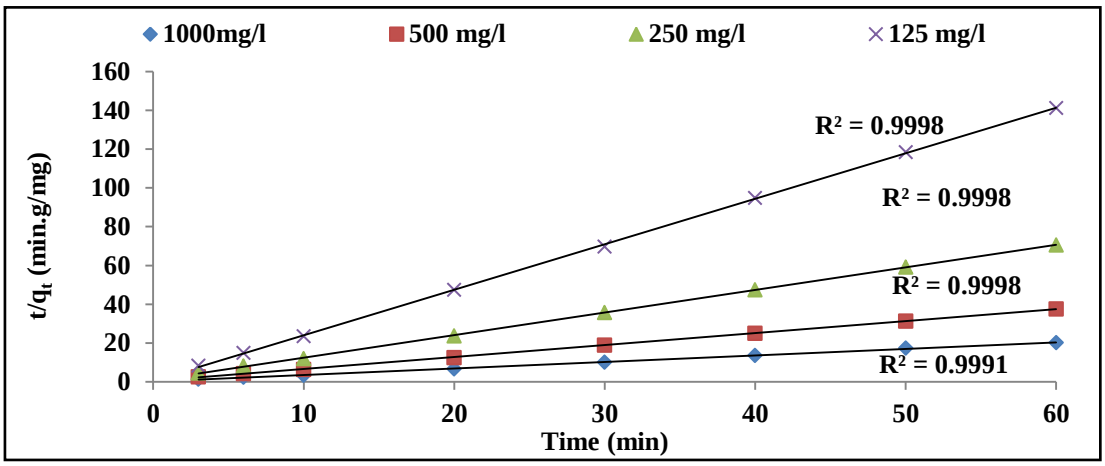

(d)

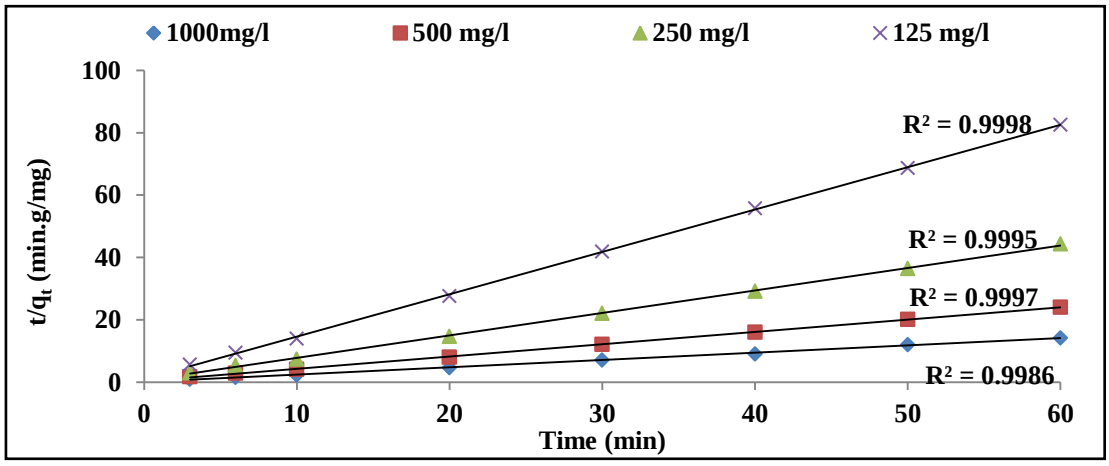

(e)

Figure 4.9: Lagergren's Pseudo Second Order Kinetic Plot for Adsorption of MB (a) 100g/100mL (b) 75g/100mL (c) 50g/100mL (d) 25g/100mL (e) 12.5g/100mL

4.3.2.3 Intraparticle Diffusion Model

The pseudo-first-order and pseudo-second-order kinetic models do not identify the diffusion mechanism. Thus the kinetic results were further analyzed by using the intraparticle diffusion model. Weber and Morris model (Weber & Morris 1963) is used to investigate intra-particle diffusion mechanism by plotting a graph between, q_t versus $t^{0.5}$. If the intra-particle diffusion is the only rate-controlled step, then the plot shall pass through the origin. Else it is understood that the boundary layer diffusion controls the adsorption to some degree. As seen from Figure 4.10 & 4.11, the plots are not linear over the entire time range, implying that more than one process affected the adsorption and a similar behaviour is reported by (Amin 2009). Further, the plots showed two regions. One, at the beginning of adsorption, representing the rapid surface loading, followed by the second representing pore diffusion. The Microsoft Excel 2010 software package was used to analyze various regions and results of linear regression are obtained for various initial concentrations. The intra-particle diffusion parameter, k_i , is determined from the slope of each region, while the intercept C of each region is proportional to the boundary-layer thickness. The values of $k_{i_1}$and k_{i_2} and the intercept, C_1 and C_2, for both the regions are given in Table B.3 in Appendix B. It is obvious from the Table B.3, that values of $k_{i_2}$for DR81 are greater than the values of k_{i_2} for MB at all the adsorbent doses and dye concentrations. And, values of C_2 for MB are greater than values of C_2 for DR81 at all the adsorbent doses and dye concentrations. Thus, it could be presumed that most of the DR81 is removed through the pore diffusion and adsorption onto the soil surface played a lesser role. However, in case of MB removal, it is the soil surface which supported dye removal. This feature of dye removal could be explained based on the molecular size of the dye and average pore size of the adsorbent. MB is reported to have a molecular size of MB is 112 Å or 11.2 nm (Simoncic & Armbruster 2005). From Table 4.10, the reported average pore size of non-modified soil is 19.861 Å. Thus, this explains the adsorption of MB on the soil surface as the dye molecule is much greater than the average pore size. Data on the molecular size of DR81 is not available in detail. However, to explain the adsorption, Congo red dye is taken as model because DR81 belongs to the same dye family and have almost same molecular weight and structure. The reported depth and width of the ionized Congo red dye is 7.4 Å and 26.2 Å. Therefore, the

width of the dye may contribute to the steric hindrance (Pelekani & Snoeyink 2001). But the process of pore diffusion is assisted as non-modified soil acquires positive charge at pH 3. But, DR81 is oppositely charged. Thus, dye anions experience physical and electrical forces to overcome steric hindrance and diffuse through pores (El Qada et al. 2008).

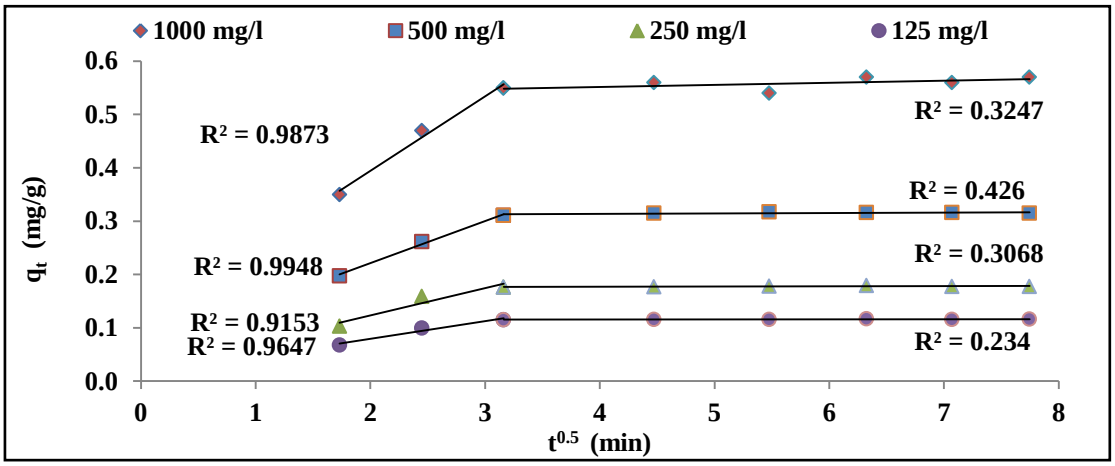

(a)

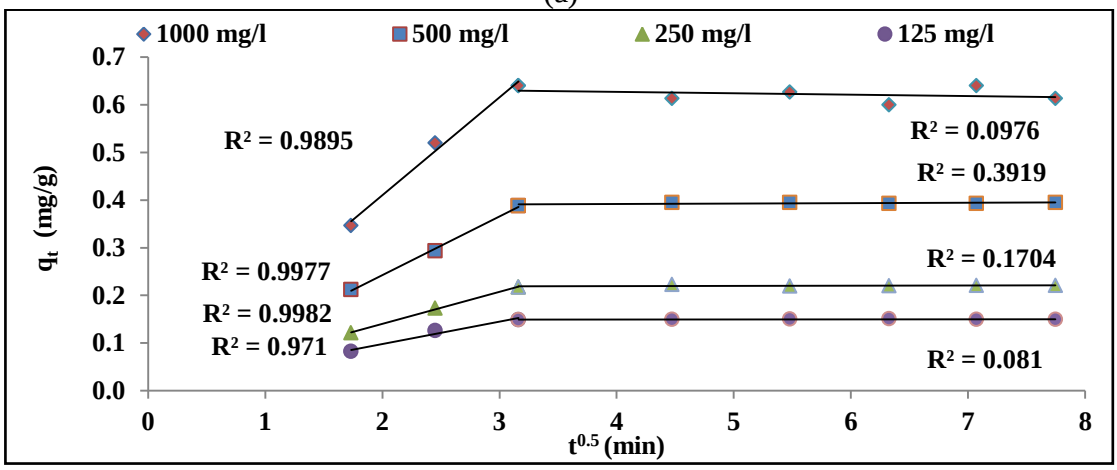

(b)

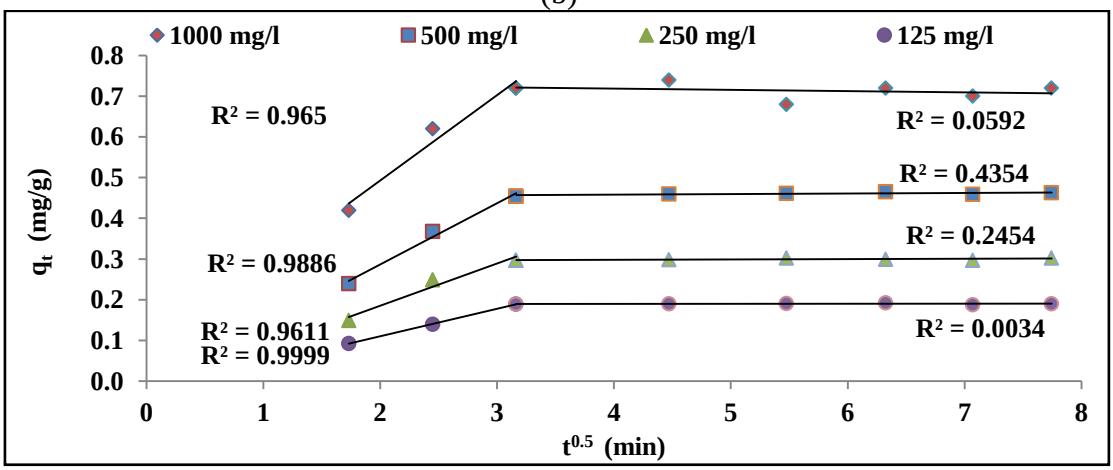

(c)

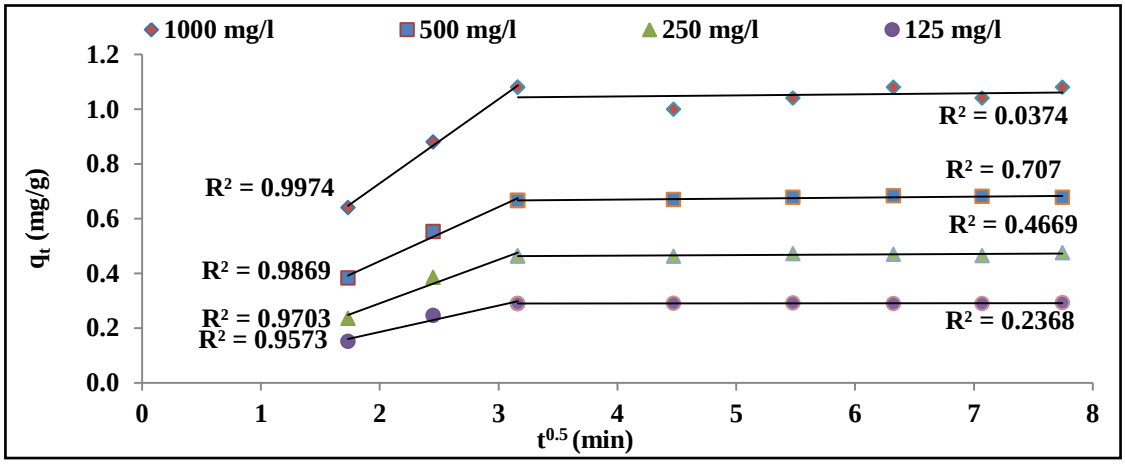

(d)

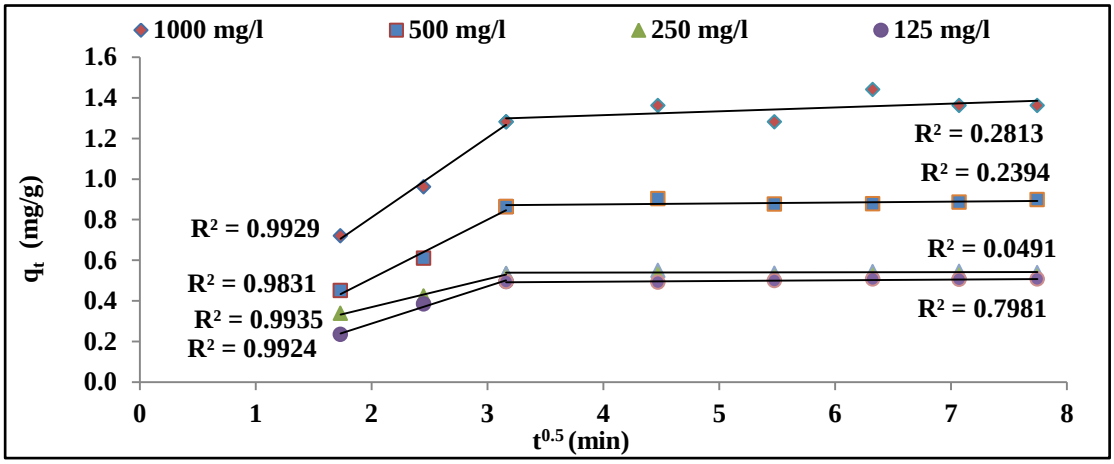

(e)

Figure 4.10: Intraparticle Diffusion Parameters for Adsorption of DR81 (a)100g/100mL (b) 75g /100mL (c) 50g/100mL (d) 25g/100mL (e) 12.5g/100mL

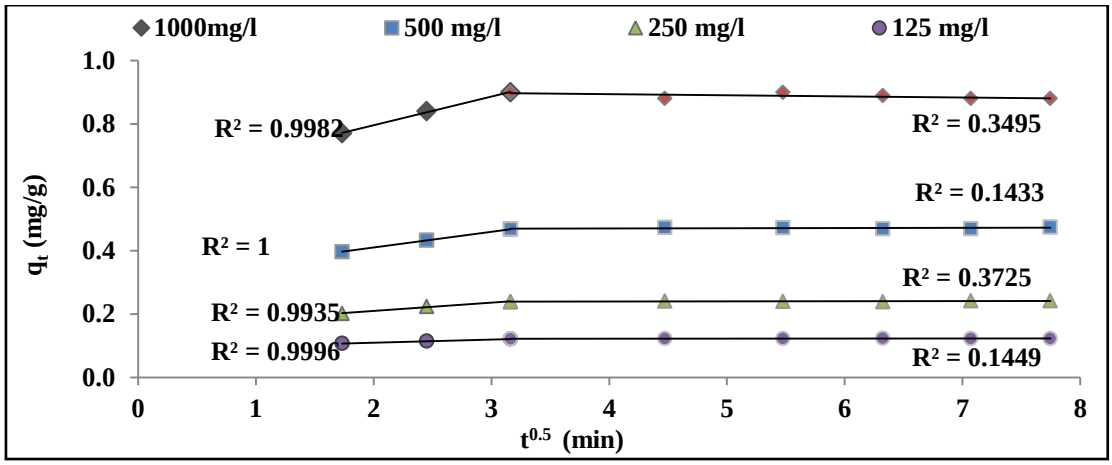
1000mg/l
500 mg/l
250 mg/l
125 mg/l
1.0
0.8
0.6
0.4
0.2
0.0
q_t (mg/g)
R^2 = 0.9982
R^2 = 0.3495
R^2 = 0.1433
R^2 = 1
R^2 = 0.3725
R^2 = 0.9935
R^2 = 0.9996
R^2 = 0.1449
0
1
2
3
4
5
6
7
8
$t^{0.5}$ (min)

(a)

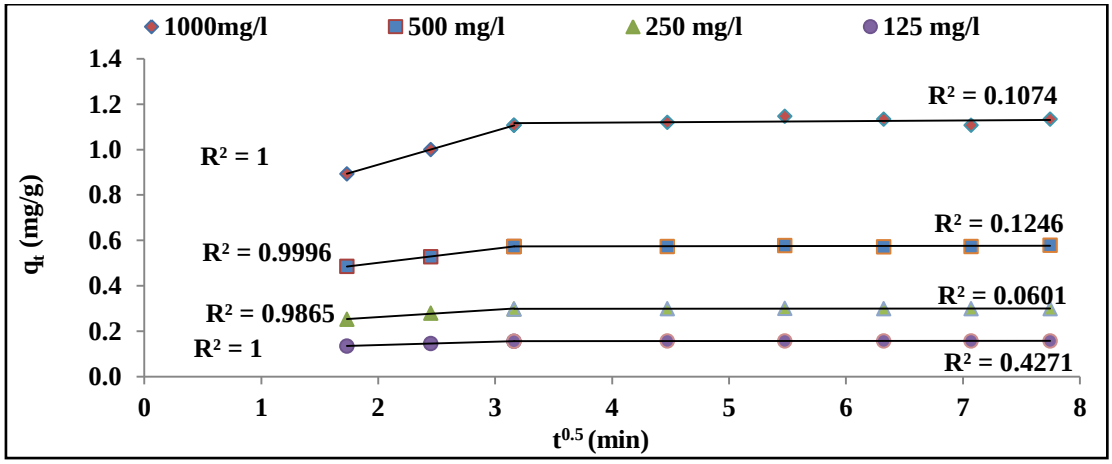
1000mg/l
500 mg/l
250 mg/l
125 mg/l
1.4
1.2
1.0
0.8
0.6
0.4
0.2
0.0
q_t (mg/g)
R^2 = 0.1074
R^2 = 1
R^2 = 0.1246
R^2 = 0.9996
R^2 = 0.0601
R^2 = 0.9865
R^2 = 1
R^2 = 0.4271
0
1
2
3
4
5
6
7
8
$t^{0.5}$ (min)

(b)

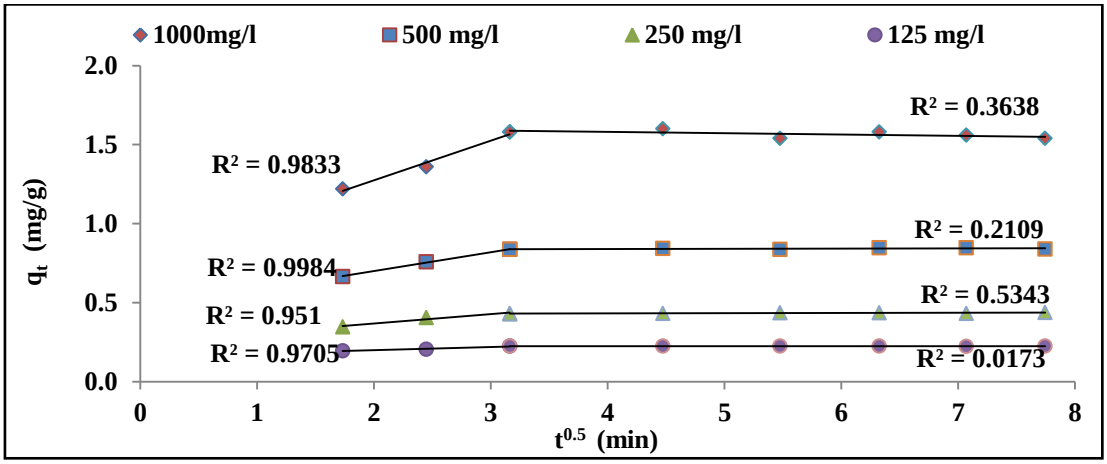
1000mg/l
500 mg/l
250 mg/l
125 mg/l
2.0
1.5
1.0
0.5
0.0
q_t (mg/g)
R^2 = 0.3638
R^2 = 0.9833
R^2 = 0.2109
R^2 = 0.9984
R^2 = 0.5343
R^2 = 0.951
R^2 = 0.9705
R^2 = 0.0173
0
1
2
3
4
5
6
7
8
$t^{0.5}$ (min)

(c)

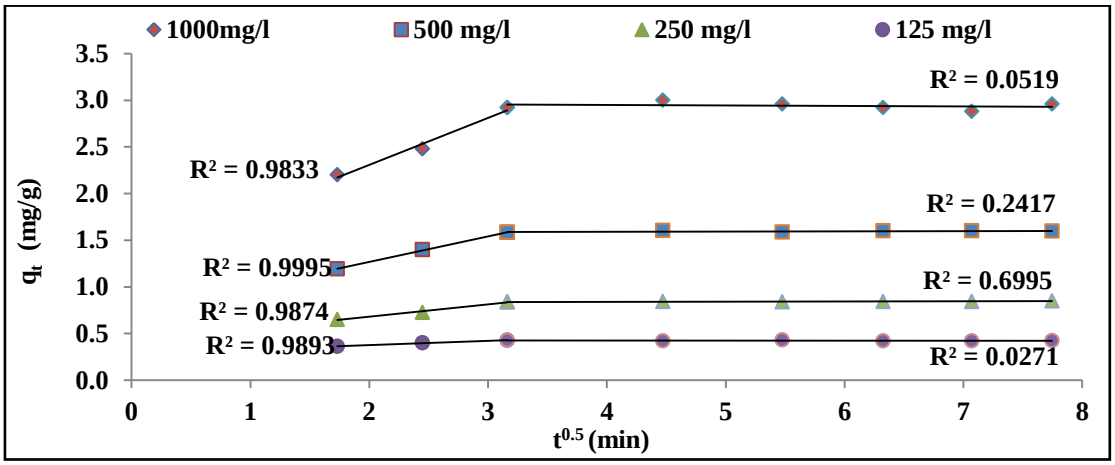

(d)

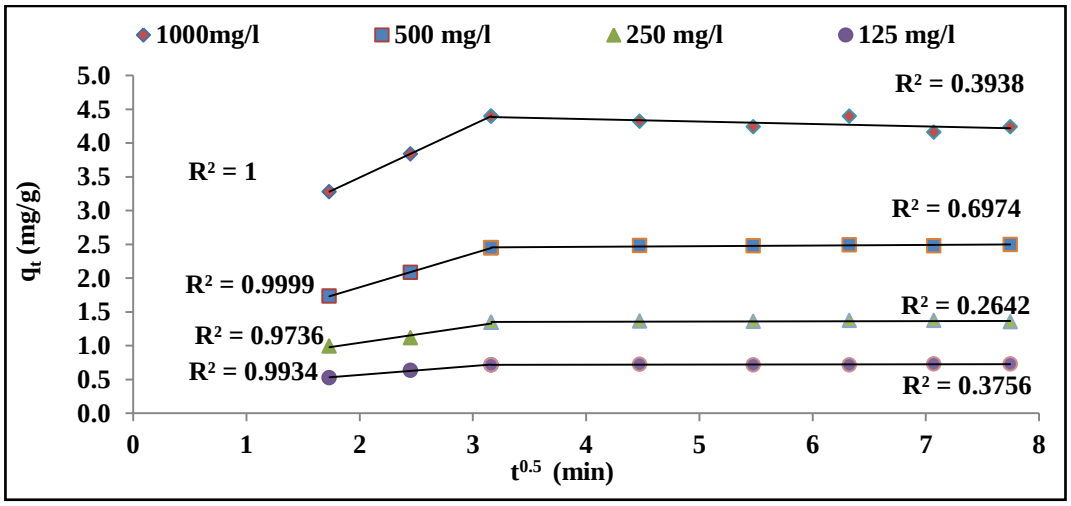

(e)

Figure 4.11: Intraparticle Diffusion Parameters for Adsorption of MB
(a)100g/100mL (b) 75g /100mL (c) 50g/100mL (d) 25g/100mL (e) 12.5g/100mL

4.3.3 Equilibrium Study

Adsorption isotherms describe of how dye molecules interact with the non-modified soil surface. They also help in optimizing the design of an adsorption system. Therefore, it is important to establish the most appropriate correlation for the equilibrium curves (Mall et al. 2005)(Somasekhara Reddy et al. 2012). Hence, two important isotherms have been used in this chapter, which are, namely Langmuir, and Freundlich isotherms. Linear regression analysis was carried out for all adsorbent doses with both the two models using Microsoft Excel.

The calculated values of the Langmuir and Freundlich equation's parameters are given in the Table 4.3. Negative values for Langmuir constants indicate the inadequacy of the isotherm model to explain the adsorption process. The positive values for the Freundlich isotherm constants indicate heterogeneous surface binding (Robinson et al. 2002)(Ramakrishna & Viraraghavan 1997). The comparison of correlation coefficients (R^2) of the linearised form of both equations also indicates that the Freundlich model yields a better fit for the experimental equilibrium adsorption data than the Langmuir model for the both the dyes; DR81 and MB. Similar results have been observed by many researchers (Ahmad et al. 2007),(Jain & Sikarwar 2008),(Kargi & Ozmihci 2004). Since the value of $n < 1$, for both the dyes in all the cases, it show that the adsorption is chemical (Khaled et al. 2009). Figure 4.12 & 4.13 shows Freundlich plots for both dyes; DR81 and MB.

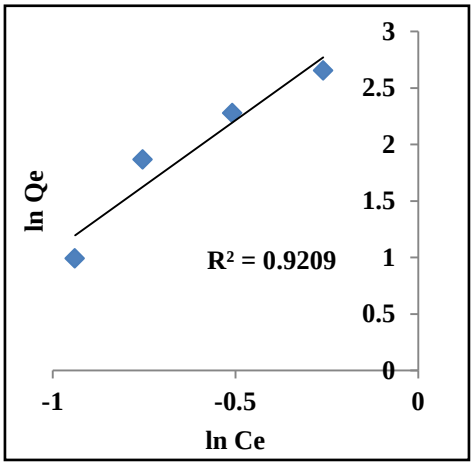

(a)

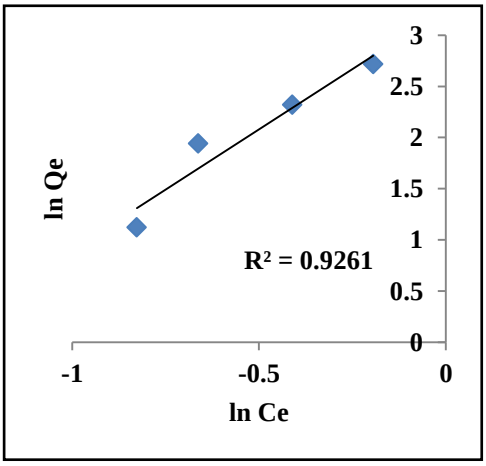

(b)

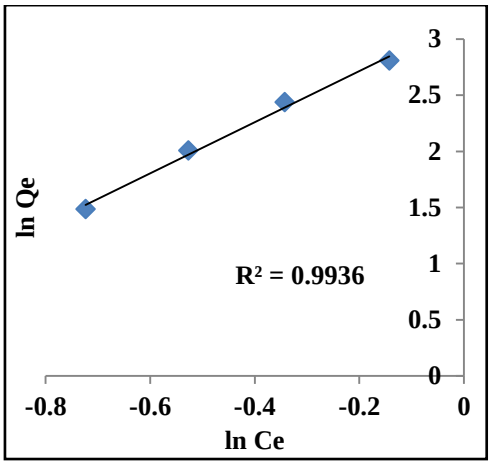

(c)

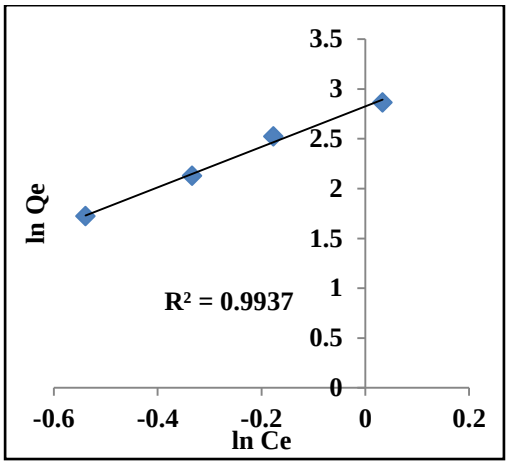

(d)

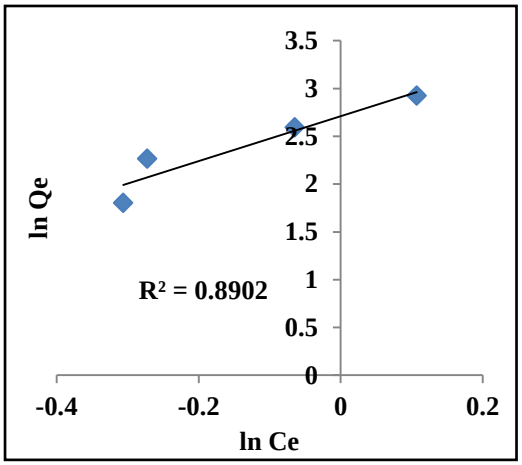

(e)

Figure 4.12: Freundlich isotherm plots For DR81 (a) 100g/100mL (b) 75g/100mL (c) 50g/100mL (d) 25g/100mL (e) 12.5g/100mL

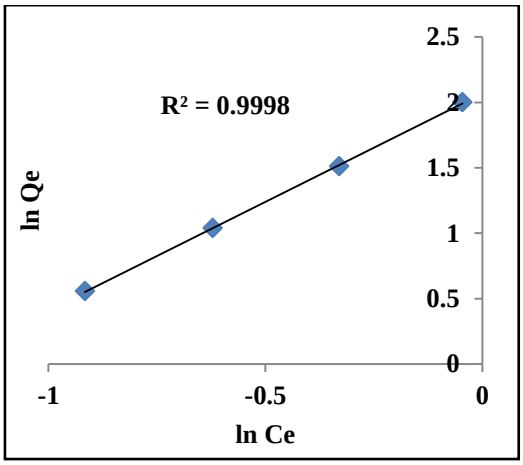

(a)

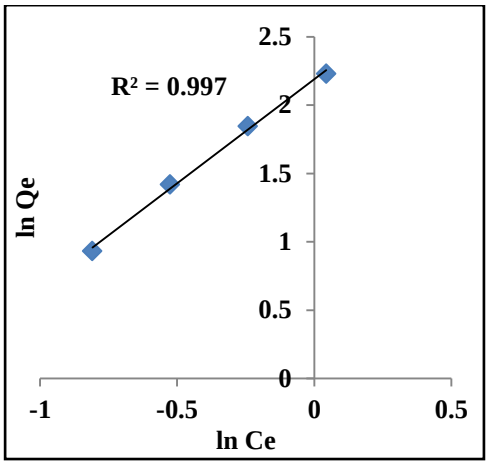

(b)

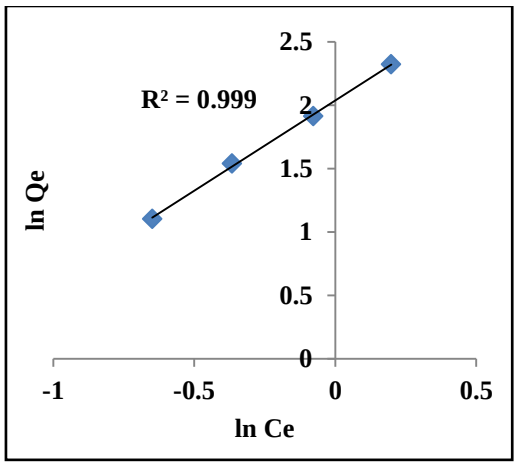

(c)

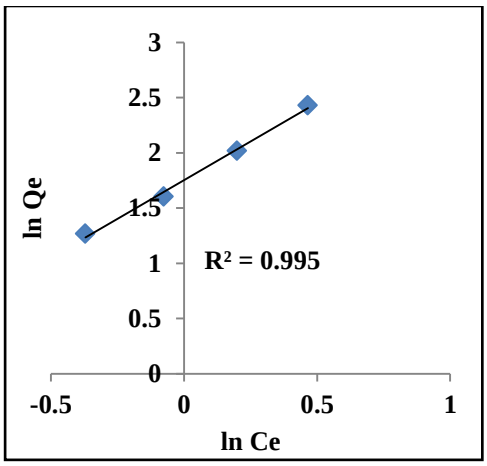

(d)

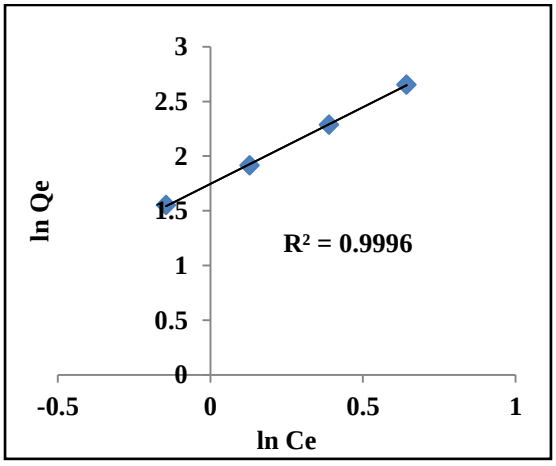

(e)

Figure 4.13: Freundlich isotherm plots for MB (a) 100g/100mL (b) 75g/100mL (c) 50g/100mL (d) 25g/100mL (e) 12.5g/100mL

Table 4.4: Isotherm parameters obtained using linear method for DR81 and MB removal on non-modified soil

		Adsorbent Dose (per 100mL of dye solution)									
		DR81					**MB**				
Isotherm	**Parameter**	**100g**	**75g**	**50g**	**25g**	**12.5g**	**100g**	**75g**	**50g**	**25g**	**12.5g**
LangmuirI	q_m	1.749	1.433	1.195	0.751	0.676	0.824	0.628	0.387	0.197	0.126
	K_l	-0.006	-0.006	-0.005	-0.006	-0.007	-0.03	-0.016	-0.016	-0.024	-0.02
	R^2	0.84	0.883	0.948	0.941	0.911	0.959	0.881	0.937	0.985	0.962
LangmuirII	q_m	-26.178	-34.13	-76.923	-149.254	-136.986	-21.008	-50	-90.909	-178.57	-270.27
	K_l	-2.69	-2.139	-1.585	-0.931	-0.785	-0.048	-0.021	-0.011	-0.006	-0.004
	R^2	0.805	0.793	0.935	0.97	0.677	0.983	0.975	0.985	0.999	0.996
LangmuirIII	q_m	0.009	0.009	0.007	0.006	0.008	0.032	0.017	0.017	0.025	0.021
	K_l	-57.471	-66.667	-119.048	-212.766	-181.818	-35.461	-96.154	-153.85	-200	-370.37
	R^2	0.447	0.478	0.725	0.803	0.492	0.818	0.714	0.819	0.964	0.912
LangmuirIV	q_m	-0.015	-0.015	-0.008	-0.007	-0.012	-0.035	-0.019	-0.018	-0.025	-0.021
	K_l	-25.644	-31.959	-86.467	-169.98	-89.432	-29.02	-125.51	-193.53	-193.53	-342.91
	R^2	0.447	0.478	0.725	0.803	0.492	0.818	0.819	0.964	0.964	0.912
Freundlich	n	0.431	0.425	0.439	0.492	0.427	0.604	0.657	0.702	0.713	0.714
	K_f	29.166	25.909	23.855	16.853	15.017	7.909	8.927	7.973	5.771	5.731
	R^2	0.921	0.926	0.994	0.994	0.89	0.999	0.997	0.999	0.995	0.999

4.3. 4 Characterisation of the Non-modified Soil

4.3.4.1 X-Ray Diffraction Analysis

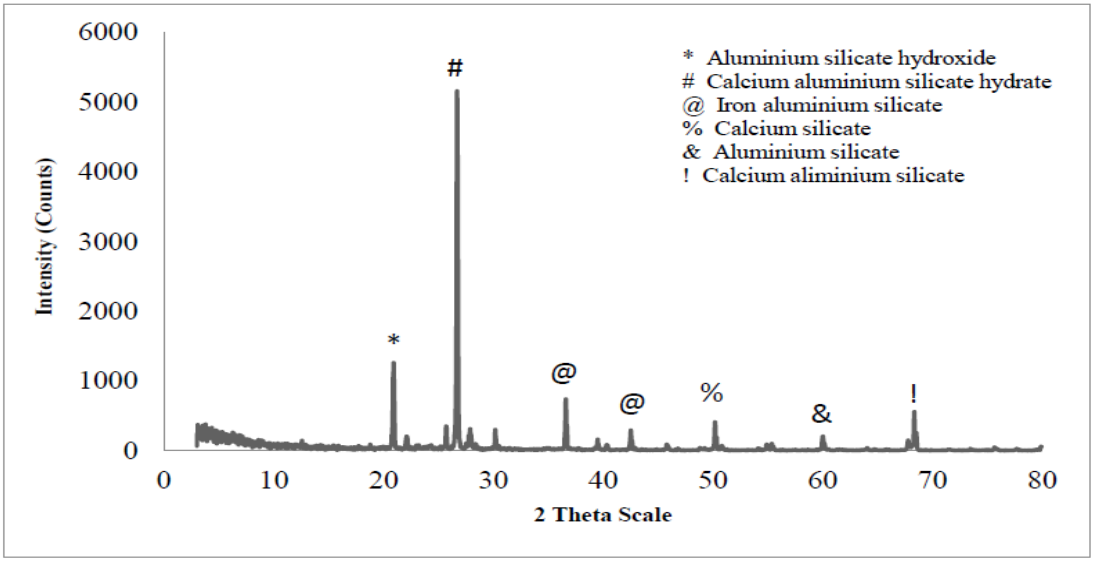

Figure 4.14: XRD pattern for Non-modified soil

The XRD results from Figure 4.14 suggest the presence of aluminium silicate hydroxide, calcium aluminium silicate hydrate, iron aluminium silicate, calcium silicate, aluminium silicate and calcium aluminium silicate in all the three soils. Two major peaks show contents as aluminium silicate hydroxide and calcium aluminium silicate hydrate. And other minor peaks are of iron aluminium silicate ($Fe_2Al_4Si_5O_{18}$; sekaninaite), calcium silicate (Ca_2SiO_4; calico-olivine), aluminium silicate (Al_2SiO_5; kyanite) and calcium aluminium silicate ($CaAl_2SiO_8$; svyatoslavite).

Aluminium silicate hydroxide ($Al_2Si_4O_{10}(OH)_2$) is a mineral namely pyrophyllite. It belongs to the family of non-swelling silicate minerals that are composed of three infinite layers formed by the sharing of oxygen ions at three corners of the silica tetrahedra. A layer of octahedrally coordinated Al–OH ions holds the two layers of tetrahedrally coordinated Si–O ions together as a three-layer sheet (Gücek et al. 2005). Calcium Aluminium Silicate hydrate ($CaAl_2Si_2O_8.4H_2O$), commonly known as gismondine is a zeolite. Zeolite is classified as framework alumosilicate. In an alumosilicate framework [AlO_4] tetrahedra are negatively charged with respect to [SiO_4] tetrahedra because of the trivalent state of Al. The charge of the whole framework is normally compensated by mono and/or divalent cations within the

cavities, while additional water molecules are present in the framework cavities (Ghobarkar & Guth 1999).

4.3.4.2 X-Ray Fluorescence Analysis

Table 4.5: XRF of Non-modified soil

Constituents	Wt%
SiO_2	15.86
Al_2O_3	3.72
Fe_2O_3	2.33
CaO	0.73
MgO	0.13
Na_2O	0.65
K_2O	0.53

The chemical composition of non-modified soil obtained by using XRF analysis, given in Table 4.5, indicates the presence of silica, alumina and iron oxide as major constituents, along with traces of sodium, potassium, calcium, and magnesium oxides. It is thus expected that the dye species may be removed mainly by SiO_2 and/or Al_2O_3.

4.3.4.3 Surface Area

Table 4.6: BET surface area analysis of non-modified soil

Parameter	Non-modified
Average Pore Size(Å)	19.861
Langmuir Surface Area(m^2/g)	19.399
BET Surface Area(m^2/g)	5.773
Total Pore Volume(cm^3/g)	$5.733X10^{-3}$

According to the International Union of Pure and Applied Chemistry (IUPAC), pores are classified as micropores (<2nm diameter), mesopores (2–50nm diameter) and macropores (>50nm diameter) (Sing et al. 1985). The microporous nature of the majority of adsorbents is well suited to many applications, including molecular sieving, adsorption and catalytic reactions of small molecules. However, there are numerous other potential applications, such as adsorption of dyes, in which the

presence of wider pores, preferably in the mesoporous range, would be advantageous (Asouhidou et al. 2009).

The surface area, average pore size and total pore volume was measured by BET method, given in Table 4.5. The porosity of the non-modified soil lies in the microporous range.

4.3.4.4 Scanning Electron Microscopy (SEM) – Energy Dispersive X-Ray (EDX) Analysis

Scanning electron microscopy has been a primary tool for characterizing the surface morphology and fundamental physical properties of the adsorbent surface. For the localisation and quantitative analysis of the elements Energy Dispersive X-Ray Analysis was performed. Figure 4.15 and Table 4.6 shows the presence of elements like oxygen, silicon, iron, aluminium, calcium, magnesium, potassium and sodium. Figure 4.16 shows the SEM images for non-modified soil before adsorption and after adsorption of MB and DR81.

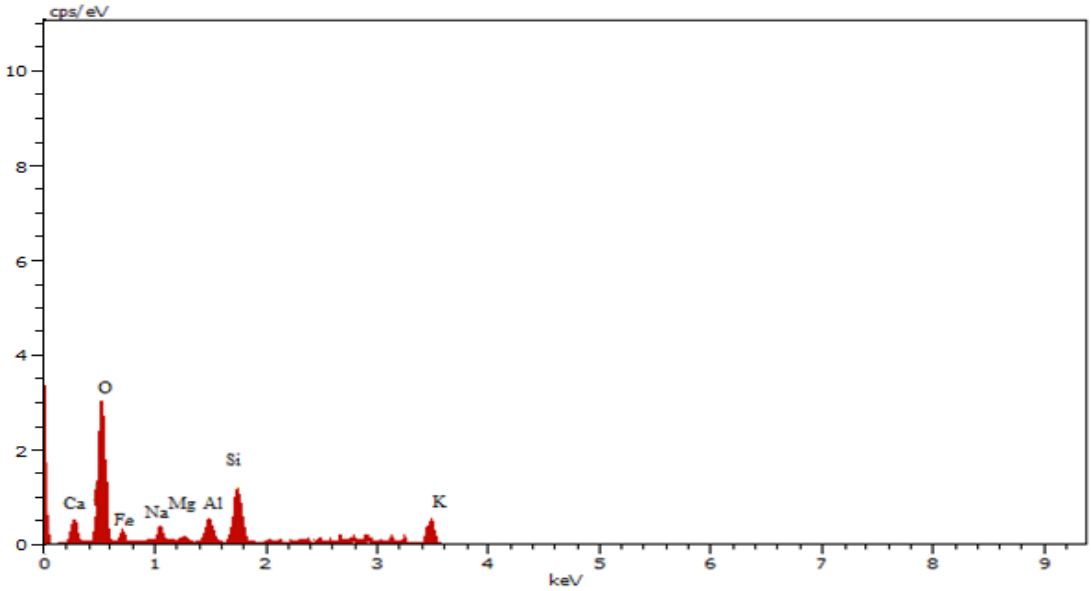

Figure 4.15: Energy Dispersive X-Ray Analysis of Non-modified soil

Table 4.7: Elemental Composition of Non-modified Soil

Element	Wt%	At%
O	62.04	52.24
Si	16.23	20.59
Al	12.53	13.87
Fe	0.31	0.99
Ca	6.04	7.04
Mg	0.22	0.39
K	0.08	0.36
Na	2.55	4.52

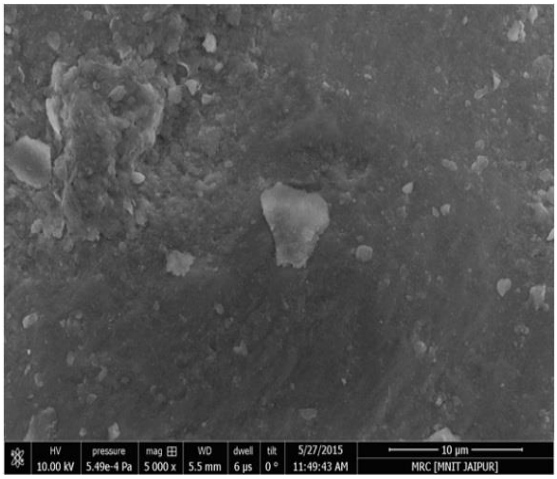

(a)

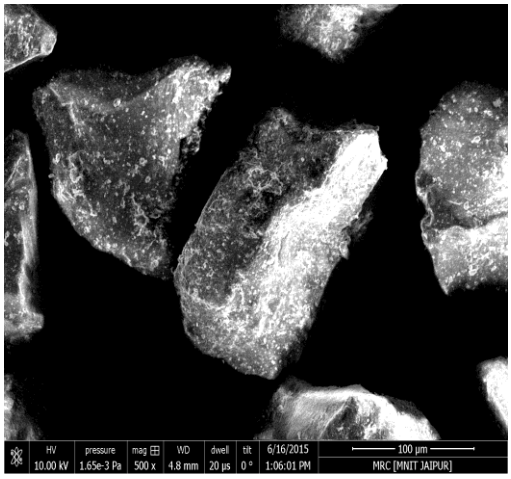

(b)

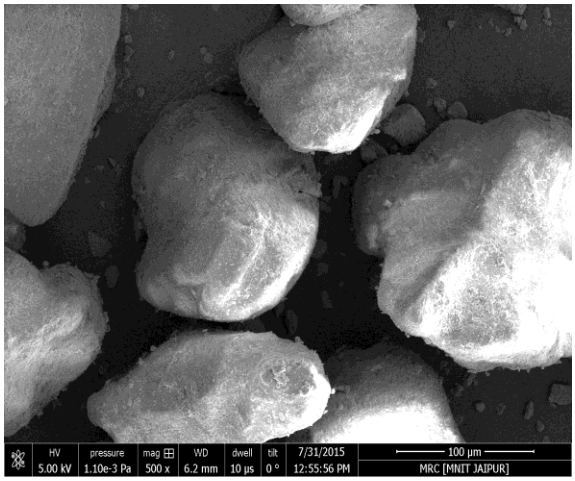

(c)

Figure 4.16: SEM images for (a) Non-modified Soil (b) DR81 adsorbed Non-modified Soil and (c) MB adsorbed Non-modified Soil

4.3.4.5 Fourier Transform Infrared Spectroscopy Analysis and Zeta Potential of the soil surface

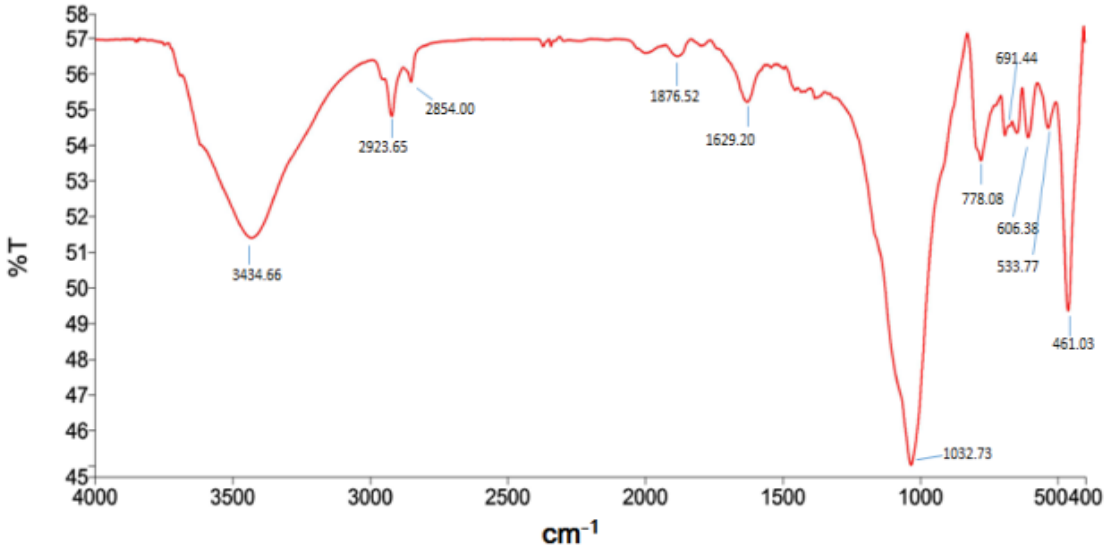

(a)

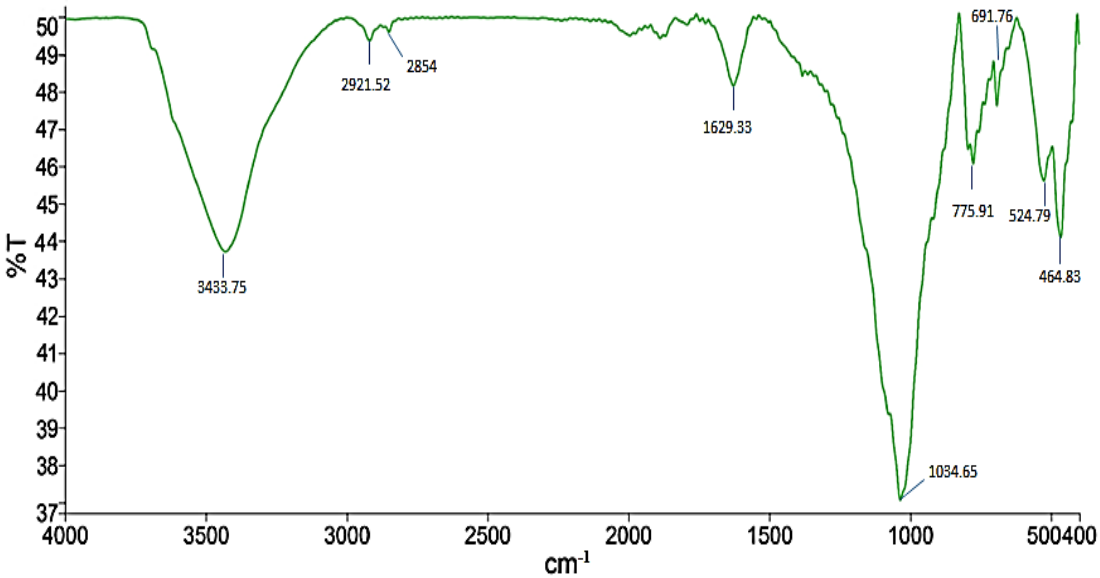

(b)

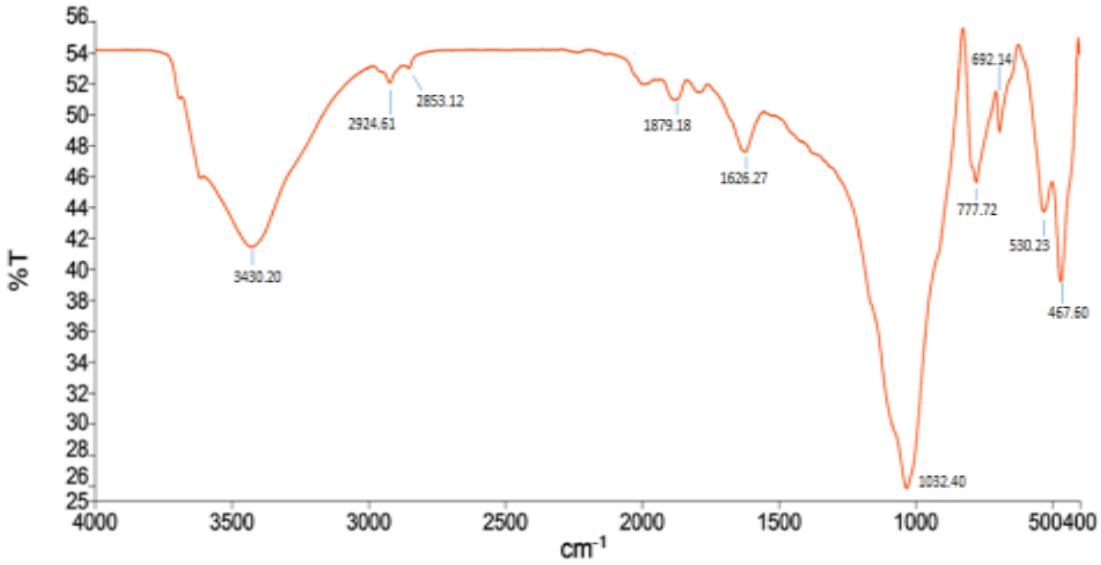

(c)

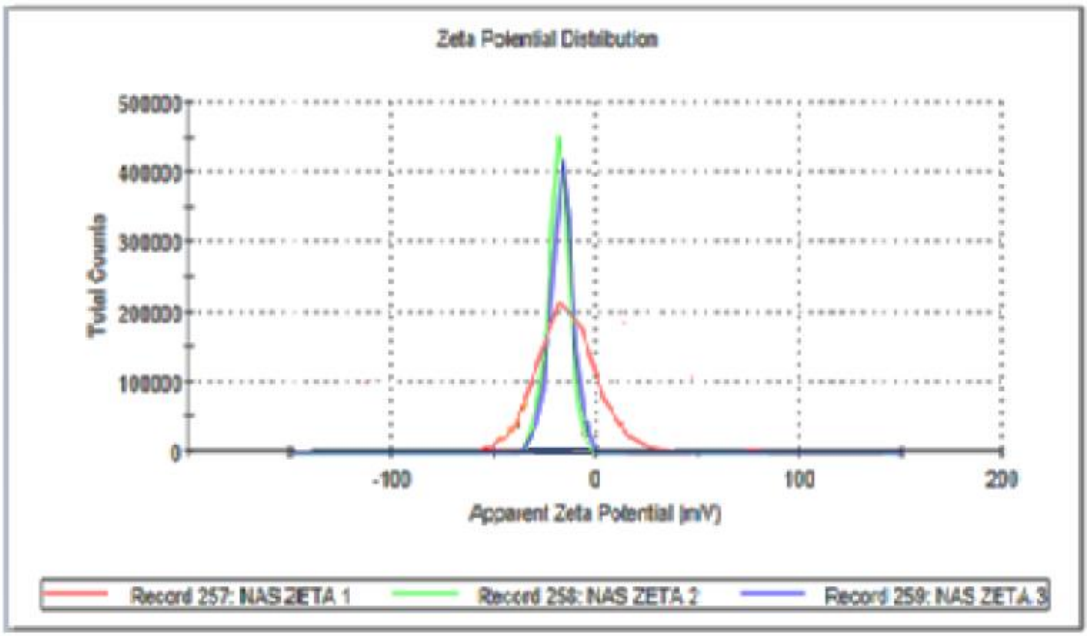

(d)

Figure 4.17: FTIR spectra for (a) non-modified soil, (b) DR81 adsorbed non-modified soil, (c) MB adsorbed non-modified soil, (d) zeta potential for non-modified soil

The infrared spectra of non-modified soil, DR81 adsorbed non-modified soil and MB adsorbed non-modified soil are illustrated in Figure 4.17 (a), (b) & (c). The main application of this technique is to detect the structure of chemical species and provide qualitative measurements based on the adsorption and molecular vibration peaks. It helps in the identification of functional groups on the surface of the adsorbents which are responsible for adsorption of dye (Bera et al. 2013),(Chowdhury & Saha 2010).

The location of hydrogen-bonded OH groups usually lie in the range of 3200–3750cm^{-1}, involved in hydrogen bonding may be due to adsorbed water (Ahmad & Hameed 2009). In Figure 4.17 (a), the peak at 3434.66 cm^{-1} is assigned to stretching vibration of silanol group (SiO-H) and H-O-H group of a water molecule (Mahmoodi et al. 2011). A pair of strong bands at 2854.00 and 2923.65 cm^{-1} can be assigned to the symmetric and asymmetric stretching vibrations of the methylene group (-CH_2) (Özcan et al. 2006). The peak at 1629.20 cm^{-1} is attributed to H-O-H bending vibration because the deep band at 3434.66 cm^{-1} suggests the presence of some interlamellar water (Mahmoodi et al. 2011), (Özcan & Özcan 2005). The strong band observed at 1876.52 cm^{-1} indicated the stretching vibrations of C-OH bonds (Abdel-Ghani et al. 2007). The deep band at 1033.8 cm^{-1} represents asymmetric stretching of siloxane (Si-O-Si) group.

The bands appearing between 800 and 500 cm^{-1} are associated with the tetrahedral vibrations formed by silicate system. These bands are typical characteristic of the double or single rings with tetrahedral bonds (Pansuk 2011). The adsorption peaks at 778.08 cm^{-1} and 606.38 cm^{-1} lies in the region of stretching vibration for Si-O symmetric and asymmetric bond vibration respectively (Bera et al. 2013) (Vijayakumar et al. 2009). Adsorption bands at 521.27 cm^{-1}, 693.91 cm^{-1} are related to the bending vibration of Si-O group in asymmetric and symmetric vibration (Bera et al. 2013). The band at 461.03 cm^{-1} is due Si-O-Si bending vibrations (Özcan & Özcan 2005), (Pansuk 2011).

Hence, FTIR spectral analysis demonstrates the existence of negatively charged functional groups like –OH,-C-OH, -CH_2, and –SiO on the soil surface. Zeta potential result also supports the negative charge on the soil surface. Zeta potential of the non-modified soil surface is -17mV (Figure 4.17 (d)).

On comparing spectrum Figure 4.17(a) of non-modified soil with the spectrum of DR81 adsorbed non-modified soil as shown in Figure 4.17(b), it could be seen that there are small shifts in some bands (3433.75 cm^{-1} and 2921.52 cm^{-1}) and some bands disappeared (606.38cm^{-1} and 1876.56 cm^{-1}). The intensity of the some peaks was minimised (2854.00cm^{-1}, 1629.33cm^{-1}, 1034.65cm^{-1}, 775.95cm^{-1},691.76cm^{-1}, 524.79cm^{-1}, 464.83cm^{-1}) as shown in the Figure 4.17(c). These changes observed in

the spectrum indicated the possible involvement of these functional groups on the surface of the non-modified soil in the adsorption process.

On comparing spectrum Figure 4.17(a) of non-modified soil with the spectrum of MB adsorbed non-modified soil as shown in Figure18 (c), it could be seen that there are small shifts in some bands (3430.20 cm^{-1} and 1626.27 cm^{-1}) and some bands disappeared (606.38cm^{-1}). The intensity of the some peaks was minimised (1879.18cm^{-1}, 1032.40cm^{-1}, 692.14cm^{-1}, 530.2cm^{-1}, 467.60cm^{-1} and 777.72cm^{-1}) as shown in the Figure 4.17 (c). These changes observed in the spectrum indicated the possible involvement of these functional groups on the surface of non-modified soil participated in the adsorption process. Table B.5, B6 & B.7 in Appendix B gives the tabular representation of FTIR data analysis.

4.4 Summary

This Chapter presents a study of the effect of operational parameters on adsorption of two classes of dyes: MB and DR81 onto the non-modified soil. It was found that the adsorption capacity of the non-modified soil is much higher for MB than DR81 because of the ionic charges on the dye and surface character of the non-modified soil. From surface characterisation results it could be concluded that non-modified soil possesses a definite negative charge on its surface. The isoelectric point of non-modified soil was found to be at around pH 9. pH plays an important role in surface hydroxylation and acid-base dissociation and surface complexation (Ho & Chiang 2001). Therefore, the adsorption of DR81 was supported in spite of the negative surface charge. Further, it was found that pH 3 and pH 11 were optimum for DR81 and MB removal, respectively.

The contact time of 10 minutes was found to be sufficient to attain the equilibrium adsorption for both the dyes. The adsorption capacity of soil increased with a decrease in particle size range of non-modified soil from 300-150µm to 150-75µm for both the dyes. This particle size range is reasonably larger than the low-cost adsorbents (mainly clayey material), with good adsorption of dyes reported earlier. Therefore, it can be said that non-modified soil will provide better hydraulics for fixed bed studies.

The kinetic modelling showed that the pseudo-second order model exhibited the best correlation for the experimental data for both the dyes and indicated that boundary

layer resistance is not the rate limiting step. Intraparticle diffusion model showed multilinearity for both the dyes which suggested diffusion of dye molecules into the pores to some extent. From equilibrium studies, it was found that Freundlich isotherm gave the best fit which reveals that adsorption of both the dyes was of chemical nature.

CHAPTER 5

Chapter 5

Removal of Direct Red 81 onto Acid-Modified Soil

This Chapter discusses the modification of non-modified soil for adsorption of Direct Red 81 dye. The effect of operational parameters like contact time, initial dye concentration and adsorbent dose on adsorption is also discussed. Investigations based on these parameters are used for kinetic modelling and equilibrium studies. The effect of surface characteristics on adsorption of the dye has also been discussed in detail.

5.1 Introduction

From the chapter 4, it is clear that the non-modified soil has negative charge at natural pH as explained in Section 4.3.4.5. Since DR81 have sulphonate groups in its structure (Section 3.3.1.2), they are repelled by the negatively charged non-modified soil surface. This induces a relatively low adsorption capacity. However, it gave better removal of Direct Red81 dye at pH 3. The surface of the non-modified soil acquires positive charge at this pH. It has been reported that the specific surface area and surface acidity of the clay samples can be greatly increased by acid activation (Özcan & Özcan 2004). (Mundada et al. 2017) have reported the presence of clayey particles in the non-modified soil of Rajasthan. Therefore, acid modification of the soil was done so that its surface attains positive charge and become receptive for anionic dye DR81. This would help in the enhancement of the adsorption property of non-modified soil. Acid activation has also been reported on various other adsorbents like rice husk (Shih & Husk 2012), neem sawdust (Khattri & Singh 2009), etc.

5.2 Materials & Methods

5.2.1 Adsorbent

As the name suggests, the soil was modified using mineral acid; sulphuric acid (H_2SO_4). For acid activation, the locally available soil from Rajasthan was collected from the premises of Malaviya National Institute of Technology, Jaipur. The collected soil was then washed with distilled water to remove the suspended impurities and then oven dried at 100°C for 2 hours. The dried soil was crushed and sieved to give particle

size 150-75 μm using ASTM Standard sieves. After sieving the soil to the desired particle size, it was stirred continuously at 10 rpm for 2 hours at room temperature in 1N H_2SO_4 in a flat bottom beaker. The soil to the acid suspension was kept at a constant ratio of 1:6 (kg: ml). Stirring was done to provide a better contact between the acid and the soil surface. The stirring was stopped after 2 hours, and the soil-acid suspension was left undisturbed for next 2 hours. This was so done to provide more reaction time between the soil surface and acid. After 2 hours, the suspension was washed several times with distilled water. The pH of the suspension was also checked, meanwhile washing. When the pH was brought down to ~3 to 3.5, washing was halted, and the modified soil was dried in an oven at 100°C for 2 hours before use.

5.2.2 Adsorbate

Direct Red 81 stock solution was prepared as discussed in Section 3.3.1.3.

5.2.3 Adsorption Studies

The adsorption measurements were carried out by the batch method given in Section 3.3.2.

5.3 Results & Discussion

5.3.1 Parametric analysis

This section elucidates the effect of contact time, initial dye concentration and adsorbent dose. Effect of pH has not been discussed in this section as the adsorbent has been modified to acquire positive charge. And also, it is reported in Chapter 4 that DR81 shows better removal at acidic pH. The particle size range chosen for all the parametric analyses is 150-75μm because this size range gave better removal, as reported in Chapter 4.

5.3.1.1 Effect of initial dye concentration and contact time

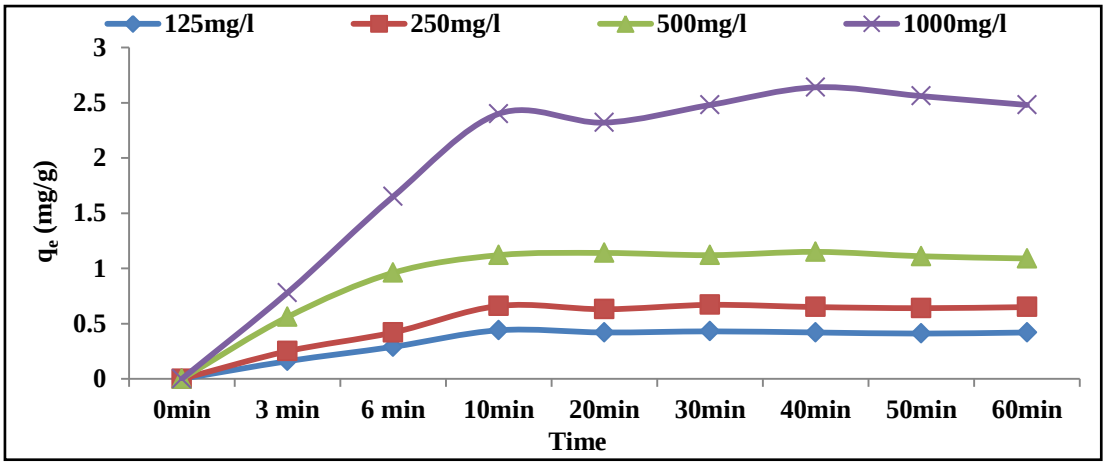

Figure 5.1: Effect of initial dye concentration and contact time on DR81 removal. (Condition: dose: 12.5g/100ml)

The adsorption of DR81 on acid modified soil was studied at different DR81 concentration (125 mg/L, 250 mg/L, 500 mg/L and 1000 mg/L). Figure 5.1 shows the result of effect of initial concentration on adsorption of DR 81 onto acid modified soil at 30°C. It is observed that dye uptake was rapid for the initial 10 minutes, and thereafter, saturation stage was attained. It could also be seen from Figure 5.1 that an increase in initial DR 81 concentration results in an increase in the adsorption of DR81onto acid modified soil. The equilibrium adsorption increases from 0.44 mgg^{-1} to 2.40 mgg^{-1} with increase in the initial DR81 concentration. However, equilibrium percent removal of dye gets decreased from 44% to 30%. This indicates that the initial dye concentration plays an important role in the adsorption capacity of dye. A rapid adsorption took place on the exterior surface of the adsorbent and thereafter, dye molecules penetrate into the pores of the adsorbent. A high dye concentration overcomes all the mass transfer resistance. Similar kind of results has been reported on direct dyes by (Ahmad et al. 2007), (Mall et al. 2005), on reactive dyes by (Özacar & Şengil 2003), etc.

Comparison between non-modified and acid modified soils for percent and mgg^{-1} removal of DR81 is given in Table 5.1. It can be observed from the Table 5.1 that there is an enhancement in the adsorption property of the soil after modification.

Table 5.1: Effect of initial dye concentration on DR81 removal (Condition: adsorbent dose: 12.5g/100ml, contact time: 10 minutes)

Dye Concentration	**% removal**		**q_e mgg^{-1}**	
	Non-modified Soil	Acid-modified Soil	Non-modified Soil	Acid-modified Soil
125mg/L	45	44	0.45	0.44
250mg/L	25	33	0.5	0.66
500mg/L	16	28	0.64	1.12
1000mg/L	12	30	0.96	2.4

5.3.1.2 Effect of adsorbent dose

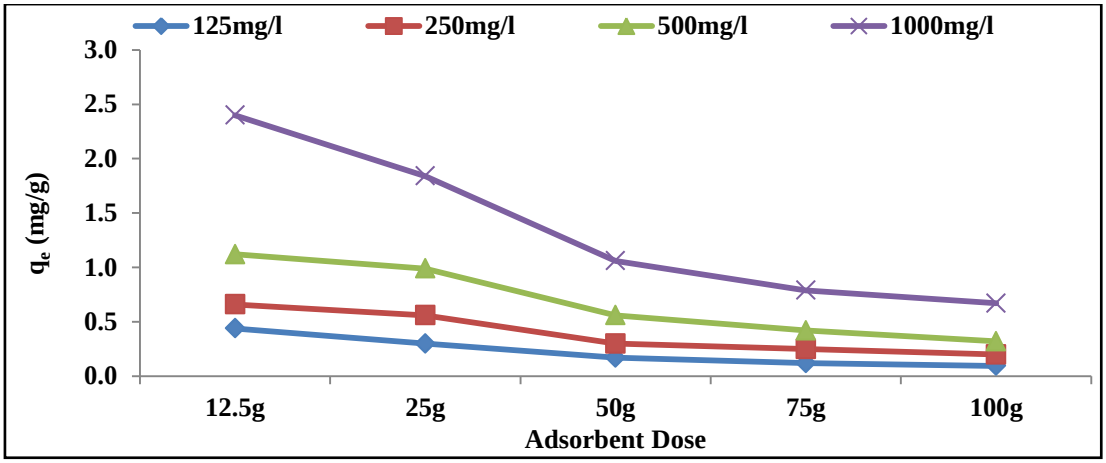

Figure 5.2: Effect of acid modified soil dose on DR81 removal. (Condition: time: 10 min)

The adsorption of DR81 on acid modified soil was investigated at different adsorbent doses (12.5g/100ml, 25g/100ml, 50g/100ml, 75g/100ml, and 100g/100ml). Figure 5.2 shows the result of effect of adsorbent dose on adsorption of DR81onto acid modified soil at 30°C. While the adsorbent dose increases from 12.5g /100ml to 100g/100ml at a contact time of 10 minutes, the adsorption capacity of DR81 onto soil surface decreases from 0.44mgg^{-1} to 0.1mgg^{-1} for 125 mg/L, 0.66mgg^{-1} to 0.2mgg^{-1} for 250 mg/L, 1.12mgg^{-1} to 0.32mgg^{-1} for 500 mg/L and 2.4mgg^{-1} to 0.67mgg^{-1} for 1000 mg/L of DR81 concentration. However, percent removal increases from 44% to 76% for 125 mg/L, 33% to 80% for 250 mg/L, 28% to 64% for 500 mg/L and 30% to 67% for 1000 mg/L of DR81 concentration. The increase in the percent removal of DR81 by increasing the adsorbent dose at a fixed DR81 concentration could be due the increased number of available adsorption sites. However, the amount of DR81

adsorbed decreased per unit mass of adsorbent as the adsorbent increased. This could be due to the fast saturation of the easily available active sites for DR81 adsorption. Similar results were obtained by (Zhu et al. 2007).

Comparison between non-modified and acid modified soils for percent and mgg^{-1} removal of DR81 is given in Table 5.2. It can be observed from the Table 5.2 that there is an enhancement in the adsorption property of the soil after modification.

Table 5.2: Effect of adsorbent dose on DR81 removal (Condition:dye concentration: 1000 mg/L, contact time: 10 minutes)

Adsorbent dose	**% removal**		**q_e mgg^{-1}**	
	Non-modified Soil	Acid-modified Soil	Non-modified Soil	Acid-modified Soil
12.5g/100ml	12	30	0.96	2.4
25g/100ml	20	46	0.8	1.84
50g/100ml	31	53	0.62	1.06
75g/100ml	42	59.25	0.56	0.79
100g/100ml	46	67	0.46	0.67

5.3.2 Kinetic modelling

5.3.2.1 Lagergren's Pseudo First Order Kinetic Model

The correlation coefficient R^2, rate constant k_1 and adsorption capacity, q_e^{exp} and q_e^{pred}, for Lagergren's pseudo first order equation for the adsorption of DR81 has been given in Table C.1 in Appendix C. The values of correlation coefficients were rather low for this model for both the operating parameters i.e. adsorbent dose and dye concentration. Also, the values of q_e^{exp} and q_e^{pred} did not match well. This suggests that adsorption of DR81 is not a pseudo first-order reaction.

5.3.2.2 Lagergren's Pseudo Second Order Kinetic Model

The correlation coefficient R^2, rate constant k_2 and adsorption capacity, q_e^{exp} and q_e^{pred}, obtained from Lagergren's pseudo second order equation (Equation 3.3) for the adsorption of DR81 has been given in Table C.1 in Appendix C. Figure 5.3 illustrates that the data show a good compliance with the pseudo second order equation and the regression coefficients for the linear plot were higher than 0.99 for all the adsorbent doses and dye concentrations. Therefore, it can be said that kinetics

for the adsorption of DR81 on acid modified soil follows pseudo second order rate expression. From Table C.1, equilibrium adsorption capacity q_e, increased with increase in the initial dye concentration. This indicates that the DR81 removal is dependent on initial dye concentration. However, values of rate constant k_2 decreased as the initial DR81 concentration increased from 125 mg/L to 1000 mg/L. The similar observation for the removal of Direct red 81 was reported by (Heravi et al. 2015). However, the rate constant k_2, increased with increase in the adsorbent dose. This might be due to increase in number of active sites with adsorbent dose.

From Table C.1, values of predicted equilibrium adsorption capacities q_e^{pred} and correlation coefficients R^2 for Lagergren's pseudo second-order model are much more reasonable when compared with results of the pseudo first-order model. Since most of the first-order predicted q_e^{pred} values deviate significantly from the experimental q_e^{exp} values, it suggests that the adsorption of dye onto acid modified soil follows the pseudo-second order model.

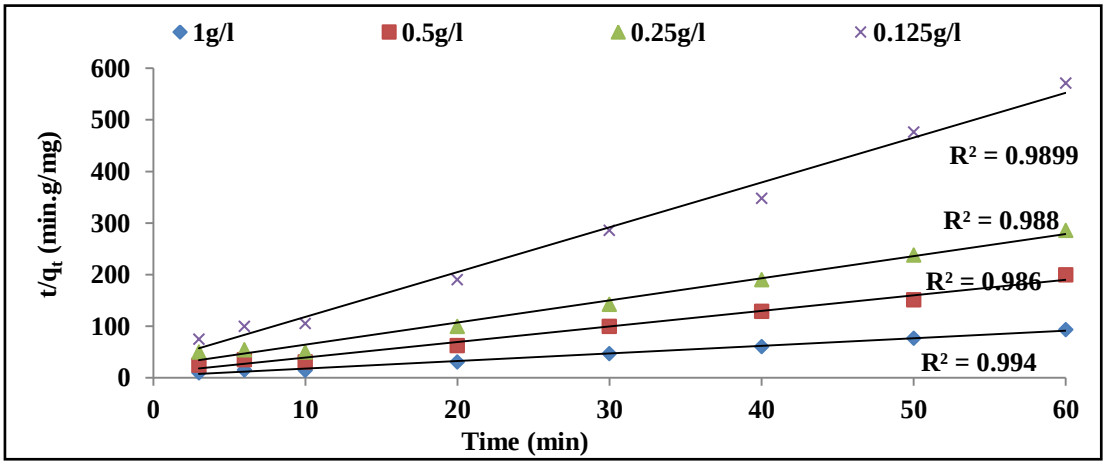

(a)

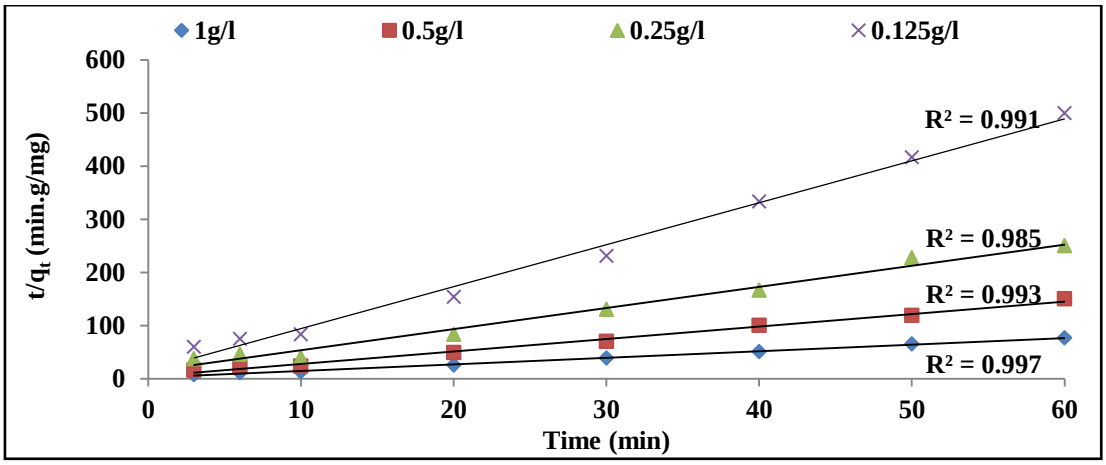
1g/l
0.5g/l
0.25g/l
0.125g/l
t/qt (min.g/mg)
600
500
400
300
200
100
0
0
10
20
30
40
50
60
Time (min)
R² = 0.991
R² = 0.985
R² = 0.993
R² = 0.997

(b)

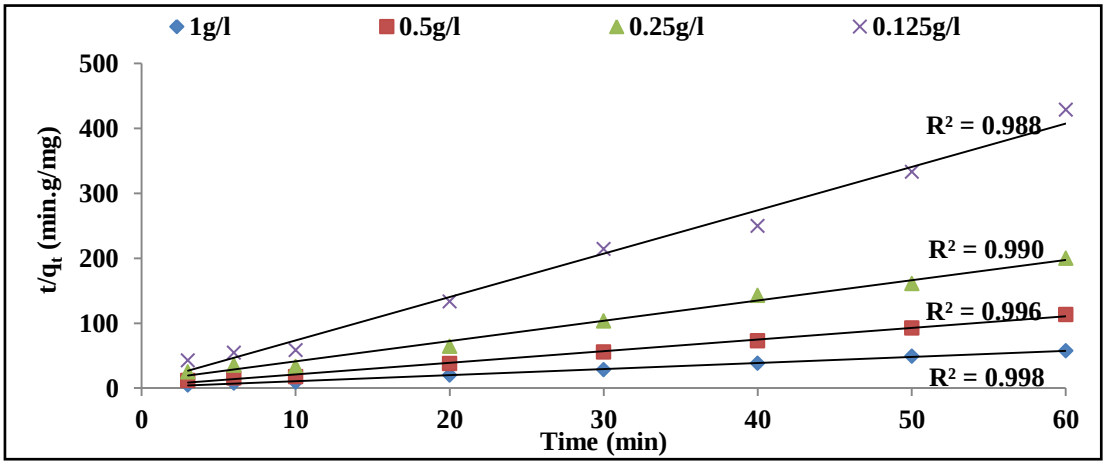
1g/l
0.5g/l
0.25g/l
0.125g/l
t/qt (min.g/mg)
500
400
300
200
100
0
0
10
20
30
40
50
60
Time (min)
R² = 0.988
R² = 0.990
R² = 0.996
R² = 0.998

(c)

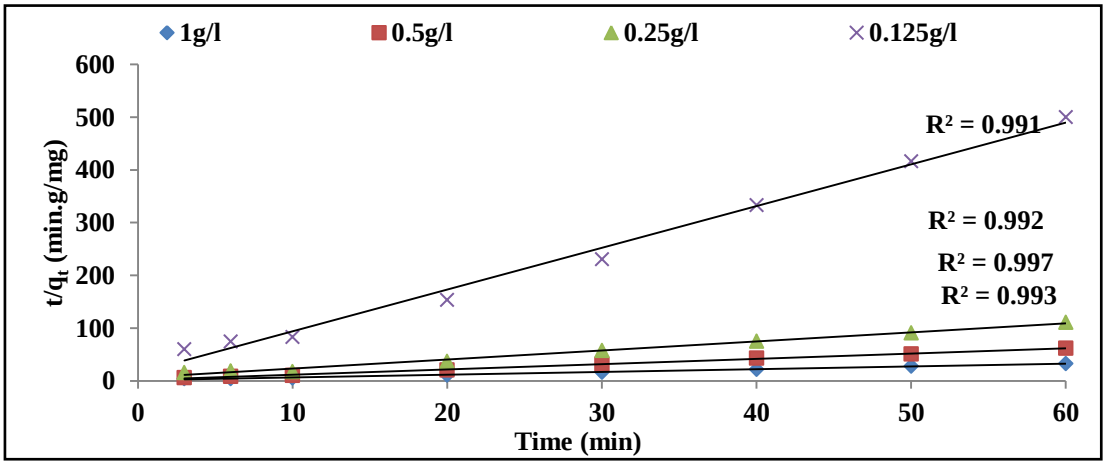
1g/l
0.5g/l
0.25g/l
0.125g/l
t/qt (min.g/mg)
600
500
400
300
200
100
0
0
10
20
30
40
50
60
Time (min)
R² = 0.991
R² = 0.992
R² = 0.997
R² = 0.993

(d)

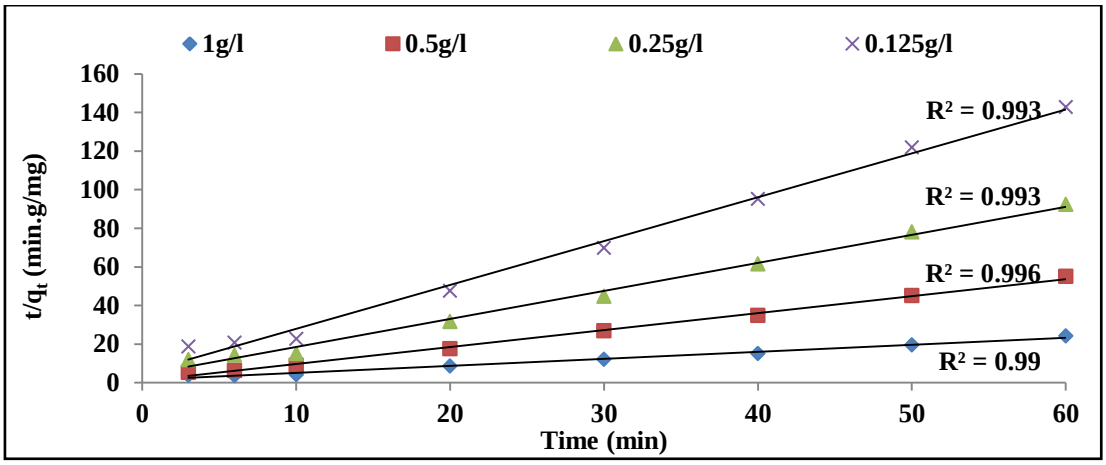

(e)

Figure 5.3: Lagergren's Pseudo Second Order Kinetic Plot for Adsorption of DR81 on Acid Modified Soil (a) 100g/100ml (b) 75g/100ml (c) 50g/100ml (d) 25g/100ml (e) 12.5g/100ml

5.3.2.3 Intraparticle Diffusion Model

Figure 5.4 show that the plots between q_t (mgg^{-1}) and the square root of time $t^{0.5}$(min). It could be observed that the plots present multi-linearity, which indicates that two steps occurred in the process. The plots show two phases: the initial curved portion of the plot indicated a boundary layer effect while the second linear portion was due to intraparticle diffusion. A similar multilinearity was observed for the adsorption of DR81 on bamboo sawdust (Khan et al. 2012). The calculated k_{i_2} and C_2 values for each initial concentration are reported in Table C.2 in Appendix C. The slope $k_{i_2}$of the second linear portion characterizes intraparticle diffusion, whereas intercept C_2 of this portion is proportional to the boundary layer thickness. The discrepancy in the k_{i_2} values may be due to the decrease in the pore size of the acid modified soil after modification. This is the reason that non modified soil showed better intraparticle diffusion than acid modified soil. The average pore size for non-modified and acid-modified soil is 19.861Å as given in Table 4.10 and 18.692 Å as given in Table 5.9 respectively. (Pelekani & Snoeyink 2001) also reported that Congo red adsorption is related to the pore size. The R^2 values for this diffusion model ranged between 0.0249 and 0.7428 as shown in Table 5. The low to high values of correlation coefficients without any definite meaning indicates some degree of boundary layer control. However, the results do not pass through the origin (the plots have intercepts in the range 0.092-0.677 for 100g/100ml, 0.129-0.801 for 75g/100ml , 0.177-1.050 for

50g/100ml, 0.312-1.872 for 25g/100ml, 0.450-2.239 for 12.5g/100ml), indicating that intraparticle diffusion is involved in the adsorption process but it is not the only rate-limiting mechanism and that some other mechanisms also play an important role. This confirms that adsorption mechanism was a multi-step process, involving adsorption on the external surface, diffusion into the interior and ion exchange, as previously reported by (Amin 2009)(Khaled et al. 2009). The values of the intercept C_2 given in the Table C.2 also give an idea about the boundary layer thickness: the larger the intercept, the greater is the boundary layer effect. Any increase in the value of C_2 indicates the abundance of dye molecules adsorbed on boundary layer (Mall et al. 2005). As seen in Table C.2, the value of C_2 increases with increasing initial dye concentration which indicates increase in the boundary layer thickness and decrease of the chance of the external mass transfer and hence increase of the chance of internal mass transfer. On the other hand, the value of C_2 decreased with increase of adsorbent dose, which reflects a decrease of the thickness of the boundary layer and hence an increase of the chance of external mass transfer. Similar results were reported by (Khaled et al. 2009) for treatment of direct yellow 12 by orange peel carbon.

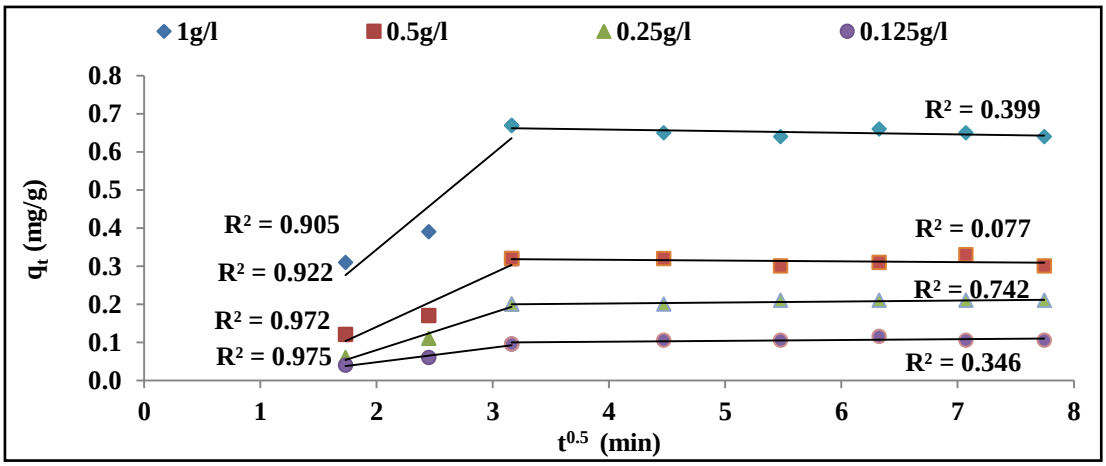

(a)

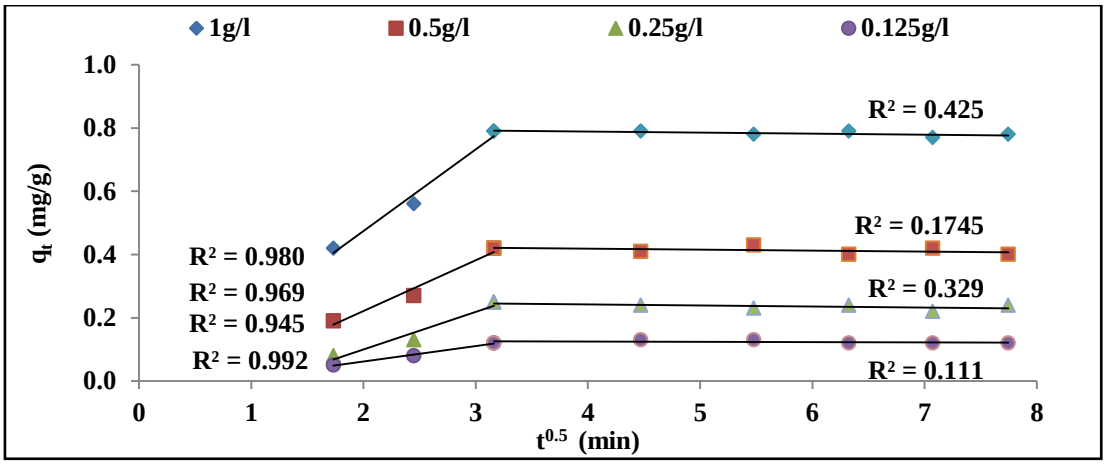
1g/l
0.5g/l
0.25g/l
0.125g/l
1.0
0.8
0.6
0.4
0.2
0.0
q_t (mg/g)
R^2 = 0.425
R^2 = 0.1745
R^2 = 0.329
R^2 = 0.111
R^2 = 0.980
R^2 = 0.969
R^2 = 0.945
R^2 = 0.992
0
1
2
3
4
5
6
7
8
$t^{0.5}$ (min)

(b)

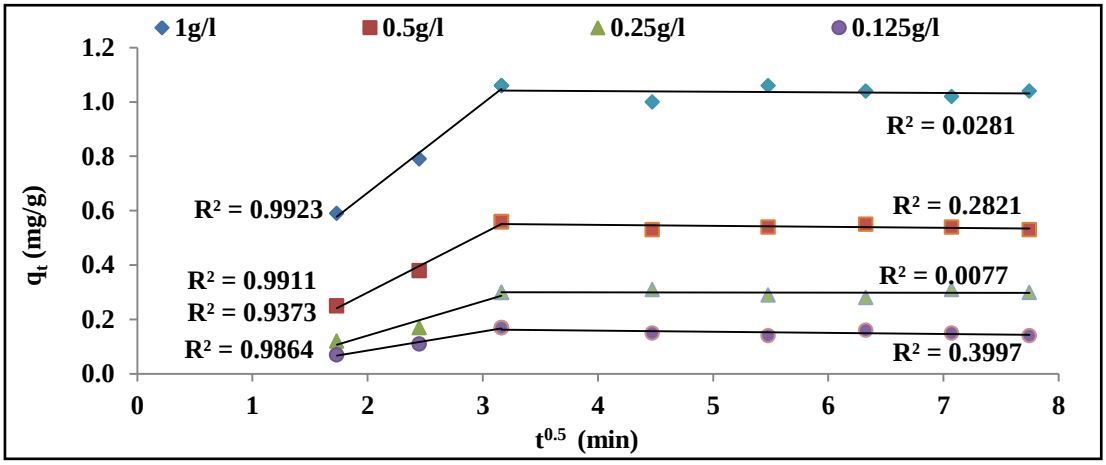
1g/l
0.5g/l
0.25g/l
0.125g/l
1.2
1.0
0.8
0.6
0.4
0.2
0.0
q_t (mg/g)
R^2 = 0.0281
R^2 = 0.2821
R^2 = 0.0077
R^2 = 0.3997
R^2 = 0.9923
R^2 = 0.9911
R^2 = 0.9373
R^2 = 0.9864
0
1
2
3
4
5
6
7
8
$t^{0.5}$ (min)

(c)

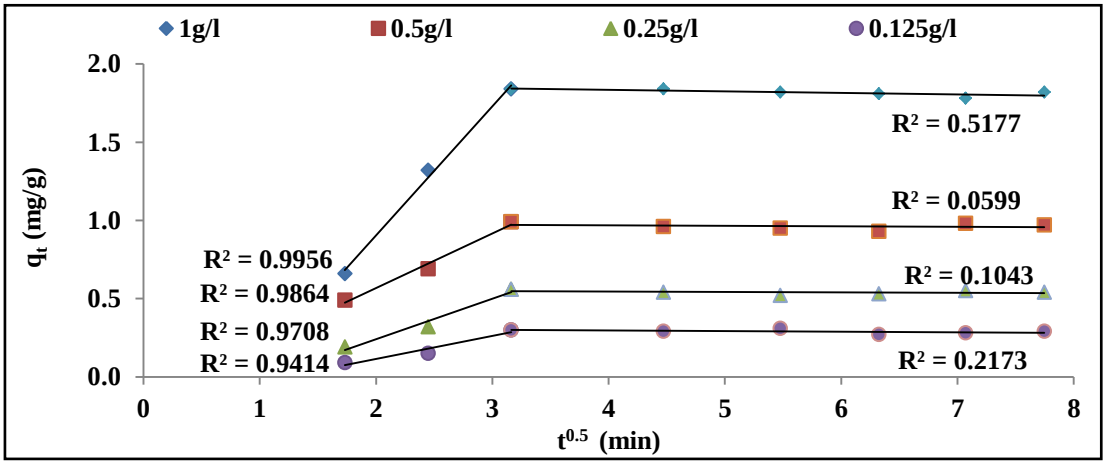
1g/l
0.5g/l
0.25g/l
0.125g/l
2.0
1.5
1.0
0.5
0.0
q_t (mg/g)
R^2 = 0.5177
R^2 = 0.0599
R^2 = 0.1043
R^2 = 0.2173
R^2 = 0.9956
R^2 = 0.9864
R^2 = 0.9708
R^2 = 0.9414
0
1
2
3
4
5
6
7
8
$t^{0.5}$ (min)

(d)

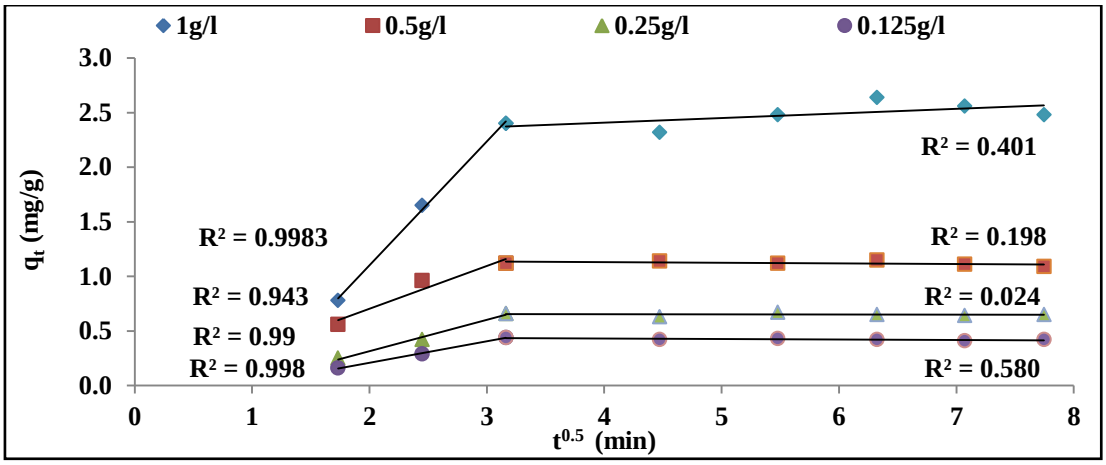

(e)

Figure 5.4: Intraparticle Diffusion Parameters for Adsorption of DR81 on Acid Modified Soil (a) 100g/100ml (b) 75g/100ml (c) 50g/100ml (d) 25g/100ml (e) 12.5g/100ml

5.3.3 Equilibrium Studies

The adsorption isotherms were developed for all the adsorbent doses i.e. 100g, 75g, 50g, 25g and 12.5g. C_e is the DR81 concentration in aqueous solution at equilibrium at contact time of 10 minutes for initial dye concentration (125 mg/L – 1000 mg/L) and q_e is calculated by Equation 3.1. Table C.3 in Appendix C shows the isotherm parameters for Langmuir and Freundlich isotherms.

5.3.3.1 Linear Regression Analysis

Table C.3 shows that the result for R^2 value in most of the cases was not going beyond 0.9. So, the interpretation of which isotherm fits the data well could not be properly done. Therefore, a non-linear approach to make isotherms was used to fit the data.

5.3.3.2 Non- Linear Regression Analysis

The non-linear regression analysis was carried out for five isotherms; Langmuir, Fruendlich, Redlich-Peterson, Sips and Toth. The experimental q_e^{exp} was calculated by the Equation 3.1 and the predicted q_e^{pred} is obtained from the non-linear expressions of the above mentioned isotherms, given in the Table 3.2.

Table 5.3 shows the non-linear regression analysis of five isotherm models, namely; Langmuir, Freundlich, Redlich-Peterson, Sips and Toth isotherm. Figure 5.5 illustrate

the plots for all the above mentioned isotherms. The order of fitness of isotherm models from the best to the least was Redlich–Peterson < Freundlich < Langmuir < Sips < Toth isotherms based on their R^2 values. The assertion that sometimes correlation coefficient, R^2 does not justify the basis for selection of best fit of adsorption model, was investigated by use of Chi-square χ^2 and RMSE statistical test (Auta & Hameed 2012). The χ^2 and RMSE test results obtained in this study further supported that Redlich–Peterson was the best model that described the process of adsorption of DR81 on acid modified soil as revealed by correlation coefficient R^2. This was revealed by smaller values of χ^2 and RMSE signifying stronger alliance between theoretical and experiment data as compared with other models tested.

The Redlich–Peterson isotherm parameter's values β determined revealed that the model was tending towards Freundlich and not Langmuir. This was because the β values obtained were far from unity as opposed to Langmuirmodel which is satisfied when the value of $\beta = 1$. This further revealed that the adsorption of DR81 was not by monolayer arrangement, but by ion-exchange and complexation interactions as a result of full coverage of surface functional groups on the acid modified soil via surface exchange reactions (Zaghouane-Boudiaf et al. 2014).

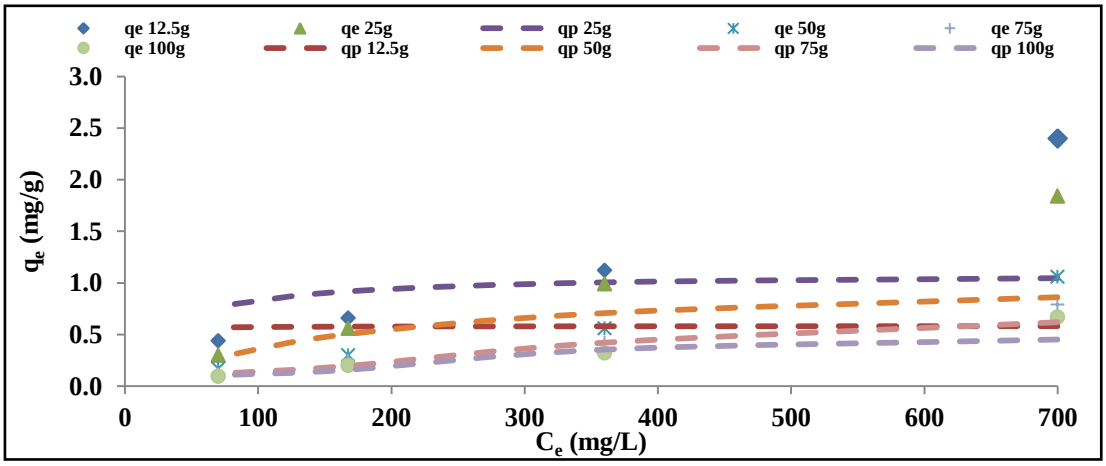

(a)

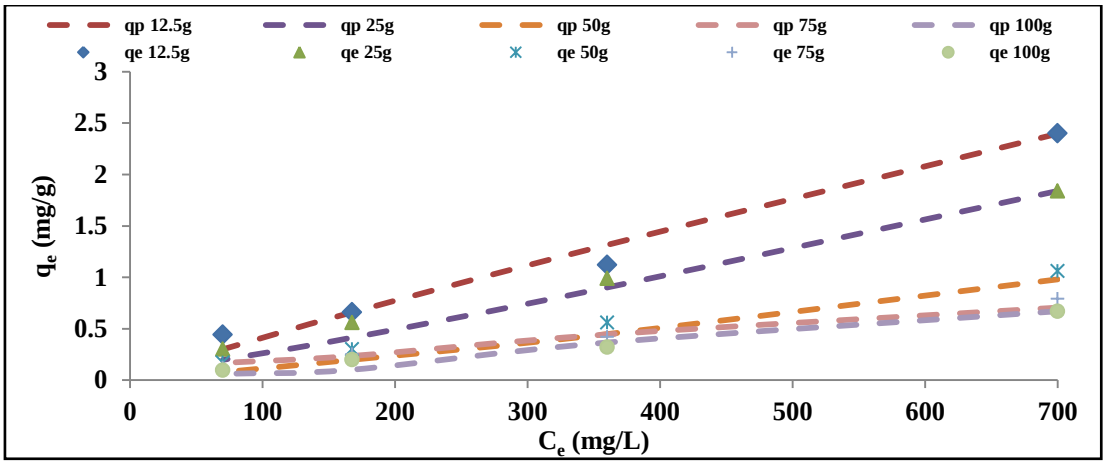
qp 12.5g
qp 25g
qp 50g
qp 75g
qp 100g
qe 12.5g
qe 25g
qe 50g
qe 75g
qe 100g
qe (mg/g)
Ce (mg/L)

(b)

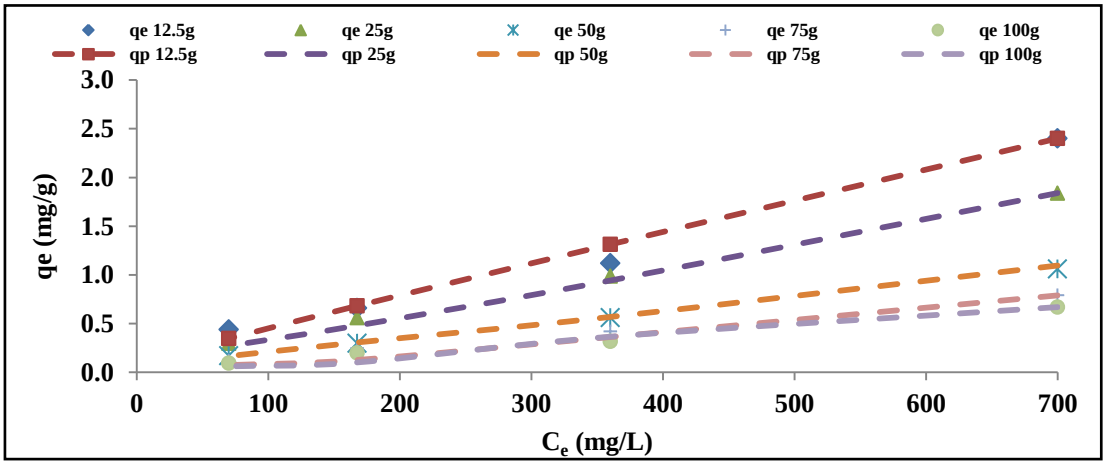
qe 12.5g
qe 25g
qe 50g
qe 75g
qe 100g
qp 12.5g
qp 25g
qp 50g
qp 75g
qp 100g
qe (mg/g)
Ce (mg/L)

(c)

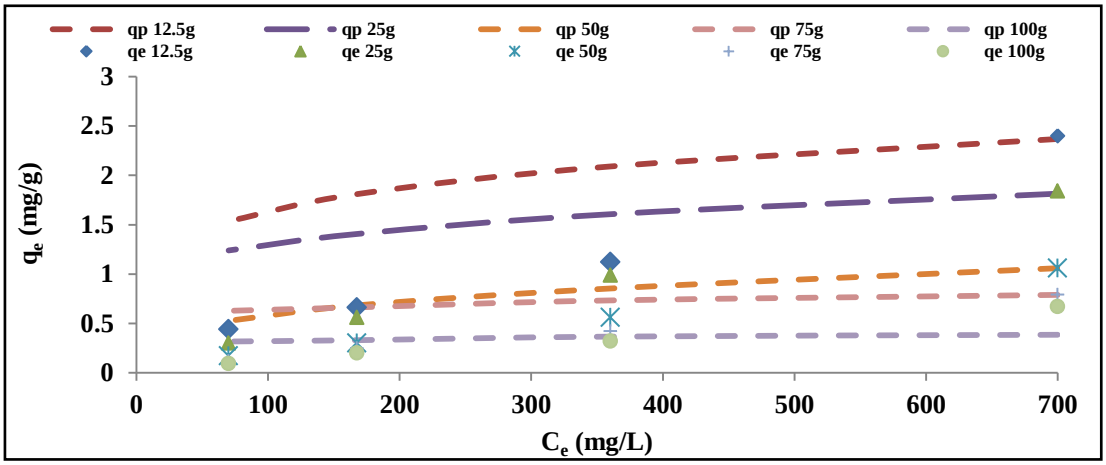
qp 12.5g
qp 25g
qp 50g
qp 75g
qp 100g
qe 12.5g
qe 25g
qe 50g
qe 75g
qe 100g
qe (mg/g)
Ce (mg/L)

(d)

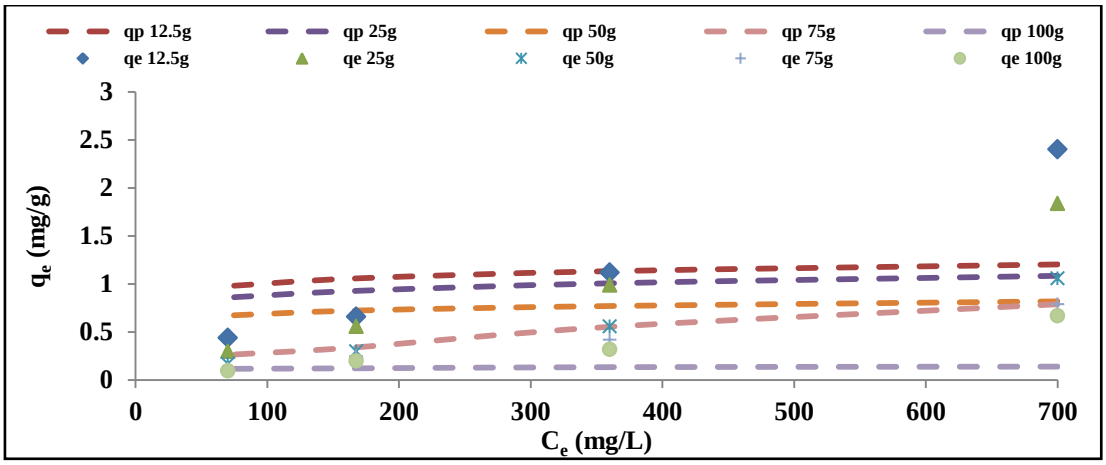

(e)

Figure 5.5: Non-Linear Regression Analysis for Isotherms (a) Langmuir (b) Fruendlich (c) Redlich-Peterson (d) Sips (e) Toth

Table 5.3: Isotherm parameters obtained using non-linear regression method for DR 81 removal onto acid modified soil

Isotherm model	Isotherm Parameter	100g/100mL	75g/100mL	50g/100mL	25g/100mL	12.5g/100mL
Langmuir	q_m	0.674	1.017	1.066	1.085	0.583
	K_l	0.006	0.004	0.009	0.05	0.61
	R^2	0.73	0.874	0.751	0.278	-0.57
	$RMSE$	0.175	0.13	0.38	0.944	1.477
	χ^2	0.084	0.049	0.289	1.327	1.687
Fruendlich	K_f	0.002	0.021	0.002	0.005	0.006
	n	1	1.708	0.969	1.065	1.108
	R^2	0.931	0.96	0.918	0.971	0.975
	$RMSE$	0.102	0.098	0.222	0.195	0.195
	χ^2	0.067	0.03	0.114	0.082	0.079
R-P	K_r	0.002	0.002	0.002	0.003	0.003
	a_r	0.001	0.006	0.039	0.042	0.041
	β	0.003	0.085	0.218	0.279	0.273
	R^2	0.932	0.92	0.997	0.993	0.98
	$RMSE$	0.101	0.129	0.032	0.089	0.177
	χ^2	0.066	0.085	0.002	0.016	0.054
Sips	K_s	0.126	0.31	0.097	0.347	0.362
	a_s	0.115	0.142	0.088	0.316	0.329
	β_s	0.081	0.093	0.284	0.16	0.188
	R^2	0.201	0.736	0.861	0.789	0.778
	$RMSE$	0.394	0.71	0.595	1.395	1.866
	χ^2	0.737	0.803	0.558	1.459	1.964

Toth	K_T	0.098	0.054	0.502	0.587	0.669
	a_T	0.873	0.05	0.05	0.05	0.05
	$1/t$	0.936	0.553	0.92	0.902	0.91
	R^2	-0.706	0.813	-0.154	0.254	0.186
	$RMSE$	0.467	0.213	0.792	0.978	1.234
	χ^2	0.558	0.25	2.222	1.599	1.497

5.3.4 Characterisation of the Acid Modified Soil

5.3.4.1 X-Ray Diffraction

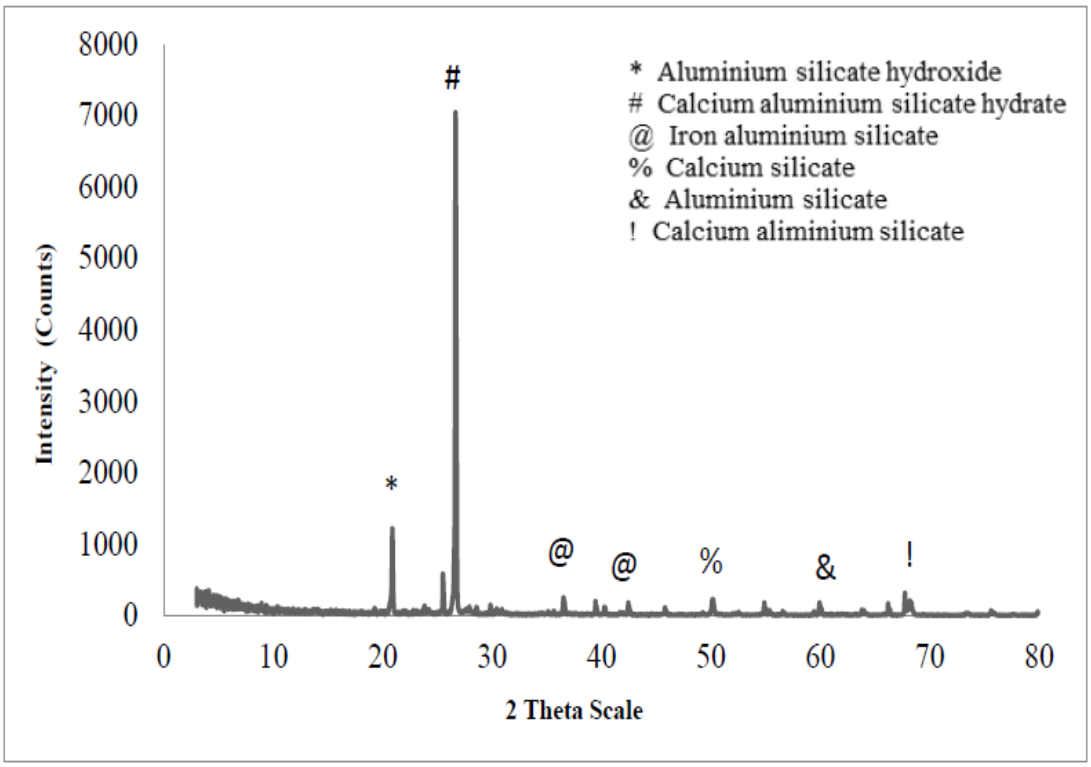

Figure 5.6: XRD pattern for Acid modified soil

Figure 5.6 shows the XRD pattern of the acid modified soil. The intensity of the peak at 2θ = 20.90 (d= 4.25Å) is decreased as compared to non-modified soil (Refer Figure 4.14). This can be due to acid washing of soil which may remove impurities that block the pores and eliminate cations to change into H-form and finally dealuminate the structure (Wang & Peng 2010). The same might have happened at the peak 2θ = 59.9. The decrease in the intensity at 2θ = 36.53, 42.45, 50.19, 59.94 and 68.19 might be the result of the dissolution of the compounds present on the soil surface due to acid attack. The position and d spacing of the peaks have no obvious change after being acid modified.

5.3.4.2 X-Ray Fluorescence Analysis

Table 5.4: XRF of Acid-modified soil

Constituents	Wt%
SiO_2	21.13
Al_2O_3	3.7
Fe_2O_3	2.01
CaO	0.73
MgO	0.14
Na_2O	0.66
K_2O	0.54

The chemical composition of acid-modified soil was obtained by using XRF analysis. Table 5.4 indicates the presence of silica, alumina and iron oxide as major constituents, along with traces of sodium, potassium, calcium, and magnesium oxides. The data in Table 5.3 shows that there is an increase in the SiO_2 content of the acid modified soil as compared to the non-modified soil (Refer Table 4.5). It is thus expected that the dye species may be removed mainly by SiO_2 and/or Al_2O_3.

5.3.4.3 Surface Area

Table 5.5: BET surface area analysis of acid-modified soil

Parameter	Acid modified
Average Pore Size(Å)	18.692
Langmuir Surface Area(m^2/g)	0.649
BET Surface Area(m^2/g)	0.213
Total Pore Volume(cm^3/g)	$1.992X10^{-4}$

The surface area, average pore size and total pore volume was measured by BET method. From Table 5.5, it is clear that the acid modified soil not only showed marked differences in its porous structure but also in the extent of surface area as compared to the non-modified soil (Refer Table 4.6).This indicates that significant structural changes took place after acid modification. It could be seen that non-modified soil have mesopores while after modification, the acid modified soil became microporous.

Non-modified soil showed relatively larger total pore volume indicating that the soil has a higher mesoporosity. Acid modified soil has a very low surface area and pore

volume. Therefore, it can be said that its adsorption characteristics could be presumed mainly due to the chemical interactions between the dye molecules and its surface functional groups (Ip et al. 2009). Acid treatment increases microporosity significantly and decreases the cation-exchange capacity due to partial dissolution of both Si-tetrahedra and free linkages, which yields secondary micropores and destroys specific exchange sites of the adsorbent (Wang & Peng 2010).

5.3.4.4 Scanning Electron Microscopy (SEM)– Energy Dispersive X-Ray (EDX) Analysis

Figure 5.7 and Table 5.6 show EDX analysis and the elemental composition of the acid modified and DR81 adsorbed acid modified soil. Table 5.6 shows the decrease in the weight percentage of the elements in the DR81 adsorbed acid modified soil as compared to acid modified soil. This indicates the utilization of the constituents of the soil for adsorption of the dye molecule. Also, when the elemental composition of the non-modified soil (Refer Table 4.7) was compared with the acid-modified soil, the weight percentage of aluminium decreased to 5.7% from 12.53%. It is because aluminium is present on the octahedral position and can be leached out (Liu & Zhang 2007).The increase in the weight percent of Fe, Ca and Mg is because these elements are precipitated as oxides from the outer silica layer (Jozefacuik & Bowanko 2000). No significant change can be noticed in potassium. The increase in the Si and O could be due to the Si-O-Si bond breakage due to modification process.

Table 5.6: Elemental Composition of Acid-modified Soil

Element	**Acid modified**		**DR 81 adsorbed acid modified soil**	
	Wt%	At%	Wt%	At%
O	63.11	56.69	57.87	52.86
Si	17.46	22.58	14.28	19.23
Al	5.7	4.01	1.98	1.38
Fe	3.09	1.1	1.61	0.54
Ca	7.25	9.15	0	0
Mg	0.61	0.55	0.27	0.21
K	0.09	0.38	0.05	0.29
Na	2.69	5.54	4.98	7.78

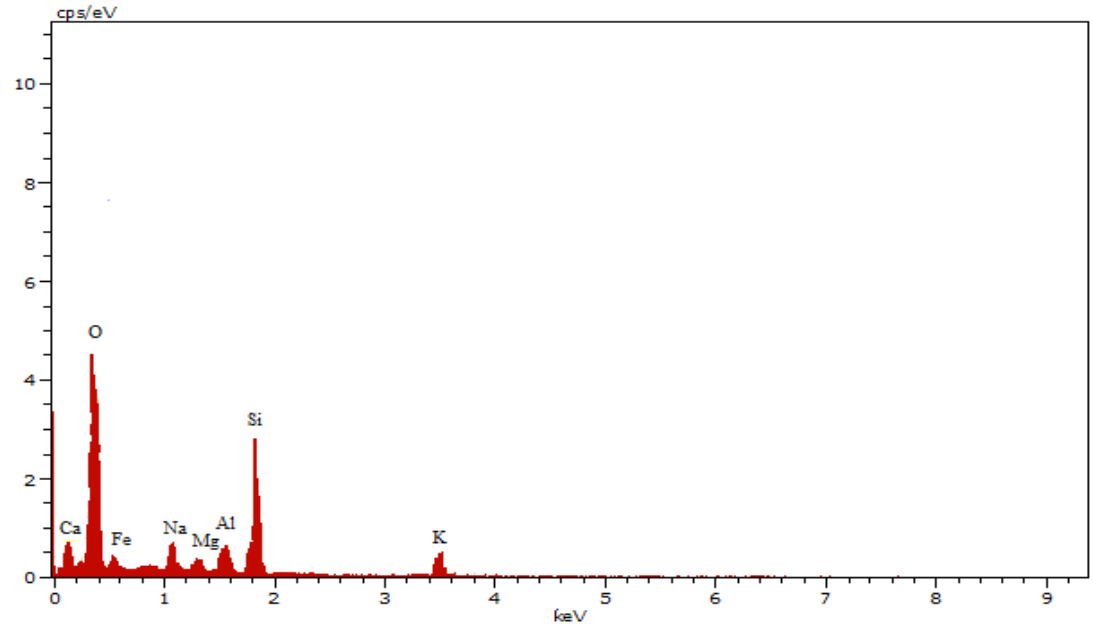

(a)

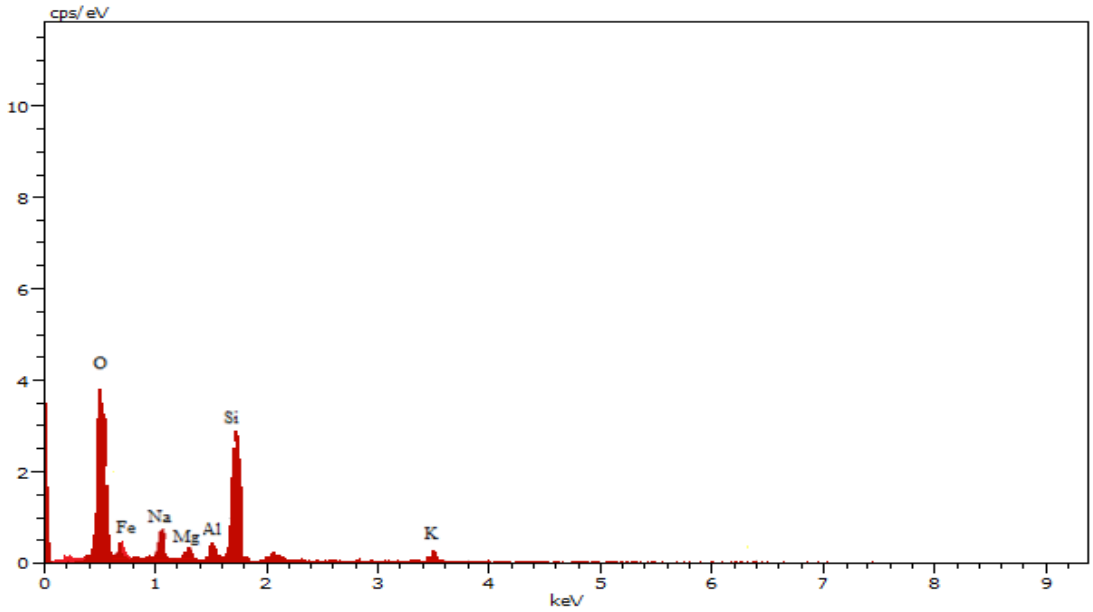

(b)

Figure 5.7: Energy Dispersive X-Ray Analysis of (a) Acid-modified soil and (b) DR81 adsorbed Acid-modified Soil

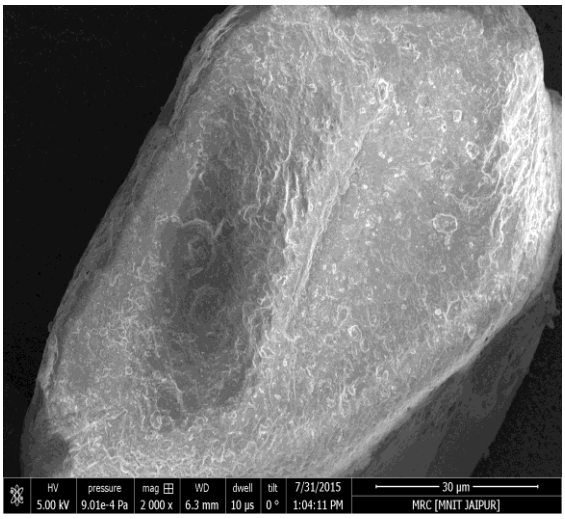

(a)

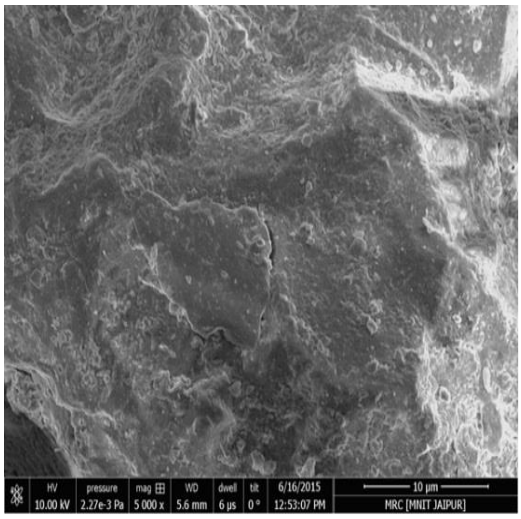

(b)

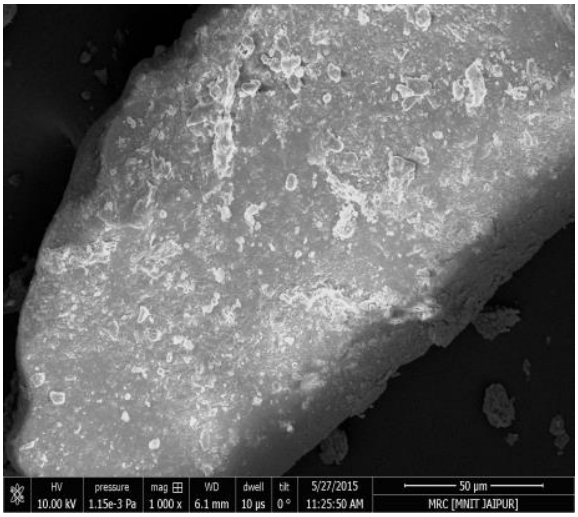

(c)

Figure 5.8: SEM images for (a) & (b) Acid-modified Soil (c) DR81 adsorbed Acid-modified Soil

Figure 5.8 shows the SEM monographs for acid-modified soil before adsorption and after adsorption of DR 81dye.

5.3.4.5 Fourier Transform Infrared Spectroscopy Analysis and Zeta Potential of the soil surface

Figure 5.9 shows the zeta potential for the acid modified soil. The acid modification resulted in the decrease in the zeta potential of the soil. Zeta potential of acid modified soil is -15.6 mV whereas non-modified soil has -17 mV. This value reveals that surface of the soil acquires some positive charges and therefore, becomes receptive to

the uptake of negatively charged dye anions through electrostatic attractions (Ziona et al. 1990).

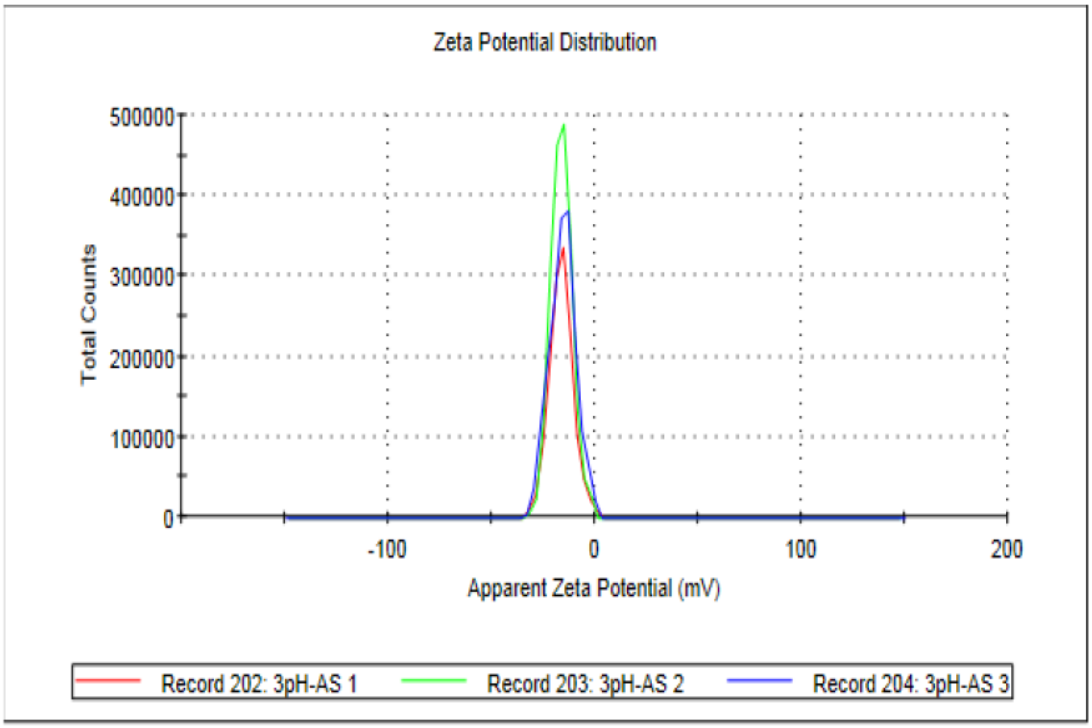

Figure 5.9: Zeta Potential for Acid modified soil

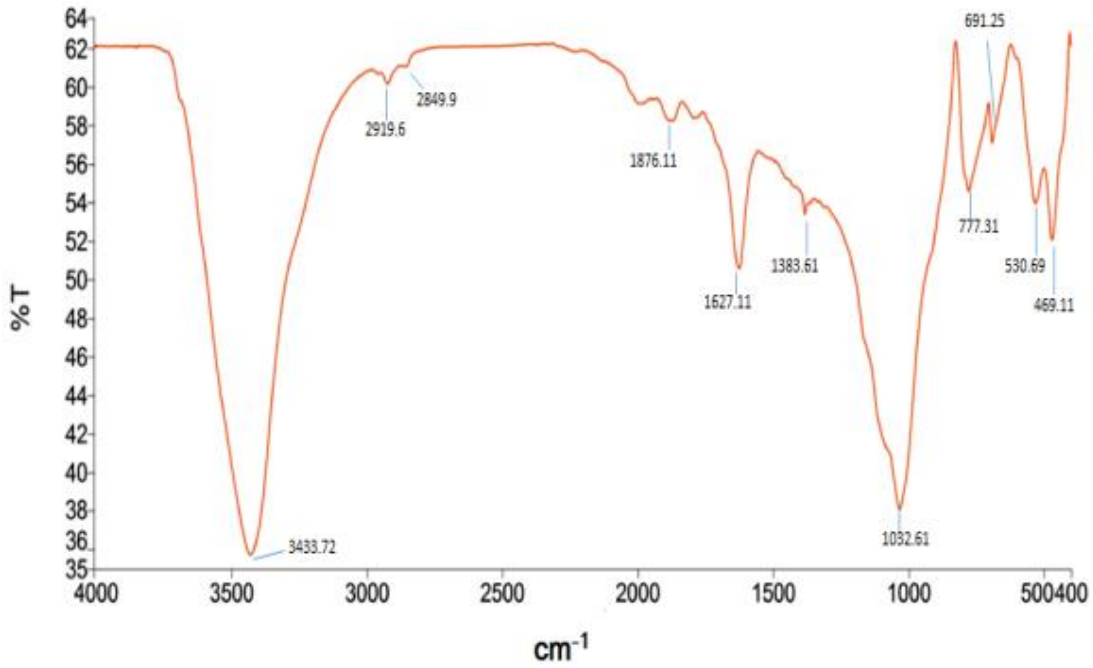

(a)

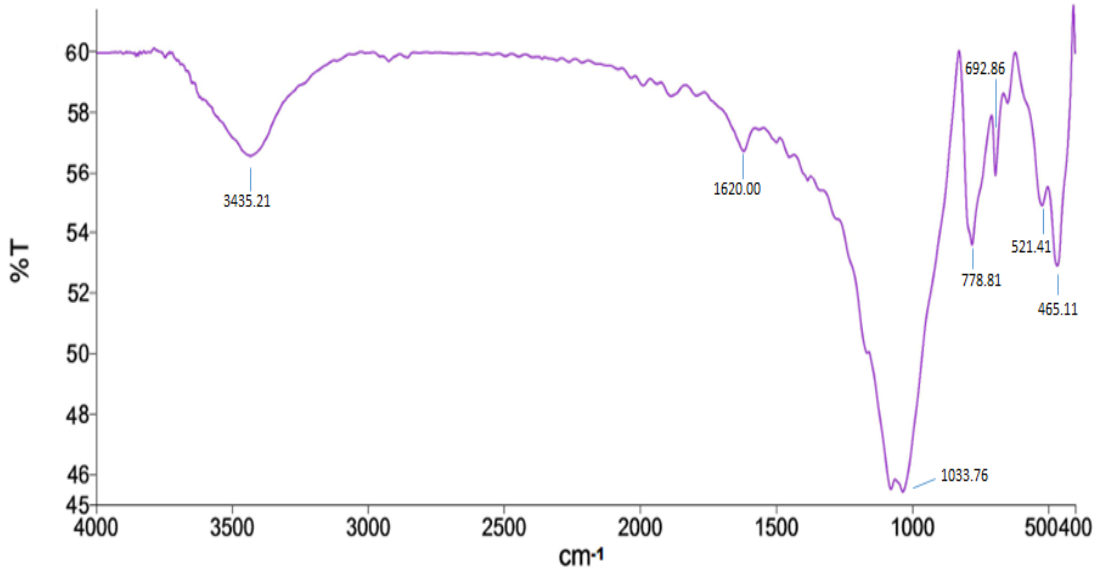

(b)

Figure 5.10: FTIR spectra for (a) Acid-modified soil (b) DR81 adsorbed Acid-modified soil

Figure 5.10 (a) shows the FTIR spectra of acid modified soil. On comparing with the FTIR spectra non-modified soil, it was found that the intensity of the stretching vibration of silanol (SiO-H) group at 3433.72cm^{-1} decreased in acid activated soil. This may be accepted as evidence for acid activation occurring on soil (Mahmoodi et al. 2011) (Özcan & Özcan 2004). The appearance of bending vibrations of a methylene group (-CH_2) at 1383.61 cm^{-1} and decrease in the intensity of H-O-H group at 1627.11cm^{-1} supports the adsorption of hydronium ions on the adsorbent surface. The band at 1383.61 cm^{-1} is not observed in non-modified soil however overlapped with different small peaks of non-modified soil (Özcan et al. 2004) (Bera et al. 2013). This result can also be supported by the zeta potential result of the acid modified soil. The zeta potential of acid modified soil is -15.6mV. This decrease in zeta potential on the surface of the soil after acid modification proves the attachment of the hydronium ions on the soil surface. No change at bands 1876.11 cm^{-1}, 1032.61 cm^{-1} and 691.25 cm^{-1} was observed. Also, the modification in the methylene group at bands 2919.6 cm^{-1}and 2849.9 cm^{-1} supports the above results.

The band at 2919.6 cm^{-1}(CH_2 asymmetric stretching), 2849.9 cm^{-1} (CH_2 symmetric stretching) and 1383.61 cm^{-1} (CH_2 bending vibrations) disappeared which indicates

that methylene group is responsible for the adsorption of DR81 dye. The increase in the intensity of the band at 1627.11 cm^{-1} modified to 1620.00 cm^{-1} indicates that the symmetric stretching and bending vibrations of the silanol group does not participate in the adsorption of DR81 dye. The intensity of the band at 1033.76 cm^{-1}also increased, indicating that symmetric stretching of the C-OH does not take part in the adsorption. The slight increase in the intensity of the bands at 692.86 cm^{-1}, 521.41 cm^{-1} and 465.11 cm^{-1} respectively indicate that the asymmetric bending of the Si-O does not participate in the adsorption.

5.4 Summary

This Chapter showed that acid modification of non-modified soil gave minor but promising enhancement of the adsorption capacity. Surface characterisation of acid-modified soil showed that negative charge on soil decreased after acid modification. This, therefore, increased adsorption of anionic DR81 dye. The contact time of 10 minutes was found to be sufficient to attain equilibrium adsorption. The acid modified soil gave the highest equilibrium adsorption upto 2.40 mgg^{-1}. The DR81 adsorption increased with the increase in dye concentration range 125 mg/L to 1000 mg/L. The pseudo second order model exhibited the best correlation for the experimental data and indicated that boundary layer resistance is not the rate limiting step. The results from assessing intraparticle diffusion model revealed that intraparticle diffusion is not the only process controlling the DR81 adsorption on acid modified soil but boundary layer effect also exists. The equilibrium analysis showed that Redlich-Peterson and Freundlich isotherm yielded better fit to the adsorption data, signifying that DR81 does not form a monolayer on the adsorbent and rather follows multilayer adsorption.

Although the generation of effluents containing direct dyes from textile industries is almost unavoidable, the results of the present study indicate that acid modified soil can be successfully employed for the removal of DR81 over a wide concentration range.

CHAPTER

6

Chapter 6

Removal of Methylene Blue onto Alkali-Modified Soil

This Chapter discusses the modification of non-modified soil for adsorption of Methylene Blue dye. The effect of operational parameters like contact time, initial dye concentration and adsorbent dose on adsorption is also discussed. Investigations based on these parameters are used for kinetic modelling and equilibrium studies. The effect of surface characteristics on adsorption of the dye has also been discussed in detail.

6.1 Introduction

From the chapter 4, it is clear that the non-modified soil has negative charge at natural pH as explained in Section 4.3.4.5. MB has positively charged nitrogen and sulphur atoms in its structure (Section 3.3.1.2). This helps in the adsorption of MB onto non-modified soil surface. However, it was also observed that MB removal became better as the pH ranges towards the alkaline region. This was because non-modified soil acquires more negative charge and hence, the better electrostatic attraction between the negatively charged Si-O group on the soil surface and positively charged methylene blue dye (Al-Ghouti et al. 2003).

$$\text{Si-OH} + {}^{-}\text{OH} \rightarrow \text{Si-O}^{-} + \text{H}_2\text{O} \quad (6.1)$$

$$\text{Si-O}^{-} + \text{MB}^{+} \rightarrow \text{Si-O}^{-}\text{MB}^{+} \quad (6.2)$$

Therefore, alkali modification of the soil was carried so that its surface attains more negative charge and enhances the adsorption property of soil. Alkali activation has also been reported on kaolinite for MB removal by (Ghosh & Bhattacharyya 2002). Also, the idea to modify the non-modified soil in such a way is to eliminate the step of pH maintenance in the adsorption process. In dye treatment process, pH maintenance adds to the cost of treatment process. Therefore, modification of the soil with alkali might help in direct removal of the dye from aqueous solution.

6.2 Materials & Methods

6.2.1 Adsorbent

As the name suggests, the soil was modified using alkali; sodium hydroxide (NaOH). For alkali activation, the locally available soil from Rajasthan was collected from the

premises of Malaviya National Institute of Technology, Jaipur. The collected soil was then washed with distilled water to remove the suspended impurities and then oven dried at 100°C for 2 hours. The dried soil was crushed and sieved to give particle size 150-75 μm using ASTM Standard sieves. After sieving the soil to the desired particle size, it was stirred continuously at 10 rpm for 2 hours at room temperature in 1N NaOH in a flat bottom beaker. The soil to alkali suspension was kept at a constant ratio of 1:6 (kg: ml). Stirring was done to provide a better contact between the alkali and the soil surface. The stirring was stopped after 2 hours, and the soil-alkali suspension was left undisturbed for next 2 hours. This was so done to provide more reaction time between the soil surface and acid. After 2 hours, the suspension was washed several times with distilled water. The pH of the suspension was also checked, meanwhile washing. When the pH was brought down to ~11 to 11.5, washing was halted, and the modified soil was dried in oven at 100°C for 2 hours before use.

6.2.2 Adsorbate

Methylene blue stock solution was prepared as discussed in Section 3.3.1.3.

6.2.3 Adsorption Studies

The adsorption measurements were carried out by the batch method given in Section 3.3.2.

6.3 Results & Discussion

6.3.1 Parametric analysis

This section elucidates the effect of contact time, initial dye concentration and adsorbent dose. Effect of pH has not been discussed in this section as the adsorbent has been modified to acquire a negative charge. And also, it is reported in Chapter 4 that MB shows better removal at alkaline pH. The particle size range chosen for all the parametric analyses is 150-75μm because this size range gave better removal, as reported in Chapter 4.

6.3.1.1 Effect of initial dye concentration and contact time

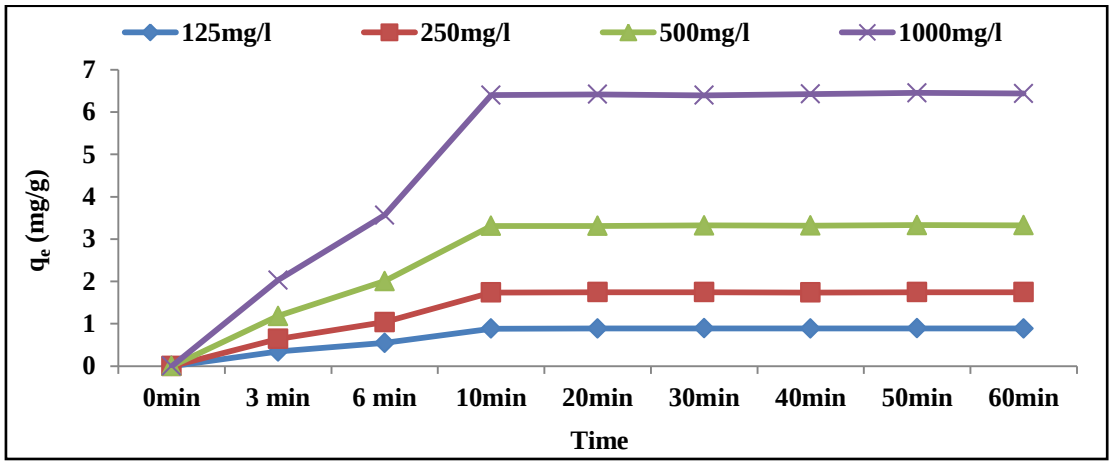

Figure 6.1: Effect of initial dye concentration and contact time on MB removal onto alkali modified soil (Condition: dose: 12.5g/100mL)

The adsorption of MB on alkali modified soil was studied at different MB concentration (125 mg/L, 250 mg/L, 500 mg/L and 1000 mg/L). Figure 6.1 shows the result of effect of initial concentration on adsorption of MB onto alkali modified soil at 30°C. It is observed that dye uptake was rapid for the first 10 minutes, and thereafter, saturation stage was attained. It could also be seen from Figure 6.1 that an increase in initial MB concentration results in an increase in the adsorption of MB onto alkali modified soil. The equilibrium adsorption increases from 0.89mgg^{-1} to 6.40mgg^{-1} with an increase in the initial MB concentration. However, equilibrium percent removal of MB gets decreased from 88.35% to 79.96%. This indicates that the initial dye concentration plays an important role in the adsorption capacity of dye. At high initial dye concentration, aggregation of the MB molecules takes place. Therefore, dye molecules get adsorbed onto the external surface. However, due to mass transfer property, dye molecules can migrate from the external surface to the interlamellar region, resulting in the deaggregation of the aggregates and restoring the monomers(Neumann et al. 2002) (Bujdák & Komadel 1997) (Gürses et al. 2006).

Comparison between non-modified and alkali modified soils for percent and mgg^{-1} removal of MB is given in Table 6.1. It can be observed from the Table 6.1 that alkali modified soil gave better MB removal than non-modified soil.

Table 6.1: Effect of initial dye concentration on MB removal (Condition: adsorbent dose: 12.5g/100mL, contact time: 10 minutes)

Dye Concentration	**% removal**		**q_e (mgg^{-1})**	
	Non-modified Soil	Alkali-modified Soil	Non-modified Soil	Alkali-modified Soil
125mg/L	55	88.55	0.55	0.89
250mg/L	49	86.93	0.98	1.74
500mg/L	43	82.79	1.72	3.31
1000mg/L	38	79.96	3.04	6.40

6.3.1.2 Effect of adsorbent dose

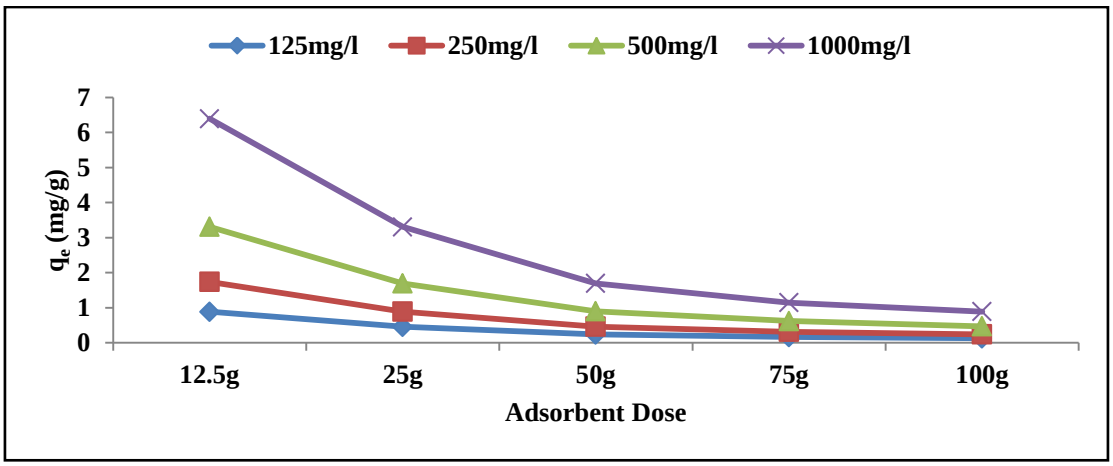

Figure 6.2: Effect of alkali modified soil dose on MB removal. (Condition: time: 10 min)

The adsorption of MB on alkali modified soil was investigated at different adsorbent doses (12.5g/100mL, 25g/100mL, 50g/100mL, 75g/100mL, and 100g/100mL). Figure 6.2 shows the result of effect of adsorbent dose on adsorption of MB onto alkali modified soil at 30°C. While the adsorbent dose increases from 12.5g/100mL to 100g/100mL at a contact time of 10 minutes, the adsorption capacity of MB onto soil surface decreases from 0.89mgg^{-1} to 0.12mgg^{-1} for 125 mg/L, 1.74mgg^{-1} to 0.25mgg^{-1} for 250 mg/L, 3.33mgg^{-1} to 0.47mgg^{-1} for 500 mg/L and 6.40mgg^{-1} to 0.89mgg^{-1} for 1000 mg/L of MB concentration. However, percent removal increases from 88.55% to 99.45%for 125 mg/L, 86.93% to 95.23%for 25 mg/L, 82.79% to 93.56% for 500 mg/L and 79.96% to 88.95% for 1000 mg/L of MB concentration. The increase in the percent removal of MB by increasing the adsorbent dose at a fixed MB concentration could be due the increased number of available adsorption sites. However, the amount of MB adsorbed decreased per unit mass of adsorbent as the adsorbent increased. This

could be due to the fast saturation of the easily available active sites for MB adsorption (Banat et al. 2003).

Comparison between non-modified and alkali modified soils for percent and mgg^{-1} removal of MB1 is given in Table 6.2. It can be observed from Table 6.2 that alkali modified soil gave better MB removal than non-modified soil.

Table 6.2: Effect of adsorbent dose on MB removal (Condition: dye concentration: 1000 mg/L; contact time: 10 minutes)

Adsorbent dose	**% removal**		**q_e (mgg^{-1})**	
	Non-modified Soil	Alkali-modified Soil	Non-modified Soil	Alkali-modified Soil
12.5g/100mL	38	79.96	3.04	6.40
25g/100mL	67	82.60	2.68	3.30
50g/100mL	69	84.56	1.38	1.69
75g/100mL	77	85.96	1.03	1.15
100g/100mL	81	88.95	0.81	0.89

6.3.2 Kinetic modelling

The study of adsorption kinetics in dye removal from textile wastewater is considered to be significant as it provides valuable insights into the mechanism of adsorption reactions. Also, the kinetics describes the rate of dye uptake which controls the contact time at the adsorbent interface. Therefore, kinetic modelling helps in the prediction of the rate at which dye is removed from the aqueous solutions and also in the designing the appropriate adsorption treatment plant (Gürses et al. 2006).

6.3.2.1 Lagergren's Pseudo First Order Kinetic Model

The correlation coefficient R^2, rate constant k_1 and adsorption capacity, q_e^{exp} and q_e^{pred}, for Lagergren's pseudo first order equation for the adsorption of MB are shown in Table D.1 in Appendix D. The values of correlation coefficients were rather low for the first order model for both the operating parameters i.e. adsorbent dose and dye concentration. Also, the values of q_e^{exp} and q_e^{pred} did not match well. This suggests that adsorption of MB is not a pseudo first-order reaction.

6.3.2.2 Lagergren's Pseudo Second Order Kinetic Model

The correlation coefficient R^2, rate constant k_2 and adsorption capacity, q_e^{exp} and q_e^{pred}, obtained from Lagergren's pseudo second order equation (Equation 3.3) for the adsorption of MB has been given in Table D.1 in Appendix D. Figure 6.3

illustrates that the data show a good compliance with the pseudo second order equation and the regression coefficients for the linear plot were higher than 0.99 for all the adsorbent doses and dye concentrations. Therefore, it can be said that kinetics for the adsorption of MB on alkali modified soil follows pseudo second order rate expression. From Table D.1, equilibrium adsorption capacity q_e, increased with increase in the initial dye concentration. This indicates that the MB removal is dependent on intial dye concentration. However, the rate constant k_2, decreased as the initial MB concentration increased from 125 mg/L to 1000 mg/L. The similar observation was reported by (Azizian 2004). Bujdak and Komadel (Bujdák & Komadel 1997) reported that at high dye concentration MB cations are adsorbed via ion exchange, frequently accompanied by aggregation of MB molecules. Also, this situation shows in an aqueous medium, the role of the exchangeable alkali ions on the surface and in the interlayer region of the alkali modified soil. However, the rate constant k_2 , increased with increase in the adsorbent dose. This might be due to increase in number of active sites with adsorbent dose.

From Table D.1, the values of predicted equilibrium adsorption capacities q_e^{pred} and correlation coefficients R^2 for Lagergren's pseudo second-order model are much more reasonable when compared with results of the pseudo first-order model. Since most of the first-order predicted q_e^{pred} values deviate significantly from the experimental q_e^{exp} values, it suggests that the adsorption of dye onto alkali modified soil follows the pseudo-second order model.

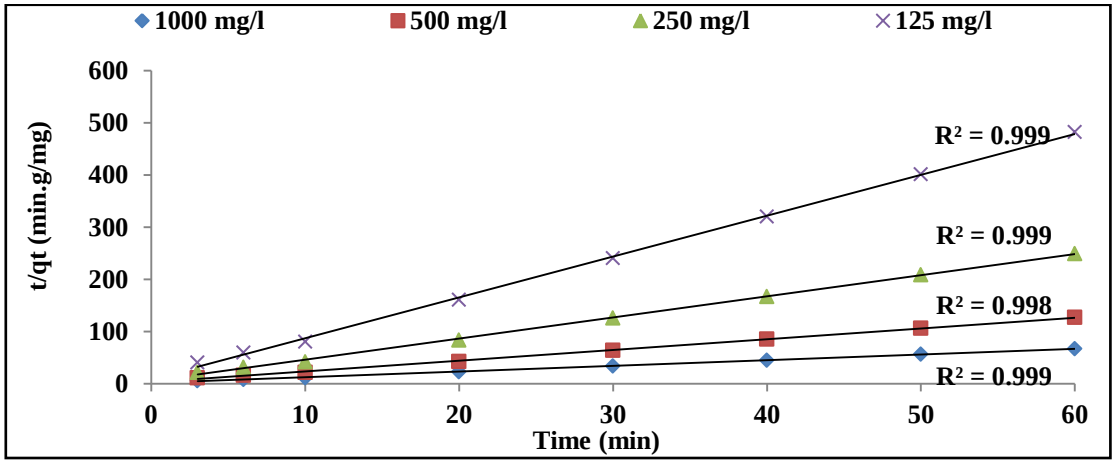

(a)

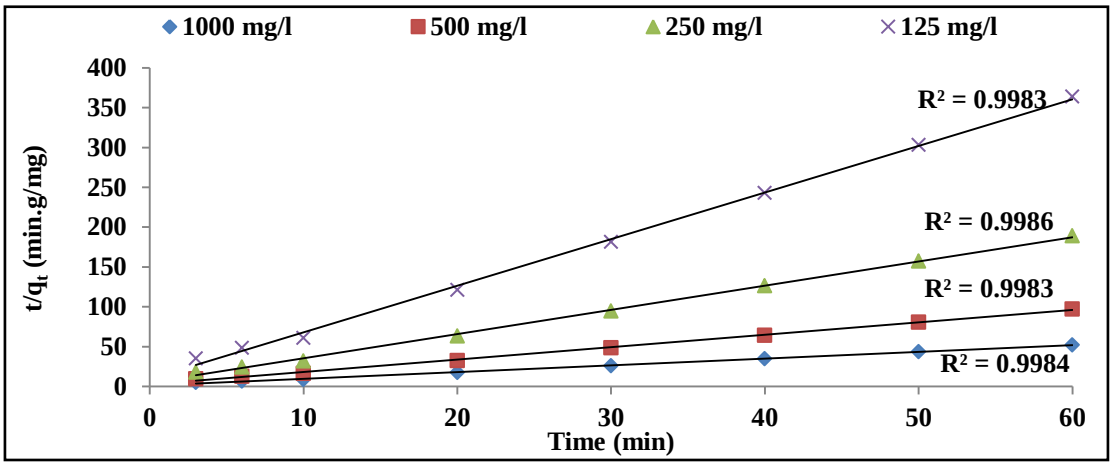
1000 mg/l
500 mg/l
250 mg/l
125 mg/l
t/qt (min.g/mg)
Time (min)
R² = 0.9983
R² = 0.9986
R² = 0.9983
R² = 0.9984

(b)

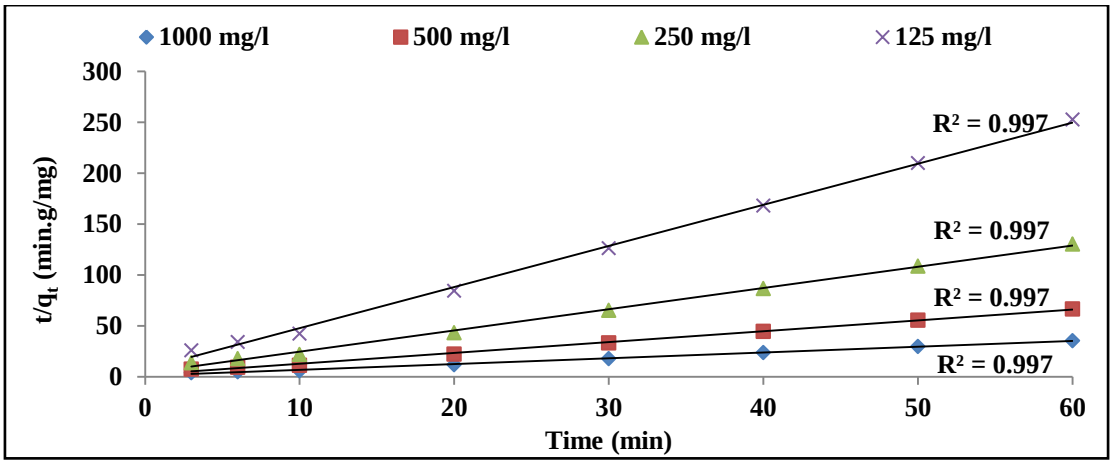
1000 mg/l
500 mg/l
250 mg/l
125 mg/l
t/qt (min.g/mg)
Time (min)
R² = 0.997
R² = 0.997
R² = 0.997
R² = 0.997

(c)

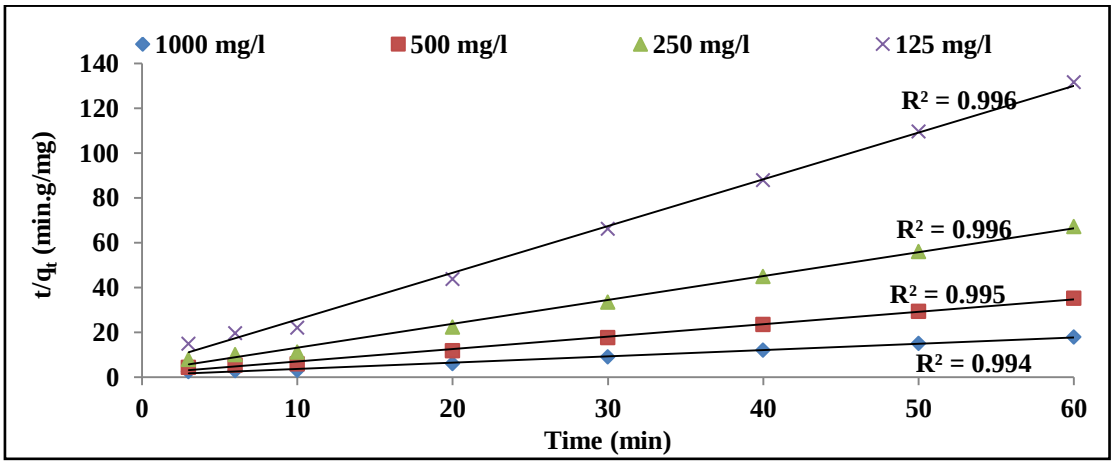
1000 mg/l
500 mg/l
250 mg/l
125 mg/l
t/qt (min.g/mg)
Time (min)
R² = 0.996
R² = 0.996
R² = 0.995
R² = 0.994

(d)

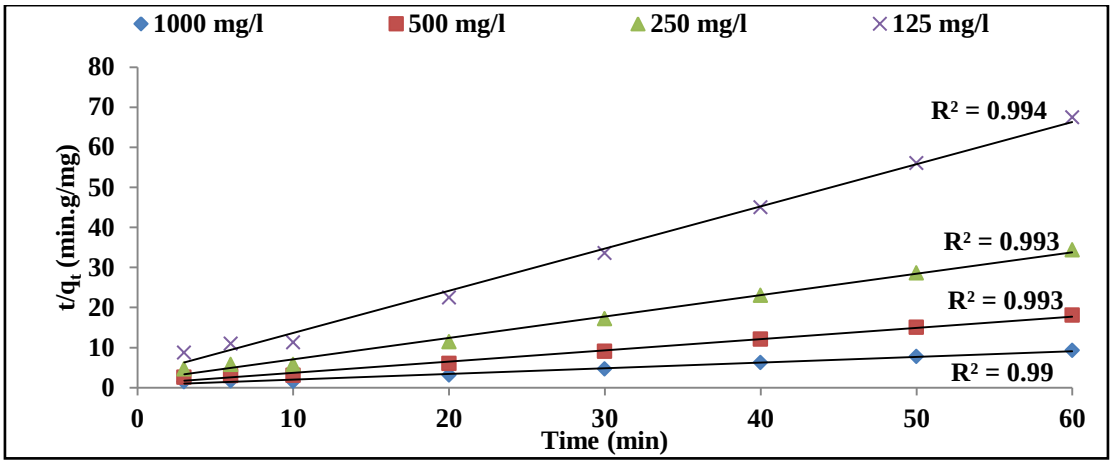

(e)

Figure 6.3: Lagergren's Pseudo Second Order Kinetic Plot for Adsorption of MB on Alkali Modified Soil (per 100mL) (a) 100g (b) 75g (c) 50g (d) 25g (e) 12.5g

6.3.2.3 Intraparticle Diffusion Model

Figure 6.4 show that the plots between q_t (mgg^{-1}) and the square root of time $t^{0.5}$(min). It could be observed that the plots present multi-linearity, which indicates that two steps occurred in the process. The plots show two phases: the initial curved portion of the plot indicated a boundary layer effect while the second linear portion was due to intraparticle diffusion. A similar multilinearity was observed by (Crini et al. 2007). The calculated k_{i_2} and C_2 values for each initial concentration are reported in Table D.2 in Appendix D. The slope $k_{i_2}$of the second linear portion characterizes intraparticle diffusion, whereas intercept C_2 of this portion is proportional to the boundary layer thickness. It was found that the value of k_{i_2} increasedwith increasing dye concentration. However, some deviations occurred at high initial dye concentration. These deviations may be attributed to some repulsion between dye–dye molecules and/or adsorbent/adsorbate molecules due to concentration density (Crini & Ndongo Peindy 2006) (Crini 2003). The R^2 values for this diffusion model are between 0.073 and 0.7923 as given in Table D.2. This indicates that the adsorption of MB onto alkali modified soil can be followed by an intraparticle diffusion model after 10 minutes of contact time. However, the results do not pass through the origin (the plots have intercepts in the range 0.124-0.887 mgg^{-1} for 100g, 0.16-1.15 mgg^{-1} for 75g, 0.236-1.694 mgg^{-1} for 50g, 0.454-3.292 mgg^{-1} for 25g, 0.885-6.361 mgg^{-1} for 12.5g), indicating that intraparticle diffusion is involved in the adsorption process but it is not the only rate-limiting mechanism and that some other mechanisms also play

an important role. This confirms that adsorption mechanism was a multi-step process, involving adsorption on the external surface, diffusion into the interior and ion exchange, as previously reported (Gürses et al. 2006) (Doğan et al. 2007). The values of the intercept C_2 given in the Table D.2 also give an idea about the boundary layer thickness: the larger the intercept, the greater is the boundary layer effect. Any increase in the value of C_2 indicates the abundance of MB adsorbed on boundary layer. As seen in Table D.2, the values of C_2 increases with increasing dye concentration. However, decreases with increase in adsorbent concentration.

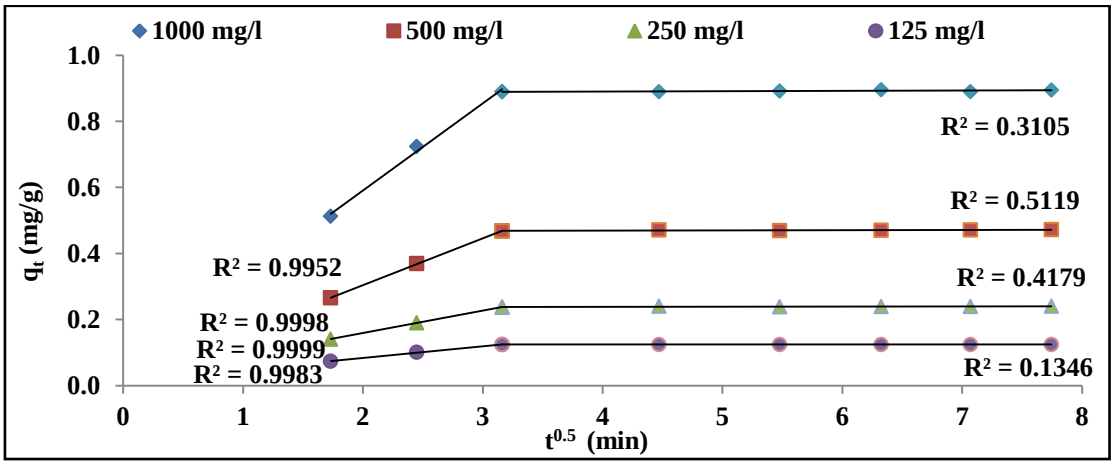

(a)

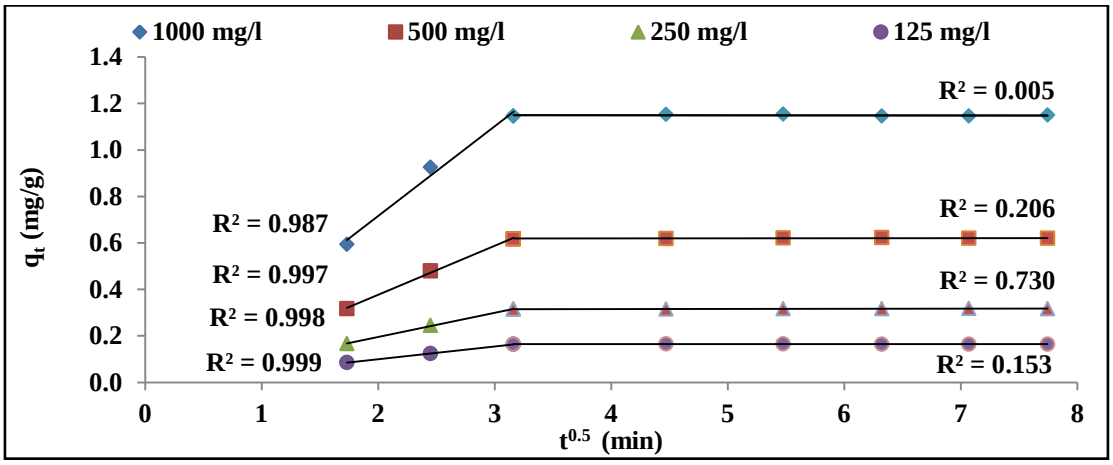

(b)

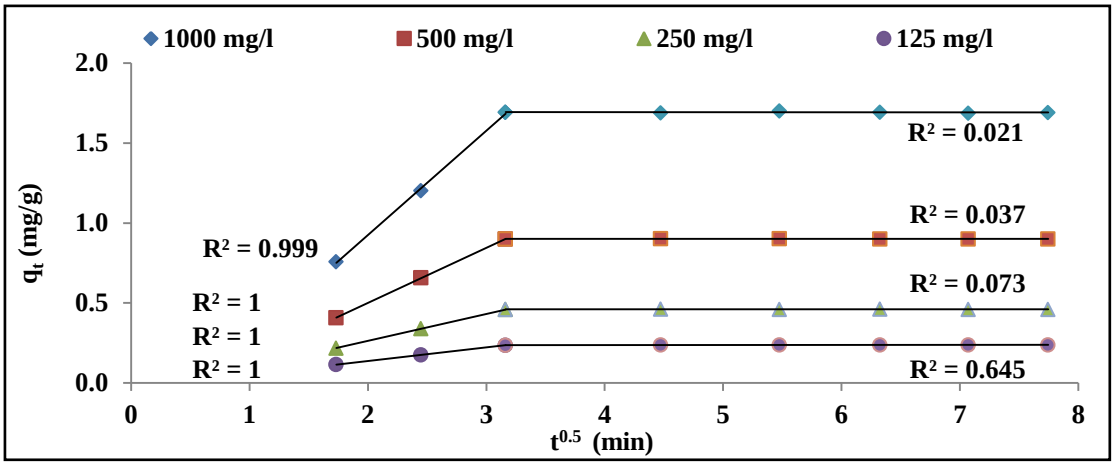

(c)

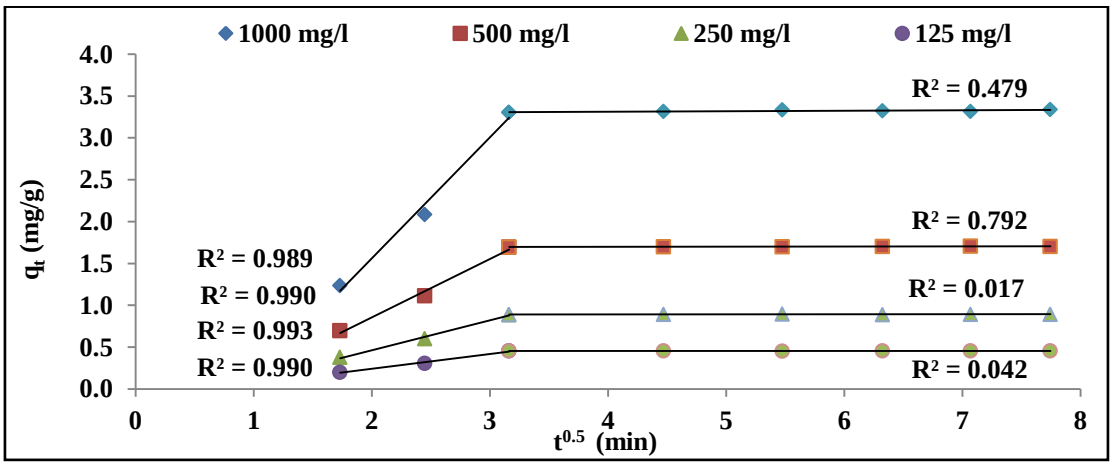

(d)

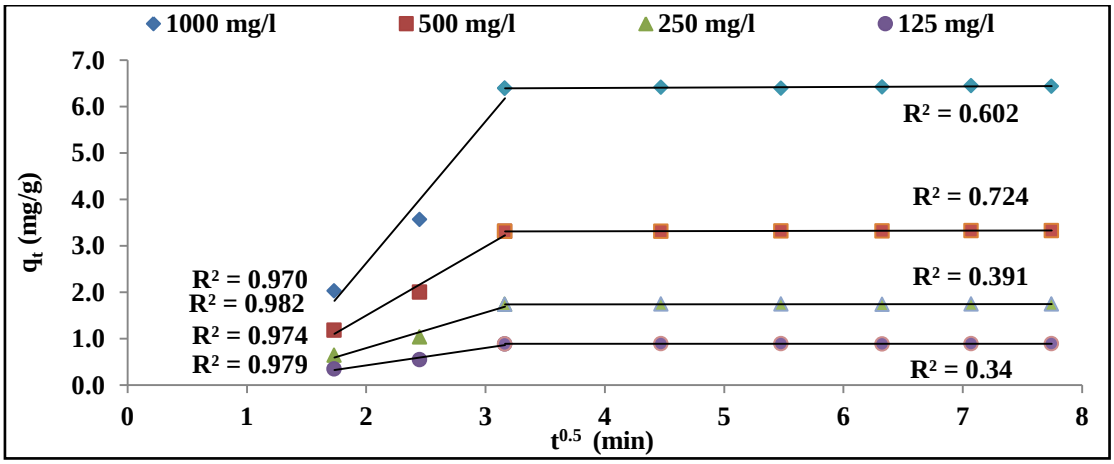

(e)

Figure 6.4: Intraparticle Diffusion Parameters for Adsorption of MB on Alkali Modified Soil (per 100mL) (a) 100g (b) 75g (c) 50g (d) 25g (e) 12.5g

6.3.3 Equilibrium Studies

The adsorption isotherms were developed for all the adsorbent doses i.e. 100g/100mL, 75g/100mL, 50g/mL, 25g/mL and 12.5g/mL. C_e is the MB concentration in aqueous solution at equilibrium at contact time of 10 minutes for initial dye concentration (125 mg/L – 1000 mg/L) and q_e is calculated by Equation 3.1. Table D.3 in Appendix D shows the isotherm parameters for Langmuir and Freundlich isotherms.

6.3.3.1 Linear Regression Analysis

Table D.3 shows that the behaviour of adsorption processes of MB onto the alkali modified soil. The Langmuir parameters q_m and K_l show negative values and hence, Langmuir isotherm failed to describe the data and will not be discussed in this case. The data exhibited the Freundlich behaviour, since $R^2 > 0.937$, which indicates adsorption is not restricted to monolayer formation as in the case of Langmuir isotherm (Robinson et al. 2002). Freundlich parameters, K_f is roughly an indicator of the adsorption capacity for an arrow sub-region having equally distributed energy sites toward specific adsorbate and n refers to adsorption tendency (Gemeay 2002). It is clear from the experimental results of Freundlich isotherm given in Table D.3 that the adsorption capacity corresponding to the initial equilibrium concentration was increased in order: 100g/100mL>75g/100mL >50g/100mL >25g/100mL >12.5g/100mL. The $(1/n)$ value from Freundlich equation indicates that the relative distribution of energy sites and depends on the nature and strength of the adsorption process. Moreover, the closer of the n value to 1, indicate homogenous surface (Khraisheh et al. 2005).

6.3.3.2 Non-Linear Regression Analysis

The non-linear regression analysis was carried out for five isotherms; Langmuir, Fruendlich, Redlich-Peterson, Sips and Toth. The experimental q_e^{exp} was calculated by the Equation 3.1 and the predicted q_e^{pred} is obtained from the non-linear expressions of the above mentioned isotherms, given in the Table 3.2.

Table 6.3 shows the non-linear regression analysis of five isotherm models, namely; Langmuir, Fruendlich, Redlich-Peterson, Sips and Toth isotherm. Figure 6.5 illustrate the plots for all the above mentioned isotherms. The order of fitness of isotherm models from the best to the least was Sips <Freundlich< Langmuir <Redlich–Peterson

<Toth isotherms based on their R^2 values. The assertion that sometimes correlation coefficient, R^2 does not justify the basis for selection of best fit of adsorption model, was investigated by use of Chi-square χ^2 and RMSE statistical test (Auta & Hameed 2012). The χ^2 and RMSE test results obtained in this study further supported that Sips isotherm was the best model that described the process of adsorption of MB on alkali-activated soil as revealed by correlation coefficient R^2. This was revealed by smaller values of χ^2 and RMSE signifying stronger alliance between theoretical and experiment data as compare with other models tested.

Sips isotherm has features of both Langmuir and Freundlich. The Sips isotherm parameter's value β_s determines whether the model tends towards Freundlich or Langmuir. The smaller is the value of this parameter, the more heterogeneous is the adsorbent surface and reduces to Freundlich equation. If β_s is equal to 1, the Sips equation isreduced to the Langmuir equation and the surface is homogeneous (Sreńscek-Nazzal et al. 2015). It can be observed from Table D.4, that β_s value at 100g/100mL, 75g/100mL and 50g/100mL of adsorbent dose is 0.547, 0.539 and 0.669 respectively. This indicates that Freundlich isotherm is approaching. Thus it can be concluded that when the adsorbent dose is high then multilayer is formed. When adsorbent dose is reduced then Langmuir isotherm governs and monolayer adsorption takes place (Hossain et al. 2012). The correlation coefficient R^2 of Freundlich and Langmuir isotherm also supports this phenomenon.

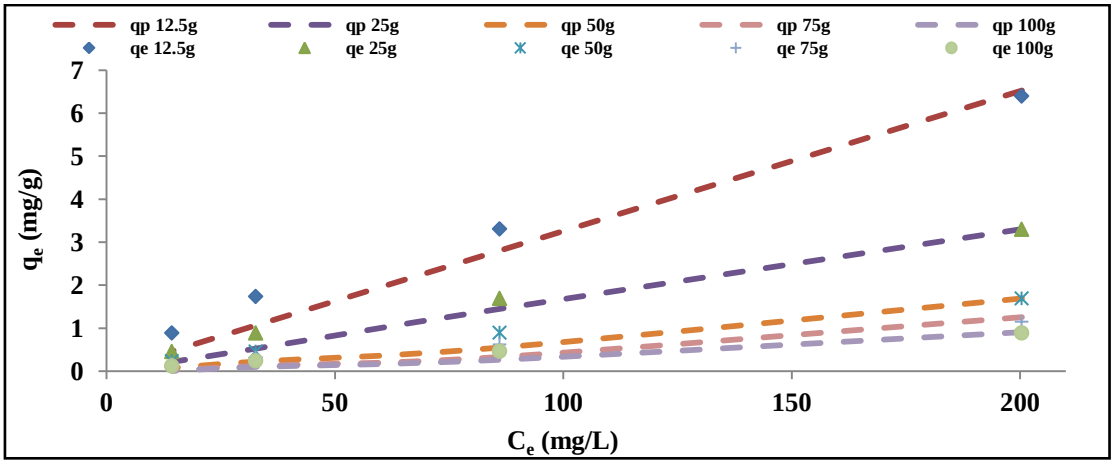

(a)

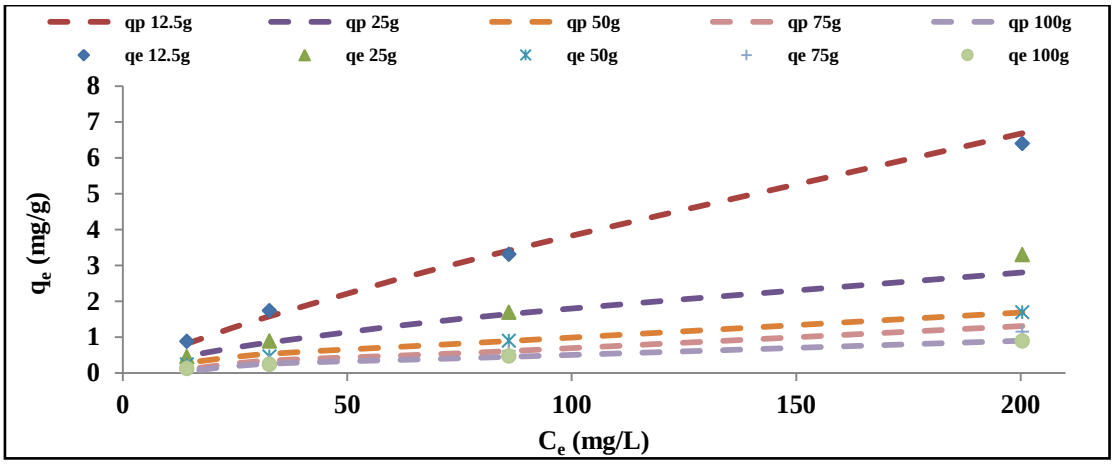
qp 12.5g
qp 25g
qp 50g
qp 75g
qp 100g
qe 12.5g
qe 25g
qe 50g
qe 75g
qe 100g
qe (mg/g)
Ce (mg/L)
0
1
2
3
4
5
6
7
8
0
50
100
150
200

(b)

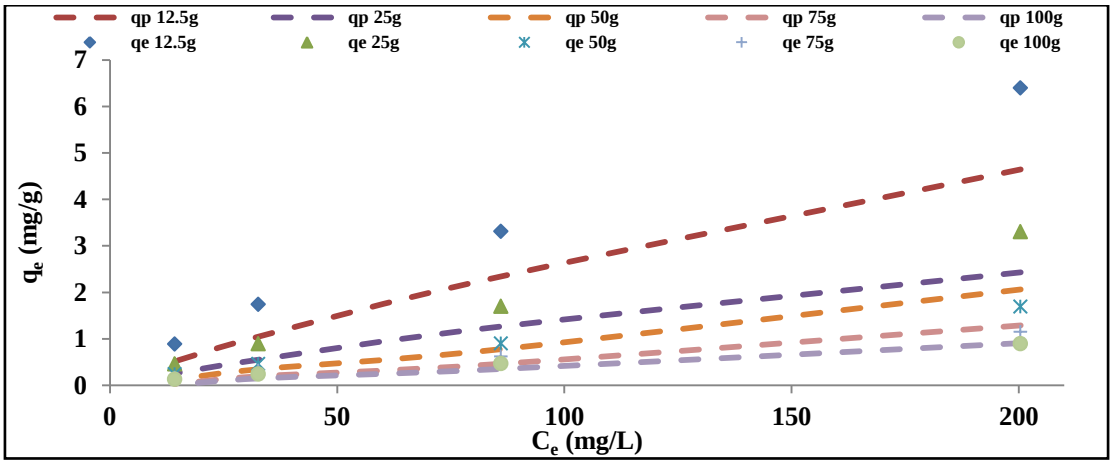
qp 12.5g
qp 25g
qp 50g
qp 75g
qp 100g
qe 12.5g
qe 25g
qe 50g
qe 75g
qe 100g
qe (mg/g)
Ce (mg/L)
0
1
2
3
4
5
6
7
0
50
100
150
200

(c)

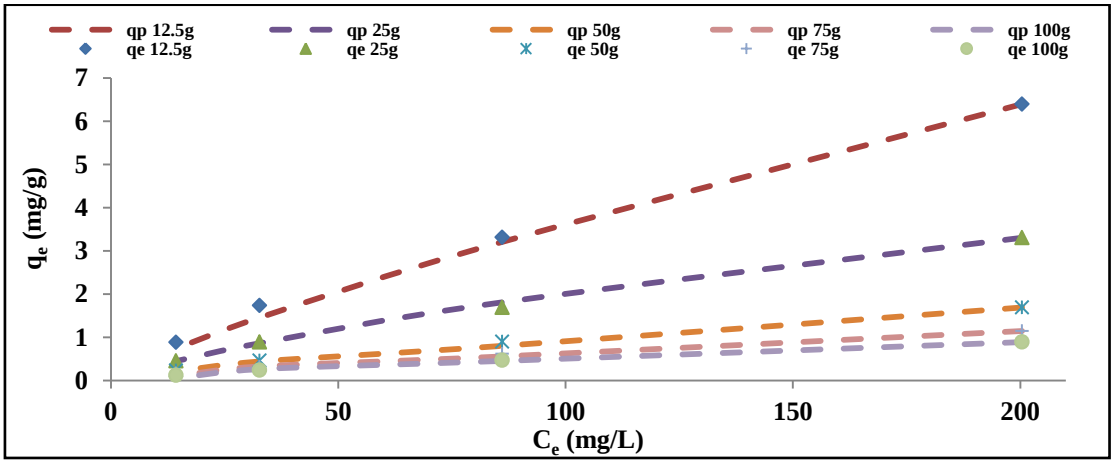
qp 12.5g
qp 25g
qp 50g
qp 75g
qp 100g
qe 12.5g
qe 25g
qe 50g
qe 75g
qe 100g
qe (mg/g)
Ce (mg/L)
0
1
2
3
4
5
6
7
0
50
100
150
200

(d)

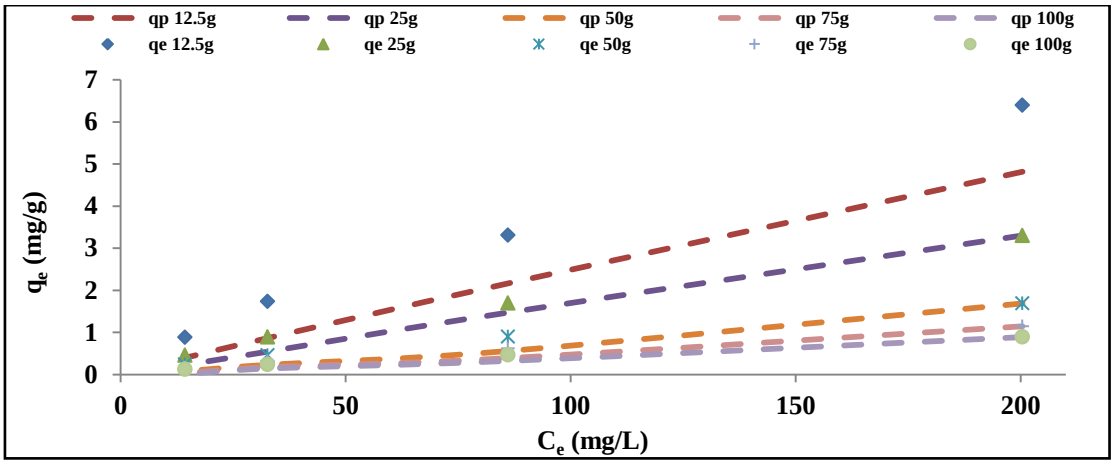

(e)

Figure 6.5: Non-Linear Regression Analysis for Isotherms (a) Langmuir (b) Freundlich (c) Redlich-Peterson (d) Sips (e) Toth

Table 6.3: Isotherm parameters obtained using non-linear regression method for MB removal onto alkali modified soil

Isotherm model	Isotherm Parameter	100g/100mL	75g/100mL	50g/100mL	25g/100mL	12.5g/100mL
Langmuir	q_m	0.020	0.096	0.048	0.020	0.021
	K_l	0.008	0.008	0.01	0.019	0.032
	R^2	0.78	0.726	0.833	0.947	0.949
	$RMSE$	0.276	0.425	0.431	0.49	0.996
	χ^2	0.285	0.399	0.371	0.313	0.541
Fruendlich	K_f	0.065	0.079	0.098	0.100	0.099
	n	1.789	1.757	1.769	1.546	1.259
	R^2	0.982	0.943	0.993	0.947	0.993
	$RMSE$	0.07	0.15	0.078	0.35	0.352
	χ^2	0.044	0.047	0.025	0.079	0.035
R-P	K_r	0.015	0.016	0.022	0.038	0.064
	a_r	0.006	0.005	0.002	0.027	0.029
	β	0.672	0.715	0.396	0.35	0.315
	R^2	0.898	0.862	0.856	0.768	0.739
	$RMSE$	0.195	0.32	0.413	1.055	2.171
	χ^2	0.169	0.218	0.179	0.553	1.191
Sips	K_s	0.012	0.013	0.003	0.005	0.006
	a_s	0.055	0.067	0.057	0.071	0.079
	β_s	0.547	0.539	0.662	0.73	0.816
	R^2	0.984	0.988	0.992	0.997	0.994
	$RMSE$	0.062	0.074	0.079	0.085	0.305

Sips	χ^2	0.041	0.026	0.013	0.009	0.073
Toth	K_T	0.019	0.021	0.012	0.021	0.032
	a_T	0.050	0.061	0.053	0.064	0.067
	$1/t$	0.179	0.194	0.019	0.02	0.053
	R^2	0.877	0.842	0.844	0.953	0.728
	$RMSE$	0.201	0.287	0.418	0.458	2.348
	χ^2	0.181	0.253	0.347	0.278	1.495

6.3.4 Characterisation of the Alkali Modified Soil

6.3.4.1 X-Ray Diffraction

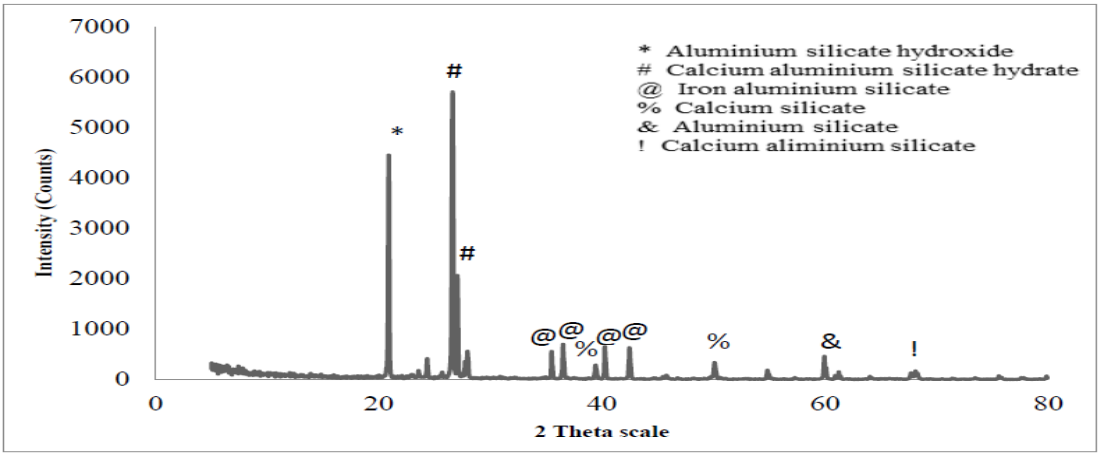

Figure 6.6: XRD pattern for Alkali modified soil

Figure 6.6 shows the XRD pattern of alkali modified soil. The appearance of the new peak or duplicate peak of calcium aluminium silicate hydrate at 2θ = 26.65 (d= 3.34958 Å) is the result of alkali modification of the non-modified soil (Refer Figure 4.14). Similarly, new peak or duplicate peaks of iron aluminium silicate at 2θ = 36.46(d= 2.46 Å), 40.23(d= 2.24Å), 42.39(d= 2.13Å). Usually, under alkali treatment, the dissolution processes affect mineral structures to a lesser extent, though the formation of new mineral phases is a frequent phenomenon (Rz 2002). The increase in the intensity of the peak at 2θ = 20.83 (d = 4.26 Å) might be because of reconstruction of the crystal structure after the partial leaching of tetrahedron Si and Al (Wang et al. 2015). Hydroxyl ions may be available from the alkali modification.

6.3.4.2 X-Ray Fluorescence Analysis

Table 6.4: XRF of Alkali-modified soil

Constituents	Wt%
SiO_2	21.71
Al_2O_3	4.75
Fe_2O_3	3.17
CaO	0.92
MgO	0.14
Na_2O	0.68
K_2O	0.55

The chemical composition of acid-modified soil obtained by using XRF analysis, given in Table 6.4, indicates the presence of silica, alumina and iron oxide as major constituents, along with traces of sodium, potassium, calcium, and magnesium oxides. The data in Table 6.4 shows that there is an increase in SiO_2, Al_2O_3 and Fe_2O_3 content of the alkali-modified soil as compared to the non-modified soil (Refer Table 4.5). It is thus expected that the dye species may be removed mainly by SiO_2, Al_2O_3 and/or Fe_2O_3.

6.3.4.3 Surface Area

Table 6.5: BET surface area analysis of alkali-modified soil

Parameter	Alkali modified
Average Pore Size(Å)	24.802
Langmuir Surface Area(m^2/g)	11.664
BET Surface Area(m^2/g)	2.165
Total Pore Volume(cm^3/g)	$2.685X10^{-3}$

The surface area, average pore size and total pore volume was measured by BET method. From Table 6.5, it is clear that the alkali-modified soil not only showed marked differences in its porous structure but also in the extent of surface area as compared to the non-modified soil (Refer Table 4.6). This indicates that significant structural changes took place after alkali modification. The average pore size of the alkali-modified soil increased as compared to non-modified soil.

Alkali-modified soil has a relatively low surface area as it lacks microporosity which contributes most for surface area (Ip et al. 2009). A decrease in the total pore volume was also observed following the alkali modification of the soil. This means the pore widening takes place as a result of wall breaking between micropores, which leads to an increase in internal porosity and reductions in micropores associated with the high surface area. The same behaviour was observed by (Khraisheh et al. 2005) (Attia et al. 2008). The mesopores have the most influence on the adsorption of organic solutes, which enables their surfaces to be accessible to solute molecules. Surface functional groups added to the surface of the soil, as a result of modification, changed the surface character of the adsorbent (Khraisheh et al. 2005).

6.3.4.4 Scanning Electron Microscopy (SEM) – Energy Dispersive X-Ray (EDX) Analysis

Figure 6.7 and Table 6.6 show the EDX analysis and the elemental composition of the alkali-modified and MB adsorbed alkali modified soil. Table 6.5 shows the decrease in the weight percentage of the elements in the MB adsorbed alkali modified soil as compared to alkali modified soil. This indicates the utilization of the constituents of the soil for adsorption of the dye molecule. Also, when the elemental composition of the non-modified soil (Refer Table 4.7) was compared with the alkali-modified soil, the weight percentage of aluminium decreased to 1.19% from 12.53%. It is because aluminium is present on the octahedral position and can be leached out (Liu & Zhang 2007).The increase in the weight percent of Fe, Ca and Mg is because these elements are precipitated as oxides from the outer silica layer (Jozefacuik & Bowanko 2000). No significant change can be noticed in potassium. The increase in the Si and O could be due to the Si-O-Si bond breakage due to modification process.

Table 6.6: Elemental Composition of Alkali-modified Soil

Element	**Alkali modified soil**		**MB adsorbed alkali modified soil**	
	Wt%	At%	Wt%	At%
O	64.09	53.92	41.49	49.68
Si	19.02	23.3	12.56	15.26
Al	1.19	2.4	0.87	2.39
Fe	4.02	2.32	3.51	2.04
Ca	8.08	12.51	7.71	3.28
Mg	0.5	0.54	0.51	0.43
K	0.09	0.39	0.06	0.41
Na	3.01	4.62	2.21	3.45

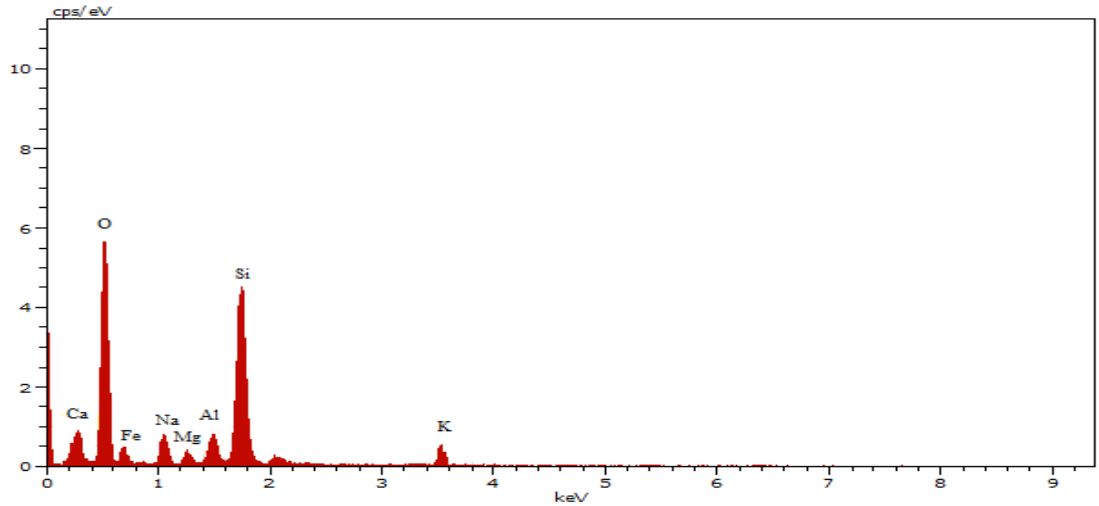

(a)

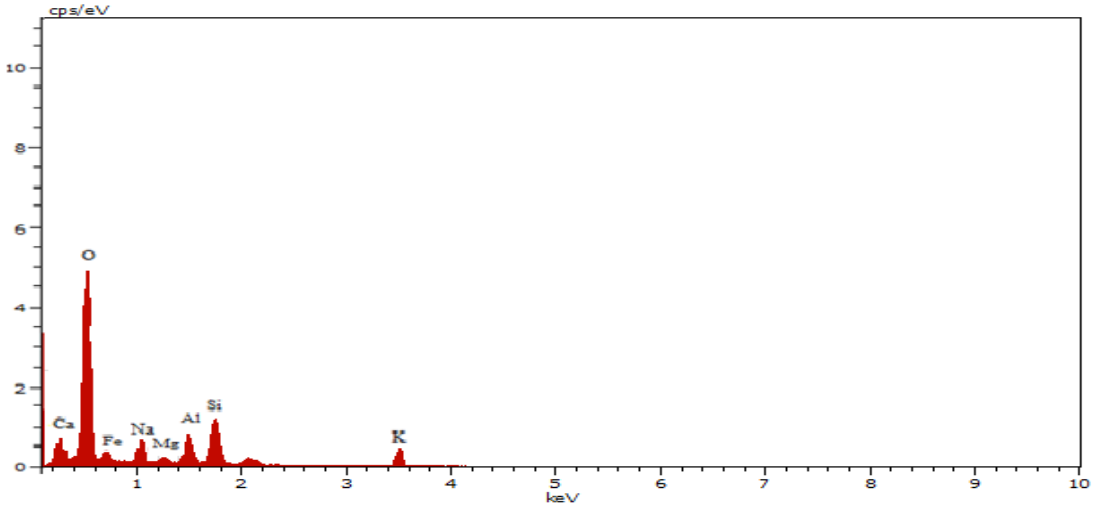

(b)

Figure 6.7: Energy Dispersive X-Ray Analysis of (a) Alkali-modified soil and (b) MB adsorbedAlkali-modified Soil

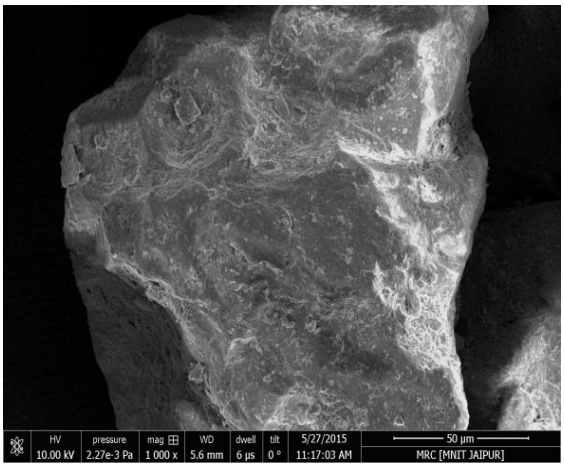

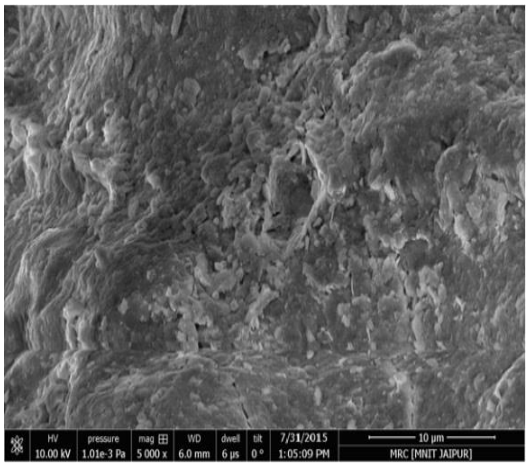

(a) (b)

(c)

Figure 6.8: SEM images for (a) & (b) Alkali-modified Soil (c) MB adsorbed Alkali-modified Soil

Figure 6.8 shows the SEM monographs for alkali-modified soil before adsorption and after adsorption of methylene blue dye.

6.3.3.5 Fourier Transform Infrared Spectroscopy Analysis and Zeta Potential of the soil surface

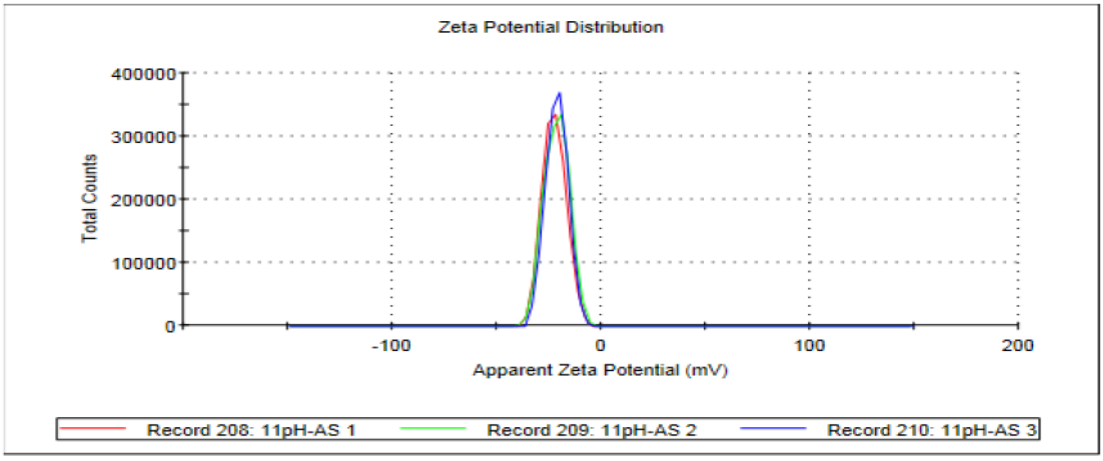

Figure 6.9: Zeta Potential for Alkali modified soil

Figure 6.9 shows the zeta potential for the alkali-modified soil. Alkali modification resulted in the increase in the zeta potential of the soil. Zeta potential of alkali modified soil is -21.6mV whereas non-modified soil has -17 mV. This value reveals that surface of the soil acquires some more negative charges and therefore, becomes more receptive to the uptake of positively charged dye cations through electrostatic attractions (Al-Ghouti et al. 2003).

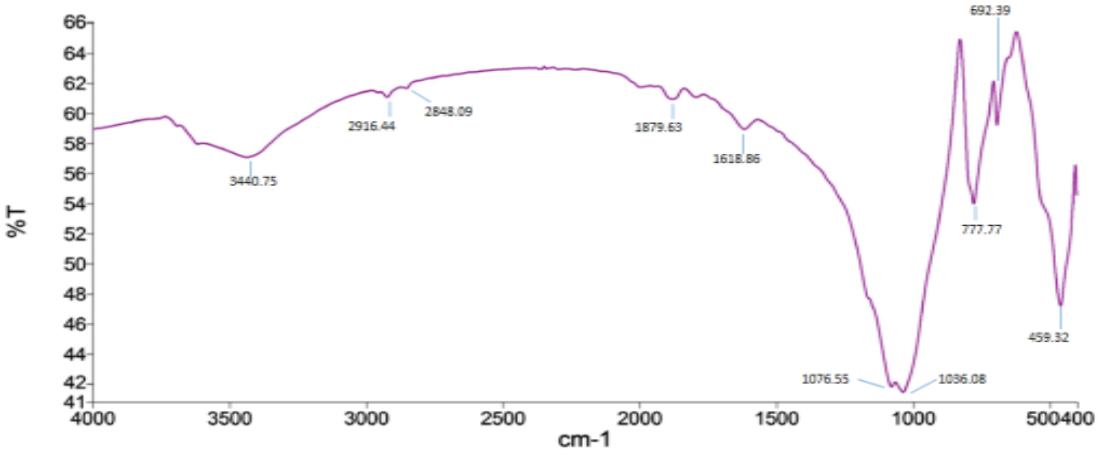

(a)

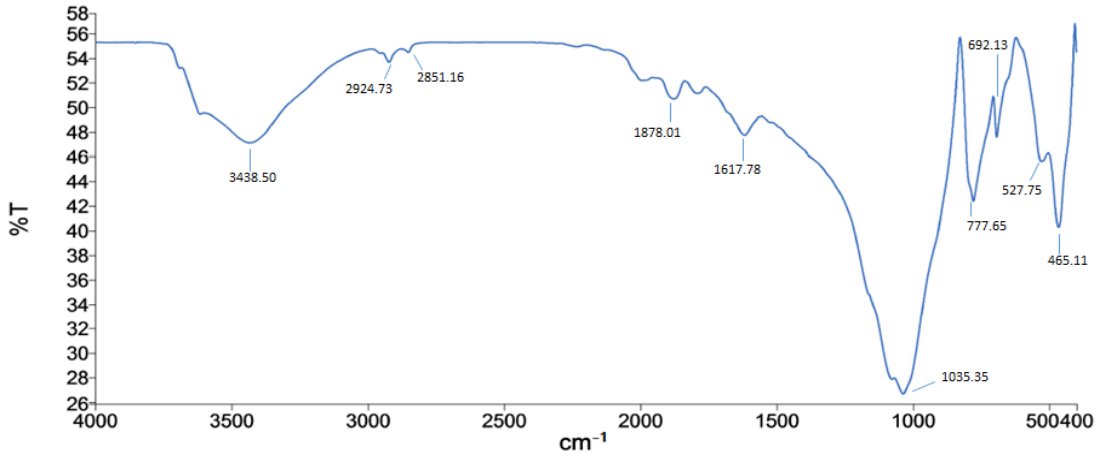

(b)

Figure 6.10: FTIR spectra for (a) Alkali-modified soil (b) MB adsorbed Alkali-modified soil

Figure 6.10 (a) shows the FTIR spectra of alkali modified soil. On comparing with the FTIR spectra non-modified soil, it was found that the increase in the intensity of the stretching vibration of silanol (SiO-H) group at 3440.75cm^{-1} supports the alkali modification of the soil. The appearance of the new band at 1076.55cm^{-1} lies in the region of asymmetric vibration of Si-O group which is presumably due to is cleavage by nucleophilic reagent; sodium hydroxide (Khraisheh et al. 2005)(Bera et al. 2013) (Abdel-Ghani et al. 2007). Also, there is a modification of carboxyl and siloxane groups at 1879.63 cm^{-1}and 1036.08 cm^{-1} support the increase in the negative charge on the soil surface. Zeta potential results of the alkali modified soil also support this phenomenon. The zeta potential of alkali modified soil increased to -21.6mV as compared to non-modified and acid modified soils.

Bands at 3440.75cm^{-1} and 1618.86cm^{-1}present on the adsorbent modified to 3438.50cm^{-1} and 1617.78cm^{-1}respectively on the MB adsorbed adsorbent indicates O-H stretching and bending takes part in the adsorption. Band at 1879.63cm^{-1} represents symmetric stretching of C-OH on the adsorbent. It gets modified to 1878.01 cm^{-1} after MB adsorption on adsorbent indicating C-OH participated in the adsorption. Similarly, the band at 1036.08cm^{-1} present on the adsorbent modified to 1035.35cm^{-1} indicates C-OH stretching participated in the MB adsorption. The disappearance of 1076.55 cm^{-1} indicated that asymmetric stretching of Si-O took part in the adsorption. The band at 692.39cm^{-1} present on adsorbent modified to 692.13cm^{-1} remained unchanged indicating asymmetric bending of Si-O does not participate in adsorption. Band at 2916.44cm^{-1} present on adsorbent modified to 2924.73cm^{-1} indicating asymmetric stretching of CH_2 participated in adsorption. Similarly, 2848.09cm^{-1} present on adsorbent modified to 2851.16cm^{-1} indicating symmetric stretching of CH_2 also participated in adsorption. The band at 778.77cm^{-1} modified to 777.65cm^{-1} showing symmetric stretching of Si-O participated in adsorption. Similarly, band at 459.32cm^{-1} modified to 465.11cm^{-1} indicating bending vibrations of Si-O-Si participated in adsorption. As a result, it can be concluded that the hydrogen bonding and the other electrostatic interactions play an important role in the MB removal on alkali modified soil.

6.4 Summary

This Chapter showed that alkali modification of non-modified soil is a promising approach for enhancement of the adsorption capacity. Surface characterisation of alkali-modified soil showed that negative charge on soil increased after alkali modification. This, therefore, increased adsorption of cationic MB dye. The contact time of 10 minutes was found to be sufficient to attain equilibrium adsorption. The alkali modified soil gave the highest equilibrium adsorption upto 6.4mgg^{-1}. The MB adsorption increased with the increase in dye concentration range 125 mg/L to 1000 mg/L. The pseudo second order model exhibited the best correlation for the experimental data and indicated that boundary layer resistance is not the rate limiting step. The results from assessing intraparticle diffusion model revealed that intraparticle diffusion is not the only process controlling the MB adsorption on alkali modified soil but boundary layer effect also exists. The equilibrium analysis showed that Sips and Freundlich isotherm yielded better fit to the adsorption data, signifying

that MB does not form a monolayer on the adsorbent and rather follows multilayer adsorption.

The results obtained from this Chapter showed that adsorption capacity of the alkali-modified soil for MB was higher than both non-modified and acid-modified soil for DR 81 adsorption. Therefore, this soil was chosen as an adsorbent for fixed bed study explained in the next chapter.

CHAPTER 7

Chapter 7

Fixed Bed Study for the Treatment of Simulated and Actual Textile Wastewater

This Chapter discusses the fixed bed adsorption studies performed using simulated textile wastewater and actual textile wastewater. The removal of colour in a fixed bed adsorption column was expressed by the breakthrough curve. The reduction in the chemical oxygen demand was also studied. Fixed bed column studies were conducted on three Perspex columns packed with alkali activated soil of three different working bed heights. The columns were charged with simulated wastewater and actual wastewater in the upflow mode. The basic engineering data were collected from the fixed bed studies to further evaluate the design parameters using various models.

7.1 Introduction

Colour and presence of organics in the textile wastewater are of major concern and are to be reduced. Wastewaters from a textile industry are characterized by their highly visible colour (3000-4000 ADMI units), COD (800-1600mg/L) and alkaline pH (9-11) (Manu & Chaudhari 2002). Most of the earlier studies were conducted using pure dye solutions. Experiments were conducted in batch modes. A very few reports are available on continuous treatment of synthetic/actual textile wastewater on low-cost adsorbents. However, continuous treatment actually describes the field operation. Also, the complex nature of the textile wastewater containing dye and various auxiliary salts is not taken into account. Study carried out on the simulated wastewater is useful in two ways: firstly it enables research to be carried out in the absence of a local source of effluent and secondly simulated effluents have constant composition and therefore enable the effect of treatment to be more readily understood (O'Neill et al. 1999). In the present work, both the simulated and actual textile wastewater has been treated on the alkali modified soil.

7.2 Materials & Methods

7.2.1 Adsorbent

From the previous chapters, it is clear that alkali modified soil gave better removal efficiency as compared to non-modified and acid modified soil. Therefore, alkali modified soil was used as an adsorbent in fixed bed study.

7.2.2 Adsorbate

Simulated textile wastewater was prepared as given in Section 3.4.1.1. Details of actual textile wastewater are given in Section 3.4.4.2.

7.2.3 Fixed Bed Studies

Column for fixed bed study was designed as given in Section 3.4.2. Study on breakthrough of the column was done as given in Section 3.4.2.1.

7.3 Results & Discussion

7.3.1 Treatment of Simulated Wastewater

7.3.1.1 Effect of Flow Rate and Bed Height on Breakthrough of Fixed Bed

Fixed Bed adsorption experiments were carried out as per method described in Section 3.4.2.1 of Chapter 3. Simulated wastewater was passed through three columns of different bed heights. Data on three different flow rates of 0.5 L/hr, 0.7 L/hr, and 1.0 L/hr were obtained on these bed heights. The breakthrough curves were plotted on each column run. The breakthrough times and exhaustion times were taken corresponding to C/C_0 = 0.005 and C/C_0 = 0.9, respectively. Breakthrough time, breakthrough volume, exhaustion time and exhaustion volume at varying bed depths of alkali-modified soil were noted, and parameters were calculated. The isotherms obtained are shown in Figures 7.1 (a) to (c) for 0.5 L/hr, 0.7 L/hr, and 1.0 L/hr. The values of the important design parameters, T_B (breakthrough time), T_E (exhaust time), V_B (volume of simulated wastewater treated up to breakthrough time) and V_E (volume of simulated wastewater treated up to exhaust time) were calculated for bed depths of 2.5cm, 3.5cm and 4.5cm corresponding to the flow rates of 0.5 L/hr, 0.7 L/hr, 1.0 L/hr and are shown in Table 7.1.

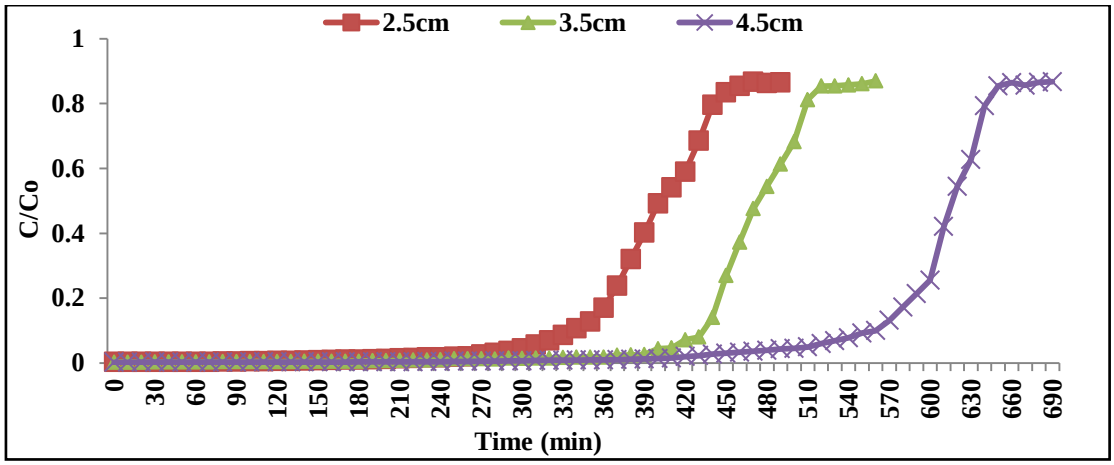

(a)

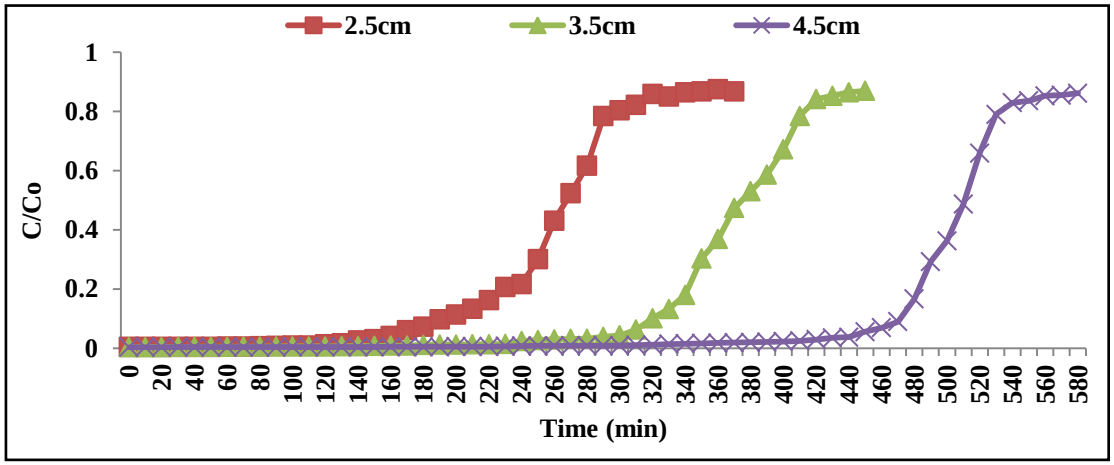

(b)

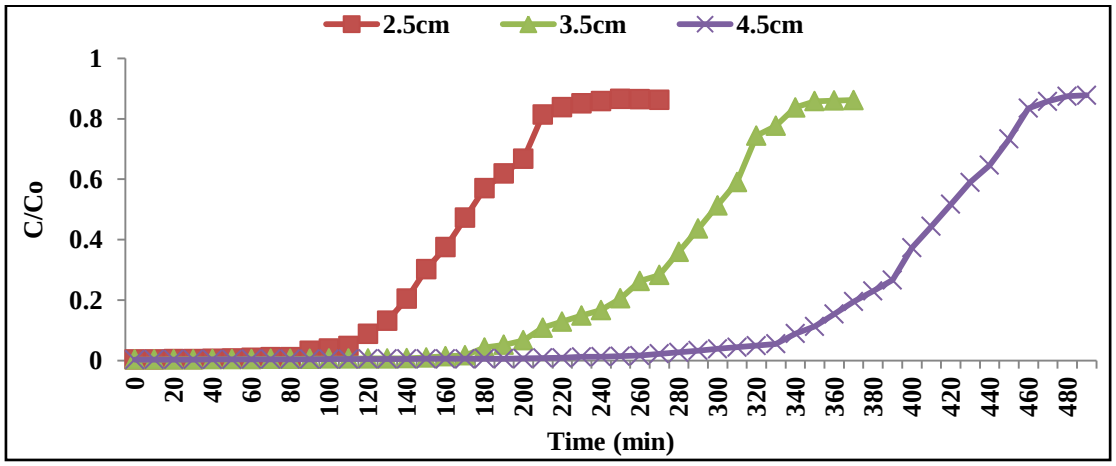

(c)

Figure 7.1: Breakthrough curves for adsorption of simulated wastewater onto alkali modified soil at varying bed depths for flow rates of (a) 0.5 L/hr, (b) 0.7 L/hr and (c)1.0 L/hr.

For 0.5 L/hr flow rate, the breakpoint time for 2.5cm, 3.5cm and 4.5cm was 110min, 180min and 280min while exhaust time for 2.5cm, 3.5cm and 4.5cm was 490min, 560min and 690min respectively. For 0.7 L/hr, the breakpoint time for 2.5cm, 3.5cm and 4.5cm were 70min, 120min and 220 min while exhaust time for 2.5cm, 3.5cm and 4.5cm was 370min, 450min and 580min respectively. For 1.0 L/hr, the breakpoint time for 2.5cm, 3.5cm and 4.5cm was 40min, 80min and 150 min while exhaust time for 2.5cm, 3.5cm and 4.5cm was 270min, 370min and 490min respectively.

It could be observed from Figures 7.1 (a) to (c) that with the increase in bed height, both breakpoint time and exhaustion time was increased. This observation may be explained on the basis of increased contact time between simulated wastewater and alkali modified soil with increased bed height. As the flow rate increased, the breakthrough time for a given bed height reduced. The increase in flow rate reduced the contact time and hence, a breakthrough occurred in lesser time. Similar results were reported by (Charumathi & Das 2012)(Kundu & Gupta 2005).

Table 7.1: Breakthrough and exhaustion times for adsorption of simulated wastewater on alkali-modified soil for different flow rates and bed heights.

Flow rate (L/hr)	**Bed depth (cm)**	**Breakthrough Time T_B (min)**	**Exhaustion Time T_E (min)**	**Breakthrough volume V_B (mL)**	**Exhaustion volume V_E (mL)**
0.5	2.5	110	490	911.9	4062.1
	3.5	180	560	1492.2	4642.4
	4.5	280	690	2321.2	5720.1
0.7	2.5	70	370	812	4292
	3.5	120	450	1392	5220
	4.5	220	580	2552	6728
1.0	2.5	40	270	664	4482
	3.5	80	370	1328	6142
	4.5	150	490	2490	8134

Various parameters for the column design have been calculated from the above mentioned data. These parameters including t_Z (time required for adsorption zone to move its own length), h_Z (height of adsorption zone), U_Z (rate of movement of adsorption zone) and bed saturation (percentage bed saturation) have been evaluated mathematically using Equations 3.15, 3.16 and 3.19. These calculated values are shown in Table 7.2. The values of h_Z and U_Z increased with increase in bed height. Bed saturation decreased with increase in both flow rates and bed heights.

Table 7.2: Column Parameters for adsorption of simulated wastewater on alkali modified soil for different flow rates and bed heights

Flow rate (L/hr)	Bed depth (cm)	t_Z (min)	h_Z (cm)	U_Z (cm/min)	Bed Saturation (%)
0.5	2.5	380	1.939	0.0051	81.52
	3.5	380	2.375	0.0063	32.43
	4.5	410	2.674	0.0065	56.45
0.7	2.5	300	2.027	0.0068	72.03
	3.5	330	2.567	0.0078	39.42
	4.5	360	2.793	0.0078	29.79
1.0	2.5	230	2.130	0.0093	66.11
	3.5	290	2.743	0.0095	42.49
	4.5	340	3.122	0.0092	13.92

Table 7.3: Adsorption capacities of different fixed bed columns for adsorption of simulated wastewater onto alkali modified soil for different flow rates and bed heights.

Flow rate (L/hr)	Bed depth (cm)	m_{total} (mg)	q_{total} (mg)	Y (%)	Weight of adsorbent(g)	q_{eq} (mgg^{-1})
0.5	2.5	812.420	660.757	81.33	125	5.286
	3.5	928.480	784.532	84.50	175	4.483
	4.5	1144.020	1006.212	87.95	225	4.472
0.7	2.5	858.400	616.144	71.78	125	4.929
	3.5	1044.000	861.933	82.56	175	4.925
	4.5	1345.600	1171.056	87.03	225	5.205
1.0	2.5	896.400	590.134	65.83	125	4.721
	3.5	1228.400	955.882	77.82	175	5.462
	4.5	1626.800	1358.473	83.51	225	6.038

The adsorption capacity, percentage removal and maximum uptake have been shown in Table 7.3. It is observed from Table 7.3 that as flow rate increased, m_{total} increased. q_{total} for a particular height of column decreased with increase in flow rate. Percentage removal of colour decreases with increase in flow rate. Value of q_{eq} increased with column depth for particular flow rate but decreased with flow rate for a particular bed height of column.

From Table 7.3, it may be noted that as the bed height increase, the removal efficiency of the column also increases. Values of maximum uptake capacity at equilibrium q_{eq} also increased with the bed height. This was due to availability of more time to contact with the alkali modified soil.

The value of percentage removal increased with increased in bed height, however, decreased with increase in flow rate. Mass transfer fundamentals can be used to explain this variation. At higher flow rates, the movement of adsorption zone along the bed was faster, reducing the time for adsorption on adsorbent bed. As expected the breakthrough time was higher with lower flow rate and lesser for higher flow rates(Han et al. 2007).

7.3.1.2 Analysis and modelling of Fixed Bed Parameters in Columns

7.3.1.2.1 BDST Model

Data collected from a set of nine column studies were evaluated using modified Bohart and Adam's model also called as Hutchins model or BDST model. The mathematical aspects of BDST model were presented in materials and methods.

From the breakthrough time (corresponding to C_t/C_0 = 0.005) and the exhaust time (corresponding to C_t/C_0 = 0.9) for bed depth 2.5 cm, 3.5 cm and 4.5 cm for simulated wastewater at 0.5 L/hr of flow rate, a graph was plotted, as shown in Figure 7.2 (a). Similar graphs, shown in Figure 7.2 (b) & (c) are plotted for 0.7 L/hr and 1.0 L/hr.

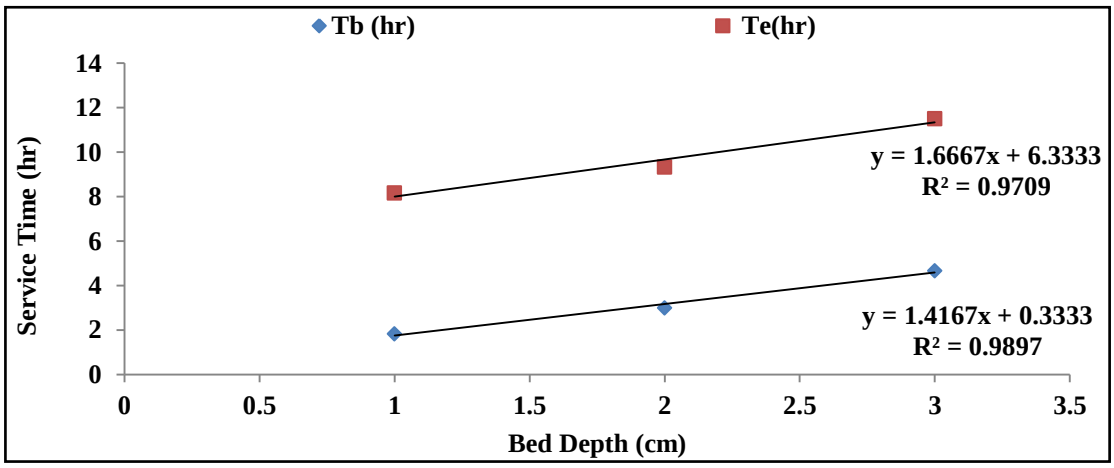

(a)

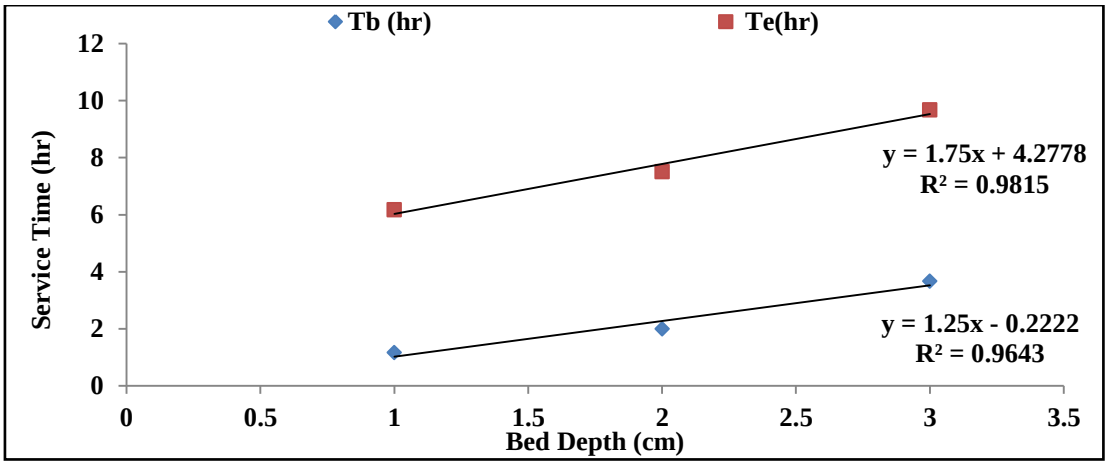

(b)

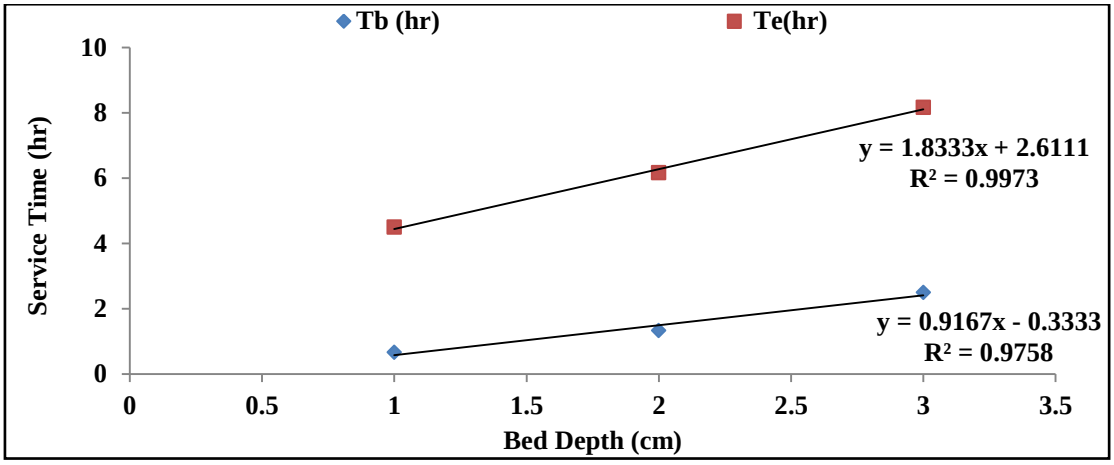

(c)

Figure 7.2: BDST model for adsorption of simulated wastewater onto alkali modified soil at varying bed depths for flow rates of (a) 0.5 L/hr, (b) 0.7 L/hr and (c) 1.0 L/hr

Figure 7.2 (a) showed the bed height versus service time for 0.5% and 90% saturation of the column at 0.5 L/hr flow rate for simulated wastewater. The equations of these lines are as follows:

t=1.6667X + 6.3333 for 90% saturation (7.1)

t=1.4167X+ 0.3333 for 5% saturation (7.2)

From the slopes, it is evident that these lines are nearly parallel, and the horizontal distance between these lines was found to be 2.66 cm. This horizontal distance is called the height of the exchange zone. This height of exchange zone shows good correlation with h_Z . From the slope and intercept of the 5% saturation line, various design parameters were obtained using Equation 7.1 and Equation 7.2. The values of K (0.079 L/mg.hr), N_o (70.821 mg/L) and X_o (0.235 cm) were obtained respectively.

Table 7.4: Parameters obtained by BDST Model at different flow rates

Sr.No.	Flow rate (cm/min)	Slope	Intercept	C_B (mg/L)	N_o (mg/g)	K	X_o (cm)
1	0.250	1.417	0.333	1	70.822	0.079	0.235
2	0.350	1.250	0.222	1	87.438	0.119	0.178
3	0.501	0.917	0.333	1	91.763	0.079	0.364

Table 7.5: Critical Bed Depth and Bed efficiency at different flow rates

Flow rate(L/hr)	Bed depth (cm)	Critical bed depth(X_o)	Efficiency (%)
0.5	2.5	0.235	90.589
	3.5	0.235	93.278
	4.5	0.235	94.772
0.7	2.5	0.178	92.890
	3.5	0.178	94.921
	4.5	0.178	96.050
1.0	2.5	0.364	85.457
	3.5	0.364	89.612
	4.5	0.364	91.920

Various design parameters were found using Equations 3.29 & 3.30 and are shown in Table 7.4. Critical bed depth and bed efficiency was found by Equation 3.27 and are shown in Table 7.5.

For 0.5 L/hr flow rate, the bed efficiencies obtained were 90.58% (2.5cm), 93.27% (3.5cm) and 94.77% (4.5cm). It is also observed that bed efficiency decreased with increase in flow rate. Critical bed depths X_o also increased with flow rates.

Table 7.6: Data obtained using BDST equation for different flow rates for adsorption of simulated wastewater onto alkali modified soil.

Flow Rate(L/hr)	Z	a	b	v'	a'	t(exp)	t(pred)
0.7	2.5	1.42	0.33	8.29	1.75	4.04	3.21
		0.92	0.33	16.60	0.87	1.85	1.96
	3.5	1.42	0.33	8.29	1.75	5.79	4.63
		0.92	0.33	16.60	0.87	2.72	2.88
	4.5	1.42	0.33	8.29	1.75	7.54	6.04
		0.92	0.33	16.60	0.87	3.60	3.79
1.0	2.5	1.42	0.33	8.29	1.84	4.26	3.21
		1.25	0.22	11.60	1.31	3.06	2.90
	3.5	1.42	0.33	8.29	1.84	6.09	4.63
		1.25	0.22	11.60	1.31	4.37	4.15
	4.5	1.42	0.33	8.29	1.84	7.93	6.04
		1.25	0.22	11.60	1.31	5.68	5.40

It is observed from Table 7.6 that the experimental value and the predicted value of service time show good agreement with each other. Thus, the BDST design has been validated. Hence it can be adopted for scaling up fixed bed reactor for field application.

7.3.1.2.2 Thomas Model

The dynamic behaviour of the columns is predicted with the help of Thomas model. The mathematical aspects of Thomas model were presented in Section 3.4.3 (b). The Thomas rate constant (k_{Th}) and maximum solid-phase concentration (q_o) were determined through the experimental column data obtained for adsorption of simulated wastewater by fitted them to the Thomas model. The respective values of $q_o$and k_{Th} were calculated from the $ln\left(\frac{C}{C_0}-1\right)$ versus t plots for all column bed heights for various flow rates and are presented in Table 7.7 along with correlation coefficients. The linear regression coefficients ranged from 0.9015 to 0.9663. The values of Thomas rate constant (k_{Th}) and q_o were found to be influenced by bed depth and flow rate. With increase in flow rate, k_{Th} increases while q_o decreases. However, k_{Th} decreases while q_{oth} increases, as the bed height increases. Similar observations were reported by (Tamez Uddin et al. 2009). This shows that high bed height and low flow rate is favourable for better adsorption (Sadaf & Bhatti 2014).

Table 7.7: Parameters predicted from Thomas model at various flow rates and bed heights

Flow rate(L/hr)	Bed depth (cm)	q_{exp}	k_{Th} (x10^{-5})	q_o	R^2
0.5	2.5	5.199	6.65	5.609	0.953
	3.5	3.983	5.45	5.057	0.883
	4.5	3.546	4.5	5.029	0.902
0.7	2.5	4.299	9.25	5.165	0.966
	3.5	4.749	6.95	5.329	0.922
	4.5	6.212	4.95	6.114	0.840
1.0	2.5	5.615	12.45	5.067	0.935
	3.5	5.925	9.15	5.655	0.951
	4.5	7.118	6.5	6.489	0.924

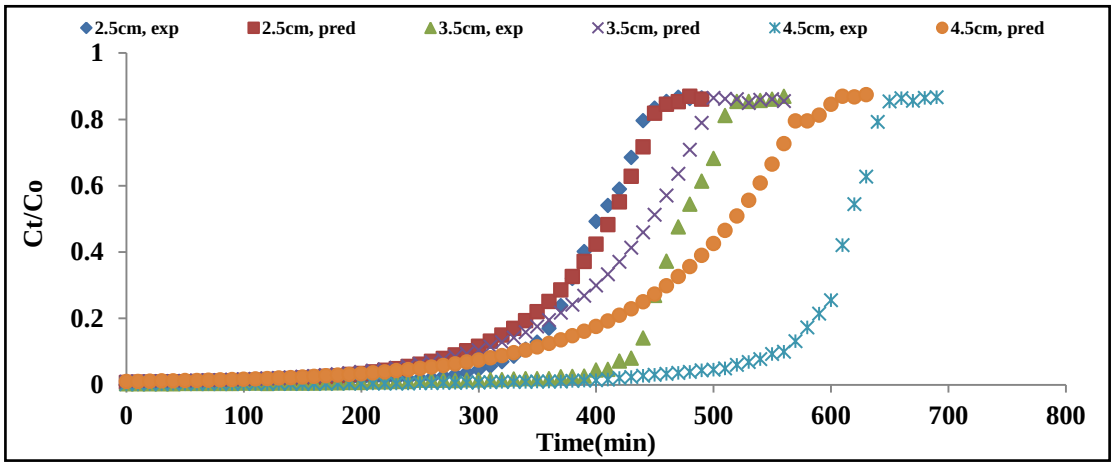

(a)

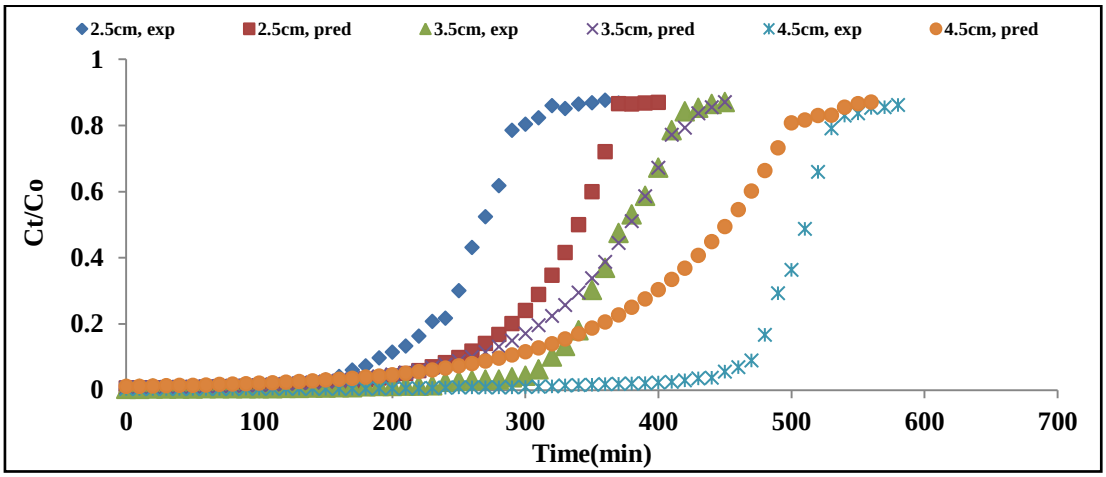

(b)

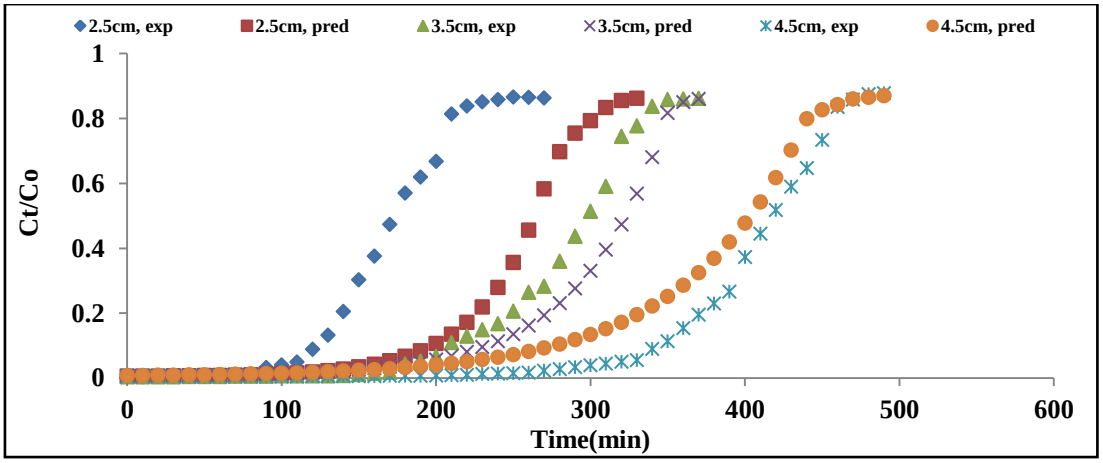

(c)

Figure 7.3: Comparison of experimental breakthrough curves with those predicted by Thomas model for adsorption of simulated wastewater at varying bed heights for flow rate (a) 0.5 L/hr, (b) 0.7 L/hr, (c) 1.0 L/hr

The breakthrough curves obtained by experiment and those predicted by Thomas model were compared and are shown in Figure 7.3. The simulation of the breakthrough for all bed heights and flow rates studied was found to be effective with the Thomas model and the breakthrough curves computed from the model were in good agreement with experimental breakthrough behavior as seen from Figure 7.3.

7.3.1.2.3 Yoon and Nelson Model

To investigate the breakthrough behaviour of adsorption on alkali modified soil in the column, the experiments were performed. The column data obtained for simulated wastewater were fitted to the Yoon and Nelson model. The mathematical aspect of Yoon and Nelson model were presented in materials and methodology. A linear regression analysis was performed on each set of experimental data obtained to determine the coefficients from slope and intercept.

The values of parameters k_{YN} (rate constant min^{-1}) and τ (the time required for 50% adsorbate breakthrough in min) of this model were determined at all three different bed heights for various flow rates. These values were used to calculate the entire breakthrough curve. A graph was plotted between sampling time (t) versus$\left(\frac{C}{C_0-C}\right)$. Value of k_{YN} and τ was determined from the graph. Value of q_{oYN} was calculated by Equation 3.36.

Table 7.8: Parameters predicted from the Yoon and Nelson model at various flow rates and bed heights

Flow rate(L/hr)	Bed depth (cm)	q_{exp}	q_{oYN}	k_{YN}	τ_{yn}	τ_{exp}	R^2
0.5	2.5	3.029	5.679	0.017	428.188	343.716	0.910
	3.5	3.473	5.111	0.013	539.425	366.610	0.820
	4.5	4.559	5.200	0.011	705.623	411.040	0.830
0.7	2.5	3.731	5.079	0.025	273.633	298.332	0.969
	3.5	4.090	5.430	0.017	409.614	308.540	0.875
	4.5	5.537	6.213	0.012	602.533	361.803	0.769
1.0	2.5	4.945	4.950	0.034	186.380	227.814	0.973
	3.5	5.470	5.724	0.023	301.707	288.307	0.944
	4.5	6.051	6.641	0.016	450.038	335.096	0.882

It is observed from Table 7.8 that as bed height increased, the values of k_{YN} decreased whereas τ and q_{oYN} increased in all column conditions. This could be due to availability of more adsorption sites. As the flow rate increased, the values of q_{oYN}- decreased, the values of k_{YN} increased and the values of τ decreased. This is because of the lesser available contact time with alkali modified soil (Rouf & Nagapadma 2015). The linear correlation coefficient varied from 0.7689 to 0.9726.

Breakthrough curves obtained by experimental study and those predicted by Yoon and Nelson model were compared and are shown in Figure 7.4. It can be seen that the breakthrough curves computed from the model were in good agreement with experimental data for adsorption of simulated wastewater studied.

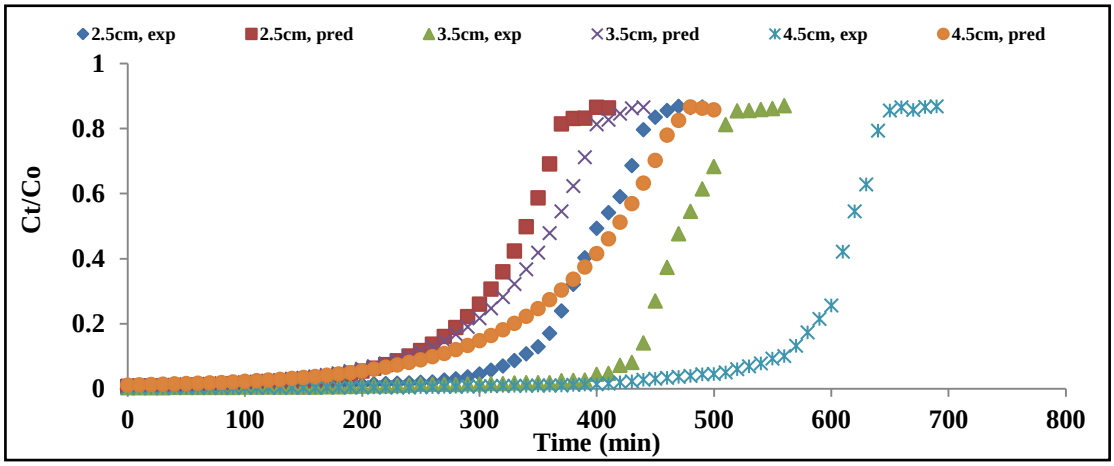

(a)

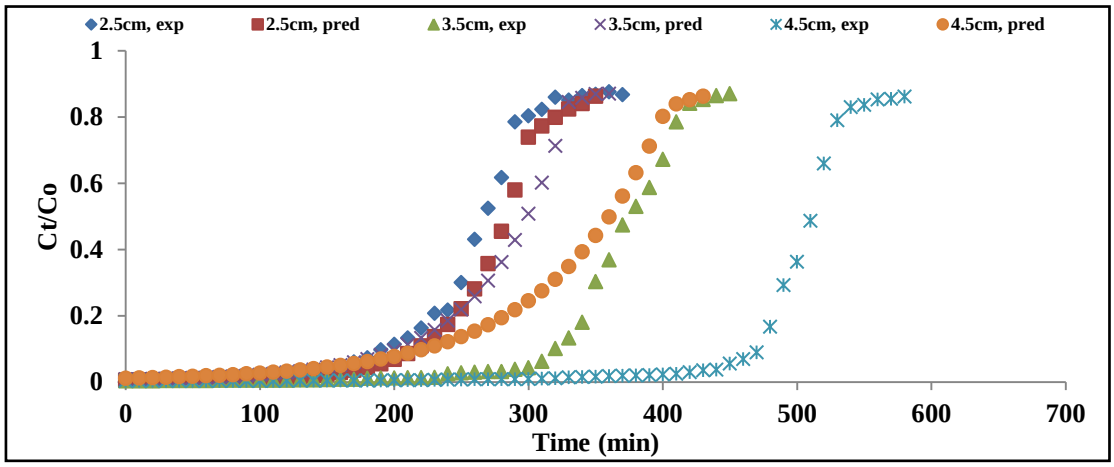

(b)

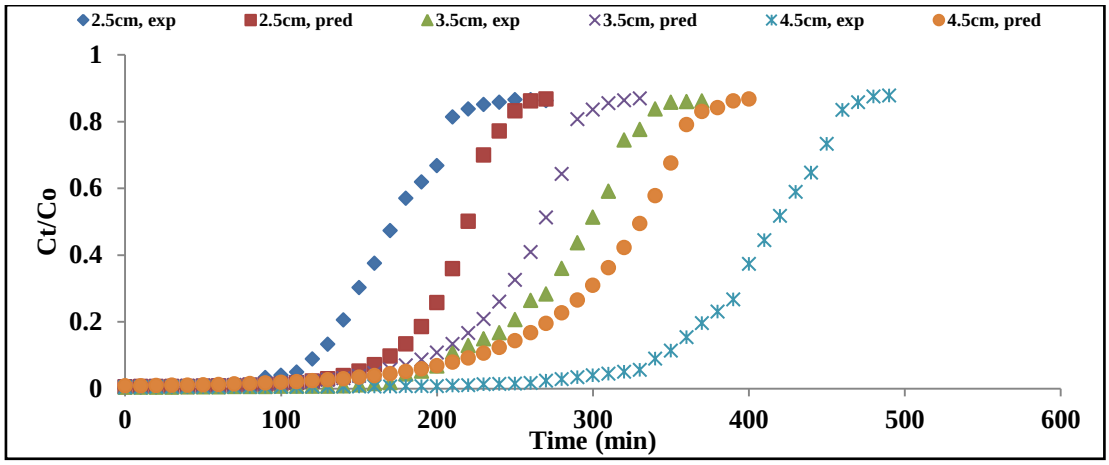

(c)

Figure 7.4: Comparison of experimental breakthrough curves with those predicted by Yoon and Nelson model for adsorption of simulated wastewater at varying bed heights for flow rate (a) 0.5 L/hr, (b) 0.7 L/hr, (c) 1.0 L/hr

7.1.3 COD Removal from Simulated Textile Wastewater

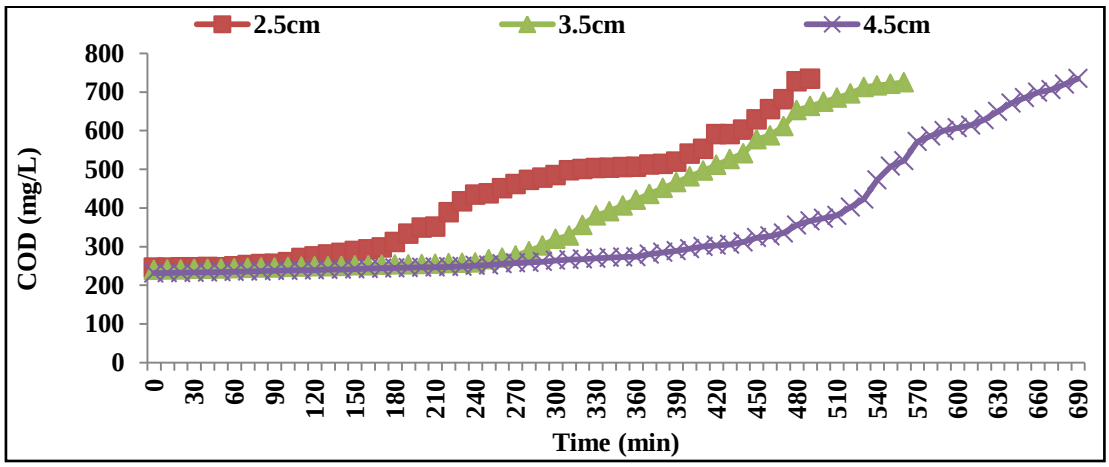

(a)

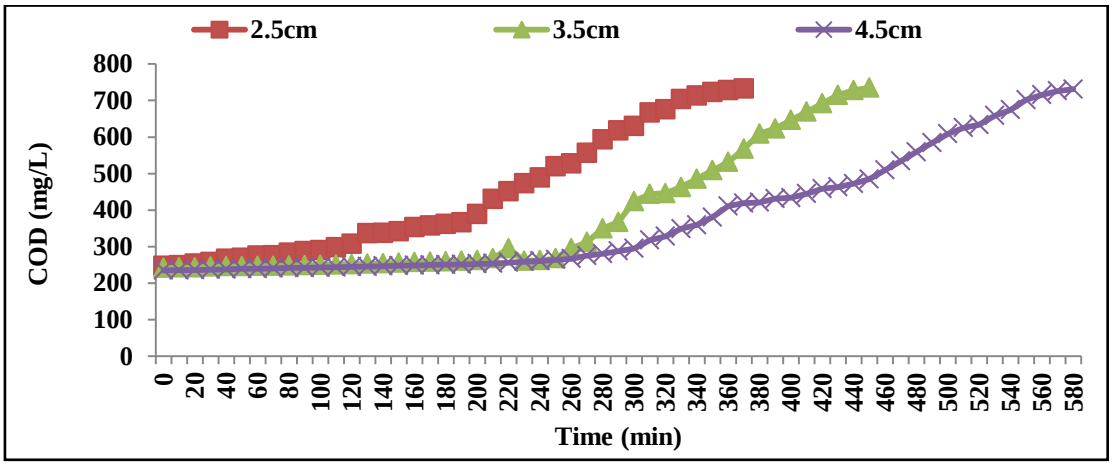

(b)

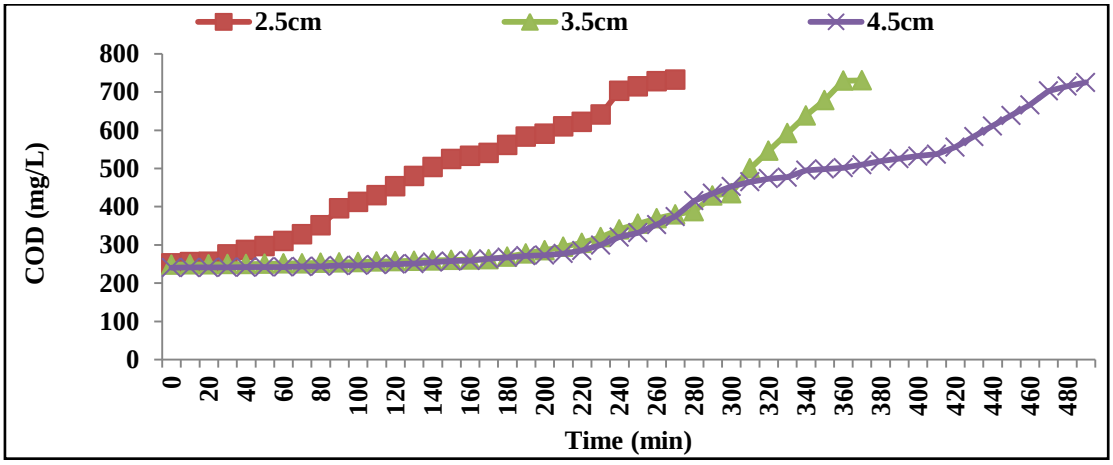

(c)

Figure 7.5: COD removal from simulated wastewater onto alkali modified soil at varying bed depths for flow rates of (a) 0.5 L/hr, (b) 0.7 L/hr and (c) 1.0 L/hr.

COD removal experiments were carried out as per method described in point 12 in Appendix A,. Simulated wastewater was passed through three columns of different bed heights; 2.5cm, 3.5cm and 4.5cm respectively. Data on three different flow rates of 0.5 L/hr, 0.7 L/hr, and 1.0 L/hr were obtained on these bed heights. COD removal was tested on the samples obtained for colour removal corresponding to to C/C_0 = 0.005 and C/C_0 = 0.9, respectively. COD removal graphs were plotted on each column run. The data obtained are shown in Figures 5 (a) to (c) for 0.5 L/hr, 0.7 L/hr, and 1.0 L/hr.

The COD for the untreated simulated wastewater was found to be 874.956mg/L. When this simulated water was passed through different bed heights at different flow rates, reduction in COD was found. For 0.5 L/hr flow rate, the COD reduction for 2.5cm was 245.638 mg/L to 733.769 mg/L, 3.5cm was 239.238 mg/L to 725.157mg/L and 4.5cm was 231.127mg/L to 734.419 mg/L, respectively. For 0.7 L/hr, the COD removal for 2.5cm was 247.238 mg/L to 732.629 mg/L, 3.5cm was 241.845mg/L to 735.146 mg/L and 4.5cm was 235.156 mg/mL to 730.932 mg/L respectively. For 1.0 L/hr, the COD removal for 2.5cm was 252.127 mg/L to 731.867 mg/L, 3.5cm was 248.563 mg/L to 730.322 mg/L and 4.5cm was 240.563 mg/L to 725.025 mg/L, respectively. It could be observed from the Figure5 (a) to (c) that as the bed height increased, COD reduction increased. However, with increase in flow rate, COD reduction decreased. Moreover, in all the cases COD reduction reached below 250

mg/L (at initial level) which is the requirement forced by Central Pollution Control Board for textile wastewater discharge.

The breakthrough time T_B for COD removal was considered to be the time when COD reduction just increased from 250mg/L. Therefore, for 0.5L/hr flow rate, the breakpoint time for 2.5cm, 3.5cm and 4.5cm was 100min, 240min and 280min, respectively. For 0.7 L/hr, the breakpoint time for 2.5cm, 3.5cm and 4.5cm were 30min, 120min and 190min, respectively. For 1.0 L/hr, the breakpoint time for 2.5cm, 3.5cm and 4.5cm were 20min, 80min and 140min, respectively. The volume V_B treated at breakpoint time for various flow rates and bed heights are given in Table 7.9. It could be observed from the Table 7.9 that both T_B and V_B increased with increase in bed height. However, with an increase in flow rate, both T_B and V_B decreased.

Table 7.9: Breakthrough times and volume treated of simulate wastewater on alkali modified soil for different flow rates and bed heights for COD removal

Flow rate (L/hr)	**Bed depth (cm)**	**Breakthrough Time T_B (min)**	**Breakthrough volume V_B (mL)**
0.5	2.5	100	829
	3.5	240	1989.2
	4.5	280	2321.2
0.7	2.5	30	348
	3.5	120	1329
	4.5	190	2204
1.0	2.5	20	332
	3.5	80	1328
	4.5	140	2324

7.3.2 Treatment of Actual Textile Wastewater

From the tests of simulated wastewater, it could be seen that the column was rapidly exhausted at higher flow rates of 0.7 L/hr and 1.0 L/hr as compared to 0.5 L/hr. This may be due to the competition of various organic matters. Therefore, the flow rate of 0.5L/hr and a bed height of 4.5cm were chosen for the treatment of actual wastewater.

The physicochemical properties of actual wastewater are described in materials and methods. Since the actual wastewater obtained for the present study was not the high clarity wastewater, it caused the rapid clogging of the bed. Therefore, for the treatment of the actual wastewater, coagulation of the suspended impurities was performed before the adsorption process.

7.3.2.1 Coagulation-Flocculation

Chemical coagulation and flocculation in textile wastewater treatment involve the addition of chemicals to alter the physical state of dissolved and suspended solids and facilitate their removal by sedimentation(Verma et al. 2012). In the present study, alum; aluminium sulphate ($Al_2(SO_4)_3.16H_2O$) was used as a coagulant. Various alum doses were tried to obtain the optimum alum dose for the colour removal. Figure 7.6 shows the effect of various alum doses. In the Figure 6 different coloured lines represent different alum doses like a: untreated wastewater, b: 0.2g/L, c: 0.4g/L, d: 0.6g/L, e: 0.8g/L, f: 1.0g/L, g: 1.2g/L, h: 1.4g/L, i: 1.6g/L, j: 1.8g/L, and k: 2.0g/L. It can also be seen from the Figure 6 that the dose of 1.6g/L gave the best colour removal after which all the lines merged. Therefore, this dose was considered to be optimum dose and was further used for the treatment of actual wastewater.

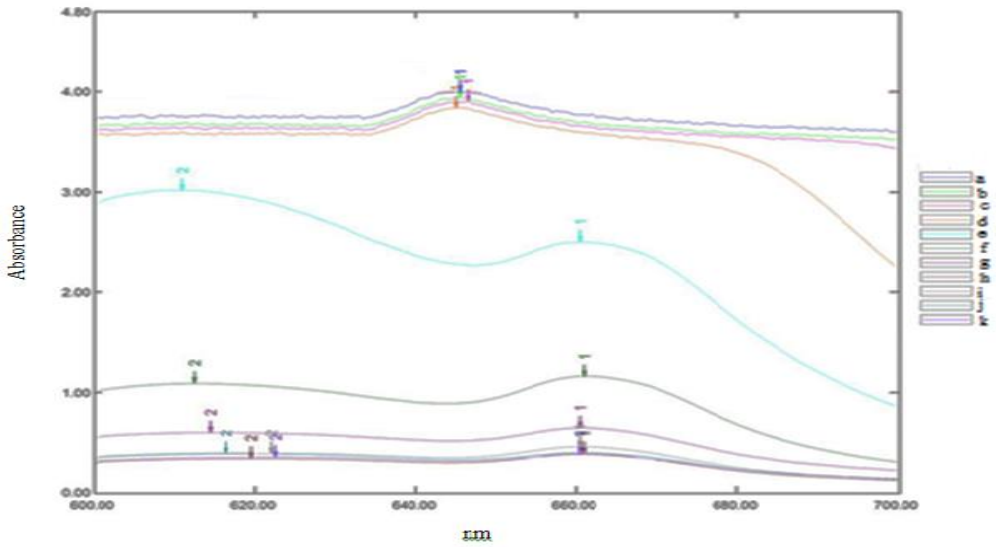

Figure 7.6: The curve of absorbance in the visible spectrum for the treated wastewater by alum.

The Figure 7.6 shows the reduction in the COD at various alum doses. The COD of the raw actual wastewater was found to be 1215.14mg/L. The COD at various doses was as follows: 0.2g/L : 1034.023mg/L, 0.4g/L : 993.665mg/L, 0.6g/L : 984.665mg/L, 0.8g/L : 975.067mg/L, 1.0g/L : 937.399mg/L, 1.2g/L : 936.55mg/L, 1.4g/L : 899.543mg/L, 1.6g/L : 858.901mg/L, 1.8g/L : 854.37mg/L and 2.0g/L : 843.702mg/L.

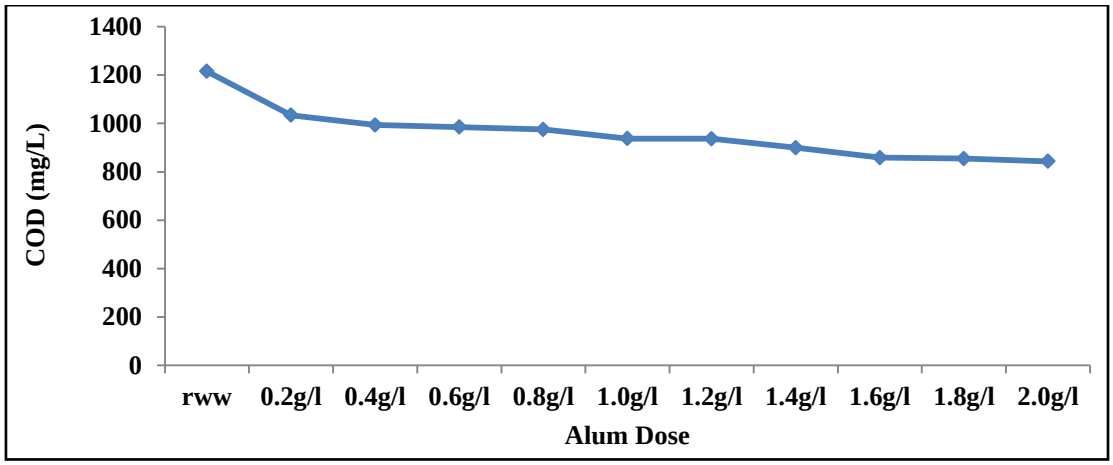

Figure 7.7: COD reduction at various alum doses

7.3.2.2 Adsorption on Fixed Bed Column

The COD for the actual textile wastewater was found to be 858.901mg/L after coagulation. When this actual textile wastewater was passed through fixed bed column of bed height 4.5cm at 0.5 L/hr flow rate reduction in COD was found. For 0.5 L/hr flow rate, the COD reduced from 858.901 mg/L to 211.051 mg/L.

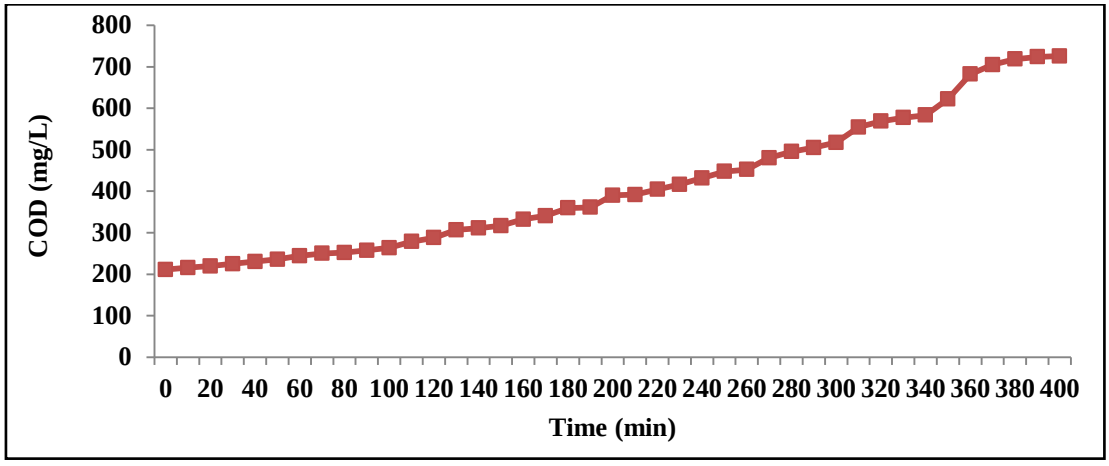

Figure 7.8: COD removal for actual wastewater at 0.5 L/hr flow rate and 4.5cm bed height

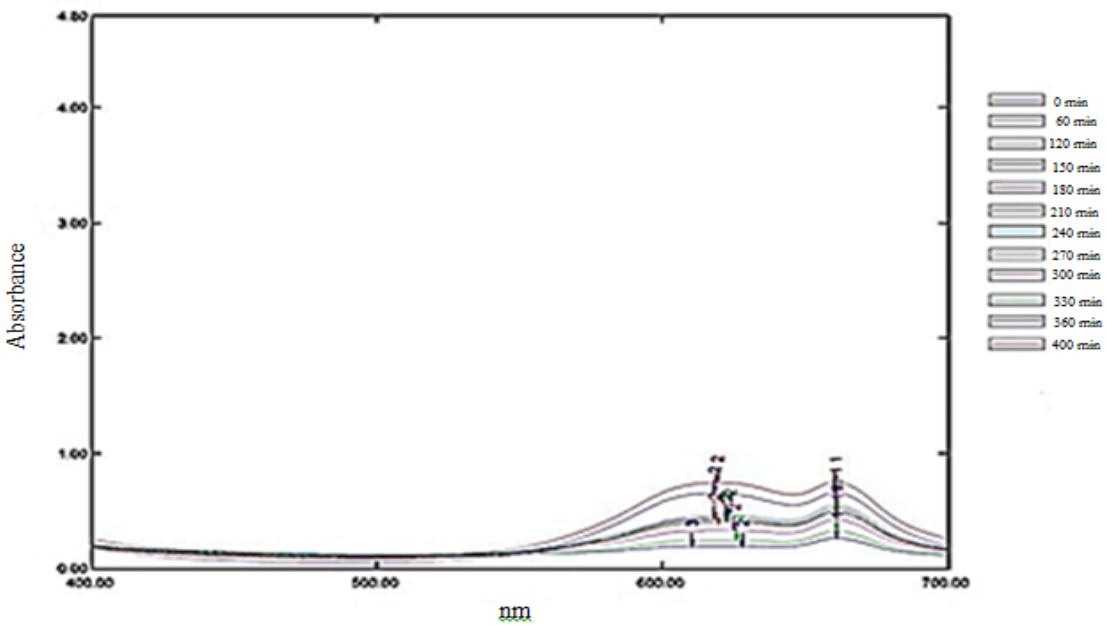

Figure 7.9: The curve of absorbance in the visible spectrum for the treated wastewater at 0.5 L/hr flow rate and 4.5cm bed height

7.4 Summary

This Chapter illustrates the fixed bed study for the treatment of simulated and actual textile wastewater. Methylene blue was used in the preparation of simulated wastewater as it is the most soluble dye and difficult to remove. Alkali modified soil was used as an adsorbent for the column study. The effect of adsorbent bed height and flow rate on the adsorption capacity for colour and COD removal were investigated. It was found that an increase in bed height and a decrease in flow rate improved the colour removal and COD reduction. Several breakthrough models reported in the literature were tested for their validity to explain the adsorption data. The BDST model was found to predict the breakthrough curve satisfactorily for all values of bed height and flow rate. The Thomas and Yoon-Nelson model were also applied for the prediction of breakthrough curves. Model constants were determined by linear regression for use in the column design. Simulations made by both the models were found to be consistent with the experimental observations. All of the models were found to be suitable for describing the dynamic behaviour of the whole or a definite part of the column with respect to all bed heights and flow rate values.

For treatment of actual textile wastewater, the combination of bed height of 4.5 cm and flow rate of 0.5 L/hr was chosen as it gave good removal for simulated wastewater. Before passing the wastewater through adsorption column, it was treated with coagulation method using alum as a coagulant. Coagulation reduced COD from 1215.14 mg/L to 858.901 mg/L. After passing this wastewater through adsorption column, COD further reduced to 211.051 mg/L. Thus, fixed bed study showed that actual textile wastewater could be brought to standard limits of COD (250 mg/L) for disposal.

CHAPTER

8

Chapter 8

Conclusion

A feasibility study was conducted on the non-modified soil to assess its dye adsorption capacity Two classes of dyes: anionic; Direct Red 81 and cationic; Methylene Blue, were used for their removal from aqueous solution. After the encouraging results obtained vis-à-vis colour removal, the study was further detailed, and the research objectives were defined.

This chapter presents the conclusions of this study against four objectives mentioned in Chapter 1. Based on the results obtained from the research, conclusions are derived on each of the research objectives and are as follows.

Objective 1:*"To study the effect of various operating parameters to identify the set of optimum parameters for colour removal on the soil."*

Chapter 4 elucidates the effect of various parameters like pH, adsorbent dose, initial dye concentration, contact time and particle size of non-modified soil on adsorption of the two dyes conducted in batch mode.

It was found that the isoelectric point of the non-modified soil was around at pH 9. Therefore, DR81 being an anionic dye, showed maximum removal towards the acidic region. The optimum ***pH*** obtained for DR81 removal was pH 3. One noteworthy fact realised is that at pH 1 almost 80% of DR81 was removed irrespective of the adsorbent dose used indicating chemical precipitation of dye. MB is a cationic dye and was removed in the basic pH region. The maximum removal for MB was found to be at pH 11.

It was observed that effect of ***contact time*** for both the dyes was same. The contact time of 10 minutes was found to be sufficient for the establishment of equilibrium.

The amount of dye uptake (mgg^{-1}) was found to decrease with an increase in ***adsorbent dose***. For instance, at initial dye concentration of 1000 mg/L, contact time 10 min, particle size 300-150 µm and pH 3, q_e for DR81 was found to be $0.96mgg^{-1}$-

0.46mgg^{-1} for adsorbent dose of 12.5g/100mL-100g/100mL respectively. However, at initial dye concentration of 1000 mg/L, contact time 10 min, particle size 300-150 µm and pH 11, q_e for MB was found to be 3.04mgg^{-1}-0.81mgg^{-1} for adsorbent dose 12.5g-100g respectively. The reason for decrease in adsorption capacity can be attributed to overlapping of adsorption sites resulting in decrease in total adsorbent surface area available to dye and increase in diffusion path length.

The effect of ***initial dye concentration*** was also studied. It was found that amount of dye uptake (mgg^{-1}) increased with increase in initial dye concentration. For instance, at adsorbent dose of 25g/100mL, contact time 10 min, particle size 300-150 µm and pH 3, q_e for DR81 was found to be 0.28mgg^{-1}-0.80mgg^{-1} for initial dye concentration of 125 mg/L-1000 mg/L respectively. However, at adsorbent dose of 25g/100mL, contact time 10 min, particle size 300-150 µm and pH 11, q_e for MB was found to be 0.42 mgg^{-1}-2.68 mgg^{-1} for initial dye concentration of 125 mg/L-1000 mg/L respectively.

It was observed that adsorption capacity of non-modified soil is increased with a decrease in the ***particle size of the adsorbent***. When the particle size was decreased from 300-150µm to 150-75µm, the adsorption capacity of soil was increased from 0.96mgg^{-1} to 1.28mgg^{-1} for DR81 and 3.04mgg^{-1} to 4.4mgg^{-1} for MB.

From the above findings, adsorption capacity of non-modified soil for cationic dye (MB) was found to be much higher than anionic dye (DR81) because of the ionic charges on the dyes and the surface charge of the non-modified soil on the above mentioned isoelectric point supported the better adsorption of MB as compared to DR81.

Kinetics of adsorption explains how fast the reaction occurs and the factors affecting it. The experimental data fitted well with Lagergren's pseudo second order kinetic model for both the dyes which suggest chemiadsorption. Also, the predicted uptake values nearly matched with experimental values. Also, values of experimental q_e increased with increase in the initial dye concentration for both the dyes, which is typical of an adsorption process. This suggests that the boundary layer resistance was not the rate limiting step. From, intraparticle diffusion model for both dyes, it was observed that intraparticle diffusion was not the only rate-limiting step but boundary layer diffusion also controlled the adsorption to some extent.

The analysis of equilibrium of adsorption provides basic fundamental data for evaluating the applicability of adsorbent for the uptake of adsorbate. The parameters of ***isotherm models*** express the surface properties and affinity of the adsorbent. Langmuir and Freundlich isotherms were tried for both the dyes. Equilibrium data for both the dyes fit very well in the Freundlich isotherm equation, confirming the adsorption is of chemical nature.

Thus, the set of optimum parameters obtained from the objective 1 for colour removal was as follows: contact time: 10 minutes, pH: 3 for DR81 and 11 for MB and particle size range of adsorbent: 150-75μm. For further analysis in the present work, these optimum parameters were considered pre-set.

Objective 2: *"To modify soil based on optimum parameters as identified from objective 1 and analyse surface characteristics of soil after modification."*

Following the objective 1, it was observed that DR81 and MB gave maximum removal at pH 3 and pH 11, respectively. Thus, it could be concluded that non-modified soil acquired positive and negative charge on its surface at pH of 3 and 11, respectively, for the removal of these oppositely charged dyes. So, modification of non-modified soil was done in such a way that it acquires surface charge opposite to the dye to be removed. This helped in the exclusion of the pH maintenance step for dye removal.

For DR81 removal, the non-modified soil was modified using 1N H_2SO_4 and was named as ***acid-modified soil***. For MB removal, the non-modified soil was modified using 1N NaOH and was named as ***alkali-modified soil***.

To investigate the modification done on non-modified soil and to compare the surface characteristics of all the three soils, this objective was designed. Six techniques were used for surface characteristics analysis, namely; Zeta potential, FTIR, BET surface area, XRD, XRF, and SEM-EDX.

- ***Zeta potential*** revealed the negative charge on the soil surface. Zeta potential of the non-modified soil surface was -17mV. However, in acid modified soil, its value decreased to -15.6 mV. This showed the attainment of positive charge by acid-modified soil. Zeta potential of alkali modified soil increased to -21.6 mV as

compared to non-modified soil. Thus, alkali modified soil acquired more negative charge after modification.

- ***FTIR spectral analysis*** demonstrated the existence of negatively charged functional groups like –OH,-C-OH, -CH_2, and –SiO on the non-modified soil surface. FTIR spectral data of acid modified soil showed that the intensity of silanol (SiO-H) group at 3433.72cm^{-1} decreased in acid activated soil. This may be accepted as evidence for acid modification occurring on soil. In alkali modified soil, there was an increase in the intensity of stretching vibration of silanol (SiO-H) group at 3440.75cm^{-1}. This may be accepted as evidence for alkali modification of soil. These results further supported zeta potential analyses.
- ***BET surface area analysis*** suggested non-modified soil to be mesoporous with average pore size of 19.861Å. However, in case of acid-modified soil average pore size of soil particle decreased as compared to non-modified soil. The value was found to be 18.692Å which indicated microporosity. Surface analysis of alkali-modified soil showed that average pore size of soil particle increased as compared to non-modified soil. The value was found to be 24.802Å which indicated better mesoporosity than non-modified soil.
- ***XRD analysis*** of non-modified soil suggested the presence of aluminium silicate hydroxide and calcium aluminium silicate hydrate. Some minor peaks of iron aluminium silicate, calcium silicate, aluminium silicate and calcium aluminium silicate were also observed. For acid modified soil, XRD pattern showed that the intensity of the peak at $2\theta = 20.90$ and $2\theta = 59.9$ was found to be decreased as compared to non-modified soil. This suggested acid modification of soil took place. For alkali modified soil, new peaks appeared at $2\theta = 26.65$ and $2\theta = 36.46$, 40.23 and 42.39 as compared to non-modified soil. This suggested alkali-modification of soil took place.
- ***XRF analysis*** of non-modified soil indicated the presence of silica, alumina and iron oxide as major constituents, along with traces of sodium, potassium, calcium, and magnesium oxides. SiO_2 content of the acid modified soil as compared to non-modified soil increased. For alkali modified soil, SiO_2, Al_2O_3 and Fe_2O_3 content increased.
- ***SEM and EDX analysis*** was also conducted. The elemental composition of all soils showed the presence of oxygen, silicon, iron, aluminium, calcium, magnesium,

potassium and sodium. SEM monographs revealed better adsorption of methylene blue.

Objective 3: *"To assess the potential of modified soil vis-a-vis colour removal."*

The purpose of this objective was to evaluate the adsorption capacity of both the modified soil; acid-modified and alkali-modified soil. The parameters which were considered for assessment were contact time, initial dye concentration and adsorbent dose.

Contact time studies revealed that 10 minutes were sufficient to attain the equilibrium state for both the modified soils for respective dye removal from aqueous solution. Thus, no change in the effect of contact time was observed as compared to non-modified soil. The amount of dye uptake (mgg^{-1}) was found to decrease with an increase in ***adsorbent dose***. For removal of DR81 on acid-modified soil, equilibrium adsorption capacity (q_e) decreased from $2.4mgg^{-1}$-$0.67mgg^{-1}$ when adsorbent dose increased from 12.5g/100mL-100g/100mL. q_e of MB onto alkali modified soil surface decreases from $6.40mgg^{-1}$-$0.89mgg^{-1}$ with increase in adsorbent dose from 12.5g/100mL-100g/100mL. The effect of ***initial dye concentration*** showed that equilibrium adsorption capacity (q_e) increased from $0.44mgg^{-1}$-$2.40mgg^{-1}$ with increase in the initial DR81 concentration from 125 mg/L-1000 mg/L. For MB, q_e increased from $0.89mgg^{-1}$-$6.40mgg^{-1}$ with increase in the initial MB concentration from 125 mg/L-1000 mg/L. On comparing the adsorption capacity with non-modified soil, it was found that both the modified soils developed better adsorption capacity. However, alkali modified soil has highest adsorption capacity.

To have detailed knowledge of the reaction mechanism of the modified soils, ***kinetic modelling and equilibrium study*** was done. The kinetic modelling for both the modified soils revealed that Lagergren's pseudo second-order kinetic model was found to describe the behaviour of DR81 and MB removal onto the respective modified soil. The values of experimental q_e suggested that boundary layer resistance was not the rate limiting step for adsorption of dyes onto both the modified soils. Intraparticle diffusion model showed multilinearity. This suggested that adsorption mechanism was a multi-step process, involving adsorption on the external surface, diffusion into the interior and ion exchange.

Linear and non-linear regression analysis of equilibrium data was performed. For DR81 onto acid-modified soil, equilibrium data did not fit well with Langmuir and Freundlich isotherms for linear regression analysis. Therefore, non-linear regression analysis approach was used. It was found that the order of fitness of isotherm models from the best to the least was Redlich–Peterson < Freundlich < Langmuir < Sips < Toth isotherms based on their R^2 values, χ^2 and RMSE.

For MB onto alkali modified soil, linear regression analysis of equilibrium data exhibited Freundlich behaviour to some extent. From non-linear regression analysis, the order of fitness of isotherm models from the best to the least was Sips < Freundlich < Langmuir < Redlich–Peterson < Toth isotherms based on their R^2 values, χ^2 and RMSE.

Objective 4: *"To conduct fixed bed study to evaluate design parameters of using the soil as an adsorbent."*

Objective 1 and 3 were performed in batch mode. However, to evaluate the adsorption capacity of the soil for commercial purpose, fixed bed study was designed. Both simulated and actual textile wastewater were used for treatment. Alkali modified soil had all the requisite characteristics for successful continuous flow mode of operation in fixed bed column. Therefore, it was used as an adsorbent. The removal of colour and COD from both the textile wastewater was studied. Effect of three different bed heights and flow rates was studied through breakthrough curves.

The adsorption was studied with ***simulated textile wastewater*** at three different flow rates of 0.5 L/hr, 0.7 L/hr, and 1.0 L/hr fixed bed column of various heights of 2.5cm, 3.5cm and 4.5cm. As flow rate increased, the breakthrough time for a given depth reduced. The increase in flow rate reduced the contact time and hence, a breakthrough occurred at the lesser time. The value of percentage colour removal increased with increased in bed height, however, decreased with increase in flow rate.

The ***COD*** reduction from the simulated textile wastewater was also studied. As the bed height increased, COD reduction increased. However, with an increase in flow rate, COD reduction decreased. Moreover, in all the cases COD reduction reached below 250mg/L (at initial level) which is the requirement forced by Central Pollution Control Board for textile wastewater discharge.

To have a better understanding of the continuous mode of operation, evaluation of design parameters using three models namely; BDST, Thomas and Yoon and Nelson were performed on the data collected from the breakthrough curve. ***BDST approach*** could successfully be applied for the evaluation of design parameters. The service time was found sufficiently long to support the economics of column operation. It is also observed that bed efficiency decreased with increase in flow rate. The dynamic behaviour of the columns was predicted with the ***Thomas model***. The values of Thomas rate constant (k_{Th}) were found to be dependent on bed height and flow rate. It decreased with increase in bed height, however, increased with increase in flow rate.The column data obtained was also fit to the ***Yoon and Nelson model***. As the bed height increased, the values of k_{YN} decreased and q_{oYN} increased in all column conditions. And, as the flow rate increased, the values of q_{oYN} decreased and k_{YN} increased.

For ***actual textile wastewater***, a combination of the flow rate of 8.29ml/min and a bed height of 4.5cm was chosen for treatment as it gave the best result for simulated wastewater. Actual wastewater caused rapid clogging of bed; therefore an additional step of coagulation was added in the treatment process. Aluminium sulphate ($Al_2(SO_4)_3.16H_2O$) was used as a coagulant. The dose of 1.6g/L of coagulant was found to be optimum. After coagulation step, COD was reduced from 1215.14mg/L to 858.901mg/L. When this treated wastewater was passed through the adsorption bed, COD further reduced to 211.051mg/L. Colour was also reduced.

Thus, for both the wastewater, alkali-modified soil reasonably met the standard limits of treatment. Therefore, it could be said that its commercial applicability is feasible as a low-cost adsorbent.

Limitations of the Study

This study could be criticised for taking a limited number of data sets for various analyses. For example,

- Data between times 0 minute to 10 minutes is less and it may influence the results.

- Analysis on effect of initial dye concentration is limited to a set of four initial dye concentrations.
- Less number of experiments performed in each experiment. This restricted to perform optimization of the process parameter.

Also, the volume of the dye is too little as compared to the adsorbent used. Experiments at various temperatures are also not conducted. However, the researcher has tried to be utterly realistic as to what can actually be achieved during the limited study time available. She has resisted the temptation to pretend that more can be achieved for the sake of appearing more 'advanced' in this research.

Overall Conclusion to the Research Problem

With the increasing industrial growth and eradicating clean water resources, low-cost treatment technologies are on high demand. Especially textile sector, which renders water unsuitable for further use, it is a big challenge for environmental engineers and scientists to develop a treatment technology for developing countries. The present research was an attempt to find a lost cost solution for textile wastewater treatment. The findings of the study discussed above successfully addresses the research gap in the available literature discussed earlier.

The easy and abundant availability of soil makes it a low-cost adsorbent. Since it is available locally, the transportation cost is reduced. This makes it a commercially viable solution for small to medium scale textile enterprises. Modification is also not a difficult step and can be carried out easily with unskilled labour. Modification of soil helped in understanding the removal mechanism in a better way. It also increased the adsorption capacity of soil.

Methylene blue is a very commonly used dye in small to medium scale textile enterprises. It is a highly soluble dye, making it very difficult to remove. The soil used in this study showed a good removal capacity for this dye, almost comparable to the colour removal capacity of the clayey substances. Also, the particle size of soil is reasonably larger than the low-cost adsorbents (mainly clayey material) reported earlier. This feature reduces the problem of choking of adsorption beds and makes it a better option to be used in adsorption columns for field applications. Overall the

locally available soil provides a good trade-off between colour removal capacity and practical problem of clogging of bed associated with field application of adsorbent beds. Fixed bed study conducted with both simulated and actual textile wastewater also indicated the competence of soil to be used in field scale. It also demonstrated that actual wastewater can be treated to standard limits of disposal.

In short, this research has made a contribution to the available adsorption technology concerning colour removal from textile wastewater. The findings of the study have immense potential for adoption in the field of treatment of textile wastewater using soil as a low-cost adsorbent.

Scope for Future Research

The proposed study achieved its objectives to investigate the adsorption efficiency of locally available soil to be used as a low-costadsorbent for textile wastewater treatment. But due to the limitations related to the availability of resources and time frame, the study has revealed a range of issues which are required to be investigated on the priority basis.The following recommendations may help to improve the treatment.

- Modification of non-modified soil using other acids and alkalis may be tried.
- Variation in the normality of the acid and alkali for modification of non-modified may also be tried to find the change in the uptake potential.
- Thermodynamic studies can be performed.
- Deeper understanding of the process is required to develop a better column design.
- Field scale-up studies can be undertaken to find out its acceptability to field situations.
- Parameters like total dissolved solids, salts, heavy metals, etc. can also be studied.
- Management and disposal of the spent adsorbent can be explored.

References

Abdel-Ghani, N.T., Hefny, M. & El-Chaghaby, G. a. F., 2007. Removal of lead from aqueous solution using low cost abundantly available adsorbents. *International Journal of Environmental Science & Technology*, 4(1), pp.67–73. Available at: http://link.springer.com/10.1007/BF03325963.

Abdulla, F. a, 2009. Roof rainwater harvesting systems for household water supply in Jordan. *Desalination*, 243(September 2015), pp.195–207.

Ahmad, A.A. & Hameed, B.H., 2009. Reduction of COD and color of dyeing effluent from a cotton textile mill by adsorption onto bamboo-based activated carbon. *Journal of Hazardous Materials*, 172(2-3), pp.1538–1543.

Ahmad, A.A., Hameed, B.H. & Aziz, N., 2007. Adsorption of direct dye on palm ash: Kinetic and equilibrium modeling. *Journal of Hazardous Materials*, 141(1), pp.70–76.

Ahn, D.-H., Chang, W.-S. & Yoon, T.-I., 1999. Dyestuff wastewater treatment using chemical oxidation, physical adsorption and fixed bed biofilm process. *Process Biochemistry*, 34(5), pp.429–439.

Ajibola, A. et al., 2015. Adsorption of dyes using different types of clay : a review. *Applied Water Science*, pp.117–129. Available at: "http://dx.doi.org/10.1007/s13201-015-0322-y.

Albadarin, A.B. et al., 2012. Kinetic and thermodynamics of chromium ions adsorption onto low-cost dolomite adsorbent. *Chemical Engineering Journal*, 179, pp.193–202.

Albanis, T. et al., 2000. Removal of dyes from aqueous solutions by adsorption on mixtures of fly ash and soil in batch and column techniques. *Global Nest. Int. J*, 2(3), pp.237–244. Available at: https://www.ath.aegean.gr/gnest/Journal/Vol2_No3/albanis.pdf.

Al-Degs, Y. et al., 2000. Effect of carbon surface chemistry on the removal of reactive dyes from textile effluent. *Water Research*, 34(3), pp.927–935.

Al-Ghouti, M.A. et al., 2003. The removal of dyes from textile wastewater: A study of the physical characteristics and adsorption mechanisms of diatomaceous earth. *Journal of Environmental Management*, 69(3), pp.229–238.

Almeida, C.A.P. et al., 2009. Removal of methylene blue from colored effluents by adsorption on montmorillonite clay. *Journal of Colloid and Interface Science*, 332(1), pp.46–53. Available at: http://dx.doi.org/10.1016/j.jcis.2008.12.012.

Alver, E. & Metin, A. ü, 2012. Anionic dye removal from aqueous solutions using modified zeolite: Adsorption kinetics and isotherm studies. *Chemical Engineering Journal*, 200-202, pp.59–67.

Al-wahbi, A.A.M., Ahmed, H. & Dammag, Q., 2011. Removal of Methylene Blue From Aqueous Solutions Using Yemen Bentonite. *Diyala Journal of Engineering Sciences*, 04(01), pp.30–53.

Alzaydien, A.S., 2009. Adsorption of methylene blue from aqueous solution onto a low cost natural Jordanian Tripoli. *American Journal of Environmental Sciences*, 6(6), pp.1047–1058.

Amin, N.K., 2009. Removal of direct blue-106 dye from aqueous solution using new activated carbons developed from pomegranate peel: Adsorption equilibrium and kinetics. *Journal of Hazardous Materials*, 165(1-3), pp.52–62.

Anjaneyulu, Y., Sreedhara Chary, N. & Samuel Suman Raj, D., 2005. Decolourization of industrial effluents - Available methods and emerging technologies - A review. *Reviews in Environmental Science and Biotechnology*, 4(4), pp.245–273.

Annadurai, G., Juang, R.S. & Lee, D.J., 2002. Use of cellulose - based wastes for adsorption of dyes from aqueous solutions. *Journal of Hazardous Materials*, 92(3), pp.263–274.

Ansari, R., Mohammad-khah, A. & Nazmi, M., 2013. Application of chemically modified beach sand as low cost efficient adsorbent for dye removal. *Current Chemistry Letters*, 2, pp.215–223. Available at: http://www.growingscience.com/ccl/Vol2/ccl_2013_19.pdf.

Arami, M. et al., 2005. Removal of dyes from colored textile wastewater by orange peel adsorbent: Equilibrium and kinetic studies. *Journal of Colloid and Interface Science*, 288(2), pp.371–376.

Armagan, B. et al., 2004. Color removal of reactive dyes from water by clinoptilolite. *Journal of Environmental Science and Health Part a-Toxic/Hazardous Substances & Environmental Engineering*, 39(5), pp.1251–1261. Available at: <Go to ISI>://WOS:000220979200007.

Asouhidou, D.D. et al., 2009. Sorption of reactive dyes from aqueous solutions by ordered hexagonal and disordered mesoporous carbons. *Microporous and Mesoporous Materials*, 117(1-2), pp.257–267. Available at: http://dx.doi.org/10.1016/j.micromeso.2008.06.034.

Ateş, A., Köklü, R. & Özer, Ç., 2014. The Adsorption of Dye Removal from Textile Industry Wastewater with Natural Adsorbents. , pp.275–282.

Attia, A.A., Girgis, B.S. & Fathy, N.A., 2008. Removal of methylene blue by carbons derived from peach stones by H3PO4 activation: Batch and column studies. *Dyes and Pigments*, 76(1), pp.282–289.

Atun, G. et al., 2003. Adsorptive removal of methylene blue from colored effluents on fuller's earth. *Journal of Colloid and Interface Science*, 261(1), pp.32–39.

Auta, M., 2012. Fixed bed adsorption studies of rhodamine b dye using oil palm empty fruits bunch activated carbon Address for Correspondence. *Journal of Engineering Research and Studies*, 3(3), pp.3–6.

Auta, M. & Hameed, B.H., 2012. Modified mesoporous clay adsorbent for adsorption

isotherm and kinetics of methylene blue. *Chemical Engineering Journal*, 198-199, pp.219–227. Available at: http://dx.doi.org/10.1016/j.cej.2012.05.075.

Azizian, S., 2004. Kinetic models of sorption: A theoretical analysis. *Journal of Colloid and Interface Science*, 276(1), pp.47–52.

Babu, B.R. et al., 2007. Cotton Textile Processing : Waste Generation and Effluent Treatment. *The journal of cotton science*, 153(11:141), pp.141–153.

Bailey, S.E. et al., 1999. A review of potentially low-cost sorbents for heavy metals. *Water Research*, 33(11), pp.2469–2479.

Banat, F., Al-Asheh, S. & Al-Makhadmeh, L., 2003. Evaluation of the use of raw and activated date pits as potential adsorbents for dye containing waters. *Process Biochemistry*, 39(2), pp.193–202.

Bello, O.S., Bello, I.A. & Adegoke, K.A., 2013. Adsorption of dyes using different types of sand: A review. *South African Journal of Chemistry*, 66(SEPTEMBER), p.0. Available at: http://www.scielo.org.za/scielo.php?script=sci_arttext&pid=S0379-43502013000100024&nrm=iso.

Bello, O.S., Olusegun, O.A. & Njoku, V.O., 2013. Fly Ash: an Alternative To Powdered Activated Carbon for the Removal of Eosin Dye From Aqueous Solutions. *Bulletin of the Chemical Society of Ethiopia*, 27(2), pp.191–204.

Bera, A. et al., 2013. Adsorption of surfactants on sand surface in enhanced oil recovery: Isotherms, kinetics and thermodynamic studies. *Applied Surface Science*, 284, pp.87–99. Available at: http://dx.doi.org/10.1016/j.apsusc.2013.07.029.

Bharathi, K.S. & Ramesh, S.P.T., 2013. Fixed-bed column studies on biosorption of crystal violet from aqueous solution by Citrullus lanatus rind and Cyperus rotundus. *Applied Water Science*, 3(4), pp.673–687. Available at: http://link.springer.com/10.1007/s13201-013-0103-4.

Bhatnagar, A. & Minocha, A.K., 2006. Conventional and non-conventional adsorbents for removal of pollutants from water - A review. *Indian Journal of Chemical Technology*, 13(3), pp.203–217.

Van der Bruggen, B. et al., 2005. Fouling of nanofiltration and ultrafiltration membranes applied for wastewater regeneration in the textile industry. *Desalination*, 175(1 SPEC. ISS.), pp.111–119.

Bujdák, J. & Komadel, P., 1997. Interaction of methylene blue with reduced charge montmorillonite. *Journal of Physical Chemistry B*, 101(44), pp.9065–9068. Available at: http://www.scopus.com/inward/record.url?eid=2-s2.0-0031251120&partnerID=tZOtx3y1.

Bukallah, S.B., Rauf, M.A. & AlAli, S.S., 2006. Removal of Methylene Blue from aqueous solution by adsorption on sand. *Dyes and Pigments*, 74(1), pp.85–87.

Bulut, E., Özacar, M. & Şengil, I.A., 2008. Adsorption of malachite green onto bentonite: Equilibrium and kinetic studies and process design. *Microporous and*

Mesoporous Materials, 115(3), pp.234–246.

Canci, M.B. & Kilic, M., 2013. Adsorption Of Dye From Aqueous Solution Onto Original And Modified Pumice. , pp.3–8.

Chan, L.S. et al., 2012. Error analysis of adsorption isotherm models for acid dyes onto bamboo derived activated carbon. *Chinese Journal of Chemical Engineering*, 20(3), pp.535–542.

Charumathi, D. & Das, N., 2012. Packed bed column studies for the removal of synthetic dyes from textile wastewater using immobilised dead C. tropicalis. *Desalination*, 285, pp.22–30. Available at: http://dx.doi.org/10.1016/j.desal.2011.09.023.

Chen, H. & Zhao, J., 2009. Adsorption study for removal of Congo red anionic dye using organo-attapulgite. *Adsorption*, 15(4), pp.381–389.

Chowdhury, S. & Saha, P., 2010. Sea shell powder as a new adsorbent to remove Basic Green 4 (Malachite Green) from aqueous solutions: Equilibrium, kinetic and thermodynamic studies. *Chemical Engineering Journal*, 164(1), pp.168–177. Available at: http://dx.doi.org/10.1016/j.cej.2010.08.050.

Cooper, P., 1995. Removing colour from dyehouse waste waters. *Asian Textile Journal*, 3(4), pp.52–56.

Crini, G., 2006. Non-conventional low-cost adsorbents for dye removal: A review. *Bioresource Technology*, 97(9), pp.1061–1085.

Crini, G. et al., 2007. Removal of C.I. Basic Green 4 (Malachite Green) from aqueous solutions by adsorption using cyclodextrin-based adsorbent: Kinetic and equilibrium studies. *Separation and Purification Technology*, 53(1), pp.97–110.

Crini, G., 2003. Studies on adsorption of dyes on beta-cyclodextrin polymer. *Bioresource Technology*, 90(2), pp.193–198.

Crini, G. & Ndongo Peindy, H., 2006. Adsorption of C.I. Basic Blue 9 on cyclodextrin-based material containing carboxylic groups. *Dyes and Pigments*, 70(3), pp.204–211.

Do, J.S. & Chen, M.L., 1994. Decolourization of dye-containing solutions by electrocoagulation. *Journal of Applied Electrochemistry*, 24(8), pp.785–790.

Doğan, M. et al., 2004. Kinetics and mechanism of removal of methylene blue by adsorption onto perlite. *Journal of Hazardous Materials*, 109(1-3), pp.141–148.

Doğan, M. & Alkan, M., 2003. Removal of methyl violet from aqueous solution by perlite. *Journal of Colloid and Interface Science*, 267(1), pp.32–41.

Doğan, M., Karaoğlu, M.H. & Alkan, M., 2009. Adsorption kinetics of maxilon yellow 4GL and maxilon red GRL dyes on kaolinite. *Journal of Hazardous Materials*, 165(1-3), pp.1142–1151.

Doğan, M., Özdemir, Y. & Alkan, M., 2007. Adsorption kinetics and mechanism of cationic methyl violet and methylene blue dyes onto sepiolite. *Dyes and*

Pigments, 75(3), pp.701–713.

Doulati Ardejani, F. et al., 2008. Adsorption of Direct Red 80 dye from aqueous solution onto almond shells: Effect of pH, initial concentration and shell type. *Journal of Hazardous Materials*, 151(2-3), pp.730–737.

Doulati Ardejani, F. et al., 2007. Numerical modelling and laboratory studies on the removal of Direct Red 23 and Direct Red 80 dyes from textile effluents using orange peel, a low-cost adsorbent. *Dyes and Pigments*, 73(2), pp.178–185.

El-Geundi, M.S., 1991. Colour removal from textile effluents by adsorption techniques. *Water Research*, 25(3), pp.271–273.

Erdem, E., Çölgeçen, G. & Donat, R., 2005. The removal of textile dyes by diatomite earth. *Journal of Colloid and Interface Science*, 282(2), pp.314–319.

Erdemoğlu, M. et al., 2004. Organo-functional modified pyrophyllite: Preparation, characterisation and Pb(II) ion adsorption property. *Applied Clay Science*, 27(1-2), pp.41–52.

Ergas, S.J., Therriault, B.M. & Reckhow, D.A., 2006. Evaluation of Water Reuse Technologies for the Textile Industry. *Journal of Environmental Engineering (Reston, VA, United States)*, 132(3), pp.315–323.

Fathi, M.R., Asfaram, A. & Branch, G., 2011. Investigation of Kinetics and Equilibrium Isotherms of Direct Red 12B Dye Adsorption on Hazelnut Shells. , 1(2), pp.1–12.

Foo, K.Y. & Hameed, B.H., 2010. Insights into the modeling of adsorption isotherm systems. *Chemical Engineering Journal*, 156(1), pp.2–10.

Gandhimathi, R. et al., 2012. Single and Tertiary System Dye Removal from Aqueous Solution Using Bottom Ash : Kinetic and Isotherm Studies. , 3(1), pp.52–62.

Garg, V.K. et al., 2003. Dye removal from aqueous solution by adsorption on treated sawdust. *Bioresource Technology*, 89(2), pp.121–124.

Gemeay, A.H., 2002. Adsorption characteristics and the kinetics of the cation exchange of rhodamine-6G with Na+-montmorillonite. *Journal of colloid and interface science*, 251(2), pp.235–241.

Ghobarkar, H. & Guth, U., 1999. Zeolites - from kitchen to space.pdf. , 27, pp.29–73.

Ghosh, D. & Bhattacharyya, K.G., 2002. Adsorption of methylene blue on kaolinite. , 20, pp.295–300.

Gimbert, F. et al., 2008. Adsorption isotherm models for dye removal by cationized starch-based material in a single component system: Error analysis. *Journal of Hazardous Materials*, 157(1), pp.34–46.

Goswami, a. & Purkait, M.K., 2011. Kinetic and Equilibrium Study for the Fluoride Adsorption using Pyrophyllite. *Separation Science and Technology*, 46(11), pp.1797–1807. Available at: http://www.tandfonline.com/doi/abs/10.1080/01496395.2011.572327#.VTDuJyG

qqko.

Gou, Y. et al., 2003. Adsoprtion of malachite green on micro- and mesoporous rice husk-based active carbon. *Dyes and Pigments*, 56(3), pp.219–229.

Gücek, A. et al., 2005. Adsorption and kinetic studies of cationic and anionic dyes on pyrophyllite from aqueous solutions. *Journal of Colloid and Interface Science*, 286(1), pp.53–60.

Gupta, V.K., Ali, I. & Saini, V.K., 2007. Adsorption studies on the removal of Vertigo Blue 49 and Orange DNA13 from aqueous solutions using carbon slurry developed from a waste material. *Journal of Colloid and Interface Science*, 315(1), pp.87–93.

Gupta, V.K., Sharma, M. & Vyas, R.K., 2015. Hydrothermal modification and characterization of bentonite for reactive adsorption of methylene blue: An ESI-MS study. *Journal of Environmental Chemical Engineering*, 3(3), pp.2172–2179. Available at: http://dx.doi.org/10.1016/j.jece.2015.07.022.

Gupta, V.K. & Suhas, 2009. Application of low-cost adsorbents for dye removal - A review. *Journal of Environmental Management*, 90(8), pp.2313–2342. Available at: http://dx.doi.org/10.1016/j.jenvman.2008.11.017.

Gürses, A. et al., 2004. Determination of adsorptive properties of clay/water system: Methylene blue sorption. *Journal of Colloid and Interface Science*, 269(2), pp.310–314.

Gürses, A. et al., 2006. The adsorption kinetics of the cationic dye, methylene blue, onto clay. *Journal of Hazardous Materials*, 131(1-3), pp.217–228.

Halimoon, N. & Yin, R.G.S., 2010. Removal of Heavy Metals from Textile Wastewater using Zeolite Normala. *Environment Asia*, 3(Special issue), pp.124–130.

Hameed, B.H., 2009. Spent tea leaves: A new non-conventional and low-cost adsorbent for removal of basic dye from aqueous solutions. *Journal of Hazardous Materials*, 161(2-3), pp.753–759.

Hameed, B.H., Din, A.T.M. & Ahmad, A.L., 2007. Adsorption of methylene blue onto bamboo-based activated carbon: Kinetics and equilibrium studies. *Journal of Hazardous Materials*, 141(3), pp.819–825.

Hameed, B.H., Mahmoud, D.K. & Ahmad, A.L., 2008a. Equilibrium modeling and kinetic studies on the adsorption of basic dye by a low-cost adsorbent: Coconut (Cocos nucifera) bunch waste. *Journal of Hazardous Materials*, 158(1), pp.65–72.

Hameed, B.H., Mahmoud, D.K. & Ahmad, A.L., 2008b. Sorption of basic dye from aqueous solution by pomelo (Citrus grandis) peel in a batch system. *Colloids and Surfaces A: Physicochemical and Engineering Aspects*, 316(1-3), pp.78–84.

Han, R. et al., 2007. Biosorption of methylene blue from aqueous solution by rice husk in a fixed-bed column. *Journal of Hazardous Materials*, 141(3), pp.713–718.

Hao, O.J., Kim, H. & Chiang, P.-C., 2000. Decolorization of Wastewater. *Critical Reviews in Environmental Science and Technology*, 30(4), pp.449–505.

Haq, I.U., Bhatti, H.N. & Asgher, M., 2011. Removal of solar red BA textile dye from aqueous solution by low cost barley husk: Equilibrium, kinetic and thermodynamic study. *Canadian Journal of Chemical Engineering*, 89(3), pp.593–600.

Heravi, M.M. et al., 2015. Journal of Applied Chemistry Biosorption of Direct red 81 dye from aqueous solution on prepared sonchus fruit plant , as a low cost biosorbent : Thermodynamic and Kinetic study. , 9(32), pp.17–22.

Ho, Y. & Chiang, C., 2001. Removal From Aqueous Solution Introduction. , 36(11), pp.2473–2488.

Ho, Y.S., 2004a. Citation review of Lagergren kinetic rate equation on adsorption reactions. *Scientometrics*, 59(1), pp.171–177.

Ho, Y.S., 2006. Review of second-order models for adsorption systems. *Journal of Hazardous Materials*, 136(3), pp.681–689.

Ho, Y.S., 2004b. Selection of optimum sorption isotherm. *Carbon*, 42(10), pp.2115–2116.

Ho, Y.S. & McKay, G., 1999. Pseudo-second order model for sorption processes. *Process Biochemistry*, 34(5), pp.451–465.

Hossain, M.A. et al., 2012. Adsorption and desorption of copper(II) ions onto garden grass. *Bioresource Technology*, 121(January), pp.386–395.

Hsu, T.C., 2008. Adsorption of an acid dye onto coal fly ash. *Fuel*, 87(13-14), pp.3040–3045.

Ip, A.W.M., Barford, J.P. & McKay, G., 2009. Reactive Black dye adsorption/desorption onto different adsorbents: Effect of salt, surface chemistry, pore size and surface area. *Journal of Colloid and Interface Science*, 337(1), pp.32–38.

Iqbal, M.J. & Ashiq, M.N., 2007. Adsorption of dyes from aqueous solutions on activated charcoal. *Journal of Hazardous Materials*, 139(1), pp.57–66.

Jain, R. & Sikarwar, S., 2008. Removal of hazardous dye congored from waste material. *Journal of Hazardous Materials*, 152(3), pp.942–948.

Joshi, M., Bansal, R. & Purwar, R., 2004. Colour removal from textile effluents. *Indian Journal of Fibre and Textile Research*, 29(2), pp.239–259.

Journal, I. & Engineering, O.F., 2013. Studies on Removal of Methylene Blue Color Using Sawdust as Adsorbent *1,2. , 2(11).

Jozefacuik, G. & Bowanko, G., 2000. Effect of Acid and Alkali Treatments on Surface Areas and Adsorption Energies of Selected Minerals. *Clays and Clay Minerals*, 50(6), pp.771–783.

Kargi, F. & Ozmihci, S., 2004. Biosorption performance of powdered activated sludge

for removal of different dyestuffs. *Enzyme and Microbial Technology*, 35(2-3), pp.267–271.

Kavitha, K. & Senthamilselvi, M.M., 2015. Removal of Malachite Green from aqueous solution using low cost adsorbent. , 3(6), pp.97–104.

Khaled, A. et al., 2009. Treatment of artificial textile dye effluent containing Direct Yellow 12 by orange peel carbon. *Desalination*, 238(1-3), pp.210–232. Available at: http://dx.doi.org/10.1016/j.desal.2008.02.014.

Khan, T. et al., 2009. Utilization of fly ash as low-cost adsorbent for the removal of methylene blue, malachite green and rhodamine B dyes from textile wastewater. *Journal of Environmental Protection Science*, 3, pp.11–22. Available at: http://aes.asia.edu.tw/Issues/JEPS2009/KhanTA2009.pdf.

Khan, T.A., Dahiya, S. & Ali, I., 2012. Removal of direct red 81 dye from aqueous solution by native and citric acid modified bamboo sawdust - kinetic study and equilibrium isotherm analyses. *Gazi University Journal of Science*, 25(1), pp.59–87.

Khattri, S.D. & Singh, M.K., 2009. Removal of malachite green from dye wastewater using neem sawdust by adsorption. *Journal of Hazardous Materials*, 167(1-3), pp.1089–1094.

Khraisheh, M.A.M. et al., 2005. Effect of OH and silanol groups in the removal of dyes from aqueous solution using diatomite. *Water Research*, 39(5), pp.922–932.

Ko, D.C.K., Porter, J.F. & McKay, G., 2000. Optimized correlations for the fixed-bed adsorption of metal ions on bone char. *Chemical Engineering Science*, 55(23), pp.5819–5829.

Koumanova, B. & Allen, S.J., 2005. Decolourisation of Water / Wastewater Using Adsorption (Review). *Journal of the University of Chemical Technology and Metallurgy*, 40, pp.175–192.

Kumar, K.V., 2006. Linear and non-linear regression analysis for the sorption kinetics of methylene blue onto activated carbon. *Journal of Hazardous Materials*, 137(3), pp.1538–1544.

Kundu, S. & Gupta, A.K., 2005. Analysis and modeling of fixed bed column operations on As(V) removal by adsorption onto iron oxide-coated cement (IOCC). *Journal of Colloid and Interface Science*, 290(1), pp.52–60.

Laasri, L., Elamrani, M.K. & Cherkaoui, O., 2007. Removal of two cationic dyes from a textile effluent by filtration-adsorption on wood sawdust. *Environmental science and pollution research international*, 14(4), pp.237–240.

Lian, L., Guo, L. & Guo, C., 2009. Adsorption of Congo red from aqueous solutions onto Ca-bentonite. *Journal of Hazardous Materials*, 161(1), pp.126–131.

Liu, P. & Zhang, L., 2007. Adsorption of dyes from aqueous solutions or suspensions with clay nano-adsorbents. *Separation and Purification Technology*, 58(1), pp.32–39.

Lorenc-Grabowska, E. & Gryglewicz, G., 2006. Adsorption characteristics of Congo Red on coal-based mesoporous activated carbon. *Dyes and Pigments*, 74(1), pp.34–40.

Mahmoodi, N.M., Khorramfar, S. & Najafi, F., 2011. Amine-functionalized silica nanoparticle: Preparation, characterization and anionic dye removal ability. *Desalination*, 279(1-3), pp.61–68.

Mall, I.D. et al., 2005. Removal of congo red from aqueous solution by bagasse fly ash and activated carbon: Kinetic study and equilibrium isotherm analyses. *Chemosphere*, 61(4), pp.492–501.

Mall, I.D., Srivastava, V.C. & Agarwal, N.K., 2006. Removal of Orange-G and Methyl Violet dyes by adsorption onto bagasse fly ash - Kinetic study and equilibrium isotherm analyses. *Dyes and Pigments*, 69(3), pp.210–223.

Mane, V.S., Mall, I.D. & Srivastava, V.C., 2007. Use of bagasse fly ash as an adsorbent for the removal of brilliant green dye from aqueous solution. *Dyes and Pigments*, 73(3), pp.269–278.

Manu, B. & Chaudhari, S., 2002. Anaerobic decolorisation of simulated textile wastewater containing azo dyes. *Bioresource Technology*, 82(3), pp.225–231.

Maurya, N.S., Mittal, A.K. & Cornel, P., 2008. Evaluation of adsorption potential of adsorbents: A case of uptake of cationic dyes. *Journal of Environmental Biology*, 29(1), pp.31–36.

McKay, G., 1982. Adsorption of dyestuffs from aqueous solutions with activated carbon I: Equilibrium and batch contact-time studies. *Journal of Chemical Technology and Biotechnology*, 32(7-12), pp.759–772. Available at: http://dx.doi.org/10.1002/jctb.5030320712.

McKay, G., 1998. Application of Surface Diffusion Model to the Adsorption of Dyes on Bagasse Pith. *Adsorption*, 4(3-4), pp.361–372. Available at: http://link.springer.com/article/10.1023/A:1008854304933.

Meriç, S., Kaptan, D. & Ölmez, T., 2004. Color and COD removal from wastewater containing Reactive Black 5 using Fenton's oxidation process. *Chemosphere*, 54(3), pp.435–441.

Mezzanotte, V. et al., 2013. Colour removal and carbonyl by-production in high dose ozonation for effluent polishing. *Chemosphere*, 91(5), pp.629–634.

Moghaddam, A.A.N. et al., 2010. Adsorption of Methylene Blue in Aqueous Phase by Fly Ash, Clay and Walnut Shell as Adsorbents. *World Applied Sciences Journal*, 8(2), pp.229–234.

Mohammed, M. a, Shitu, A. & Ibrahim, A., 2014. Removal of Methylene Blue Using Low Cost Adsorbent : A Review. *Research Journal of Chemical Sciences*, 4(1), pp.91–102.

Mondal, S., 2008. Methods of Dye Removal from Dye House Effluent—An Overview. *Environmental Engineering Science*, 25(3), pp.383–396. Available at: http://dx.doi.org/10.1089/ees.2007.0049.

Morais, L.C. et al., 1999. Reactive dyes removal from wastewaters by adsorption on eucalyptus bark: Variables that define the process. *Water Research*, 33(4), pp.979–988.

El Mouzdahir, Y. et al., 2010. Equilibrium modeling for the adsorption of methylene blue from aqueous solutions on activated clay minerals. *Desalination*, 250(1), pp.335–338. Available at: http://dx.doi.org/10.1016/j.desal.2009.09.052.

Mundada, P., Brighu, D.U. & Gupta, D.A.B., 2017. Removal of methylene blue on soil: an alternative to clay. *Desalination and Water Treatment*, 58.

Neumann, M.G. et al., 2002. Influence of the layer charge and clay particle size on the interactions between the cationic dye methylene blue and clays in an aqueous suspension. *Journal of colloid and interface science*, 255(2), pp.254–259.

Nidheesh, P.V. et al., 2012. Adsorption and desorption characteristics of crystal violet in bottom ash column. *Journal of Urban and Environmental Engineering*, 6(1), pp.18–29.

O'Neill, C. et al., 1999. Colour in textile effluents - Sources, measurement, discharge consents and simulation: A review. *Journal of Chemical Technology and Biotechnology*, 74(11), pp.1009–1018.

Olajire, A.A., Giwa, A.A. & Bello, I.A., 2015. Competitive adsorption of dye species from aqueous solution onto melon husk in single and ternary dye systems. *International Journal of Environmental Science and Technology*, 12(3), pp.939–950.

Ozacar, M., 2002. Adsorption of Acid Dyes from Aqueous Solutions by Calcined Alunite. , pp.301–308.

Özacar, M. & Şengil, I.A., 2003. Adsorption of reactive dyes on calcined alunite from aqueous solutions. *Journal of Hazardous Materials*, 98(1-3), pp.211–224.

Özcan Safa, A., Erdem, B. & Özcan, A., 2005. Adsorption of Acid Blue 193 from aqueous solutions onto BTMA-bentonite. *Colloids and Surfaces A: Physicochem. Eng. Aspects*, 266, pp.73–81.

Özcan, A., Oncu, E.M. & Özcan, A.S., 2004. Adsorption of Acid Blue 193 from aqueous solutions onto Na-bentonite and DTMA-bentonite. *Journal of Colloid and Interface Science*, 280(1), pp.44–54.

Özcan, A., Öncü, E.M. & Özcan, A.S., 2006. Kinetics, isotherm and thermodynamic studies of adsorption of Acid Blue 193 from aqueous solutions onto natural sepiolite. *Colloids and Surfaces A: Physicochemical and Engineering Aspects*, 277(1-3), pp.90–97.

Özcan, A. & Özcan, A.S., 2005. Adsorption of Acid Red 57 from aqueous solutions onto surfactant-modified sepiolite. *Journal of Hazardous Materials*, 125(1-3), pp.252–259.

Özcan, A.S. & Özcan, A., 2004. Adsorption of acid dyes from aqueous solutions onto acid-activated bentonite. *Journal of Colloid and Interface Science*, 276(1), pp.39–46.

Ozdemir, O. et al., 2009. Feasibility analysis of color removal from textile dyeing wastewater in a fixed-bed column system by surfactant-modified zeolite (SMZ). *Journal of Hazardous Materials*, 166(2-3), pp.647–654.

Pang, Y.L. & Abdullah, A.Z., 2013. Current status of textile industry wastewater management and research progress in malaysia: A review. *Clean - Soil, Air, Water*, 41(8), pp.751–764.

Pansuk, C., 2011. A Comparative Study of the Adsorption of Acid Brown 75 and Direct Yellow 162 onto Unmodified and Surfactant Modified Granule Developed from Coal Fly Ash. *IPCBEE vol.6 (2011)*, 6, pp.49–54.

Papić, S. et al., 2004. Removal of some reactive dyes from synthetic wastewater by combined Al(III) coagulation/carbon adsorption process. *Dyes and Pigments*, 62(3), pp.291–298.

Pathak, P.D., Mandavgane, S.A. & Kulkarni, B.D., 2015. Fruit peel waste as a novel low-cost bio adsorbent. *Reviews in Chemical Engineering*, 31(4), pp.361–381.

Pavan, F.A., Mazzocato, A.C. & Gushikem, Y., 2008. Removal of methylene blue dye from aqueous solutions by adsorption using yellow passion fruit peel as adsorbent. *Bioresource Technology*, 99(8), pp.3162–3165.

Pelekani, C. & Snoeyink, V.L., 2001. Kinetic and equilibrium study of competitive adsorption between atrazine and Congo red dye on activated carbon: The importance of pore size distribution. *Carbon*, 39(1), pp.25–37.

Ponnusami, V., Vikram, S. & Srivastava, S.N., 2008. Guava (Psidium guajava) leaf powder: Novel adsorbent for removal of methylene blue from aqueous solutions. *Journal of Hazardous Materials*, 152(1), pp.276–286.

El Qada, E.N., Allen, S.J. & Walker, G.M., 2008. Adsorption of basic dyes from aqueous solution onto activated carbons. *Chemical Engineering Journal*, 135(3), pp.174–184.

Rafatullah, M. et al., 2010. Adsorption of methylene blue on low-cost adsorbents: A review. *Journal of Hazardous Materials*, 177(1-3), pp.70–80. Available at: http://dx.doi.org/10.1016/j.jhazmat.2009.12.047.

Ramakrishna, K.R. & Viraraghavan, T., 1997. Dye removal using low cost adsorbents. *Water Science and Technology*, 36(2-3), pp.189–196. Available at: http://dx.doi.org/10.1016/S0273-1223(97)00387-9.

Rauf, M.A., Shehadi, I.A. & Hassan, W.W., 2007. Studies on the removal of Neutral Red on sand from aqueous solution and its kinetic behavior. *Dyes and Pigments*, 75(3), pp.723–726.

Robinson, T. et al., 2001. Remediation of dyes in textile effluent: A critical review on current treatment technologies with a proposed alternative. *Bioresource Technology*, 77(3), pp.247–255.

Robinson, T., Chandran, B. & Nigam, P., 2002. Removal of dyes from a synthetic textile dye effluent by biosorption on apple pomace and wheat straw. *Water Research*, 36(11), pp.2824–2830.

Rodrı̀guez, A. et al., 2009. Adsorption of anionic and cationic dyes on activated carbon from aqueous solutions: Equilibrium and kinetics. *Journal of Hazardous Materials*, 172(2-3), pp.1311–1320.

Rouf, S. & Nagapadma, M., 2015. Modeling of Fixed Bed Column Studies for Adsorption of Azo Dye on Chitosan Impregnated with a Cationic Surfactant. , 6(2), pp.538–545.

Roy, B.B., Dhir, R.P. & Kolarkar, A.S., 1978. Soils of Rajasthan Desert and their Characteristics. *Proc. Indian natn. Sci. Acad*, 44(4B), pp.161–167.

Sadaf, S. & Bhatti, H.N., 2014. Batch and fixed bed column studies for the removal of Indosol Yellow BG dye by peanut husk. *Journal of the Taiwan Institute of Chemical Engineers*, 45(2), pp.541–553.

Saha, P. et al., 2010. Insight into adsorption equilibrium, kinetics and thermodynamics of Malachite Green onto clayey soil of Indian origin. *Chemical Engineering Journal*, 165(3), pp.874–882. Available at: http://dx.doi.org/10.1016/j.cej.2010.10.048.

Salleh, M.A.M. et al., 2011. Cationic and anionic dye adsorption by agricultural solid wastes: A comprehensive review. *Desalination*, 280(1-3), pp.1–13.

Sanghi, R. & Bhattacharya, B., 2002. Review on decolorisation of aqueous dye solutions by low cost adsorbents Coloration Technology. *Coloration Technology*, 118, pp.256–269.

Sauer, T.P. et al., MODELING OF ADSORPTIVE FILTRATION OF A LEATHER DYE IN A FIXED BED COLUMN. , pp.1–10.

Senthilkumaar, S. et al., 2005. Adsorption of methylene blue onto jute fiber carbon: Kinetics and equilibrium studies. *Journal of Colloid and Interface Science*, 284(1), pp.78–82.

Shih, M. & Husk, R., 2012. Kinetics of the batch adsorption of methylene blue from aqueous solutions onto rice husk : effect of acid- modified process and dye concentration onto rice husk : effect of acid-modifi ed process and dye concentration. *Desalination and Water Treatment*, 37(1-3), pp.200–214.

Simoncic, P. & Armbruster, T., 2005. Cationic methylene blue incorporated into zeolite mordenite-Na: A single crystal X-ray study. *Microporous and Mesoporous Materials*, 81(1-3), pp.87–95.

Sing, K.S.W. et al., 1985. International union of pure and applied chemistry(IUPAC). *Pure Appl. Chem.*, 57, pp.603–619.

Singh, K. & Arora, S., 2011. Removal of Synthetic Textile Dyes From Wastewaters: A Critical Review on Present Treatment Technologies. *Critical Reviews in Environmental Science and Technology*, 41(9), pp.807–878.

Singh, K.P. et al., 2003. Color Removal from Wastewater Using Low-Cost Activated Carbon Derived from Agricultural Waste Material. *Industrial & Engineering Chemistry Research*, 42(9), pp.1965–1976. Available at: http://dx.doi.org/10.1021/ie020800d.

Somasekhara Reddy, M.C., Sivaramakrishna, L. & Varada Reddy, A., 2012. The use of an agricultural waste material, Jujuba seeds for the removal of anionic dye (Congo red) from aqueous medium. *Journal of Hazardous Materials*, 203-204(April 2016), pp.118–127.

Soni, M. et al., 2012. Adsorptive Removal of Methylene Blue Dye From an Aqueous Solution Using Water Hyacinth Root Powder As a Low Cost Adsorbent. *International Journal of Chemical Sciences and Applications*, 3(3), pp.338–345. Available at: http://bipublication.com/files/IJChSA-V3I3-2012-1.pdf.

Sreńscek-Nazzal, J. et al., 2015. Comparison of Optimized Isotherm Models and Error Functions for Carbon Dioxide Adsorption on Activated Carbon. *Journal of Chemical and Engineering Data*, 60(11), pp.3148–3158.

Srivastava, V.C. et al., 2008. Prediction of breakthrough curves for sorptive removal of phenol by bagasse fly ash packed bed. *Industrial and Engineering Chemistry Research*, 47(5), pp.1603–1613.

Sulak, M.T. & Yatmaz, H.C., 2012. Removal of textile dyes from aqueous solutions with eco-friendly biosorbent. *Desalination and Water Treatment*, 37(1-3), pp.169–177.

Tamez Uddin, M. et al., 2009. Adsorption of methylene blue from aqueous solution by jackfruit (Artocarpus heteropyllus) leaf powder: A fixed-bed column study. *Journal of Environmental Management*, 90(11), pp.3443–3450. Available at: http://dx.doi.org/10.1016/j.jenvman.2009.05.030.

Tan, B.H., Teng, T.T. & Omar, A.K.M., 2000. Removal of dyes and industrial dye wastes by magnesium chloride. *Water Research*, 34(2), pp.597–601.

Thomas, C., 1943. G = gl. , (2), pp.1943–1945.

Thompson, G. et al., 2001. The treatment of pulp and paper mill effluent: A review. *Bioresource Technology*, 77(3), pp.275–286.

Tor, A. & Cengeloglu, Y., 2006. Removal of congo red from aqueous solution by adsorption onto acid activated red mud. *Journal of Hazardous Materials*, 138(2), pp.409–415.

Tunali, S. et al., 2006. Kinetics and equilibrium studies for the adsorption of Acid Red 57 from aqueous solutions onto calcined-alunite. *Journal of hazardous materials*, 135(1-3), pp.141–8. Available at: http://www.sciencedirect.com/science/article/pii/S0304389405007405.

Vandevivere, P.C., Bianchi, R. & Verstraete, W., 1998. Treatment and reuse of wastewater from the textile wet-processing industry: Review of emerging technologies. *Journal of Chemical Technology and Biotechnology*, 72(4), pp.289–302.

Vasanth Kumar, K. & Sivanesan, S., 2007. Sorption isotherm for safranin onto rice husk: Comparison of linear and non-linear methods. *Dyes and Pigments*, 72(1), pp.130–133.

Verma, A.K., Dash, R.R. & Bhunia, P., 2012. A review on chemical

coagulation/flocculation technologies for removal of colour from textile wastewaters. *Journal of Environmental Management*, 93(1), pp.154–168. Available at: http://dx.doi.org/10.1016/j.jenvman.2011.09.012.

Vijayakumar, G. et al., 2009. Removal of Congo red from aqueous solutions by perlite. *Clean - Soil, Air, Water*, 37(4-5), pp.355–364.

Vijayaraghavan, K. et al., 2006. Biosorption of nickel(II) ions onto Sargassum wightii: Application of two-parameter and three-parameter isotherm models. *Journal of Hazardous Materials*, 133(1-3), pp.304–308.

Walker, G.M. & Weatherley, L.R., 2001. Adsorption of dyes from aqueous solution - The effect of adsorbent pore size distribution and dye aggregation. *Chemical Engineering Journal*, 83(3), pp.201–206.

Walker, G.M. & Weatherley, L.R., 2000. Textile Wastewater Treatment Using Granular Activated Carbon Adsorption in Fixed Beds . *Separation Science and Technology*, 35(9), pp.1329–1341.

Wang, S., Li, H. & Xu, L., 2006. Application of zeolite MCM-22 for basic dye removal from wastewater. *Journal of Colloid and Interface Science*, 295(1), pp.71–78.

Wang, S. & Peng, Y., 2010. Natural zeolites as effective adsorbents in water and wastewater treatment. *Chemical Engineering Journal*, 156(1), pp.11–24.

Wang, S. & Zhu, Z.H., 2006. Characterisation and environmental application of an Australian natural zeolite for basic dye removal from aqueous solution. *Journal of Hazardous Materials*, 136(3), pp.946–952.

Wang, W. et al., 2015. Enhanced Adsorptive Removal of Methylene Blue from Aqueous Solution by Alkali-Activated Palygorskite. *Water, Air, & Soil Pollution*, 226(3). Available at: http://link.springer.com/10.1007/s11270-015-2355-0.

Weber, W.J. & Morris, J.C., 1963. Kinetics of adsorption on carbon from solution. *Journal of the Sanitary Engineering Division*, 89, pp.31–60.

Xu, Z., Cai, J.-G. & Pan, B.-C., 2013. Mathematically modeling fixed-bed adsorption in aqueous systems. *Journal of Zhejiang University-SCIENCE A (Applied Physics & Engineering)*, 14(3), pp.155–176.

Yagub, M.T. et al., 2014. Dye and its removal from aqueous solution by adsorption: A review. *Advances in Colloid and Interface Science*, 209(January 2016), pp.172–184.

Zaghouane-Boudiaf, H. et al., 2014. Adsorption characteristics, isotherm, kinetics, and diffusion of modified natural bentonite for removing the 2,4,5-trichlorophenol. *Applied Clay Science*, 90, pp.81–87. Available at: http://dx.doi.org/10.1016/j.cej.2012.01.089.

Zhang, W. et al., 2011. Removal of methylene blue from aqueous solutions by straw based adsorbent in a fixed-bed column. *Chemical Engineering Journal*, 173(2), pp.429–436. Available at: http://dx.doi.org/10.1016/j.cej.2011.08.001.

Zhao, M., Tang, Z. & Liu, P., 2008. Removal of methylene blue from aqueous solution with silica nano-sheets derived from vermiculite. *Journal of Hazardous Materials*, 158(1), pp.43–51.

Zhu, M.X. et al., 2007. Removal of an anionic dye by adsorption/precipitation processes using alkaline white mud. *Journal of Hazardous Materials*, 149(3), pp.735–741.

Ziona, N., Engineering, F. & Mechanics, S., 1990. T H E R M a L a N a L Y S I S of S E P I O L I T E a N D Palygorskite Treated With Butylamine. , pp.107–119.

Appendix A

A.1 pH Measurement

The pH of a solution measures molar concentration of hydrogen ions in the solution. It is a measure of the acidity or basicity of the solution. pH of the adsorbate solution used for the batch study was adjusted to various pH (1,3,5,7,9,11) using 0.01N H_2SO_4 and 0.01N NaOH. It was determined by using the portable Haana HI-98128, with an accuracy of ±0:02 pH. Electrodes were thoroughly rinsed with distilled water before being immersed into the dye solution.

A.2 Incubator Shaker

The batch study samples were shaken at a constant speed and temperature of 150rpm and 30°C±1 for one hour. Incubator shaker (Model MSW-232) was used for this purpose. It has the ability to shake the content at constant rpm in the range 50 to 250 rpm while maintaining the temperature in the range 5°C to 60°C. This equipment helps in maintaining a constant contact between adsorbent and adsorbate molecules.

A.3 Centrifuge

At regular intervals, a measured amount of sample was taken out from the incubator shaker and centrifuged at a constant speed of 2000rpm in the centrifuge tubes. A centrifuge (Model Remi R8C-BL) works on the principle of sedimentation. The centripetal acceleration causes adsorbent particle to settle at the bottom of the tube while the adsobate rises to the top. It can work at a constant speed in the range of 0 to 6000 rpm with maximum RCF 3600g. The separated adsorbate was then pipetted out in test tube.

A.4 Spectrophotometer

UV-Vis spectrophotometer (Model UV-1800 Shimadzu UV-Vis Spectrophotometer) was used in the present study for measuring color and COD removal. It works in the ultraviolet and visible wavelength range of ~200-700nm. The spectrophotometer compares the intensity of light that passes through a reference solution and a test solution and computes the percentage of transmission of the compared to the reference standard. The measurement of the absorbance value is based on the logarithmic

function of the linear transmittance ratio. The absorbance value is proportional to the concentration of the sample being measured.

For the measurement of the amount of removal of methylene blue and direct red 81, a standard calibration graph were made at wavelength of 663nm and 548nm respectively for a given range of concentration. For further measurement of the dye samples, the standard graph was referred.

For the measurement of COD removal, a standard calibration graph was made at wavelength of 600nm for a given range of concentration. For further measurement of the COD removal from samples, the standard graph was referred.

A.5 Particle size analyzer

Particle size measurements for the non-modified soil were taken using Malvern Mastersizer-2000. The instrument operates between 0.02-2000 µm. It is a laser diffractometer used for particle sizing. Laser diffraction measures particle size distributions by measuring the angular variation in intensity of light scattered as a laser beam passes through a dispersed particulate sample. Large particles scatter light at small angles relative to the laser beam and small particles scatter light at large angles. The angular scattering intensity data is analyzed to calculate the size of the particles responsible for creating the scattering pattern. A known amount of sample of non-modified soil was mixed with about 50ml of distilled water and sonicated for 10 minutes. The sonicated sample was kept in analyser for measurement of size.

The analyzer provided size distribution in number, volume and surface area in one measurement for an overall size range of 300-150µm and 150-75µm. Its response was unaffected by color, shape, composition or refractive index of particles. The size trend function was used to plot the statistics of several sample runs on one graph or report. The result was a particle size distribution displayed as volume %in discrete size classes.

A.6 Fourier- Transform Infrared (FTIR) Spectrometer

The infrared spectra of seven soil samples; non-modified, acid-modified and alkali-modified soil; dye adsorbed and non-adsorbed respectively, were obtained by using Perkin Elmer Spectrum 2 spectrophotometer. The range was 4000cm^{-1} to 400 cm^{-1}. The soil samples were completely dried before taking the spectra. Then, a properly

grounded soil sample was mixed with KBr (AR grade, Merck, India) and put into a manual press at 10 tons. The sample turns into transparent pellet or disc. This pellet was mounted on the FTIR spectrophotometer operated by an online computer. IR radiation was passed through the sample. Performing a mathematical Fourier transform on this signal resulted in a spectrum identical to that of conventional (dispersive) infrared spectroscopy. The instrument gave the result in the form of intensity versus wavelength of the light incident on the sample, creating a molecular fingerprint of the sample.

A.7 Field Emission Scanning Electron Microscope (FE-SEM) and Energy Dispersive X-ray Spectrometry (EDX)

SEM is one of the most versatile and well known analytical techniques. Compared to the conventional optical microscope, an electron microscope offers advantages, including high magnification, large depth of focus, great resolution and ease of sample preparation and observation. Electrons generated from an electron gun enter a surface of a sample and generate many low energy secondary electrons. The intensity of these secondary electrons is governed by the surface topography of the sample. An image of the sample surface is therefore constructed by measuring secondary electron intensity as a function of the position of the scanning primary electron beam. EDX analysis is widely used for chemical analysis. The characteristic X-rays emitted from the sample serve as fingerprints and give elemental information of the samples. To know the external morphology of sludge and electrodes, SEM was used. SEM was performed using Nova Nano FE-SEM 450. It gives a resolution of 1:4 kV (TLD-SE) and 1 nm at 15 kV (TLD-SE). The samples were coated with Platinum to ensure conductivity. The SEM uses a focused beam of high-energy electrons to generate a variety of signals at the surface of solid specimens. The signals that derive from electron-sample interactions reveal information about the sample including external morphology (texture), chemical composition, crystalline structure and orientation of materials making up the sample. The FE-SEM is coupled to an EDX detector for measuring the elemental chemical composition. EDX analysis usually involves the generation of an X-ray spectrum from the entire scan area of the SEM. The Y-axis shows the counts (number of X-rays received and processed by the detector) and the X-axis shows the energy level of those counts.

A.8 X-ray Diffraction (XRD)

XRD analysis is based on constructive interference of monochromatic X-rays and a crystalline sample. The X-rays are generated by a cathode ray tube, filtered to produce monochromatic radiation, collimated to concentrate, and directed towards the sample. The interaction of the incident rays with the sample produces constructive interference (and a diffracted ray) when conditions satisfy Bragg's Law (nl = 2dsinq). This law relates the wavelength of electromagnetic radiation to the diffraction angle and the lattice spacing in a crystalline sample. These diffracted X-rays are then detected, processed and counted. By scanning the sample through a range of 2q angles, all possible diffraction directions of the lattice should be attained due to the random orientation of the powdered material. Conversion of the diffraction peaks to d-spacings allows identification of the mineral because each mineral has a set of unique d-spacings. Typically, this is achieved by comparison of d-spacings with standard reference patterns. The XRD measurements were carried out by PANanalytical Xpert powder.

A.9 Zeta Potential

Zeta (ζ) potential is used for quantification of the magnitude of the charge on the adsorbent surface. The magnitude of the zeta potential indicates the degree of electrostatic repulsion between adjacent, similarly charged particles. In the present study, Malvern Zetasizer Nano ZSP (ZEN5600) was used to measure the zeta potential on the surface of the non-modified, acid modified and alkali modified soil. This model uses micro-electrophoresis/electrophoretic light scattering technology to measure zeta potential. An electric field is applied to a solution of dispersion of adsorbent, which then move with velocity related to their zeta potential. This velocity is measured using laser interferometric technique which enables the calculation of electrophoretic mobility and from which zeta potential is calculated.

A.10 BET Surface Area

Surface area and pore size distribution are important parameters of porous materials. Physiadsorption techniques are used to determine the surface area and pore structure. For the present study, this test was conducted at ACMS, IIT-Kanpur for non-modified, acid modified and alkali modified soil. BET surface analyser (Model Autosorb I, Quantachrome) was used to perform the test. It is equipped to provide the data on the

pore volume. The average pore diameter is determined from the surface area and total pore volume. It uses nitrogen gas as the standard adsorptive gas to perform single-point and multi-point Langmuir surface area and BET surface area analysis.

A.11 X-Ray Fluoresence Spectroscopy

XRF spectroscopy (PANAlytical, PW 2404) is used to accurately measure both the major constituents of a material and its trace elements. This technology involves X-ray to dislodge an atom from the sample. Since the leaving atom creates a space, another atom comes and fills that space. The difference in energy is accompanied by emission of radiation - this is known as fluorescence. XRF spectroscopy involves measuring the energy of radiation, and since the energy of fluorescent radiation is element-specific, the amount of a certain element in the sample can be determined. This test for the present study was conducted at SAIF-IIT Bombay for non-modified, acid modified and alkali modified soil.

A.12 Chemical Oxygen Demand Analysis

COD was calculated by the closed reflux method. It works on the principle that boiling chromic and sulphuric acids oxidize almost all organic matter. The sample is refluxed in a solution having known excess of potassium dichromate. After digestion (for 2 hrs. approx.) the chromium ion changes from hexavalent state to trivalent state, which absorbs radiation at 600nm. The amount was calculated by formation of a standard calibration curve. This was done for the entire sample. (Standard methods for the examination of water and waste water, 5220 D. Closed Reflux, Colorimetric Method)

Appendix B

Operating Parameters		DR 81				MB			
Adsorbent Dose (g)	**C_0 (g/L)**	q_e^{exp}	q_e^{pred}	k_1	R^2	q_e^{exp}	q_e^{pred}	k_1	R^2
100g/100mL	**1**	0.550	0.370	0.045	0.657	0.900	0.293	0.013	0.159
	0.5	0.311	0.206	0.064	0.452	0.468	0.224	0.065	0.575
	0.25	0.176	0.161	0.058	0.473	0.239	0.173	0.061	0.729
	0.125	0.115	0.144	0.053	0.489	0.121	0.102	0.046	0.399
75g/100mL	**1**	0.640	0.310	0.029	0.185	1.107	0.415	0.026	0.452
	0.5	0.388	0.290	0.047	0.521	0.573	0.296	0.020	0.491
	0.25	0.217	0.217	0.042	0.460	0.298	0.242	0.014	0.425
	0.125	0.149	0.176	0.039	0.449	0.155	0.195	0.012	0.479
50g/100mL	**1**	0.720	0.327	0.022	0.140	1.580	0.409	0.018	0.151
	0.5	0.455	0.328	0.040	0.529	0.836	0.350	0.027	0.495
	0.25	0.297	0.272	0.037	0.509	0.431	0.288	0.019	0.515
	0.125	0.189	0.215	0.040	0.429	0.225	0.244	0.010	0.422
25g/100mL	**1**	1.080	0.414	0.049	0.345	2.920	0.552	0.027	0.229
	0.5	0.666	0.365	0.066	0.655	1.584	0.423	0.041	0.500
	0.25	0.464	0.339	0.047	0.626	0.840	0.407	0.094	0.746
	0.125	0.289	0.231	0.048	0.513	0.426	0.265	0.014	0.353
12.5g/100mL	**1**	1.280	0.649	0.043	0.366	4.400	0.520	0.015	0.048
	0.5	0.862	0.407	0.054	0.359	2.449	0.586	0.050	0.638
	0.25	0.534	0.294	0.041	0.362	1.344	0.447	0.040	0.522
	0.125	0.494	0.379	0.061	0.746	0.716	0.365	0.029	0.553

Table B.1: Lagergren's Pseudo First Order Kinetic Parameters for Adsorption of DR81 and MB on non-modified soil

Operating Parameters		DR 81				MB			
Adsorbent Dose (g)	**C_0 (g/L)**	q_e^{exp}	q_e^{pred}	k_2	R^2	q_e^{exp}	q_e^{pred}	k_2	R^2
100g/100mL	**1**	0.550	0.581	6.797	0.999	0.900	0.886	0.140	0.9997
	0.5	0.311	0.323	30.745	0.999	0.468	0.476	3.802	0.9999
	0.25	0.176	0.182	164.189	0.999	0.239	0.243	31.045	0.9999
	0.125	0.115	0.119	634.718	0.999	0.121	0.123	141.547	0.9999
75g/100mL	**1**	0.640	0.635	4.420	0.997	1.107	1.139	0.347	0.9994
	0.5	0.388	0.408	23.631	0.999	0.573	0.581	2.148	0.9999
	0.25	0.217	0.227	119.640	0.999	0.298	0.302	11.761	0.9999
	0.125	0.149	0.154	328.178	0.999	0.155	0.158	85.326	0.9999
50g/100mL	**1**	0.720	0.727	2.621	0.998	1.580	1.567	0.087	0.9993
	0.5	0.455	0.478	13.943	0.999	0.836	0.852	0.816	0.9998
	0.25	0.297	0.311	51.275	0.998	0.431	0.441	5.776	0.9999
	0.125	0.189	0.197	228.719	0.998	0.225	0.226	26.418	0.9999
25g/100mL	**1**	1.080	1.096	1.081	0.998	2.920	2.972	0.023	0.9991
	0.5	0.666	0.700	3.957	0.999	1.584	1.622	0.153	0.9998
	0.25	0.464	0.488	14.157	0.998	0.840	0.860	1.135	0.9998
	0.125	0.289	0.300	50.731	0.999	0.426	0.427	3.528	0.9998
12.5g/100mL	**1**	1.280	1.429	0.722	0.996	4.400	4.270	0.003	0.9986
	0.5	0.862	0.930	2.610	0.998	2.449	2.540	0.056	0.9997
	0.25	0.534	0.555	6.714	0.999	1.344	1.386	0.298	0.9995
	0.125	0.494	0.529	14.177	0.998	0.716	0.737	1.956	0.9998

Table B.2: Lagergren's Pseudo Second Order Kinetic Parameters for Adsorption of DR81 and MB on non-modified soil

Operating	Parameters	DR81						MB					
Adsorbent Dose (g)	C_0 **(g/L)**	k_{i_1}	C_1	R_1^2	k_{i_2}	C_2	R_2^2	k_{i_1}	C_1	R_1^2	k_{i_2}	C_2	R_2^2
100g	**1**	0.140	0.114	0.987	0.004	0.536	0.325	0.091	0.614	0.998	-0.003	0.908	0.350
	0.5	0.079	0.063	0.995	0.001	0.310	0.426	0.050	0.311	1.000	0.001	0.468	0.143
	0.25	0.051	0.020	0.915	0.0003	0.176	0.307	0.026	0.157	0.994	0.001	0.238	0.373
	0.125	0.033	0.013	0.965	0.0002	0.115	0.234	0.010	0.089	1.000	0.000	0.121	0.145
75g	**1**	0.205	0.000	0.990	-0.003	0.639	0.098	0.149	0.635	1.000	0.003	1.107	0.107
	0.5	0.123	-0.004	0.998	0.001	0.388	0.392	0.062	0.378	1.000	0.001	0.571	0.125
	0.25	0.067	0.006	0.998	0.0004	0.218	0.170	0.032	0.198	0.987	0.000	0.299	0.060
	0.125	0.047	0.005	0.971	0.0001	0.149	0.081	0.015	0.109	1.000	0.000	0.155	0.427
50g	**1**	0.210	0.073	0.965	-0.003	0.730	0.059	0.252	0.771	0.983	-0.009	1.616	0.364
	0.5	0.151	-0.015	0.989	0.001	0.452	0.454	0.119	0.461	0.998	0.001	0.834	0.211
	0.25	0.104	-0.022	0.961	0.001	0.295	0.245	0.058	0.252	0.951	0.001	0.427	0.534
	0.125	0.068	-0.025	1.000	0.0001	0.190	0.003	0.021	0.158	0.971	0.000	0.225	0.017
25g	**1**	0.308	0.114	0.997	0.004	1.032	0.037	0.503	1.301	0.983	-0.006	2.972	0.052
	0.5	0.198	0.049	0.987	0.003	0.656	0.707	0.274	0.722	1.000	0.002	1.582	0.242
	0.25	0.160	-0.029	0.970	0.002	0.456	0.467	0.131	0.418	0.987	0.002	0.832	0.700
	0.125	0.097	-0.008	0.957	0.0003	0.289	0.237	0.045	0.285	0.989	0.000	0.427	0.027
12.5g	**1**	0.392	0.028	0.993	0.019	1.239	0.281	0.783	1.923	1.000	-0.036	4.498	0.394
	0.5	0.288	-0.065	0.983	0.004	0.859	0.234	0.502	0.862	1.000	0.008	2.432	0.697
	0.25	0.137	0.096	0.994	0.001	0.537	0.049	0.245	0.551	0.974	0.003	1.342	0.264
	0.125	0.182	-0.075	0.992	0.004	0.480	0.798	0.132	0.303	0.993	0.002	0.709	0.376

Table B.3: Intraparticle Diffusion Parameters for Adsorption of DR81 and MB

S.No.	Frequency (cm^{-})	Intensity of band	Chemical group	Remarks
1	3434.65	Strong	SiO-H, H-O-H	Symmetric stretching
2	2923.65	Medium	CH_2	Asymmetric stretching
3	2854.00	Medium	CH_2	Symmetric stretching
4	1876.52	Weak	C-OH	Symmetric stretching
5	1629.20	Medium	H-O-H	Bending vibrations
6	1032.73	Strong	Si-O-Si	Asymmetric stretching
7	778.08	Medium	Si-O	Symmetric stretching
8	691.44	Medium	Si-O	Asymmetric bending
9	606.38	Medium	Si-O	Symmetric stretching
10	533.77	Medium	Si-O	Asymmetric bending
11	461.03	Strong	Si-O-Si	Bending vibrations

Table B.4: FTIR spectra for non-modified soil

S.No.	Frequency (cm^{-1})	Intensity of band	Chemical group	Remarks
1	3433.75	Strong	SiO-H, H-O-H	Symmetric stretching
2	2921.52	Weak	CH_2	Asymmetric stretching
3	2854.00	Weak	CH_2	Symmetric stretching
4	1629.33	Medium	H-O-H	Bending vibrations
5	1034.65	Strong	Si-O-Si	Asymmetric stretching
6	775.95	Medium	Si-O	Symmetric stretching
7	691.76	Medium	Si-O	Asymmetric bending
8	524.79	Weak	Si-O	Asymmetric bending
9	464.83	Strong	Si-O-Si	Bending vibrations

Table B.5: FTIR spectra for DR81 adsorbed non-modified soil

S.No.	Frequency (cm^{-1})	Intensity of band	Chemical group	Remarks
1	3430.20	Strong	SiO-H, H-O-H	Symmetric stretching
2	2924.60	Weak	CH_2	Asymmetric stretching
3	2853.12	Weak	CH_2	Symmetric stretching
4	1879.18	Weak	C-OH	Symmetric stretching
5	1626.27	Medium	H-O-H	Bending vibrations
6	1032.40	Strong	Si-O-Si	Asymmetric stretching
7	777.72	Medium	Si-O	Symmetric stretching
8	692.34	Medium	Si-O	Asymmetric bending
9	530.23	Medium	Si-O	Asymmetric bending
10	467.60	Strong	Si-O-Si	Bending vibrations

Table B.6: FTIR spectra for MB adsorbed non-modified soil

Appendix C

Operating Parameters		Pseudo first order model				Pseudo second order model			
Adsorbent Dose (g)	**C_0 (g/L)**	q_e^{exp}	q_e^{pred}	k_1	R^2	q_e^{exp}	q_e^{pred}	k_2	R^2
100g/100mL	**1**	0.670	0.338	0.027	0.154	0.670	0.679	7.196	0.995
	0.5	0.320	0.328	0.039	0.312	0.320	0.332	85.649	0.986
	0.25	0.200	0.314	0.198	0.781	0.200	0.233	397.686	0.989
	0.125	0.095	0.265	0.028	0.517	0.095	0.115	2355.075	0.990
75g/100mL	**1**	0.790	2.832	0.405	0.228	0.790	0.806	2.886	0.998
	0.5	0.420	0.385	0.317	0.261	0.420	0.426	24.065	0.994
	0.25	0.250	0.274	0.216	0.109	0.250	0.251	217.486	0.985
	0.125	0.120	0.235	0.248	0.210	0.120	0.126	948.328	0.991
50g/100mL	**1**	1.060	0.409	0.322	0.156	1.060	1.067	1.126	0.998
	0.5	0.560	0.401	0.267	0.243	0.560	0.559	10.305	0.996
	0.25	0.300	0.398	0.421	0.368	0.300	0.320	100.147	0.991
	0.125	0.170	0.231	0.090	0.035	0.170	0.150	299.904	0.988
25g/100mL	**1**	1.840	0.447	0.331	0.125	1.840	1.908	0.352	0.994
	0.5	0.990	0.468	0.327	0.208	0.990	1.005	1.896	0.997
	0.25	0.560	0.415	0.308	0.208	0.560	0.581	17.743	0.992
	0.125	0.300	0.358	0.283	0.172	0.300	0.126	948.328	0.991
12.5g/100mL	**1**	2.400	1.300	0.532	0.400	2.400	2.746	0.191	0.990
	0.5	1.120	0.508	0.366	0.275	1.120	1.135	0.655	0.997
	0.25	0.660	0.485	0.384	0.311	0.660	0.688	8.349	0.994
	0.125	0.440	0.328	0.227	0.135	0.440	0.440	26.989	0.993

Table C.1: Lagergren's Pseudo first order and Pseudo second order model for DR81 removal on acid modified soil

Adsorbent Dose (g)	C_0 (g/L)	k_{i_1}	C_1	R_1^2	k_{i_2}	C_2	R_2^2
100g/100mL	**1**	0.252	-0.159	0.906	-0.004	0.677	0.400
	0.5	0.140	-0.139	0.922	-0.002	0.325	0.077
	0.25	0.098	-0.116	0.973	0.003	0.192	0.743
	0.125	0.038	-0.029	0.975	0.002	0.093	0.346
75g/100mL	**1**	0.259	-0.043	0.980	-0.003	0.801	0.426
	0.5	0.161	-0.100	0.969	-0.003	0.430	0.175
	0.25	0.119	-0.138	0.946	-0.004	0.257	0.330
	0.125	0.049	-0.037	0.993	-0.001	0.129	0.112
50g/100mL	**1**	0.329	0.009	0.992	-0.002	1.050	0.028
	0.5	0.217	-0.134	0.991	-0.004	0.563	0.282
	0.25	0.126	-0.111	0.937	-0.001	0.302	0.008
	0.125	0.070	-0.055	0.986	-0.004	0.177	0.400
25g/100mL	**1**	0.825	-0.747	0.996	-0.009	1.872	0.518
	0.5	0.350	-0.132	0.986	-0.003	0.981	0.060
	0.25	0.259	-0.276	0.971	-0.003	0.555	0.104
	0.125	0.147	-0.179	0.941	-0.004	0.312	0.217
12.5g/100mL	**1**	1.133	-1.163	0.998	0.042	2.239	0.401
	0.5	0.392	-0.079	0.943	-0.006	1.154	0.199
	0.25	0.287	-0.258	0.990	-0.001	0.658	0.025
	0.125	0.196	-0.183	0.998	-0.005	0.450	0.580

Table C.2: Intraparticle diffusion model for DR 81 removal on acid modified soil

Isotherm	Parameter	Adsorbent Dose				
		100g/100mL	**75g/100mL**	**50g/100mL**	**25g/100mL**	**12.5g/100mL**
LangmuirI	q_m	1.380	0.790	0.521	0.274	0.367
	K_l	-201.588	-238.28	-243.148	-162.76	-137.43
	R^2	0.586	0.867	0.814	0.913	0.479
LangmuirII	q_m	-500.000	-526.32	-277.778	-434.78	-370.37
	K_l	-1.750	-2.000	-1.306	-2.870	-2.556
	R^2	0.943	0.972	0.978	0.996	0.931
LangmuirIII	q_m	0.004	0.004	0.004	0.006	0.005
	K_l	-384.615	-357.14	-555.556	-625.00	-1000.0
	R^2	0.410	0.689	0.683	0.860	0.365
LangmuirIV	q_m	-0.005	-0.004	-0.004	-0.006	-0.007
	K_l	-154.920	-249.25	-369.320	-536.05	-368.67
	R^2	0.410	0.689	0.683	0.860	0.365
Freundlich	n	0.764	0.739	0.749	0.755	-0.356
	K_f	15.957	15.359	14.313	10.904	0.013
	R^2	0.936	0.970	0.995	0.999	0.777

Table C.3: Isotherm parameters obtained using linear regression method for DR81 removal onto acid modified soil

S.No.	Frequency (cm^{-1}) Acid Activated	Intensity of the Band Acid Activated	Frequency(cm^{-1}) DR 81 Adsorbed	Intensity of the Band DR 81 Adsorbed	Chemical group	Remarks
1	3433.72	Strong	3435.21	Medium	SiO-H, H-O-H	Symmetric stretching
2	2919.6	Weak	-	-	CH_2	Asymmetric stretching
3	2849.9	Weak	-	-	CH_2	Symmetric stretching
4	1876.11	Weak	-	-	C-OH	Symmetric stretching
5	1627.11	Medium	1620.00	Weak	H-O-H	Bending vibrations
6	1383.61	Medium	-	-	CH_2	Bending vibrations
7	1032.61	Strong	1033.76	Strong	Si-O-Si	Stretching primary alcohol
8	777.31	Medium	778.81	Medium	Si-O	Symmetric stretching
9	691.25	Medium	692.86	Medium	Si-O	Asymmetric bending
10	530.69	Medium	521.41	Medium	Si-O	Asymmetric bending
11	469.11	Medium	465.11	Medium	Si-O-Si	Bending vibrations

Table C.4: FTIR of acid modified and DR 81 adsorbed acid modified soil

Appendix D

Operating Parameters		Pseudo first order model				Pseudo second order model			
Adsorbent Dose (g)	**C_0 (g/L)**	q_e^{exp}	q_e^{pred}	k_1	R^2	q_e^{exp}	q_e^{pred}	k_1	R^2
100g/100mL	**1**	0.890	0.345	0.062	0.541	0.890	0.918	0.873	0.999
	0.5	0.468	0.270	0.085	0.645	0.468	0.485	1.497	0.999
	0.25	0.238	0.226	0.102	0.689	0.238	0.247	3.127	0.999
	0.125	0.124	0.115	0.077	0.455	0.124	0.128	6.873	0.999
75g/100mL	**1**	1.146	0.478	0.615	0.404	1.146	1.185	0.595	0.998
	0.5	0.618	0.457	0.691	0.583	0.618	0.642	0.997	0.998
	0.25	0.315	0.416	0.849	0.774	0.315	0.328	1.964	0.999
	0.125	0.164	0.243	0.716	0.584	0.164	0.171	3.644	0.998
50g/100mL	**1**	1.691	0.619	0.655	0.368	1.691	1.770	0.273	0.998
	0.5	0.900	0.438	0.705	0.439	0.900	0.941	0.536	0.998
	0.25	0.459	0.397	0.744	0.568	0.459	0.480	1.121	0.997
	0.125	0.236	0.360	0.835	0.728	0.236	0.247	2.237	0.997
25g/100mL	**1**	3.304	1.634	1.095	0.692	3.304	3.559	0.092	0.994
	0.5	1.695	1.058	1.009	0.755	1.695	1.804	0.211	0.996
	0.25	0.890	0.562	0.584	0.567	0.890	0.940	0.445	0.996
	0.125	0.455	0.418	0.735	0.565	0.455	0.480	0.891	0.997
12.5g/100mL	**1**	6.397	2.241	1.035	0.700	6.397	7.027	0.035	0.990
	0.5	3.312	1.503	1.028	0.745	3.312	3.573	0.084	0.993
	0.25	1.739	1.023	1.008	0.748	1.739	1.872	0.165	0.994
	0.125	0.886	0.646	0.867	0.600	0.886	0.950	0.356	0.995

Table D.1: Lagergren's Pseudo first order and Pseudo second order model for MB removal on alkali modified soil

Adsorbent Dose (g)	C_0 (g/L)	k_{i_1}	C_1	R_1^2	k_{i_2}	C_2	R_2^2
100g/100mL	**1**	0.264	0.063	0.995	0.001	0.887	0.311
	0.5	0.141	0.022	1.000	0.001	0.467	0.512
	0.25	0.068	0.023	1.000	0.0004	0.237	0.418
	0.125	0.035	0.014	0.998	0.00004	0.124	0.135
75g/100mL	**1**	0.001	0.887	0.311	-0.0002	1.150	0.006
	0.5	0.001	0.467	0.512	0.001	0.617	0.206
	0.25	0.0004	0.237	0.418	0.001	0.314	0.731
	0.125	0.00004	0.124	0.135	0.0001	0.164	0.153
50g/100mL	**1**	0.652	-0.380	0.999	-0.0004	1.694	0.021
	0.5	0.343	-0.185	1.000	-0.0001	0.902	0.038
	0.25	0.169	-0.075	1.000	0.0001	0.460	0.073
	0.125	0.085	-0.031	1.000	0.0003	0.236	0.646
25g/100mL	**1**	1.446	-1.331	0.989	0.006	3.292	0.480
	0.5	0.697	-0.538	0.990	0.002	1.689	0.792
	0.25	0.357	-0.251	0.994	0.0002	0.891	0.018
	0.125	0.178	-0.114	0.990	0.0002	0.454	0.042
12.5g/100mL	**1**	3.053	-3.477	0.971	0.010	6.361	0.602
	0.5	1.488	-1.477	0.983	0.004	3.298	0.725
	0.25	0.765	-0.733	0.974	0.001	1.736	0.391
	0.125	0.378	-0.333	0.980	0.001	0.885	0.340

Table D.2: Intraparticle diffusion model for MB removal on alkali modified soil

Isotherm	Parameter	Adsorbent Dose				
		100g/100mL	**75g/100mL**	**50g/100mL**	**25g/100mL**	**12.5g/100mL**
LangmuirI	q_m	1.052	0.768	0.405	0.184	0.086
	K_l	-0.047	-0.046	-0.032	-0.040	-0.063
	R^2	0.890	0.940	0.967	0.889	0.927
LangmuirII	q_m	-2.297	-6.281	-42.553	-90.090	-135.13
	K_l	-2.033	-1.408	-0.601	-0.249	-0.109
	R^2	0.857	0.897	0.981	0.994	0.997
LangmuirIII	q_m	0.125	0.074	0.033	0.040	0.063
	K_l	-6.250	-14.815	-69.930	-142.86	-188.67
	R^2	0.420	0.523	0.836	0.813	0.876
LangmuirIV	q_m	-1.623	-0.798	-0.036	-0.003	-0.065
	K_l	-0.339	-0.936	-58.593	-1704.7	-166.57
	R^2	0.403	0.465	0.836	0.728	0.876
Freundlich	n	0.406	0.457	0.640	0.715	0.740
	K_f	9.908	7.809	6.123	4.619	3.372
	R^2	0.937	0.977	0.997	0.998	0.999

Table D.3: Isotherm parameters obtained using linear regression method for MB removal onto alkali modified soil

S.No.	Frequency (cm^{-}) Alkali Activated	Intensity of the Band Alkali Activated	Frequency(cm^{-1}) Alkali Activated	Intensity of the Band MB Adsorbed	Chemical group	Remarks
1	3440.75	Strong	3438.50	Medium	SiO-H, H-O-H	Symmetric stretching
2	2916.44	Weak	2924.73	Weak	CH_2	Asymmetric stretching
3	2848.09	Weak	2851.16	Weak	CH_2	Symmetric stretching
4	1879.63	Weak	1878.01	Medium	C-OH	Symmetric stretching
5	1618.86	Weak	1617.78	Medium	H-O-H	Bending vibrations
6	1076.55	Strong	-	-	Si-O	Asymmetric stretching
7	1036.08	Strong	1035.35	Strong	Si-O-Si	Stretching primary alcohol
8	778.77	Strong	777.65	Strong	Si-O	Symmetric stretching
9	692.39	Medium	692.13	Medium	Si-O	Asymmetric bending
10	459.32	Strong	465.11	Strong	Si-O-Si	Bending vibrations

Table D.4: FTIR of alkali modified and MB adsorbed alkali modified soil

Biographical Profile of Researcher

Priya is a research scholar at Department of Civil Engineering, Malaviya National Institute of Technology (MNIT), Jaipur. She has received B.Tech degree in Biotechnology from Maharishi Arvind Institute of Engineering & Technology, Jaipur. She completed M.Tech degree from MNIT, Jaipur in Environmental Engineering. After that she joined PhD in 2013 under supervision of Dr. Urmila Brighu, Department of Civil Engineering, MNIT, Jaipur. Her research interests are mainly in the areas of water and wastewater treatment. During her research work she has published four research papers in journals and has attended one International Conference. She also has papers published in two International Conferences from her M.Tech research work.

List of Publications

International Journal

- Priya Mundada, Dr.Urmila Brighu, Dr. A.B. Gupta, (2016), "Removal of methylene blue on soil: an alternative to clay", *Desalination and Water Treatment, Taylor & Francis* (doi: 10.1080/19443994.2016.1197856).

National Journal

- Priya Mundada, Dr. Urmila Brighu, "Remediation of textile effluent using siliceous materials: A review with a proposed alternative", *International Journal of Innovative and Emerging Research in Engineering*, Vol 3, Number 1, 2016, ISSN No. 2394-3343.
- Aakansha Soni, Priya Mundada, Dr.Urmila Brighu,"A comparative study on treatment of simulated and actual dye wastewater by coagulation process", *Journal of Indian Water Works Association*, Vol 47, Number 4, Oct-Dec 2015, ISSN No. 0970-275X.
- Priya, Dr. Urmila Brighu, "Study of feasibility of soil as an adsorbent for textile industry effluent treatment", *Journal of Civil Engineering and Environmental Technology*, Vol 1, Number 4, 2014, ISSN No. 2349-8404.

Conferences

- Priya, Dr. U. Brighu,"Sorption study of anionic dye from aqueous solution onto locally available soil", 47thAnnual Convection, Indian Water Works Association, Kolkata Centre held on 30th, 31st January and 1st February, 2015. The paper got published in the proceedings of the conference.

Desalination and Water Treatment
www.deswater.com

xx (2016) 1–8
September

1944-3994 / 1944-3986 © 2016 Desalination Publications. All rights reserved.
doi: 10.5004/dwt.2016.0215

Removal of methylene blue on soil: an alternative to clay

Priya Mundada*[,a], Dr. UrmilaBrighu[b], Dr. A.B. Gupta[c]

[a]*Research Scholar, Malaviya National Institute of Technology, Jaipur, India, Tel. +91-9001147871; email: priya19788@gmail.com*
[b]*Associate Professor, Malaviya National Institute of Technology, Jaipur, India, Tel/Fax: +1412713487; email: ubrighu@gmail.com*
[c]*Professor, Malaviya National Institute of Technology, Jaipur, India, Tel/Fax: +1412713259; email: akhilendra_gupta@yahoo.com*

Received 21 February 2016; Accepted 29 May 2016

ABSTRACT

The present study exploits the adsorption capacity of locally available soil from Rajasthan, India. Removal of methylene blue (MB), a cationic dye, from aqueous solution by the batch adsorption technique under different conditions of initial dye concentration, adsorbent concentration, contact time and solution pH was studied. In order to analyse the chemical composition of soil, zeta potentials, FTIR and XRF were conducted. The results showed that the adsorption reached to equilibrium within 10 min of contact time. It was found that the amount of methylene blue adsorbed per unit mass of adsorbent dose decreases with increasing adsorbent dosage but increases with the increase in initial dye concentration. Adsorption capacity increases with increasing pH in a range of 9 to 11. The equilibrium data for methylene blue adsorption well fitted to Freundlich equation. The results indicate that locally available soil from Rajasthan, India, could be employed as a low cost alternative in textile wastewater treatment for removal of methylene blue dye.

Keywords: Dyes; Soil; Clay; Textile effluent; Low cost adsorbent

1. Introduction

Water contamination from dyeing and finishing in the textile industry is a major concern. The colour produced by the synthetic dyes not only harms the aesthetic nature of the environment but these dyes are also toxic to aquatic life also [1, 2]. Therefore, removal of these dyes from wastewater is indispensible. In recent years, stricter directives coupled with increased enforcement concerning wastewater discharges have been established in many countries. To meet the effluent discharge limits set by the legislation, various biological and chemical methods have been employed. However, non-biodegradable nature of most of the dyes makes them difficult to treat [3].

Adsorption is known to be a promising technique to produce good quality effluents. The ease of operation and comparable low cost of application in decolouration process [4] makes this process more suitable for small-scale industries which cannot afford to treat their wastes due to their limited resources [5].

Although activated carbons have been most widely used for the adsorption of dyes, clay minerals have been increasingly gaining attention because they are cheaper than activated carbons and they usually have chemical and mechanical stability, high surface area and structural properties [4, 6]. Presence of net negative charge and exchangeable cation on their surface make them more efficient for colour removal. A number of studies have been reported on clay and various clay minerals for MB adsorption from its aqueous solution such as montmorillonite clay [2], kaolinite [7], bentonite [8], etc.. However, its low particle size creates separation/filtration problems after adsorption [9].

* Corresponding author.

Journal of Civil Engineering and Environmental Technology
Print ISSN: 2349-8404; Online ISSN: 2349-879X; Volume 1, Number 4; August, 2014 pp. 62 – 66
© Krishi Sanskriti Publications
http://www.krishisanskriti.org/jceet.html

Study of Feasibility of Soil as an Adsorbent for Textile Industry Effluent Treatment

Priya, Urmila Brighu
Research Scholar
Malaviya National Institute of Technology
JLN Marg, Jaipur

Abstract **:The control of water pollution has become of increasing importance in recent years. Though the release of dyes into the environment constitutes only a small proportion of water pollution but dyes are visible in small quantities due to their brilliance. Besides aesthetics, tightening government legislation is also forcing textile industries to treat their waste effluents to an increasingly high standard.**

Adsorption as a treatment technique has shown to be highly efficient for the removal of dyes and other organic content from the textile effluent. Normally reported studies are with the use of activated carbon and other low cost adsorbent which are not available abundantly locally making the cost of the treatment prohibitive, especially for MSMEs (Micro small and medium enterprises). Thus, the present scenario requires developing an adsorbent which is economically and commercially feasible.
In the present study, the feasibility of using soil of Indian origin as a low cost adsorbent for treating real textile effluent was studied. Two stage process i.e. coagulation followed by adsorption on modified soil was studied.
Coagulation followed by adsorption on modified soil as a combined unit process has shown encouraging results to treat textile wastewater through this process.
Keywords: Soil, Textile effluent, low cost adsorbents, coagulation.

1. INTRODUCTION

Wastewater generated by the industries which uses dyes and pigments is high in both colour and organic content. It is reported that about 1,00,000 different commercial dyes and pigments exist, and over 7×10^5 tons are produced annually worldwide. It was estimated that about 10-15% of these are released in effluents during dyeing processes [1]. The unexhausted dyes in the effluents are the issue for discharge in the environment because of their high brilliance and oxygen demand that are aesthetically and environmentally unacceptable [2]. They reduce light penetration and photosynthesis thus upsetting biological processes within a stream. In addition, most of dyes are either toxic or mutagenic and carcinogenic [3], [4]. Removal of dyes from effluents is important to regions where water resources might be scarce or sensitive [5]. Wastewater containing dyes is very difficult to treat, since the dyes are recalcitrant organic molecules, resistant to aerobic digestion, and are stable to light, heat and oxidizing agents [6].

Several physical, chemical and biological methods have been reported for colour removal but very few have been accepted by the textile industry. The advantages and disadvantages of some methods of dye removal from industrial effluents are given in Table 1. Amongst the numerous technologies of dye removal, adsorption is the procedure of choice and removes different types of colouring materials to give a high-quality treated effluent [7].

Activated carbon (powdered or granular) is the most widely used adsorbent because it has excellent adsorption efficiency for organic compounds, but its use is usually limited due to its high cost. Also, regeneration using solutions produces a small additional effluent, whereas regeneration by refractory technique results in a 10-15% loss of adsorbent and its uptake capacity [8].

Various low cost adsorbents have been investigated as alternatives to activated carbon such as fly ash [9], saw dust [10], bagasse fly ash [11], rice husk [12], agricultural waste [13], diatomaceous earth [14], clay [15], etc.

In the present study, soil of Indian origin has been used as a low cost adsorbent to treat real textile effluent on a fixed bed column for continuous adsorption. Only a few papers have reported the dye adsorption using continuous flow conditions, which is more useful in large-scale textile wastewater treatment.

The objective of the present study is to evaluate the efficiency of soil of Indian origin to treat the textile effluent. In addition, parameters like chemical oxygen demand and pH are also reported.

A Comparative Study on Treatment of Simulated and Actual Dye Wastewater by Coagulation Process

Aakanksha Soni[a] • Priya Mundada[b] • Dr. Urmila Brighu[c]*

Abstract

Textile industries are known to discharge effluents containing highly toxic compounds and have high COD. Chemical treatment of dye wastewater with a coagulating/flocculating agent is one of the robust ways to remove colour and COD. In this study, the coagulant dose was optimized for simulated as well as actual wastewater. For this, jar test was carried out using four different coagulants: Aluminium Sulphate, Ferric Chloride, Magnesium Chloride and Poly Aluminium Chloride. PAC was observed to give good colour and COD removal as compared to other three coagulants, in both the types of wastewater mentioned.

Keywords: *Textile wastewater, Dyes, Colour removal, Coagulants*

1. INTRODUCTION

The operations used in textile industry includes bleaching, mercerizing, dyeing and printing in which chemicals like sodium hypochlorite, H_2O_2, organics, NaOH, acids, surfactants, sodium hydroxide, dyestuffs urea, reducing agents, oxidizing agents, detergents and wetting agents are used which results in high BOD, COD, pH, TDS, toxicity, strong colour etc. (Mathur et al., 2012, Verma et al., 2012). Textile waste can contaminate water with grease, oils and waxes. They may also contain heavy metals such as copper, zinc, chromium and mercury (EPA 1974).

There are many methods used for treating textile waste including physical, chemical and biological methods. Chemical methods like coagulation/ flocculation, fentons reagent, ozonation, chlorination, photochemical, photocatalysis, electrochemical destruction etc are used. Physical methods include sedimentation, filtration, adsorption etc. Various bacteria, viruses etc are used to biologically treat the waste.

Coagulation is one of the robust ways to treat the textile waste. Colour removal by coagulation involves two principal coagulants i.e. Al(III) and Fe(III) coagulants which are readily hydrolysable cations available as sulphate or chloride salts in both liquid and solid form but large quantity of sludge is a major drawback (Gupta et al., 2009, Gao Bao et al., 2007). There are four mechanism involved in coagulation theory. They are- ionic layer compression, adsorption and charge neutralization, sweep coagulation and interparticle bridging. Either of the methods or combination of them accomplishes the coagulation phenomenon (Peavy H.S, 1985). There is a need to develop a cheap process to treat the textile waste for effective colour removal.

Prehydrolysed coagulants like Polyaluminium ferric chloride (PAFCl), Polyaluminium chloride (PAC), Polyferric chloride (PFCl) and Polyferrous sulphate (PFS) look to give better colour removal even at low temperature and may also fabricate lower volume of sludge. Strong flocs are formed using PAC as coagulant as compared to alum and there is more rapid flocculation at

a,b,c Dept. of Civil Engg., Malaviya National Institue of Technology, Jaipur – 302017, India

International Journal of Innovative and Emerging Research in Engineering
Volume 3, Issue 1, 2016

Available online at www.ijiere.com

International Journal of Innovative and Emerging Research in Engineering

e-ISSN: 2394 - 3343 p-ISSN: 2394 - 5494

Remediation of textile effluent using siliceous materials: A review with a proposed alternative

Priya Mundada[a], Dr. Urmila Brighu[b]
[a]Research Scholar, Malaviya National Institute of Technology, Jaipur, India
[b]Associate Professor, Malaviya National Institute of Technology, Jaipur, India

ABSTRACT:
Treatment of the colored effluent from the textile industries is a major challenge. Many treatment techniques have been reported in the recent past. However, adsorption on low cost adsorbents has received a worthy attention. A number of low cost adsorbents have been researched. This paper discusses the potential of the siliceous materials in dye removal. A new low cost adsorbent, soil from Rajasthan, India, has also been reported.

Keywords: Dyes, low cost adsorbents, siliceous adsorbents, direct red 81, soil

I. INTRODUCTION

The discharge of wastewater from textile and dyeing industries to the environment is a major concern due to its toxicity. These dyes can consume the dissolved oxygen required by aquatic life and some of them have direct toxicity to microbial populations and even can be toxic and/or carcinogenic to mammals [1]. Therefore, it is necessary to remove the dye stuff from the effluents. However, due to the synthetic origin and complex aromatic molecular structures of dyes (Table I & II), they become more stable and more difficult to degrade. Hence, it is imperative that a suitable treatment method should be devised to treat dyes [2].

Dye class	Description
Acid	Water-soluble anionic compounds
Basic	Water-soluble, applied in weakly acidic dyebaths; very bright dyes
Direct	Water-soluble, anionic compounds; can be applied directly to cellulosics without mordants (or metals like chromium and copper)
Disperse	Not water-soluble
Reactive	Water-soluble, anionic compounds; largest dye class
Sulfur	Organic compounds containing sulfur or sodium sulfide
Vat	Water-insoluble; oldest dyes; more chemically complex

TABLE I: TYPICAL DYES USED IN TEXTILE DYEING OPERATIONS [3]

Dye	Structure
Crystal violet	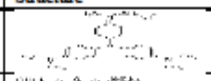
Rhodamine b	
Methylene blue	
Acid red 57	
Malachite green	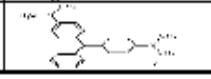

TABLE II: DYES AND THEIR STRUCTURES

Sorption Study of Anionic Dye from Aqueous Solution onto Locally Available Soil

Priya[1], Dr. U. Brighu[2]
[1, 2] Department of Civil Engineering, Malaviya National Institute of Technology, Jaipur, India
[1]Email: priya19788@gmail.com
[2]Email: ubrighu@gmail.com

***Abstract*—Textile industry is extensively water dependent and discharges intensely coloured effluent in the environment. Keeping in view the toxicity of the dyes used in this industry, zero discharge from industries across Asian and other countries have been enacted. Removal of colour from the effluent of textile industry is difficult because colour is visible even in very minute quantities. Adsorption on activated charcoal provides a high quality treated wastewater but its application is limited due to its high cost and regeneration complexities. Availability in less quantity of other low cost adsorbents restricts their use for commercial purpose. In the present study, authors have tried to investigate the potential of using locally available sandy soil for colour removal and sorption properties of this soil for an anionic dye i.e. Direct Red 81.**

***Index Terms*— adsorption, textile wastewater, low cost adsorbent, soil, anionic dye.**

I. INTRODUCTION

Textile wastewater is a by-product of textile industry and it is a mixture of colorants (dyes & pigments) and various organic compounds used as cleaning solvents, plasticizers, etc. [1]. Of all dyes produced across the world, 11% goes out as effluents, 2% from manufacturing and as much as 9% from colouring. Beside aesthetic reasons, dyes are not easily degradable and are toxic to aquatic life, if discharged untreated [2]. Not only the dye in the effluent is a major issue of concern, but this industry also uses a large amount of water during the production process. About 200L of water are used to produce 1kg of textile [3].

Rajasthan is an arid state and textile mills represent an important economic sector to this state. Owing to the easy availability of the cheaper labour and less stringent waste disposal norms by the Rajasthan government, a large number of small and medium scale enterprises (SMSEs) have come up in the last decade. Due to the limited resources in terms of finance, space and technology, these industries discharge large quantities of effluents in nearby seasonal rivers like Bundi, Jojri and Luni present in the districts; Pali, Jodhpur and Barmer respectively. This not only causes geo-environmental pollution but also anthropogenic hazards [4].

Recycling and reuse of the textile wastewater has become a necessary element to control pollution due to textile wastewater. It can be considered as the most practical solution to effectively treat the effluent so that it conforms to specified discharge requirements as shown in the Table I [5]. Consequently, on the 17th and 24th of February, 2012, the Rajasthan High Court issued two court orders. These orders placed a zero discharge requirement on local industries and mandated a reduction to 40% of their original capacity unless they could effectively create a closed loop water system. The High Court requires that industries no longer freely release effluent, but rather mitigate and reduce wastewater [6].

Rajasthan's 52% of the textile-fibre market is cotton [7]. Table III shows the typical composition of cotton textile mill waste. The most commonly used dye for cellulose textile is reactive dyes. The other types of dyes used are direct dyes, vat dyes, sulphur dyes, indigo dyes and naphtol dyes. The reactive dyes are sometimes called as fibre reactive dyes as they form covalent bond with the fibre molecule and are considered to be the most effective and permanent dyes used while direct dyes do not form strong bonds and are loosely associated with the fibre molecules. One of the advantages of direct dyes is that they are the cheapest among all other dyes [3]. Other dyes like sulphur dyes also form a low cost and good wash fastness group of dyes [8]. Table II shows the percentage of dyes lost to the effluent.

TABLE I. STANDARDS FOR TREATED EFFLUENTS FROM TEXTILE INDUSTRY. [15]

Parameter	Concentration (mg/l), except pH
pH	5.5 – 9.0
Total suspended solids	100
Bio-chemical oxygen demand (BOD)	30
Chemical oxygen demand (COD)	250
Total residual chlorine	1
Oil and grease	10
Total chromium as Cr	2
Sulphide as S	2
Phenolic compounds as C_6H_5OH	1